Studies Towards the Total Synthesis of Phormidolide A and the Synthesis of C4'-modified Nucleoside Analogues

by

Garrett Muir

B.Sc., Mount Allison University, 2017

Thesis Submitted in Partial Fulfillment of the
Requirements for the Degree of
Doctor of Philosophy

in the
Department of Chemistry
Faculty of Science

SIMON FRASER UNIVERSITY
Summer 2024

Declaration of Committee

Name:	**Garrett Muir**
Degree:	**Doctor of Philosophy (Chemistry)**
Title:	**Studies Towards the Total Synthesis of Phormidolide A and the Synthesis of C4'-modified Nucleoside Analogues**
Committee:	**Chair: Niel Branda** Professor, Chemistry
	Robert Britton Supervisor Professor, Chemistry
	Andrew Bennet Committee Member Professor, Chemistry
	Pete Wilson Committee Member Associate Professor, Chemistry
	Robert Young Examiner Professor, Chemistry
	Corey Stephenson External Examiner Professor, Chemistry University of British Columbia

Abstract

The research presented in this thesis details efforts towards the total synthesis of the natural product phormidolide A. The synthesis of various fragments and eventual completion of the macrocyclic fragment of phormidolide A is reported. As part of these efforts, a stereochemical reassignment of phormidolide A was undertaken. Finally, the discovery and use of a unique halide effect in Grignard reactions of β-hydroxyketones was identified and exploited for the synthesis of C4'-modified nucleoside analogues.

Phormidolide A is a THF-containing marine macrolide natural product, isolated from a marine cyanobacterium *Leptolyngbya sp*. by the Gerwick group. Reported in 2002, its planar structure was determined primarily through 1D and 2D NMR spectral analysis while the relative stereochemistry of phormidolide A was assigned using nuclear Overhauser effect (NOE) information and Murata's *J*-based configurational analysis. In collaboration with the Paterson group at Cambridge University, we developed a synthesis of 5 key fragments of phormidolide A. Collaborative efforts, including the synthesis of C10-C23 fragments of the natural product and comparison of computational results to data reported for the natural product led to a stereochemical reassignment. Following this, the prepared fragments were used to construct the macrocycle of phormidolide A. These synthesis efforts included the examination of a wide range of macrocyclization strategies, ultimately using macrolactonization to form the macrocycle. Finally, efforts towards linking the side chain fragments to the macrocycle are described.

During an investigation of the 1,2-addition of Grignard and other organometallic reagents to β-hydroxy ketones, we identified a unique effect of halide on diastereoselectivity, with alkylmagnesium iodide reagents demonstrating the highest levels of stereoselectivity. Detailed DFT calculations and mechanistic studies suggest that the Lewis acidity of a chelated magnesium alkoxide can be tuned by choice of halide. Exploiting this finding, we demonstrate that the diastereoselective addition of alkyl magnesium iodide reagents to ketofluorohydrins enables rapid access to naturally configured C4'-modified nucleosides. This work now provides a platform to support antiviral and anticancer drug discovery and development efforts.

Keywords: Marine natural products; phormidolide A; total synthesis; macrocyclization; Grignard reaction; C4'-modified nucleoside analogue

Dedication

To my incredible family,

who have supported me through everything.

Thank you.

Acknowledgements

So many people supported me and the work done in this thesis. My heartfelt thanks goes out to everyone who helped me get through this PhD and who supported me through the struggles.

I would like to thank my supervisor Robert Britton for his kindness, support, and optimism throughout this work. I am grateful to him for accepting me into the lab, letting me work on the chemistry that I was interested in, and letting me take every opportunity I could to grow as a chemist. The opportunity to go to Cambridge was amazing and the constant support I received from Rob learning both in and outside the lab made my learning experience incredible. His unending optimism and ideas always helped me fight through the obstacles I faced. In addition, I have to thank Ian Paterson for his support during this thesis work. Letting me come to study in the lab and getting to experience Cambridge was an unforgettable experience and I will always be grateful to him for meeting with me every two weeks to talk about results and offer suggestions. I also would like to thank Andy Bennet and Pete Wilson, my committee members, for their support and suggestions.

I have to thank Nelson Lam for his constant support and guidance during my PhD. I am so thankful for the opportunity to get to know such an amazing and insightful researcher and I would be a lesser chemist having not known him. In addition, I want to thank Venugopal Rao Challa for taking me under his wing when I arrived and teaching me everything he knew about organic chemistry.

Thank you to all the members of the Britton lab over my many years there, of which there are too many to name. I cannot express the support and kindness that so many people have shown me. From helping with lab instruments to solving NMR spectra to going to coffee or grabbing beers, to the random endless debates, to helping find challenging reaction conditions, to all the encouragement, I am forever grateful that you all made my experience in the group better. And thanks to Yejin for being the best undergraduate student that I could have supervised!

I have to thank Greg, Laurel, and Curtis for taking me in when I first got here and finding a place to live. Moving to a new city with people I knew made everything easier. I also have to thank Shane, Callum, and Steph for living with me afterwards so that I never

had to find a place on my own. Thanks to everyone who joined me on the mountain, especially Matt (Deen and Alteen), Greg, Curtis, and Deb because you all pushed me to try the slopes I never though I would. Thank you to everyone I made friends with when I arrived, especially Bryton, Shane, Marco, Saeid, and Aryan who showed me all the great parts of Vancouver and helped me feel comfortable in a new place. The Penticton trips will always be a highlight of my time here and I am thankful for you all introducing me to new adventures.

I also want to thank the friends I made along the way who were always ready to relax and have fun with me and distract from the hardships, especially Victoria, Kelsey, Albert, Cohan, Callum, Scheryn, Bryce, Brooklyn, Carolyn, and Makenzy. Our hangouts, adventures, hikes, parties, game nights, downtown adventures, zoom chats, games, and group chats were always the things that made life exciting, fun, and different. A PhD is too long of a time to go through without support and fun and you were always there to provide both. I cannot wait to celebrate with everyone when everything is finished.

Thank you to all my friends back home and everyone who got together when I came back to visit. Keeping in touch with everyone from MTA, especially Sarah, Katie, Dylan, Mike, Jacob, Allison, Jess, and Emilie, was incredibly special and I cannot wait for our next reunion. Thanks to my high school friends for always making time when I came back to visit and getting together every holiday to see each other. Thank you to my book club for giving me fun and distractions while writing my thesis.

I could also not be luckier than to have my incredible partner Ana by my side. I was so happy to meet her here and go through graduate school with her. Thank you, Ana, for getting coffees with me, being down for every adventure I wanted to try, finding places to live with me, climbing with me, putting up with my many weird and different hobbies, going on cycling and skiing trips with me, and everything you do to support me through this. Meeting you will always be the best part of this degree.

Finally, I have to thank my sister, Teagan, and parents, Paul and Philomena. My family has always supported my goals no matter what, and I will always be grateful for your support in moving across the country. I love seeing you every time I come home and I cannot wait to celebrate with you.

Table of Contents

List of Tables

List of Figures

List of Schemes

List of Acronyms and Abbreviations

$[\alpha]_D^{20}$	Specific rotation at the sodium D line (589 nm)
°C	Degrees Celsius
µL	Microlitre
µmmol	Micromole
Aq.	Aqueous
BPin	Pinacolborane
Bu	Butyl
COSY	Correlation Spectroscopy
CSA	10-Camphorsulfonic acid
DCC	N,N′-Dicyclohexylcarbodiimide
DDQ	2,3-Dichloro-5,6-dicyano-1,4-benzoquinone
DFT	Density Functional Theory
DIBAL	Diisobutylaluminium hydride
DIPA	Diisopropylamine
DMAP	*N,N*-dimethyl-4-aminopyridine
DMF	*N,N*-Dimethylformamide
DMP	Dess-Martin periodinane
DMSO	Dimethylsulfoxide
d.r.	Diastereomeric ratio
E	*Entgegen* (alkene geometry)
e.e.	Enantiomeric excess
eq.	Equivalents
ESI	Electrospray ionization
Et	Ethyl
Et_2O	Diethyl ether
EtOAc	Ethyl acetate
EtOH	Ethanol
g, mg	Grams, milligrams
h	Hours

HCl	Hydrochloric acid
HMBC	Heteronuclear multiple bond correlation
HMPA	Hexamethylphosphoramide
HPLC	High performance liquid chromatography
HRMS	High resolution mass spectrometry
HSQC	Heteronuclear single quantum coherence
HWE	Horner-Wadsworth-Emmons
Hz	Hertz
IC_{50}	Half maximal inhibitory concentration
*i*Pr	*iso*-Propyl
IR	Infrared spectroscopy
KR	Ketoreductase
LDA	Lithium diisopropylamide
LiHMDS	Lithium bis(trimethylsilyl)amide
M	Molar (mol/L)
[M]	Unspecified metal/metal halogen
Me	Methyl
MeCN	Acetonitrile
mL	Millilitre
mmol	Millimole
MNBA	2-Methyl-6-nitrobenzoic anhydride
NCS	N-chlorosuccinimide
NHK	Nozaki-Hiyama-Kishi
NMR	Nuclear magnetic resonance
NOE	Nuclear Overhauser effect
NP	Natural Product
NR	No reaction
PCy_3	Tricyclohexylphosphine
PG	Protecting group
Ph	Phenyl
PKS	Polyketide Synthase

PMBM	*p*-methoxybenzyloxymethyl
PPTS	Pyridinium *para*-toluenesulfonate
py	Pyridine
R	Substituent
R	*Rectus* (chiral designation)
rt	Room temperature
S	*Sinister* (chiral designation)
SEM	2-trimethylsilylethoxymethyl
TBAF	Tetrabutylammonium fluoride
TBDPS	*tert*-Butyldiphenylsilyl
*t*BuLi	*tert*-Butyllithium
TBS	*tert-B*utyldimethylsilyl
TE	Thioesterase
TES	Triethylsilyl
Tf	Trifluoromethanesulfonyl
TFBA	4-trifluoromethylbenzoic anhydride
THF	Tetrahydrofuran
TIPS	Triisopropylsilyl
TLC	Thin Layer Chromatography
TMS	Trimethylsilyl
Z	*Zusammen* (alkene geometry)

Chapter 1. Introduction

1.1. Marine Natural Products

Living organisms produce a variety of chemicals referred to as natural products (NPs), which are essential to life, growth, and reproduction. NPs that are crucial to basic survival are referred to as primary metabolites and include carbohydrates, proteins, fats, and nucleic acids.[1] The biosynthesis of primary metabolites is generally conserved across all organisms and is important for metabolism and reproduction.[1,2] In contrast, secondary metabolites are NPs that are not essential to the internal mechanisms that govern growth, development, and reproduction.[1,3] The production of secondary metabolites is typically specific to an organism or group of organisms and imparts an evolutionary advantage that could include defense against predation, communication, or hunting prey through chemical means.[1,4]

Organisms living in marine environments produce a wide variety of secondary metabolites owing to the extreme environmental conditions and sessile nature of many marine organisms, which are often soft-bodied, slow-moving, or lack significant physical protection.[5–8] Most commonly, these organisms produce secondary metabolites as a means of defense against predators and infectious microbes, to compete with encroaching neighbours for food and space, or to paralyze prey.[7–9] In many cases it is critical that these secondary metabolites are also highly potent so that they maintain effectiveness when diluted in the surrounding aqueous marine environment.[5] As a result, secondary metabolites from marine organisms have long been of interest to researchers as leads for drug discovery.[5,7,10] For example, marine NPs have been used clinically as anti-cancer, anti-bacterial, and anti-inflammatory agents, have shown painkilling effects and beneficial effects on neurodegenerative and heart diseases, and have shown the potential to combat drug-resistant pathogens.[11–13]

1.1.1. Marine Natural Products in Drug Discovery

Throughout history, marine NPs have been exploited for medicinal and other purposes. Ancient Chinese and Japanese mariners ate seaweed for its health benefits and records from ancient Rome showed that they used concoctions made from stingray spines to alleviate pain.[14] South-eastern Asian mariners used a flatworm, which was later

found to contain a paralyzing toxin, to stun fish to catch them more easily.[15] In the 1960s, interdisciplinary groups were brought together to systematically investigate and assess the potential of marine NPs in drug discovery. Since this time, the clinically relevant biological activity of marine NPs has been widely recognized.[15] To date, almost 40,000 marine NPs have been isolated and 23 marine NPs or marine-derived drugs are in clinical use.[16] Notably, the ratio of successful marine NP-based drugs compared to all marine NPs isolated is approximately 1:1700. This ratio is significantly better than the success rate of drugs identified from synthetic compound libraries, indicating the importance of marine NPs as drug leads.[15]

Prominent examples of marine NPs that have inspired the development of approved drugs include cytarabine (**1**, **Figure 1.1**) and vidarabine (**2**, **Figure 1.1**), which are synthetic analogues of the marine NPs spongothymidine and spongouridine, respectively.[15] In 1969, cytarabine was the first marine-derived drug to be approved by the US Food and Drug Association (FDA) and is still a prominent leukemia therapeutic.[17,18] Vidarabine was approved by the FDA in 1976 for the treatment of herpes simplex virus but was later discontinued due to better commercial alternatives.[17] The early discovery of these drugs prompted further investigation into marine NPs as drug candidates.[15,19]

The peptide ziconotide is an example of a marine-derived peptidic toxin isolated from the venom of the cone snail and is used naturally for both hunting and defense. Ziconotide and other ω-conotoxins have attracted interest due to their ability to block certain mammalian ion channels and ultimately cause pain relief. The realization of their therapeutic potential inspired considerable research that ultimately led to their approval for the treatment of chronic neuropathic pain in 2004.[15,17] Notably, ziconotide is 1000 times more potent than morphine, a commonly used opioid for pain relief, and does not show the addictive effects that opioids like morphine display.[17,20]

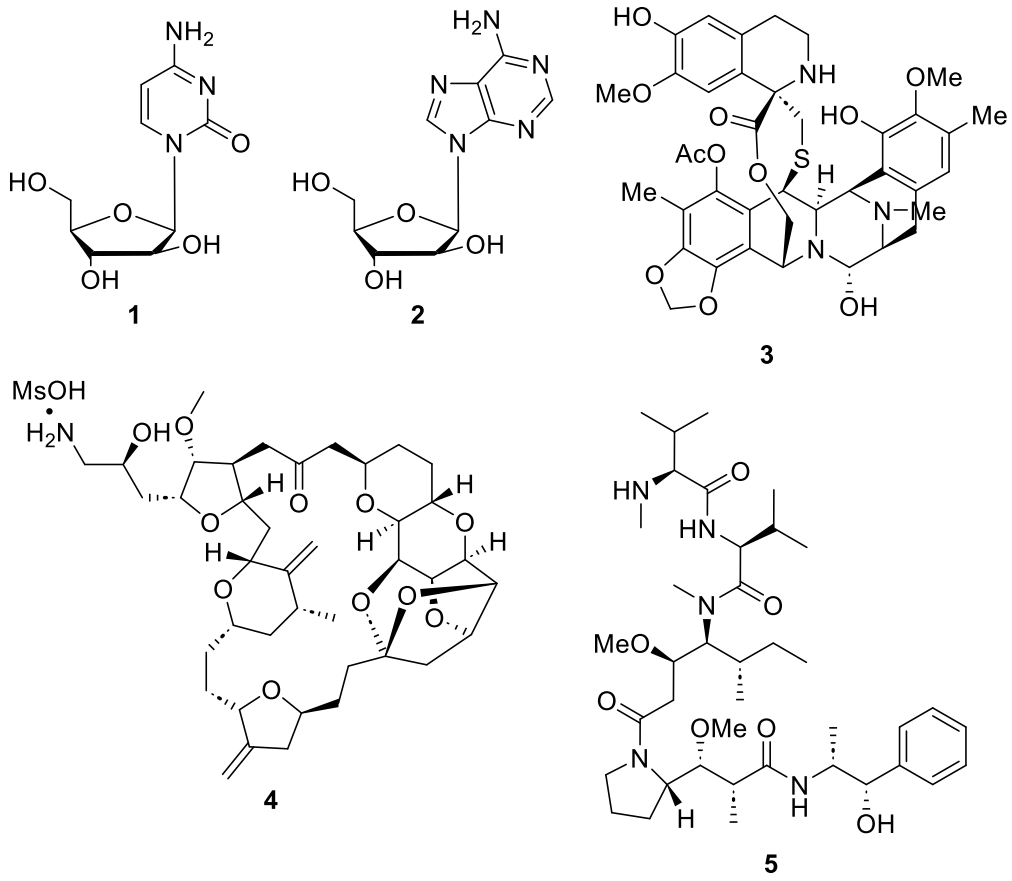

Figure 1.1. Select examples of drugs derived from marine natural products.

Trabectedin (**3**), isolated from a tunicate, was the first marine NP approved for cancer treatment. The isolation of small amounts of trabectedin led to challenges with structural identification, though bioactivity studies showed potent activity towards leukemia cells. Based on these results, further studies revealed that trabectedin had strong *in vivo* anti-cancer activity in mouse models.[21] Due to the limited amounts of the NP available from the tunicate source, efforts to produce this compound by synthetic methods were examined. PharmaMar, a Spanish pharmaceutical company, found that trabectedin could be synthesized from cyanosafracin B, which could be produced on a large scale from bacterial fermentation. The semi-synthesis from cyanosafracin B supported the development of trabectedin into an approved drug in 2007 for the treatment of soft-tissue sarcoma.[15,19,21] Trabectedin is currently in use in over 70 countries with studies ongoing to assess its further pharmaceutical potential.[15,17,20]

Much like cytarabine and vidarabine, eribulin mesylate (**4**) is a synthetic marine-inspired drug as a simplified synthetic analogue of the marine NP halichondrin B.

Halichondrin B showed incredibly potent anti-cancer activity, which inspired a synthesis campaign that was completed by Kishi and co-workers in 1992.[22] Biological testing of synthetic intermediates from this work demonstrated that the macrocyclic portion of halichondrin B was responsible for the observed activity and so, in collaboration with scientists at Eisai, over 200 additional structural analogues were synthesized and tested. Eribulin mesylate was one of the best-performing compounds in this study and showed similar potency to the parent NP.[15] In 2010, eribulin mesylate was approved by the FDA and Health Canada for the treatment of metastatic breast cancer and in 2016 for inoperable liposarcoma and acts as a microtubule aggregating agent, inhibiting mitosis and causing cell death.[20,23]

Marine-derived drugs have also been used as toxic payloads in antibody-drug conjugates (ADCs). For example, the ADC brentuximab vedotin incorporates the cytotoxic drug monomethyl auristatin E (MMAE, **5**), a synthetic analogue of the marine NP dolastatin 10. While dolastatin 10 is a potent cytotoxin and has demonstrated impressive antitumor activity, it did not proceed beyond phase II clinical trials.[15] However, Seattle Genetics was able to link MMAE to a tumor-specific antibody, resulting in the drug combination commercialized as brentuximab vedotin. Brentuximab vedotin was approved by the FDA in 2011 for the treatment of lymphomas and now several other ADCs featuring MMAE or other derivatives of dolastatin 10 have been approved as drugs.[17,19]

1.1.2. Supporting Drug Discovery with Total Synthesis

A major challenge in marine NP research is the supply of the NP itself,[24] as many of these compounds are isolated in low (mg or µg) quantities from the producing organism. Thus, their development as therapeutics may not be sustainable due to ecological concerns, including the harvesting of endangered or protected species, or practical challenges, such as the need for expensive collection techniques and jurisdictional issues surrounding organism collection.[11,19,21] While some marine species, such as bacteria, can be cultured in a laboratory setting and support sustainable access to NPs, other delicate marine organisms are more challenging, and sometimes impossible, to grow outside of their natural environment.[19] These supply issues continue to place limitations on the study of marine NPs as drug candidates.

To address these issues, total synthesis provides an alternative, sustainable access to NPs starting from commercially available starting materials. These syntheses bypass the need for collection and extraction and can be scaled up or repeated to access suitable quantities of the NP for further study.[24,25] A notable example is the Novartis synthesis of the anticancer marine polyketide discodermolide, a NP that showed potent microtubule-stabilising activity and was originally isolated from a deep-sea sponge *Discodermia Dissoluta*. Isolation efforts of discodermolide provided only 0.002% by weight from the sponge. Given that the isolated quantities were quite low, it was recognized that total synthesis would be critical to advance studies of this NP. The total synthesis of discodermolide reported by Novartis was inspired by the academic groups of Smith and Paterson.[26–29] Ultimately, the industrial synthesis delivered 64 grams of the NP over a total of 39 steps and provided sufficient material to support clinical trials. While these studies were eventually halted due to unavoidable toxicity, this effort highlights the importance of the use of total synthesis in supporting drug discovery efforts.[29]

In addition to supporting advanced biological or clinical studies, total synthesis can also provide a framework to prepare synthetic analogues or fragments of the NP. These analogues can be used to better understand the relationship between the chemical structure and the observed biological activity.[24,25] As noted above, Eisai and the Kishi group assessed the biological activity of synthetic intermediates produced during the total synthesis of halichondrin B, which led to the realization that only the macrocyclic portion of the NP was required and, ultimately, the development of eribulin mesylate.[30] From a fundamental perspective, total synthesis also plays a key role in structural assignment by providing material whose analytic data can be used to confirm the structure of the NP. Despite the abundance of analytical techniques available, structural assignment of NPs can be challenging owing to complex structural architectures or limited material, and in many cases total synthesis has resulted in structural reassignments.[31] In 2011, Suyama, Gerwick and McPhail surveyed the structural reassignments of all NPs characterized from 2005 to 2010. Here, they found that 48% of NP structural revisions that occurred during this period were based on the total or partial synthesis of the NP and more than double the percentage of the next most common form of structural reassignment; the use of NMR spectroscopy.[32]

1.2. Tetrahydrofuran-Containing Macrolides

Tetrahydrofuran (THF)-containing macrolides are a group of polyketide NPs that are characterized by their macrolactone structure that incorporates one or more embedded and often functionalized THF rings.[33] Several members of this family also contain side chains extending out from the macrolide core. Many members of this family exhibit potent and potentially useful biological activities and have attracted interest from NP and total synthesis groups.[33]

1.2.1. Biological Activity of THF-Containing Macrolides

While many THF-containing macrolides have demonstrated potentially useful biological activity, a notable example is amphidinolide C (**6**, **Figure 1.2A**), which contains two embedded THF rings. Isolated from marine plankton, amphidinolide C is active against murine lymphoma cells and human carcinoma cells with IC_{50} values of 8.1 and 6.4 nM, respectively. Interestingly, the alcohol functionality at C29 in the side chain is essential to the anticancer activity, as amphidinolides C2 and C3 (**7** and **8**, **Figure 1.2**), which differ only at this position, are three orders of magnitude less active than amphidinolide C against the same cell lines.[34] Similarly, caribenolide I (**9**, **Figure 1.2**), often referred to amphidinolide N, was isolated from the same genus of marine plankton and is the most potent member of the amphidinolide family. Caribenolide I displayed activity against both a human colon carcinoma cell line and a drug-resistant version of the cell line with an IC_{50} of 1.6 nM.[33,35]

Several structurally similar chlorinated THF-containing macrolides named the haterumalides and biselides have been isolated from marine sponges and ascidians collected in the Okinawa prefecture of Japan.[34] Two of these NPs, haterumalide NA (**10**, **Figure 1.2**) and biselide A (**11**, **Figure 1.2**), exhibited cytotoxicity against a broad panel of human cancer cell lines. Among this family, haterumalide NA proved to be most potent with IC_{50} values in a range of 0.13 to 0.74 μM, while biselide A was generally 5-10-fold less active against the same pane of cell lines. Interestingly, while haterumalide NA proved to be toxic towards brine shrimp, biselide A showed no such toxicity, suggesting biselide A could be a better drug-development candidate.[36,37]

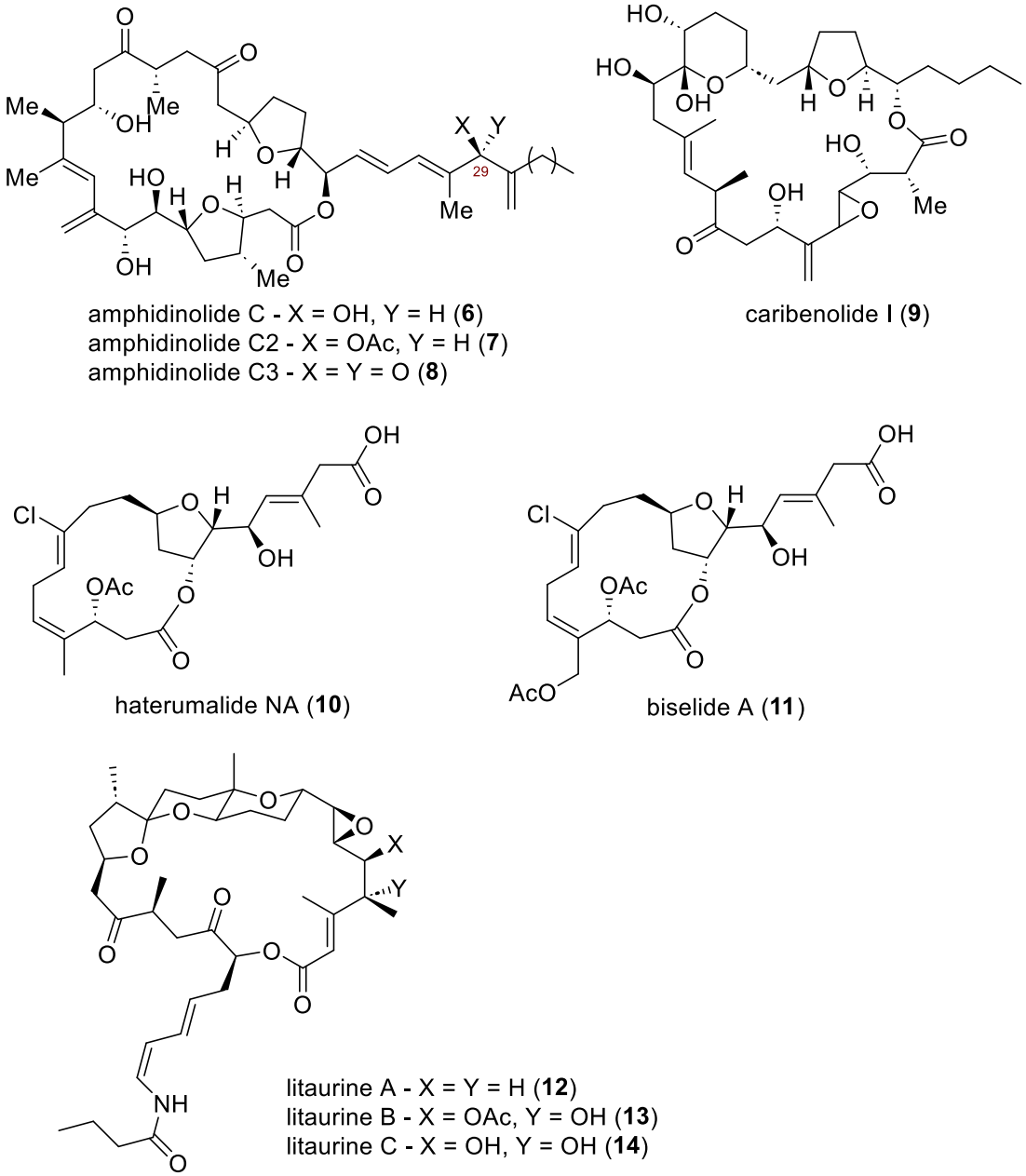

Figure 1.2. Examples of THF-containing macrolides with clinically relevant biological activity.

The lituarines A-C (**12-14**, **Figure 1.2**) are complex THF-containing macrolides, with an embedded spiro-linked tetrahydrofuran/tetrahydropyran duet. These NPs were isolated from a sea pen, which is a sessile marine filter feeder, and were shown to inhibit the growth of several fungi. The lituarines also showed potent cytotoxicity against KB cells, a human carcinoma cell line, with IC_{50} values of 3.7-5.0 nM, 1.0-2.0 mM, and 5.0-6.0 nM for lituarines A, B, and C, respectively.[33,38] This potent activity has inspired efforts towards

their total synthesis. Unfortunately, completion of the total synthesis of lituarines B and C revealed that these NPs were incorrectly assigned, an issue that has not yet been resolved.[39]

1.2.2. Macrocyclization of THF-Containing Macrolides

Polyketides are biosynthesized by large multi-enzyme complexes called polyketide synthases (PKSs), categorized based on whether the enzymes are covalently linked or free-standing.[40] PKSs bind and catalyze the iterative coupling of small building blocks and contain groups of enzymes for the modification of each unit, such as dehydrating, reducing, or deoxygenating. With these groups of enzymes, PKSs can rapidly assemble long, structurally complex polyketide chains that are later assembled into macrolide NPs by a thioesterase (TE) enzyme in the PKS complex.[40–42] For example, the proposed biosynthetic macrolactonization of oomycin A (**15**) is depicted in **Figure 1.3**. Here, once the C1-C19 chain is formed through an iterative coupling and modification strategy, the thioesterase (TE) in the PKS catalyzes the transesterification of the C13 alcohol with the bound thioester, releasing macrolide **16**, which is further modified to form oomycin A.[43]

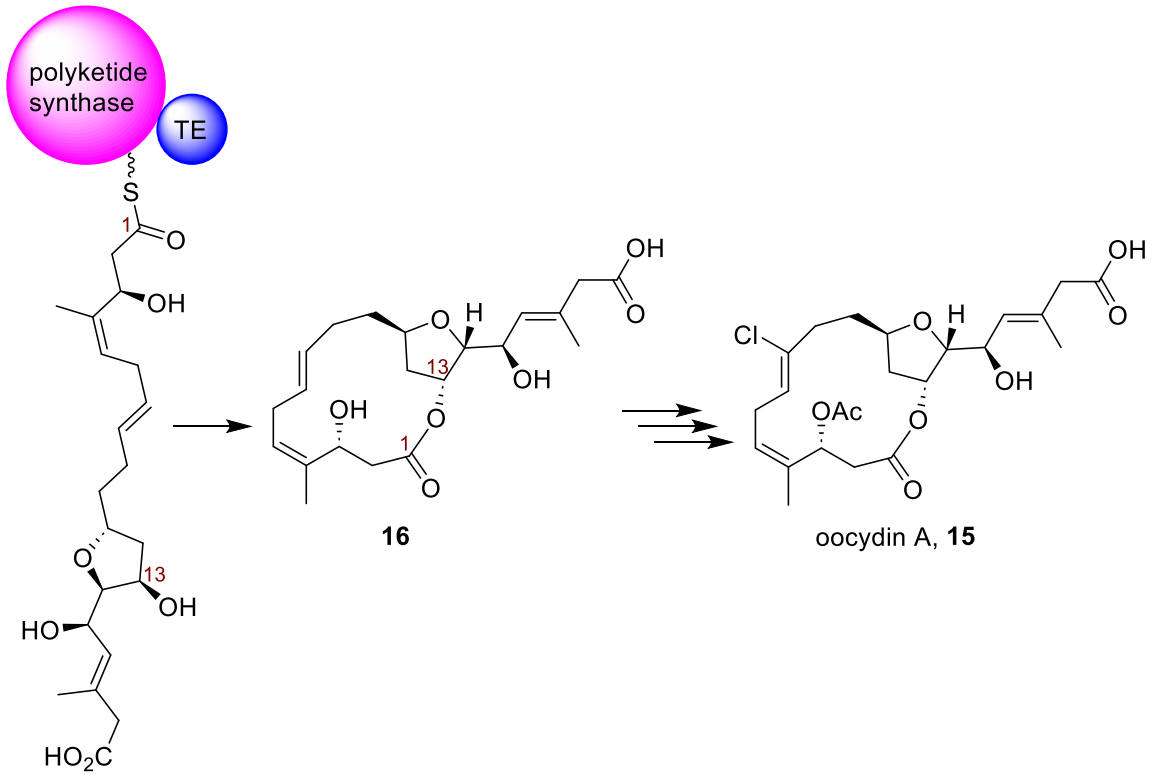

Figure 1.3. **The proposed macrocyclization step in the biosynthesis of oomycin A.**
TE = thioesterase.

Similar to Nature's strategy, many total syntheses of THF-containing macrolides take advantage of macrolactonization strategies. For example, in the Nicolaou synthesis of des-epoxy-caribenolide I (**Scheme 1.1**), seco acid **17** was prepared in 24 linear steps from commercial starting materials. Here, a Yamaguchi macrolactonization[44] was employed to perform a site-selective macrocyclization of **17** and afforded the macrocycle **18** which constitutes the core framework of caribenolide I. Unfortunately, a late-stage epoxidation could not be accomplished to complete the synthesis of the NP.[45]

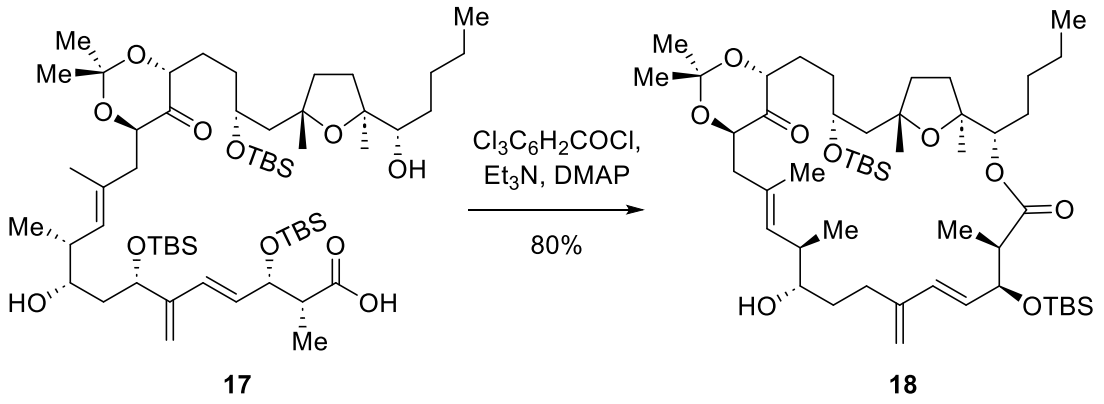

17 18

Scheme 1.1. Macrolactonization Strategy for the Synthesis of Des-Epoxy-Caribenolide I.

Lee and coworkers used a different macrolactonization strategy in the synthesis of amphidinolide E (**Scheme 1.2**). In this case, seco acid **19** was prepared in 28 linear steps from commercial starting materials. Here, Yamaguchi macrolactonization failed to form the desired product, but the use of a ruthenium-catalyzed macrolactonization afforded macrolactone **20** in 44% yield. This ruthenium-catalyzed macrolactonization methodology was initially developed by Kita *et al.* for esterification[46] then expanded to macrolactonization by Trost *et al*,[47] and is known to be milder than common macrolactonization strategies, including Yamaguchi conditions. Subsequent deprotection of macrolactone **20** afforded access to the NP.[48]

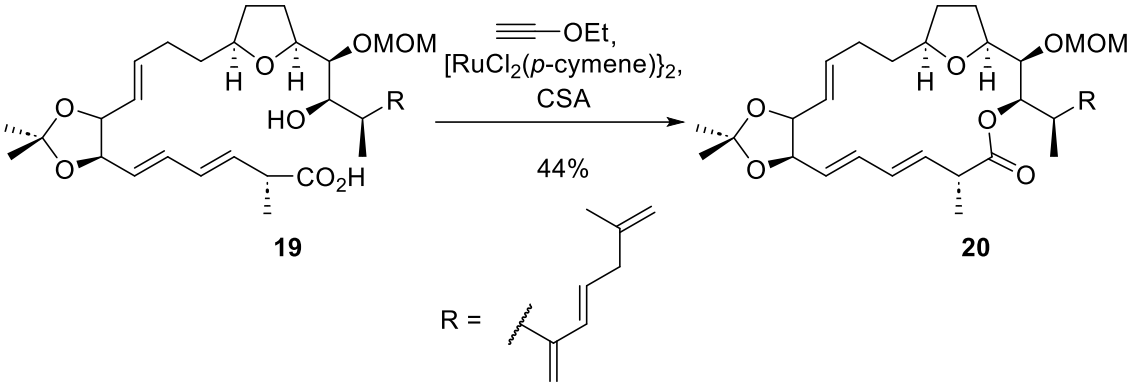

19 20

Scheme 1.2. Macrolactonization Strategy for the Synthesis of Amphidinolide E.

Ring-closing metathesis (RCM) is also a commonly used macrocyclization strategy for the synthesis of THF-containing macrolides. For example, in the synthesis of the proposed structure of lytophilippine A by Lee and co-workers (**Scheme 1.3**) the macrocycle precursor **21** was prepared in 22 steps from D-ribose and a subsequent RCM

reaction converted this diene into macrocycle **22** in excellent (88%) yield. Global deprotection of **22** afforded the proposed structure of lytophilippine A. Unfortunately, the comparison of spectroscopic data derived from the synthetic material to that recorded on the NP cast doubt on the structural assignment of lytophilippine A.[49]

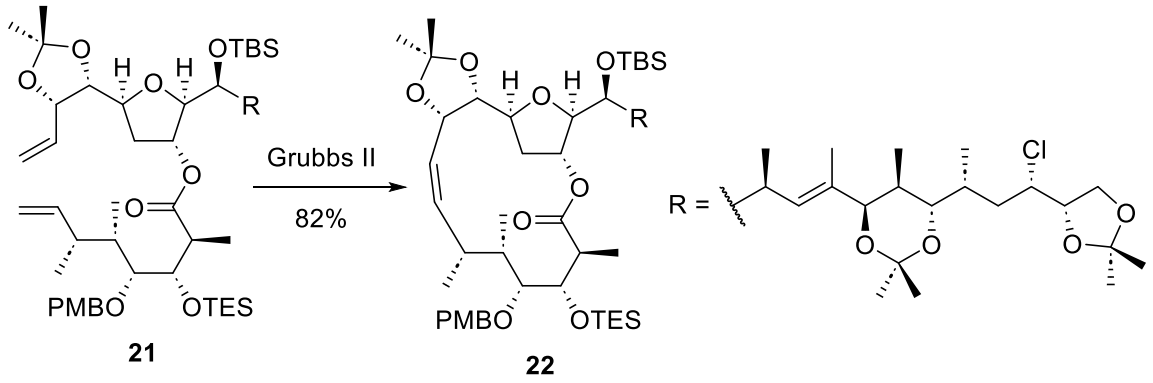

Scheme 1.3. Ring-Closing Metathesis (RCM) Strategy for the Synthesis of Lytophilippine A.

The Reformatsky reaction has also been used in the macrocyclization step of total syntheses of the THF-containing macrolides family. Most recently, the Britton group has used this strategy for the synthesis of biselide A (**Scheme 1.4**). Here, aldehyde **23** was prepared in 12 steps from commercial materials. Treatment of **23** under macrocyclic Reformatsky conditions formed alcohol **24** as a mixture of epimers. The choice of the primary *t*-butyldimethylsilyl (TBS) protection was crucial to ring formation as the use of the larger *t*-butyldiphenylsilyl (TBDPS) protecting group prevented ring closure, highlighting just one of the many complex factors present in the macrocyclizations of these NPs. The NP was then accessed from macrolactone **24** in 5 steps.[37]

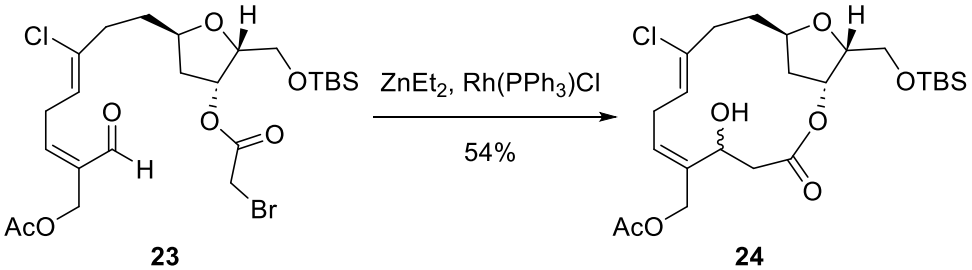

Scheme 1.4. Reformatsky Macrocyclization Strategy for the Synthesis of Biselide A.

A unique $CrCl_2$-mediated macrocyclization was also reported in the synthesis of haterumalide NC by Schomaker and Borhan (**Scheme 1.5**). In this case, aldehyde **25** was prepared in 12 steps from 2-deoxy-D-ribose and, when treated with $CrCl_2$, gave the vinyl chloride **26** in 55% yield. Importantly, this strategy simultaneously affected macrocyclization and installed the vinyl chloride functionality present in the target NP. This synthetic effort led to both a total synthesis of haterumalide NC and NA.[50]

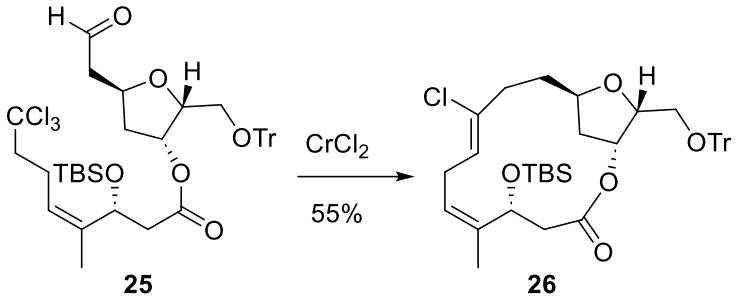

Scheme 1.5. $CrCl_2$-Mediated Macrocyclization for the Synthesis of Haterumalide NC and Formal Synthesis of Haterumalide NA.

1.3. Phormidolide A and The Phormidolide Family

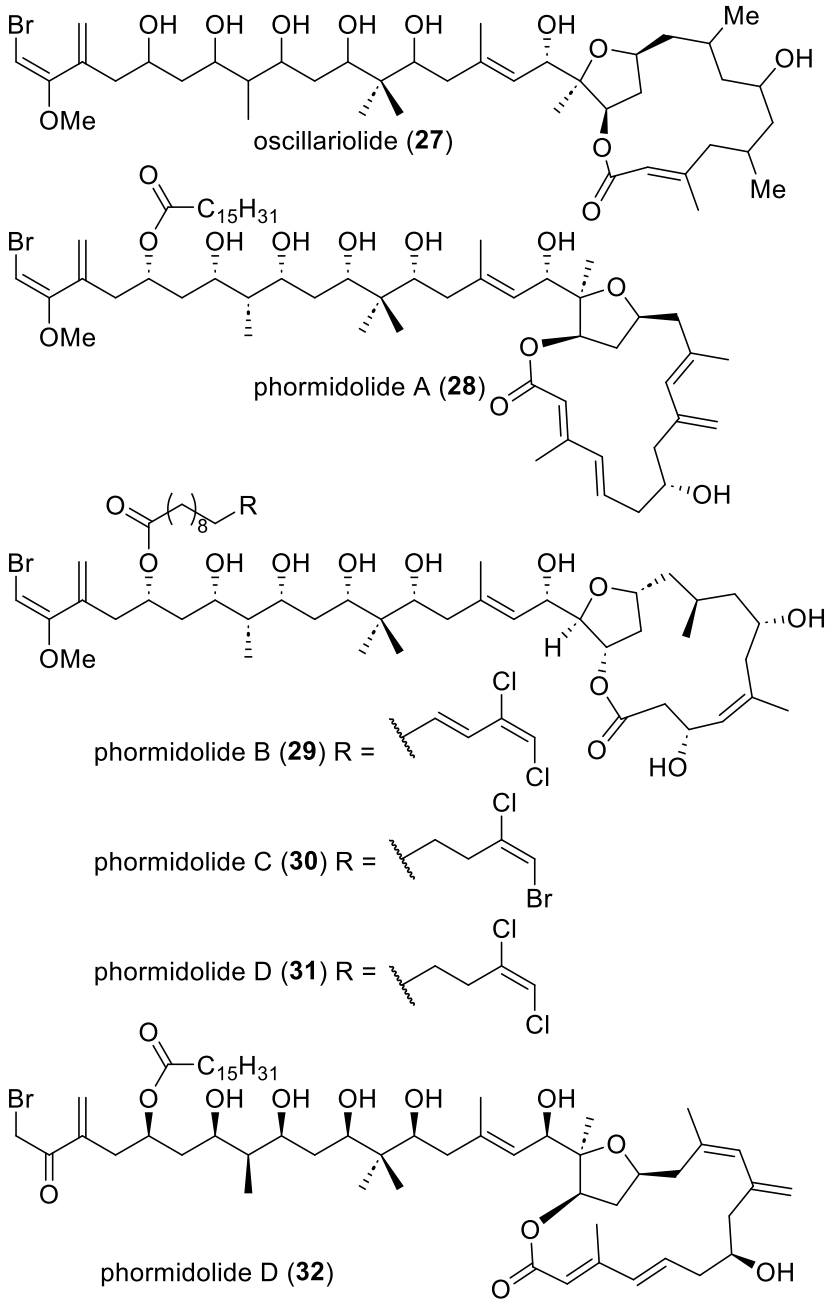

Figure 1.4. The members of the phormidolide family, a family of THF-containing macrolide NPs.

One of the most structurally complex families of THF-containing marine macrolides are the phormidolides (**Figure 1.4**), which includes oscillariolide (**27**),[51] phormidolide A (**28**),[52] phormidolide B (**29**), phormidolide C (**30**),[53] phormidolide D (**31**),[54] and an analogue also named phormidolide D (**32**).[55] These NPs have been Isolated from marine

cyanobacteria and sponges, and all exhibit similar structural features that include a macrocyclic core with an embedded THF linked to a polyhydroxylated side chain. Additionally, all members, except for the phormidolide D (**32**), contain a bromomethoxydiene unit at the end of the side chain and most incorporate a C_{14}-C_{16} fatty acid ester. Notably, three additional THF-containing macrolides were recently isolated from the same genus of cyanobacteria as phormidolide A. These NPs have been named leptolyngbyalide A-C (**33**-**35**, **Figure 1.5**) and are structurally related to oscillariolide (**27**).[56] While the stereochemistry of these NPs was not determined, the relative stereochemistry of the macrocycle, shown in **Figure 1.5**, was proposed based on comparison between calculated spectroscopic data for macrocycle diastereomers and data derived from the NPs.[57]

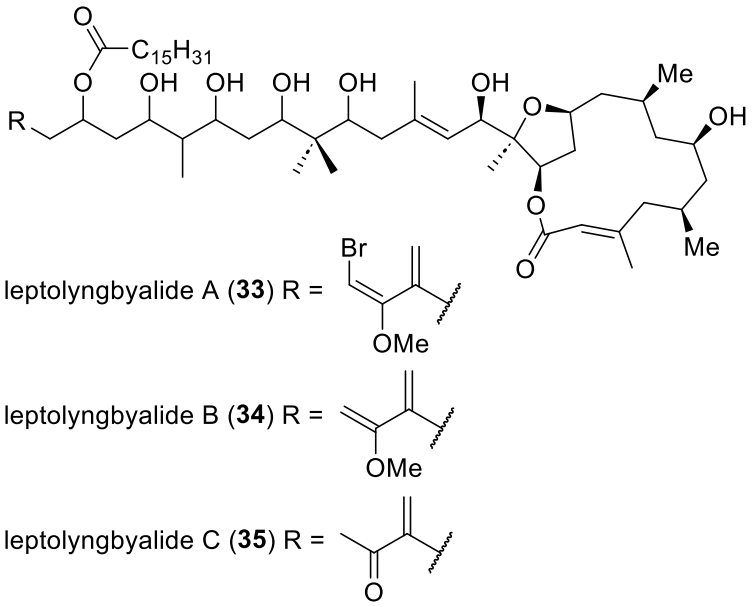

Figure 1.5. The recently discovered leptolynbyalides which share significant structural features with the phormidolide family.

With respect to the biological activity within this family, oscillariolide (**27**) has been shown to inhibit cell division of fertilized starfish eggs at a concentration of 0.61 μM,[51] and phormidolide D (**32**) was reported to be an antifouling agent and cytotoxic towards human colon carcinoma cells, with an IC_{50} of 1.21 μM.[55] Phormidolides B and C (**29** and **30**) have shown anti-cancer activity, with the side chain being of critical importance to this activity.[53,58] Phormidolide A (**28**) demonstrated toxicity towards brine shrimp but displayed no anti-cancer activity at concentrations tested.[52] The biological activities and synthetic

studies of phormidolides A, B, and C are discussed in more detail in the following two sections.

1.3.1. Phormidolides B and C

Phormidolides B and C (**29** and **30**) were isolated from a sponge of the *petrosiidae* family and initially, their planar structure was assigned through a combination of ^{1}H, ^{13}C, and 2D NMR, mass spectrometry (MS), and comparison with previously reported data. The relative stereochemistry of the THF moiety was determined using ROESY spectroscopy and the relative configuration of a section of the macrocycle and side chain was determined using a *J*-based configurational analysis.[53] Phormidolides B and C showed cytotoxic activity against 3 human tumor cell lines (lung, colon, and breast), with GI_{50} values for phormidolide B between 1.0 – 1.4 μM and phormidolide C between 0.5 – 1.3 μM for the same 3 cell lines. These were the first members of this family to show clinically-relevant activity.[53] There have been significant efforts invested in the total syntheses of phormidolides B and C. Summarized here are specific efforts directed towards constructing the macrocyclic portion of these compounds.

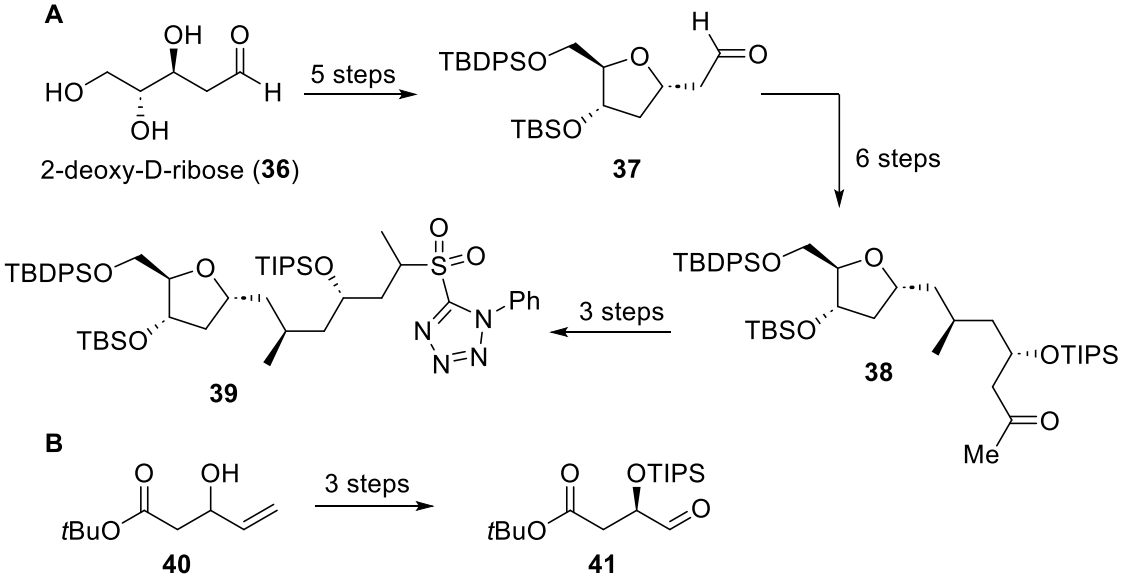

Scheme 1.6. Preparation of Sulfone 39 and Aldehyde 41 for the Synthesis of the Macrocycle of Phormidolides B and C.

In 2015, the Álvarez group reported their first-generation synthesis of the macrocycle (**Schemes 1.6** and **1.7**). This strategy relied on a one-pot modified Julia-

olefination,[59] for which the key coupling partners are a sulfone and an aldehyde. Beginning with 2-deoxy-D-ribose (**36**), THF **37** was prepared in 5 steps and further elaborated into the ketone **38** which was transformed into the desired sulfone **39** following an additional 9 steps (**Scheme 1.6A**). The aldehyde coupling partner **41** was synthesized from racemic β-hydroxyketone **40** (**Scheme 1.6B**).[53] Coupling of the two fragments afforded **42** in a 38% yield, favouring the desired *Z*-isomer in a ratio of 7:3. Mild hydrolysis of **42** to reveal the carboxylic acid followed by Yamaguchi macrolactonization[44] afforded macrocycle **43** in a 39% yield (**Scheme 1.7**).[53]

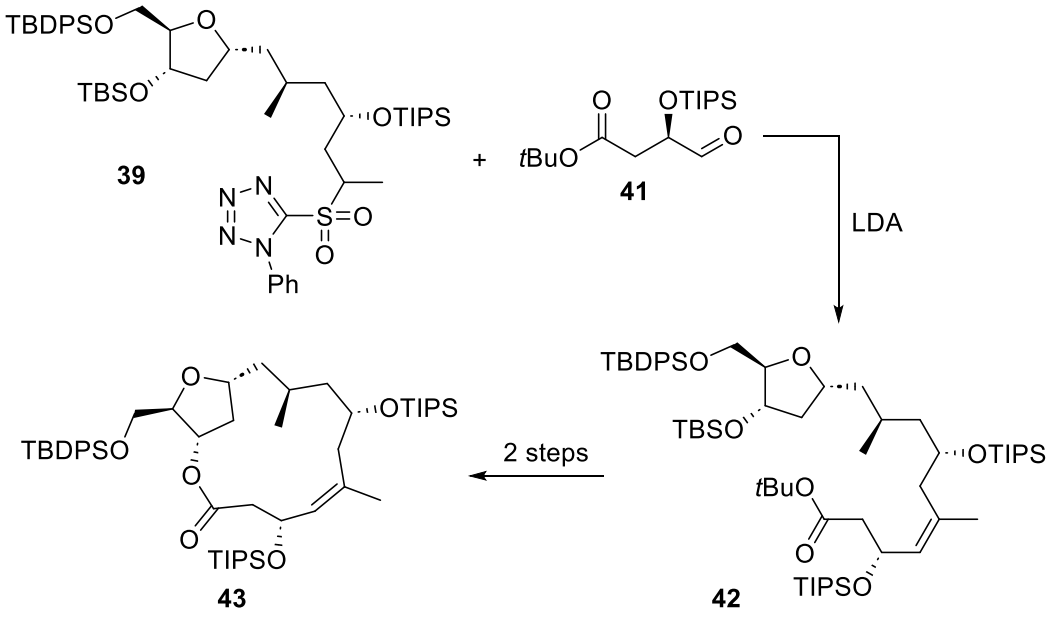

Scheme 1.7. Julia Coupling and Macrolactonization to Form the Protected Macrocycle of Phormidolides B and C.

To confirm the stereochemical assignment of the THF ring, stereoisomers of macrocycle **43** were synthesized (**Scheme 1.8**) that are diastereomeric in the THF ring. Sulfone **44** was synthesized in 16 steps, using an analogous methodology as described above, starting with 2-deoxy-L-ribose. A *tert*-butyl tetrazole substitution was used on the sulfone instead of a phenyl substitution to obtain higher *Z*-selectivity[60] and a trimethylsilyl (TMS) protecting group was used at the C13 position instead of a TBS group for more facile deprotection. Coupling **44** to aldehyde **41** afforded the macrocyclic precursor **45** with high diastereoselectivity (97:3) and subsequent selective hydrolysis and Yamaguchi macrolactonization[44] afforded a mixture of two C13 diastereomers, macrocycles **46** and **47**. Comparison of NMR spectroscopic data derived from the three macrocycles **43**, **46**,

and **47** with that derived from the NPs suggested that the NP possessed the stereochemistry consistent with macrocycle **43**, which supported the original proposal by the Álvarez group depicted in **Figure 1.3**.[53]

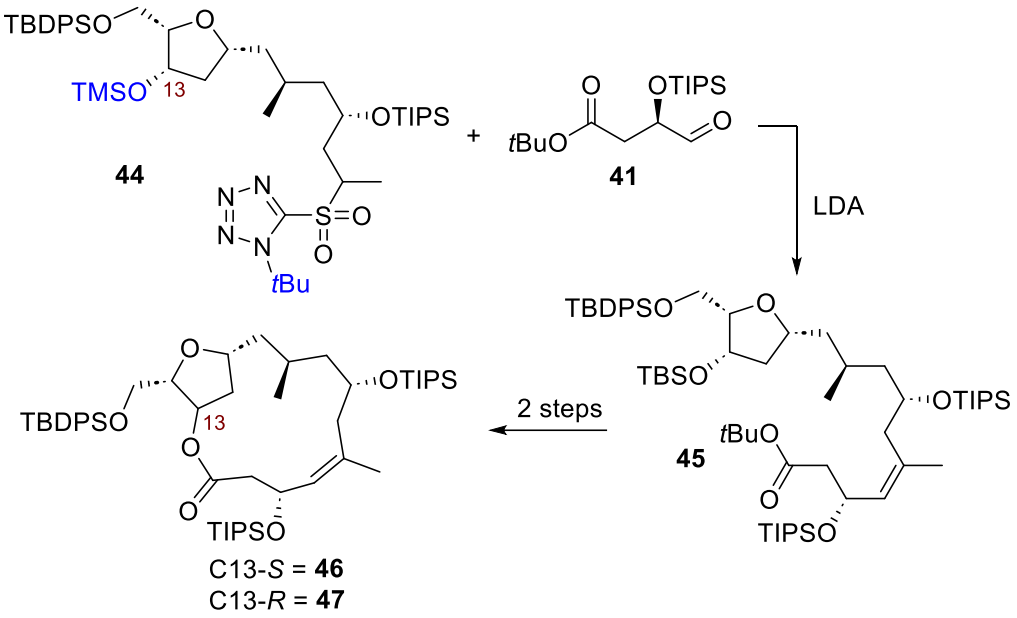

Scheme 1.8. Preparation of 46 and 47 for Spectral Comparison.

Later that same year, the Álvarez group reported a second-generation synthesis of the macrocycle using a stereoselective allylsilane 1,2-addition.[58] Analogous to the first-generation synthesis, the THF **48** was synthesized from 2-deoxy-D-ribose (**36**) in 7 steps. Aldehyde **48** was then elaborated to the key coupling partner **49** in 4 additional steps. To synthesize the second coupling partner, previously prepared **41** was transformed into alcohol **50** *via* a Wittig reaction to form the alkene and introduce a terminal ester followed by ester reduction to form the aldehyde. Xanthate formation and rearrangement afforded **51**. Radical reaction with Bu_3SnH[61] formed allyl silane **52** as a mixture of Z/E isomers in a 7:3 ratio (**Scheme 1.9**).[58]

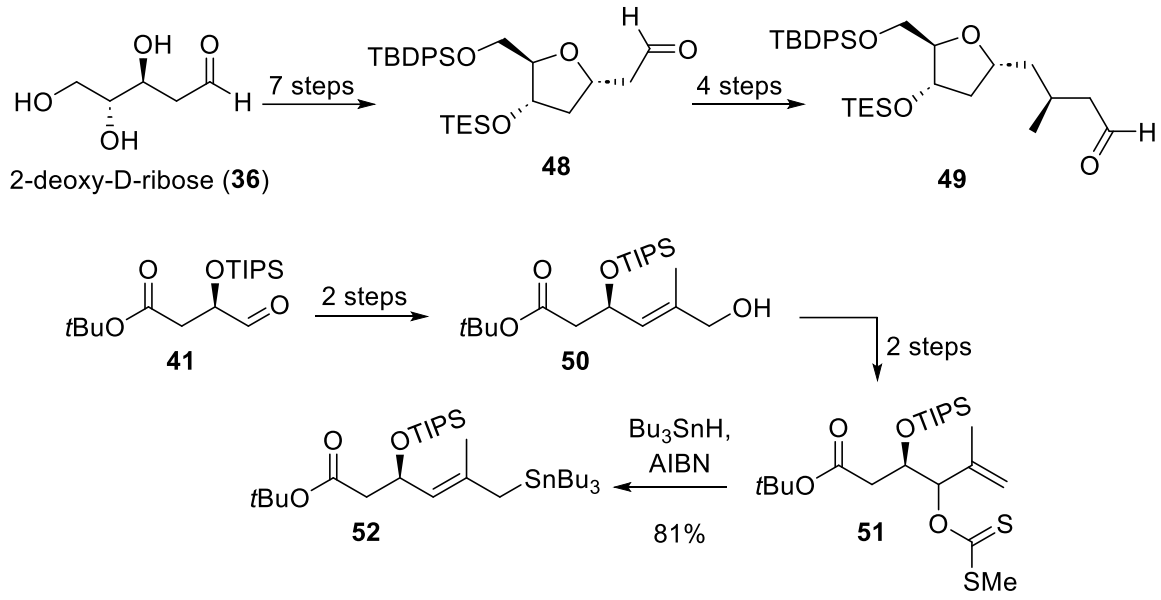

Scheme 1.9. Synthesis of Aldehyde 49 and Allyl Stannane 52 for the Second-Generation Synthesis of the Macrocycle of Phormidolides B and C.

Compounds **49** and **52** were then coupled through a $SnCl_4$-mediated process (**Scheme 1.10**).[61] This allyl stannane addition not only afforded **53** with the desired stereochemistry at the secondary alcohol center but was also selective for the formation of the desired Z-alkene. With the carbon skeleton of the macrocycle in hand, **53** was deprotected and subjected to Shiina macrocyclization conditions, affording macrocycle **54** in 67% yield. Deprotection of **54** afforded the macrocycle for spectral comparison with the NP, which supported the original stereochemical assignment of the macrocycle. When the deprotected macrocycle was tested in the same assays as the phormidolides B and C, it showed no activity, highlighting the importance of the side chain and/or fatty acid function for the observed biological activity.[58]

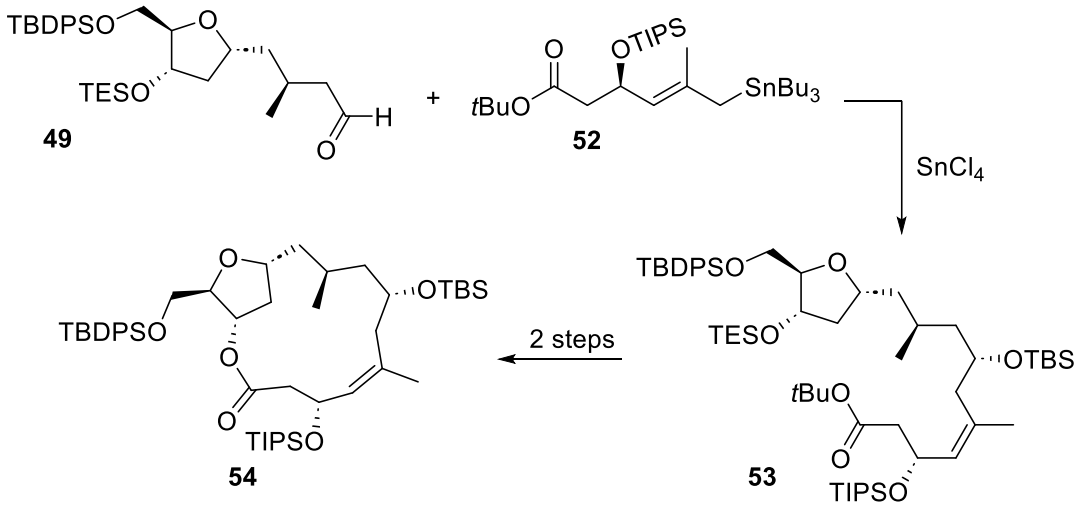

Scheme 1.10. Completion of the Second-Generation Synthesis of the Phormidolide B and C Macrocycle.

1.3.2. Phormidolide A

Phormidolide A (**28**, **Figure 1.4**) was reported in 2002 by the Gerwick group and was isolated from a marine cyanobacteria originally identified as *Phormidium sp*. based on the filament morphology of the bacteria. The producing organism was later corrected to be a *Leptolyngbya sp*. following RNA analysis.[52,62] Phormidolide A was isolated following bioassay-guided fractionation, based on inhibition of the Ras-Raf protein interaction, which is of interest as a target pathway for anti-cancer therapeutics. While phormidolide A was found to be the major secondary metabolite present in bioactive fractions, the activity was ultimately linked to a minor chlorophyll-type contaminant. Phormidolide A itself was found to be toxic towards brine shrimp, with an LC_{50} = 1.5 μM but inactive towards cancer cells.[52]

The planar structure of phormidolide A was assigned using 1D and 2D NMR spectroscopic methods as well as mass spectrometry, ultraviolet-visible (UV) spectroscopy, and infrared (IR) spectroscopy. Key to this analysis was the preparation of a ^{13}C-enriched sample of phormidolide A, which was prepared by culturing the marine cyanobacteria with [1,2-$^{13}C_2$]acetate. With ^{13}C-enriched phormidolide, correlations between adjacent carbons were observable and necessary to confidently assign connections between fragments of the NP using an ACCORD-ADEQUATE pulse program.[52,63]

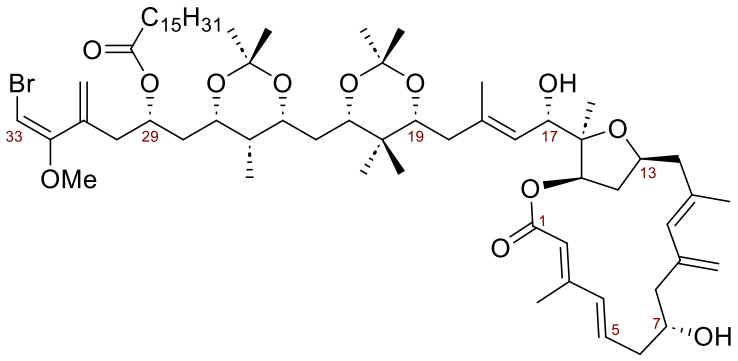

phormidolide A bisacetonide derivative (**55**)

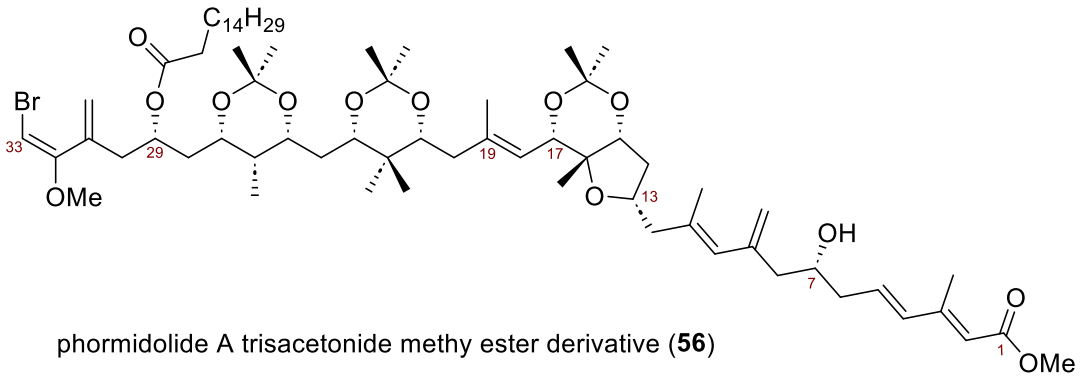

phormidolide A trisacetonide methy ester derivative (**56**)

Figure 1.6. The prepared acetonide derivatives of phormidolide A for stereochemical and structural analysis.

The relative stereochemistry of phormidolide A was assigned using nuclear Overhauser effect (NOE) information from GROESY analysis as well as employing Rychnovsky's method[64] to analyse a bisacetonide derivative of the NP, **55** (**Figure 1.6**). In addition, Murata's *J*-based configuration analysis was used to assign relative stereochemistry within stereoclusters using both homonuclear (H-H) and heteronuclear (C-H) coupling constants.[65] In *J*-based configurational analysis, each coupling constant of a two-centre system is categorized as small or large depending on its magnitude, providing a 'barcode' which represents a specific relative stereochemistry.[65] Finally, the absolute stereochemistry at the C7 alcohol in the macrocycle was determined via variable temperature analysis of the methoxyphenylacetic ester derivative of **55**. Notably, this analysis enables the assignment of absolute stereochemistry with a single Mosher's ester derivative, thus reducing the amount of NP required.[66,67] Based on this collection of data, the structure of phormidolide A was proposed as shown in **Figure 1.4**.[52] In a later publication from the Gerwick group, a triacetonide methyl ester derivative of phormidolide

A, **56** (**Figure 1.6**), was prepared from the NP. A standard Mosher's ester analysis was performed, using both the *R*- and *S*-Mosher's ester derivatives of **56** at the C7 position. Based on the data from this analysis, the group confirmed their original assignment.[62]

The Gerwick group were also able to determine the biosynthetic pathway for phormidolide A. Here, isotope feeding revealed that most of the NP was derived from acetate and *S*-methionine starting units and there was one 3-carbon unit for which the precursors could not be determined. Genome sequencing and bioinformatic analysis allowed for the characterization of the gene cluster that codes for the enzymes involved in the synthesis of phormidolide A as a *trans*-acyltransferase biosynthetic pathway. Furthermore, it was found that the NP is assembled by four polyketide-synthase (PKS) megaunits that extend the chain from a 3-carbon starter unit by the repeated addition of acetyl-CoA. Certain enzymes were also found that add specific functionalities to the NP, such as a halogenase to introduce the bromine atom. From this study, it was predicted that the unassigned 3-carbon precursor is a 1,3-bisphosphoglycerate unit, produced by the bacteria. This analysis allowed the isolation group to propose a biosynthetic pathway where the macrocycle is formed *via* transesterification, which releases the macrocycle from the PKS. Post-release, the fatty acid palmitic acid is transferred onto the NP which is then halogenated to produce the final phormidolide A. This biosynthetic proposal was consistent with the original structural assignment of phormidolide A.[62]

1.4. The Approach to Stereochemically-Rich THFs

With the varied biological activities of THF-containing NPs, the Britton group has invested considerable efforts in developing robust methodologies to access stereochemically rich THFs. Typically, the starting materials are simple, commercially available, or easily prepared, aldehydes and ketones. This particularly practical approach to THFs relies on proline catalysis, an easily accessible inexpensive amino acid available in either enantiomeric form.

The formation of these THF rings involves a robust 3-step sequence which begins with a one-pot tandem α-halogenation aldol reaction which proceeds through a dynamic kinetic resolution and results in a product with 3 new stereocentres and >99% e.e.[68] Shown for the formation of an example chlorohydrin in **Scheme 1.11**, the first step in this process is an L-proline catalyzed α-chlorination of aldehyde **57**, affording **58a** and **58b**.

Notably, L-proline also catalyzes the racemization of the chloroaldehydes. The next step is an L-proline catalyzed aldol reaction with ketone **59**, which first undergoes condensation with L-proline to form an imine, followed by imine-enamine tautomerism. The nucleophilic enamine then reacts with the chloroaldehydes to provide the aldol products **60a** and **60b**. Critically, the racemization of the chloroaldehyde is significantly faster than the subsequent aldol reaction, which proceeds via **TS-1** or **TS-2** to form the *syn*- or *anti*-chlorohydrin respectively. In general, the major product of this process is aldol **60a**, the *syn*-chlorohydrin. The lower energy of **TS-1** is rationalized by the avoidance of destabilizing electrostatic interactions between the halogen and oxygen atoms present in **TS-2**.[68,69] This process affords aldol products with 3 new stereocenters and high enantioselectivity.

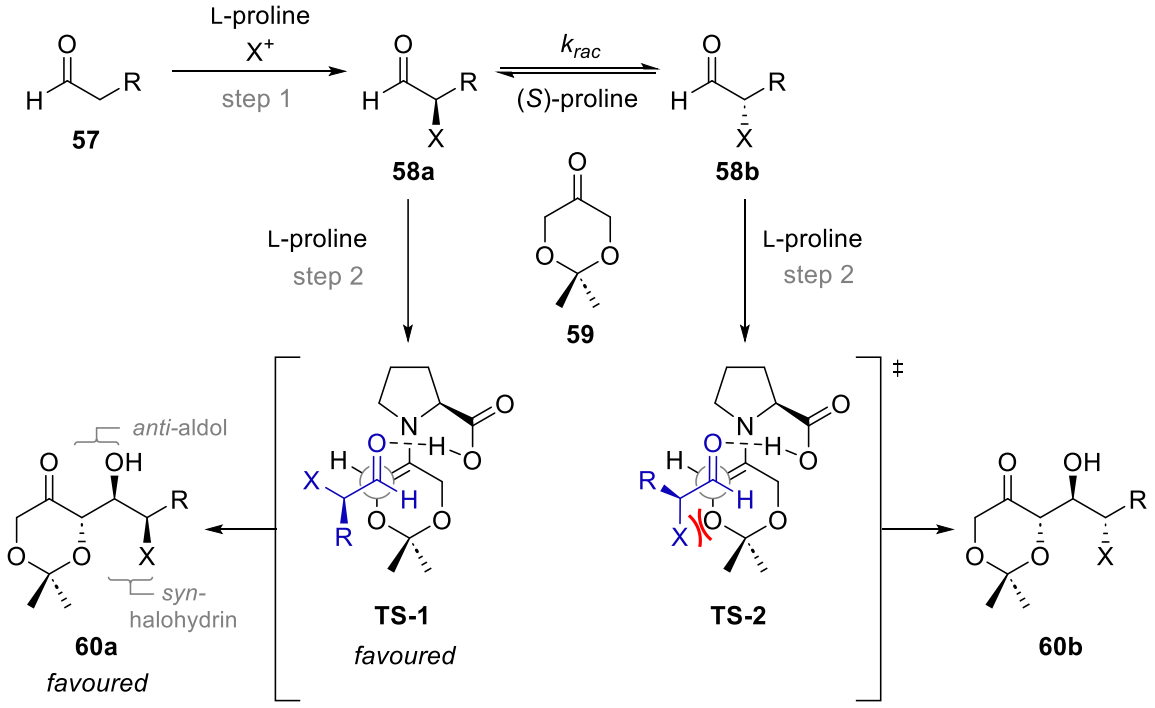

Scheme 1.11. Mechanism of the α-chlorination Aldol Reaction.

There are several options for controlling the stereochemical outcome of the α-halogenation aldol reaction, depending on the desired product. The first is the choice of L- or D-proline to control which enantiomer is formed in the reaction. Additionally, while in most solvents the syn-chlorohydrin is the major product, acetonitrile can be used to give a ~1:1 diastereomeric ratio of the *syn*- to *anti*-chlorohydrin, allowing for easier access to the minor diastereomer.[68]

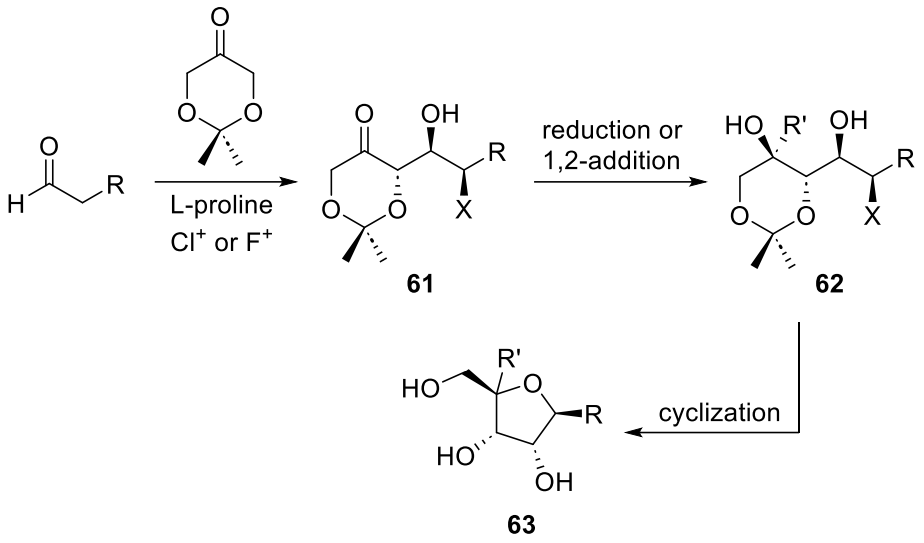

Scheme 1.12. Preparation of Stereochemically Rich THF Rings pioneered by Britton and co-workers.

Stereochemically rich THFs can be accessed in two more steps from the halohydrin product **61** (**Scheme 1.12**). Reduction of, or 1,2-addition to the ketone affords a diol product **62**. Following this, cyclization under heating, basic conditions, or Lewis acidic conditions forms the THF rings **63**.[68–70] The ability to form a stereochemically rich product in 3 steps from simple starting materials and to have a degree of control over the stereochemical outcome of each position in the THF ring during this process allows for a wide range of valuable materials to be produced using this methodology. Consequently, it has been expanded upon and used in the synthesis of NPs,[23,71] nucleoside analogues,[70,72] medicinally relevant iminosugars,[73,74] and carbohydrate analogues.[69,75–77]

1.4.1. α-Chlorination Aldol Methodology in Total Synthesis

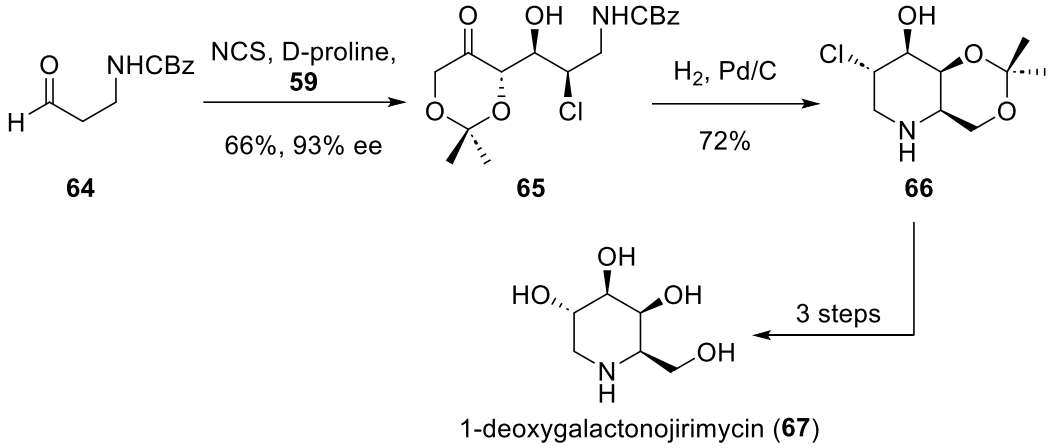

Scheme 1.13. The α-chlorination Aldol Reaction Used in the Total Synthesis of 1-deoxygalactonojirimycin.

As depicted in **Scheme 1.13**, the α-chlorination aldol methodology was used in the total synthesis of 1-deoxygalactonojirimycin (**67**). Here, an NCS/D-proline catalyzed reaction between aldehyde **64** and ketone **59** afforded aldol **65** in 66% yield with 93% ee. The material then underwent a one-pot cyclization/reductive amination when treated with H_2, catalyzed by palladium on carbon to afford **65**. The resulting chloropiperidine **65** was elaborated to the NP **67** in 3 steps.[71]

Our lab's recent formal synthesis of eribulin also involved the use of this methodology to construct two different THF moieties (**Scheme 1.14**). Here, aldehyde **68** was prepared in 5 steps while aldehyde **69** was prepared in 2 steps from commercial starting materials. Both were subjected to the D-proline catalyzed tandem α-chlorination aldol reaction with ketone **70** to afford aldols **71** and **72,** respectively. These products could be produced on a multi-gram scale which was critical in demonstrating a practical route for generating eribulin. Aldols **71** and **72** could then be reduced and cyclized using $SrCO_3$ to afford THFs **73** and **74,** respectively, which included synthetic handles for a key Corey-Chaykovsky reaction and provided the framework for THF parts of the target intermediates.[23]

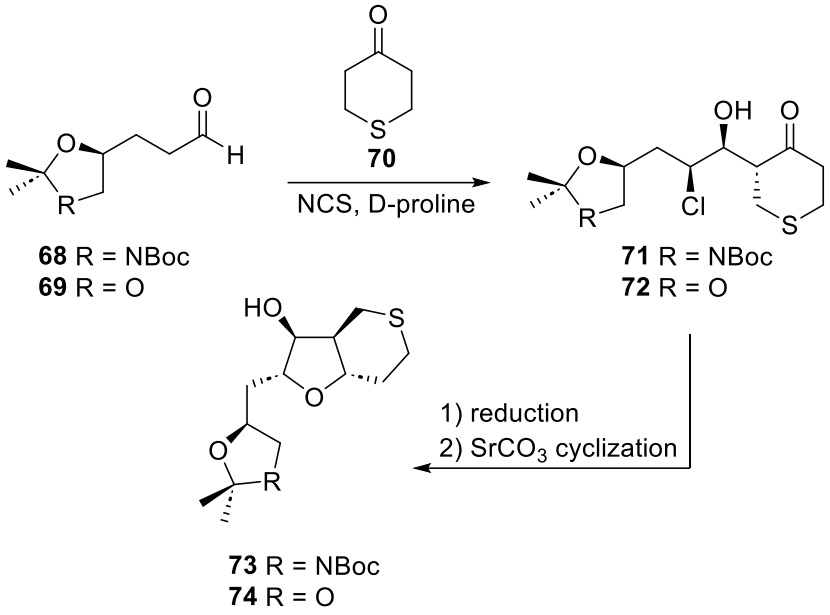

68 R = NBoc
69 R = O

71 R = NBoc
72 R = O

73 R = NBoc
74 R = O

Scheme 1.14. The α-chlorination Aldol Reaction Used in the Formal Synthesis of Eribulin.

Based on uncertainties regarding the stereochemistry of phormidolide A, the potentially useful bioactivity, and our group's interest in the THF-containing macrolides, we were interested in probing whether our methods would prove useful for accessing this NP. Therefore, we set out to develop a total synthesis of phormidolide A, using this methodology as the critical step to form the THF ring. Upon commencing the total synthesis of phormidolide A, we sought to first assess the previous stereochemical assignment of the NP.

Chapter 2 will detail the assessment of the phormidolide A stereochemical proposal, and, based on conclusions from this assessment, the proposed stereochemical reassignment of phormidolide A. This stereochemical reassignment gives a new target structure for the total synthesis of phormidolide A and Chapters 3 to 5 detail the efforts towards the total synthesis of this NP. Chapter 3 covers the variety of macrocyclization strategies explored to form the macrocycle of phormidolide A, culminating in a successful macrolactonization. Chapter 4 covers the efforts towards linking the side chain to the macrocycle while Chapter 5 outlines proposed alternative strategies for the completion of the total synthesis of phormidolide A. Finally, Chapter 6 covers a separate topic, the use of an observed halide effect in Grignard reactions for the synthesis of C4'-modified nucleoside analogues and the computational investigation of this halide effect.

Chapter 2. Stereochemical Reassignment of Phormidolide A

2.1. Stereochemical Reassignment of Natural Products by Chemical Synthesis

Structural assignment is a key component of natural product (NP) research. Historically, structural determination involved the chemical degradation of NPs to known and well-characterized small molecule fragments. Challenging and tedious, this process often required significant quantities of the NP and time. Despite these limitations, countless NP structures have been elucidated using this process, including cholesterol (**75**), quinine (**76**), and haemin (**77**).[31] Presently, advances in analytical techniques have streamlined the structure determination process, allowing for NPs to be characterized with only microgram quantities.[78] However, even with modern tools, misassignment of NP structures still occurs with some frequency.[32,78,79]

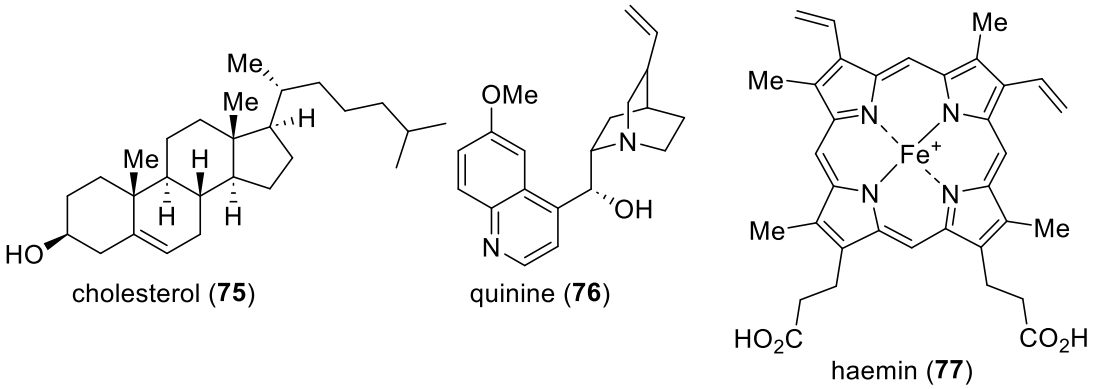

Figure 2.1. Examples of chemical structures elucidated using chemical synthesis.

In 2011, Suyama, Gerwick, and McPhail outlined the structural misassignments of all NPs reported between 2005 to 2010. They found that misassignments resulting from errors in NOE analysis were the most common type of structural misassignment, with 22% of misassignments coming from these errors (11% arose from HMBC-based misassignments and 7% arose from errors in *J*-based analysis). The frequency of NOE-based misassignments suggests that stereochemical assignments are among the more challenging aspects of structural elucidation.[32] The authors also found that structural reassignments of these NPs most commonly resulted from total or partial synthesis, with

48% of all structural reassignments being made based on comparison with synthetic data. Thus, synthesis continues to play a key role in the structural assignment of NPs.[31,32]

2.2. Ambiguities in the Stereochemical Assignment of Phormidolide A

A

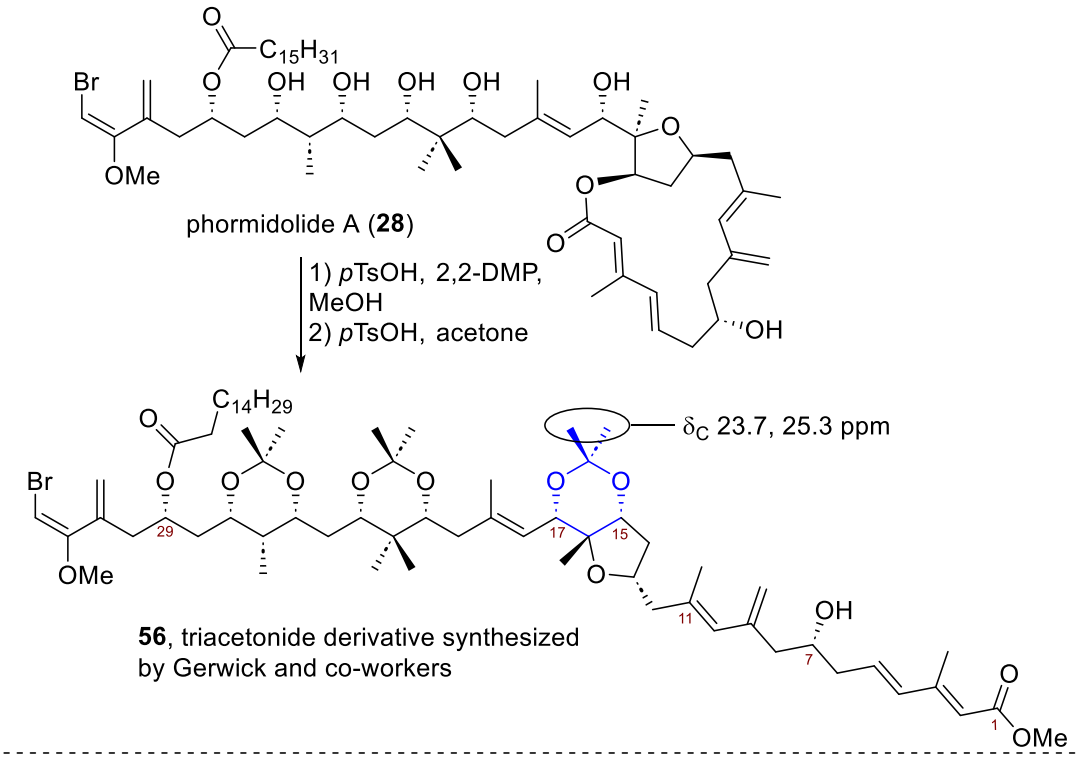

B Partial ^{1}H NMR chemical shift comparison of the *S*- and *R*-Mosher's ester derivative of **56**

Position	δH *S*-Mosher's Ester (ppm)	δH *R*-Mosher's Ester (ppm)	Δ δ^{S-R}
H2	5.71	5.72	-0.01
H4	6.17	6.19	-0.02
H5	6.17	6.18	-0.01
H6	2.38	2.43	-0.05
H6	2.34	2.36	-0.02
H8	2.28	2.24	+0.04
H8	2.25	2.21	+0.04
H10	5.73	5.71	+0.02
H12	2.55	2.42	+0.13
H12	2.43	2.40	+0.03
H13	3.97	3.96	+0.01

C2-C12 *S*-Mosher's ester derivative

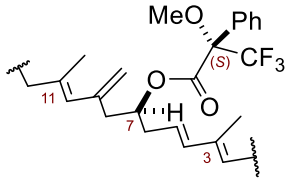

C2-C12 *R*-Mosher's ester derivative

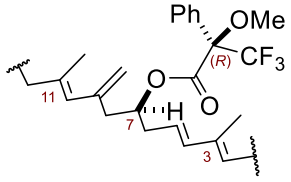

Figure 2.2. A: The ^{13}CNMR spectroscopic chemical shifts of the 17,15-acetonide methyl groups of the phormidolide A triacetonide derivative 56 B: The Mosher's ester analysis of the triacetonide derivative 56.

Our group was interested in pursuing a total synthesis of phormidolide A. While there is significant spectroscopic data to support the planar structural assignment of phormidolide A, several issues became evident upon close inspection of the published spectroscopic data. First, analysis of the *R*- and *S*- Mosher's ester derivatives of **56** (**Figure 2.2A**) at the C7-alcohol suggested that the stereochemical assignment should be *S,* not *R* (shown in **Figure 2.2B** with representative Mosher's ester derivatives).[56,67]

In addition to concerns regarding the stereochemistry at C7, a close examination of the ^{13}C NMR spectroscopic data recorded on the triacetonide derivative **56** revealed that the methyl carbons of the C15,C17 acetonide resonate at 23.7 and 25.3 ppm (**Figure 2.2A**). Based on Rychnovsky's acetonide analysis,[64] this data suggests that the C15 and C17 alcohols have a 1,3-*anti* configuration rather than the proposed 1,3-*syn*-configuration.

Finally, the biosynthetic analysis raised additional questions. Here, the Gerwick group carefully characterized the ketoreductases in the biosynthetic pathway, which are the enzymes responsible for the stereospecific reduction of ketone functions. In the original disclosure, the carbinol groups at positions C7, C17, C21, C23, C25, C27, and C29 (the macrocyclic alcohol and side chain alcohols) were L-configured. However, the ketoreductases responsible for setting the stereochemistry at each of these positions are predicted to form D-configured alcohols, due on the presence of an aspartate residue at position D1758 in each ketoreductase. This aspartate residue is typically a predictor for the formation of D-configured alcohols.[62] Therefore, this biosynthetic data suggests that the alcohols at these positions are actually D-configured and the original stereochemical assignment was incorrect.[62] Based on these uncertainties, we developed a strategy to assess the stereochemical proposal before the completion of the total synthesis through spectral comparison with fragments of the NP.

2.3. Synthesis of the THF moiety

The work contained in this subchapter was performed in collaboration with Dr. Venugopal Rao Challa. Dr. Challa and the author were jointly responsible for the development of the synthesis of compounds 78-85.

To assess the stereochemical proposal for phormidolide A (**28**, **Figure 2.2**), we aimed to construct fragments containing the characteristic tetrahydrofuran (THF) core of

this NP. Therefore, we first envisioned constructing THF **89** (**Scheme 2.1**). THF **89** contains a vinyl iodide functional group and differentially protected alcohols and therefore could not only serve as a fragment for stereochemical reassignment studies, but also as a key intermediate in the synthesis of phormidolide A.

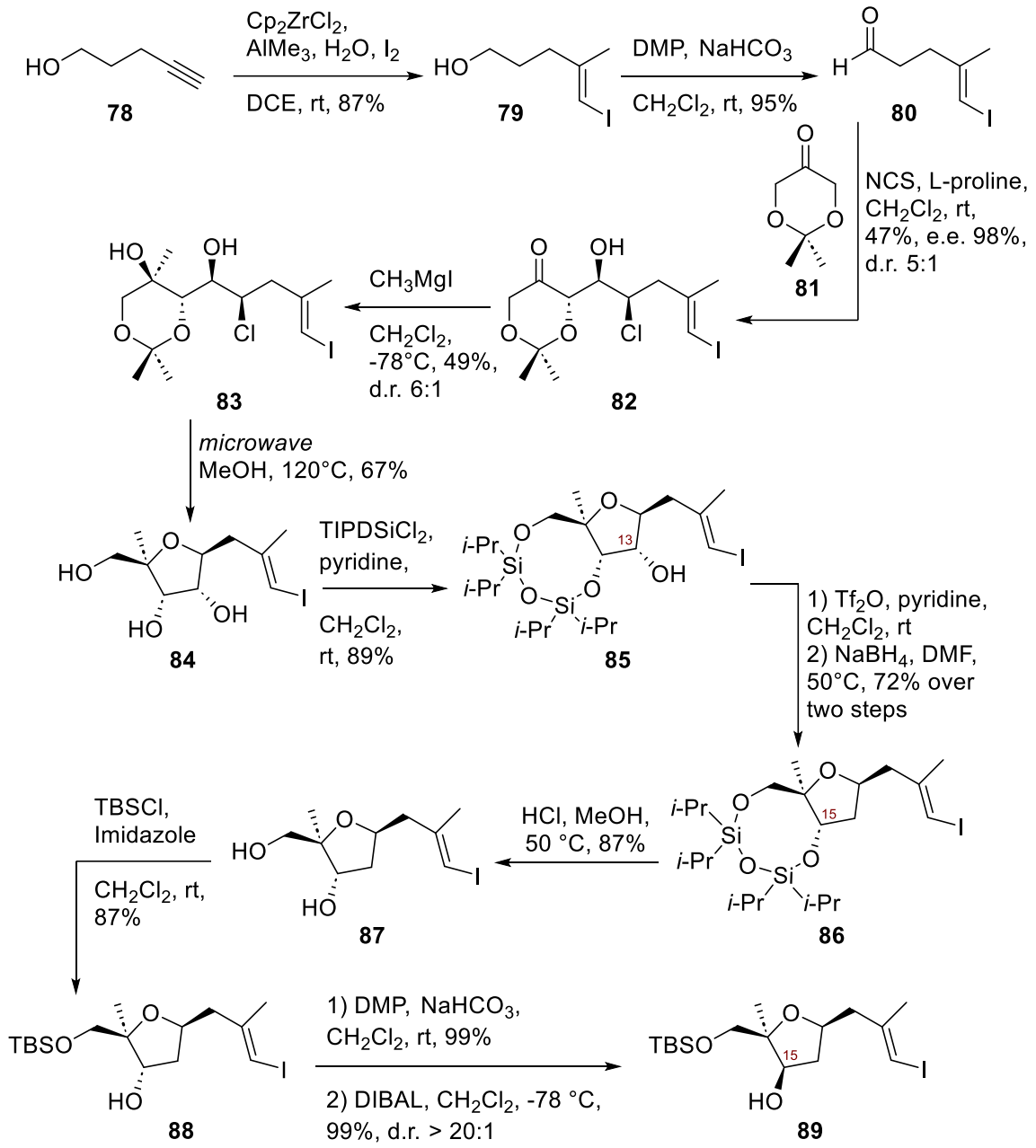

Scheme 2.1. Synthesis of the THF Moiety 89.

The synthesis of the THF moiety (**Scheme 2.1**) relied on a tandem α-chlorination aldol reaction developed in our lab.[68] Toward this goal, preparation of aldehyde **80**

commenced with a Negishi carboalumination reaction of 4-pentyn-1-ol (**78**) to afford vinyl iodide **79**, followed by DMP oxidation to provide aldehyde **80**. The L-proline catalysed tandem α-chlorination aldol reaction was executed using commercially available 2,2,-dimethyl-1,3-dioxan-5-one (**81**) to generate the chlorohydrin **82** as a separable mixture of diastereomers. Subsequent Grignard addition provided alcohol **83**. Mosher's ester derivatives (*R*)- and (*S*)-**90** were prepared and Mosher's ester analysis[67] was used to confirm the absolute stereochemistry of this compound (**Figure 2.3**). Cyclization and *in-situ* acetal deprotection under microwave conditions afforded triol **84**. This latter material was then protected as the cyclic disiloxane to afford THF **85**.

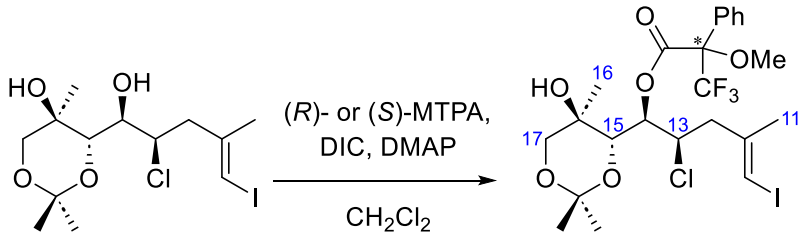

83 (*R*)- or (*S*)-**90**

Partial ^{1}H NMR chemical shift comparison of the (*S*)- and (*R*)-Mosher's ester derivative, **90**

Position	δH *S*-Mosher's Ester (ppm)	δH *R*-Mosher's Ester (ppm)	Δ δ^{S-R}
Me11	1.80	1.86	-0.06
H12	2.11	2.40	-0.29
H12	2.48	2.60	-0.12
H13	4.37	4.43	-0.06
H15	4.20	4.11	+0.09
Me16	1.29	1.14	+0.15
H17	3.70	3.60	+0.10
H17	3.45	3.34	+0.11

Figure 2.3. The preparation of Mosher's ester derivatives (R)- and (S)-90 and analysis of the resulting chemical shift differences.

At this stage, it was necessary to deoxygenate the C13 position. Our initial strategy to accomplish this task involved triflation of the secondary alcohol followed by reduction using tetrabutylammonium borohydride to afford **86**. However, while this reaction successfully afforded the deoxygenation product in 68% yield over two steps times, after several synthetic campaigns, protodeiodination began complicating the use of this strategy. After careful experimentation and examination of the compatibility of each

reagent with the vinyl iodide **85**, it was found that protodeiodination resulted from the reaction of the vinyl iodide with tetrabutylammonium borohydride. Unfortunately, despite much effort, we could not determine why this outcome was not observed in our original experiments. For example, the use of newly purchased tetrabutylammonium borohydride or purified (recrystallization) tetrabutylammonium borohydride did not prevent protodeiodination. Fortunately, a screen of alternative reducing agents revealed that sodium borohydride was also capable of reducing the triflate without protodeiodination. Careful optimization of the solvent revealed that the use of DMF at 50 °C allowed for effective reduction of the triflate to afford **86** in a 72% yield over two steps.

Recognising that the configuration at C15 required inversion, silyl deprotection and selective TBS protection of **87** afforded C17-protected THF **88**. At this stage, we were unable to affect Mitsunobu esterification.[80] Fortunately, oxidation of alcohol **88** and reduction afforded alcohol **89** as a single diastereomer. With the THF core of the macrocycle successfully synthesized, we began efforts to assess the phormidolide A stereochemical reassignment.

2.4. Phormidolide A Stereochemical Reassignment

2.4.1. Reassignment from Synthetic Models

Reproduced from Lam, N. Y. S.; Muir, G.; Challa, R.; Paterson, I.; Britton, R. Chem. Commun. 2019, 55, 9717–9720 with permission from the Royal Society of Chemistry:

*The work contained in this subchapter chapter was performed in collaboration with Dr. Nelson Lam. Dr. Lam was responsible for the preparation of compounds **97**, **100-107**, and the preparation of this manuscript. The author was responsible for the preparation of compound **89** as well as reviewing and editing this manuscript.*

As discussed in Chapter 1, Phormidolide A (**28**, **Figure 2.3**) is a complex polyketide isolated by the Gerwick group in 2002 from the marine cyanobacterium Leptolyngbya sp. collected off the coast of Sulawesi, Indonesia.[52,62] At the time of its isolation, the relative stereochemistry of phormidolide A was wholly determined through the application of Murata's *J*-based method,[65] taking into account NOE correlations, $^{2/3}J$ homo and heteronuclear coupling constants to ascertain the configuration of all 11 stereogenic centres. The relative stereochemistry of the all-*syn* polyol side chain was

corroborated through the preparation of the corresponding diacetonide, with the absolute configuration initially determined through a variable-temperature NMR spectroscopic experiment with a methoxyphenyl acetic acid derivative of the C7 alcohol,[52] and subsequently by the preparation and analysis of the two diastereomeric Mosher esters of a phormidolide A triacetonide derivative at the same position.[62] Through the synthesis of a series of model C10-C23 diacetonides and detailed NMR spectroscopic comparisons with the triacetonide derivative of phormidolide A, we herein report the stereochemical reassignment of phormidolide A from **28** to **91** (**Figure 2.4**).

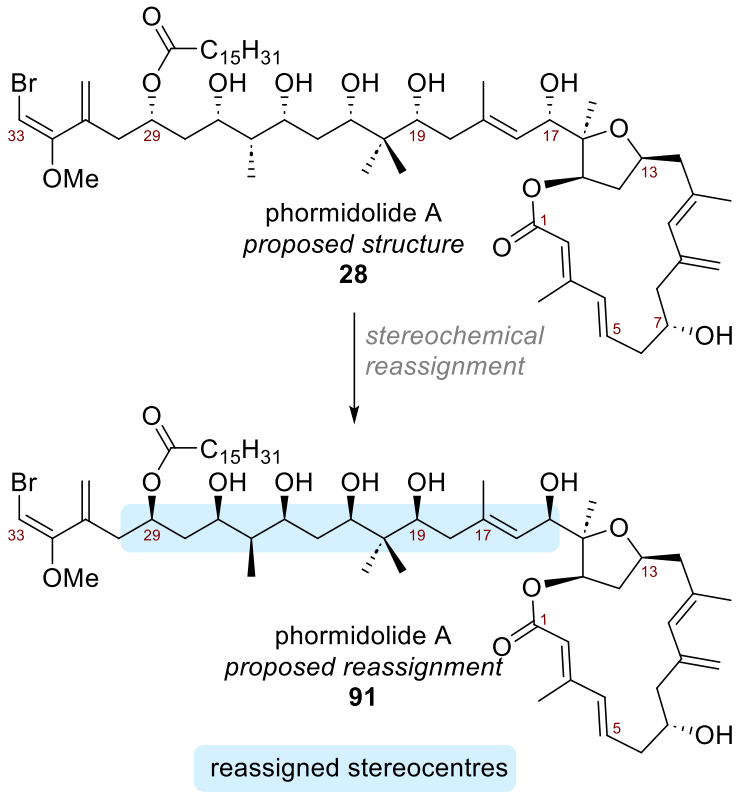

Figure 2.4. The proposed reassignment of Phormidolide A, 91.

Drawn to its gamut of structural features and unknown but potentially interesting biological activity, we sought to embark on a synthetic campaign towards phormidolide A. Noting that the side chain was a conserved structural feature across related congeners, we chose to disconnect across C17-C18 *via* a vinyl metal addition[81] to reveal the macrolactone C17 aldehyde and the C18-C33 side chain. We surmised that the reported 17*S* configuration could be set up via a chelation-controlled aldehyde addition with the nucleophile selectively approaching from the side of the small methyl substituent at C16.

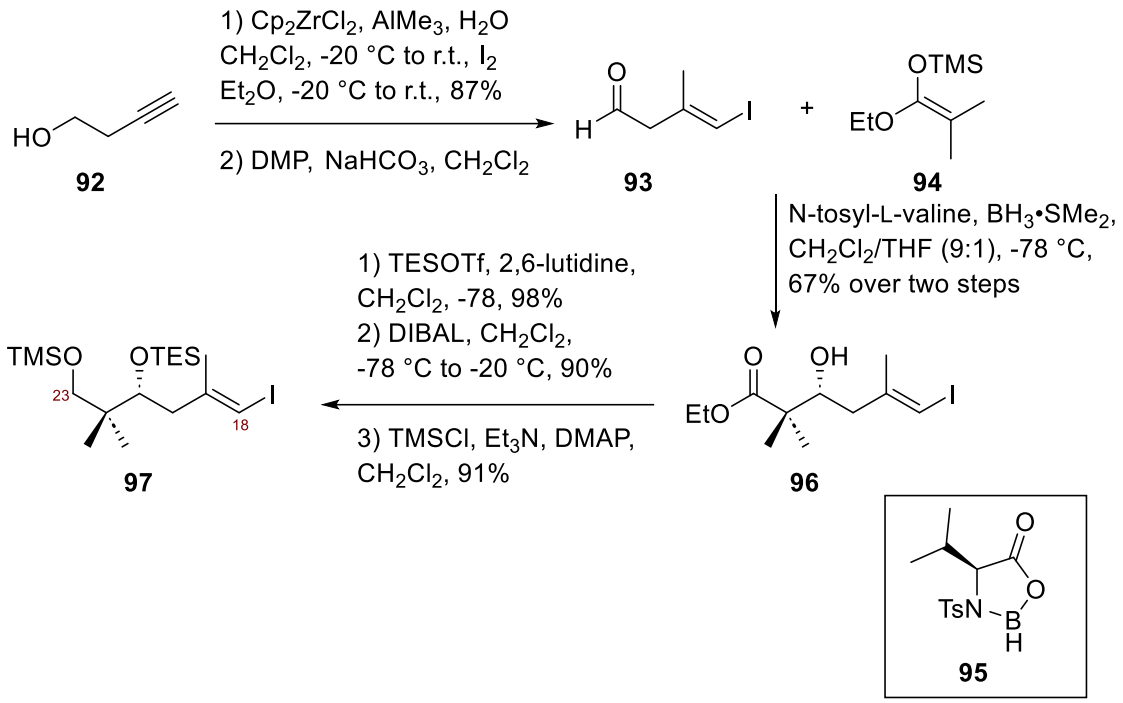

Scheme 2.2. Preparation of Vinyl Iodide 97.

To test this rationale, a facile route to the truncated C18–C23 vinyl iodide **97** was developed. Vinyl iodide **97** (**Scheme 2.2**) was obtained from a Negishi carbalumination[82] of 3-butyn-1-ol (**92**) followed by oxidation to afford the sensitive aldehyde **93**. An asymmetric Mukaiyama aldol reaction[83] with silyl ketene acetal **94** mediated by the chiral Lewis acid **95**[84] gave adduct **96** (91% e.e.). Subsequent TES ether formation, reduction (DIBAL) and TMS protection afforded the C18–C23 vinyl iodide **97** in six steps. The C10-C17 aldehyde **100** was prepared from THF **89** (**Scheme 2.3**). Noting that the NP contains an α,β-unsaturated ester motif at C15 and recognising that our model system required suitable functionalities to mirror the NP, we transformed alcohol **89** into the dimethylacrylate ester **99** (DCC, DMAP, DMAP•HCl).[85] Finally, desilylation of **99** followed by a Dess–Martin oxidation gave the C10–C17 aldehyde **100**.

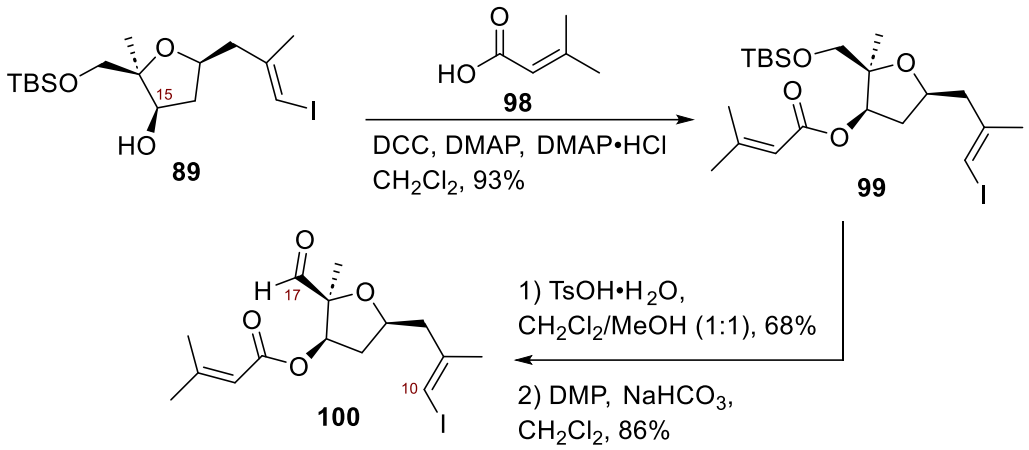

Scheme 2.3. Preparation of Aldehyde 100.

With both C18-C23 vinyl iodide **100** and C10-C17 aldehyde **97** in hand, we explored the planned vinyl metal addition using the in situ generated Grignard species (**Scheme 2.4**, Method A).[81] Encouragingly, we obtained a 5:1 mixture of alcohols, epimeric at C17 in 77% yield. To unambiguously ascertain the stereochemistry, and noting that the triacetonide derivative of phormidolide A, **56**, was known,[62] we transformed **101** into the corresponding diacetonide **103**. Unexpectedly, analysis of the ^{13}C chemical shifts and NOE enhancements from the diacetonide revealed that we had formed the 15,17-anti acetonide **103**, corresponding to the 17R configuration. Next, we conducted the vinyl lithium addition by omitting $MgBr_2 \cdot OEt_2$ (**Scheme 2.4**, Method B), expecting to favour the 17S adduct dictated by polar Felkin-Anh rather than chelation control.

The vinyl lithium addition indeed delivered the other epimer **102**, which yielded the diacetonide **104** corresponding to the originally proposed 17S configuration for phormidolide A (**Scheme 2.4**). Interestingly, the NMR spectroscopic data for 15,17-*syn* product, **104**, did not match that reported for the analogous region of triacetonide **56**. In particular, through Rychnovsky's acetonide analysis,[86] the ^{13}C NMR spectroscopic chemical shifts for the two acetonide methyl groups of **56** (25.3 and 23.7 ppm) appeared to us to be diagnostic for the 15,17-*anti* rather than the originally proposed 15,17-*syn* stereochemistry.

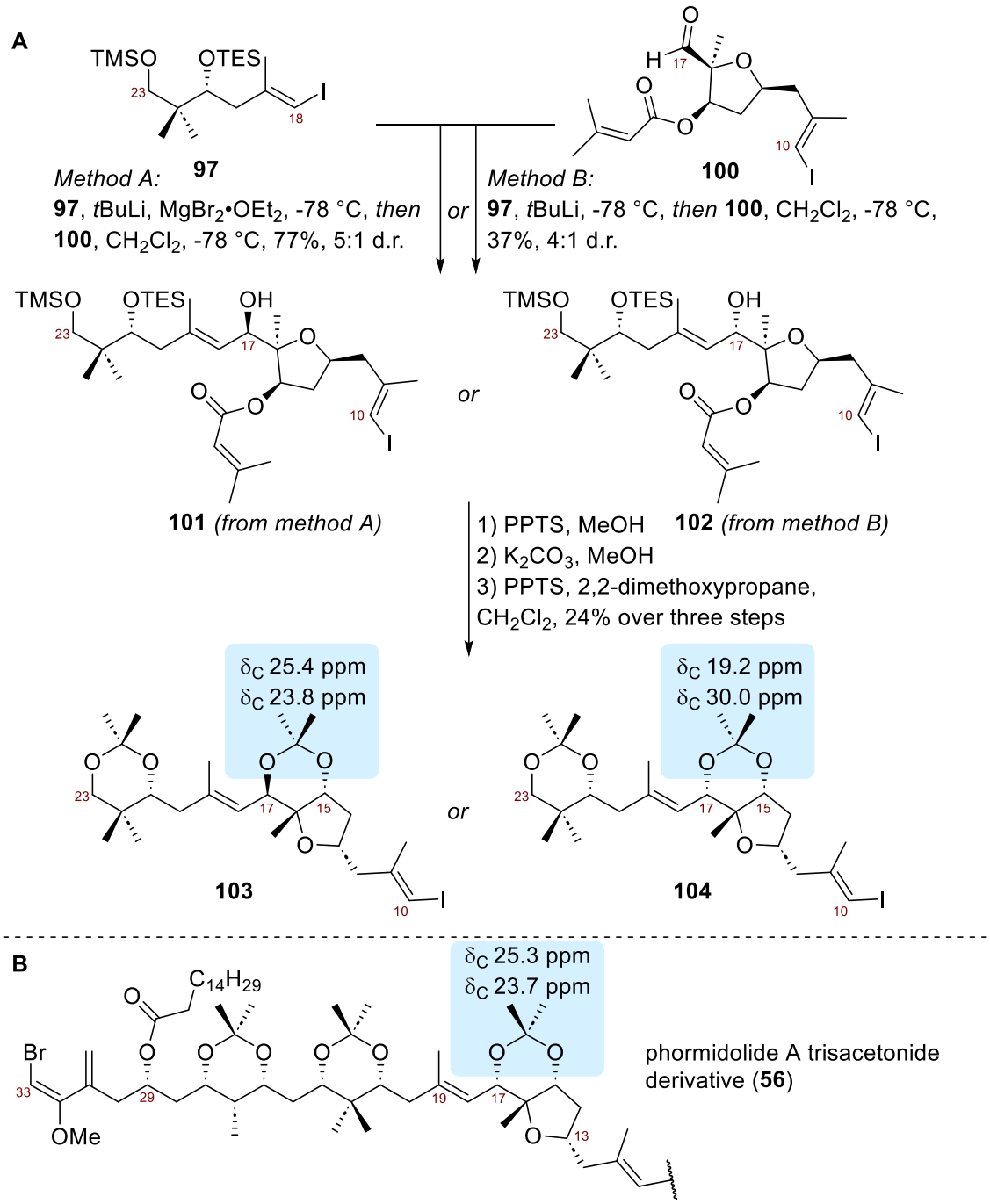

Scheme 2.4. A: Preparation of Models 103 and 104. B: Phormidolide A Trisacetonide Derivative 56.

At this juncture, it appeared that the configuration of one of the two stereocentres in the 15,17-acetonide in **56** was misassigned. Analysis of chemical shifts, NOE data and comparison between THF intermediates **88**, **89**, and **99**, and the NP supports the assigned configuration at C15, leaving C17 as the likely suspect stereocentre. A reanalysis of the

reported $^{3}J_{CH}$, $^{3}J_{HH}$ and NOE data for phormidolide A indeed provided evidence that the NP possessed the 17R configuration rather than the reported 17S configuration. This observation suggested that the Grignard nucleophile in the chelation-controlled addition preferentially approached the C17 carbonyl from the face opposite the C16 methyl group (**Figure 2.5**, TS1), indicating that it was exerting a disproportionately large steric influence over the preferred trajectory of the incoming nucleophile, so disfavouring TS2. Notably, this chelation structure may be more complex than what is depicted in **Figure 2.5**, with further chelation to the C15 ester being possible.[87]

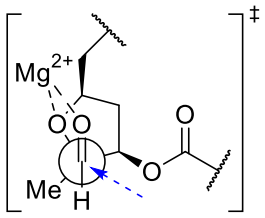

TS1
major transition state

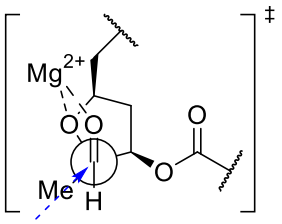

TS2
minor transition state

Figure 2.5. The transition state models for the vinyl metal addition to 100.

Following our reassignment of C17 to the *R* configuration, it was prudent to check whether or not C21 and the remainder of the side chain were configured correctly. In pursuit of this, the enantiomeric C18-C23 vinyl iodide **105** was prepared. A chelation-controlled vinyl Grignard addition gave predominantly the alcohol **106** (**Scheme 2.5**), and the corresponding diacetonide **107** was prepared.

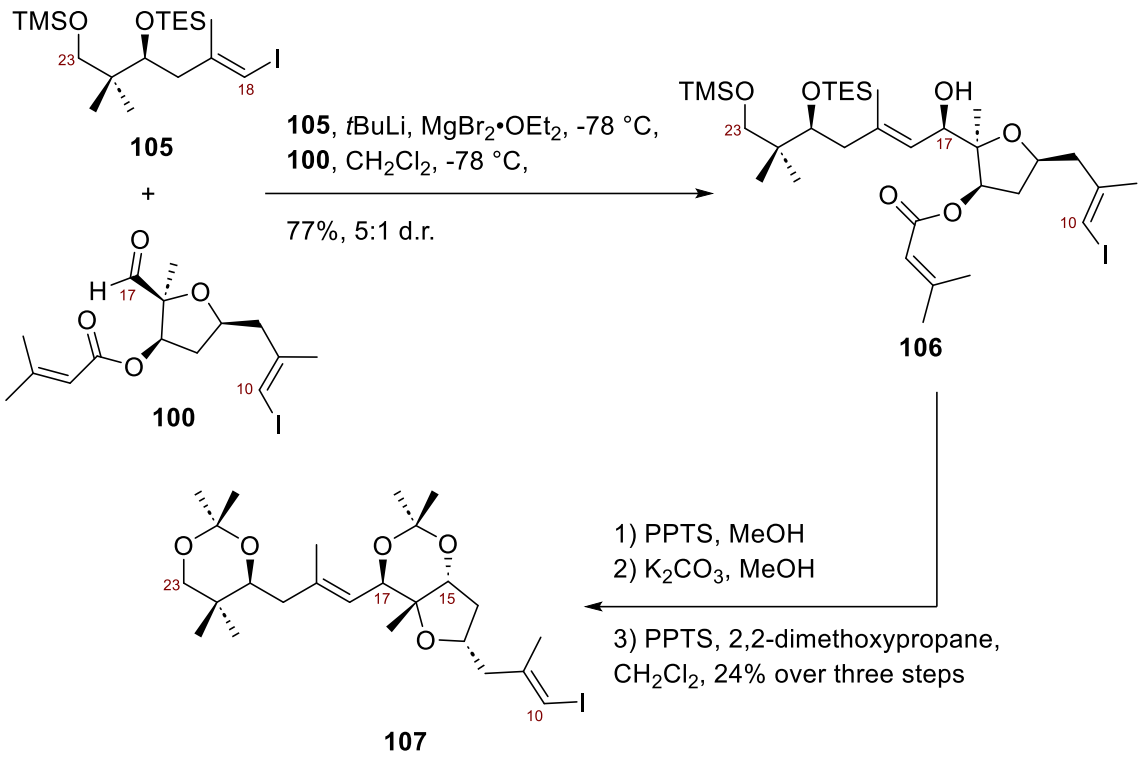

Scheme 2.5. Preparation of Model 107.

With the three diastereomeric diacetonides in hand, a thorough spectroscopic comparison to the phormidolide A triacetonide **56** was undertaken. Analysis of ^{1}H and ^{13}C NMR spectroscopic shifts revealed that the 21-*epi*-17,15-*anti* diacetonide **107** (**Table 2.1**, entry 1) matched the triacetonide derivative of the NP much better than the 17,15-*anti* diacetonide **103** (**Table 2.1**, entry 2 and **Scheme 2.4**). Notably, the 17,15-*syn* diacetonide **104** corresponding to the originally proposed (17*S*, 21*R*) configuration was the poorest match (**Table 2.1**, entry 3), even by excluding the signals attributed to the acetonide. As the relative configuration of the remainder of the side chain was relayed back to C21 *via* *J*-based methods,[52] and confirmed *via* the previously synthesised diacetonide derivatives of phormidolide A,[52,62] we propose that the configuration of **28** should be reassigned to 17*R*, 21*S*, 23*R*, 25*S*, 26*R*, 27*R* and 29*R*, as shown in **91** (**Figure 2.4**).

Table 2.1. Sum of Absolute Errors |Σ| (ppm) For Each Diastereomer Compared to the Reported Spectra of Phormidolide A Triacetonide 56

Entry	|Σ| for ^{1}H	Max error for ^{1}H	|Σ| for ^{13}C	Max error for ^{13}C
1. 21-*epi*-17,15-*anti* **107**	0.24	0.08	3.2	1.5
2. 17,15-*anti* **103**	0.32	0.11	8.2	2.7
3. 17,15-syn **104**	1.34	0.37	30.0	8.2

Subsequent to their isolation paper, the Gerwick group reported a detailed analysis of the biosynthesis of phormidolide A. Here, they noted that the ketoreductases responsible for setting carbinol configuration were inconsistent with the absolute stereochemistry proposed for the NP.[62] Specifically, it was noted that Type B-like ketoreductases present in the phormidolide A polyketide synthase system catalyse the formation of D-OHs in polyketide motifs.[88,89] However, the original isolation report presents all 10 carbinol stereocentres as L-configured. Our proposed reassignment of the six carbinol stereocenters as D-configured in **91** is also consistent with the stereochemistry predicted by analysis of the ketoreductase domain, which now gives a better rationalisation for the biosynthesis of phormidolide A.

In summary, an unexpected stereochemical outcome from a chelation-controlled vinyl Grignard addition of **97** into aldehyde **100** prompted a re-examination of the stereochemical assignment of phormidolide A. Subsequent NMR spectroscopic analyses of three diastereomeric diacetonides 17,15-*anti* **103**, 17,15-*syn* **104,** and 21-*epi*-17,15-*anti* **107** (**Figure 2.6**) revealed the relative configuration between C21, C17 and the macrolactone. Combining this with the previously reported analysis then resulted in the reassignment of seven of the 11 stereocentres, leading to the revised structure **91**. Importantly, this work validates the choice of suitable fragments as well as a key fragment union strategy for our ongoing total synthesis campaign directed at **91** and reaffirms the power of synthesis in its role in the unambiguous stereochemical elucidation of complex NPs.

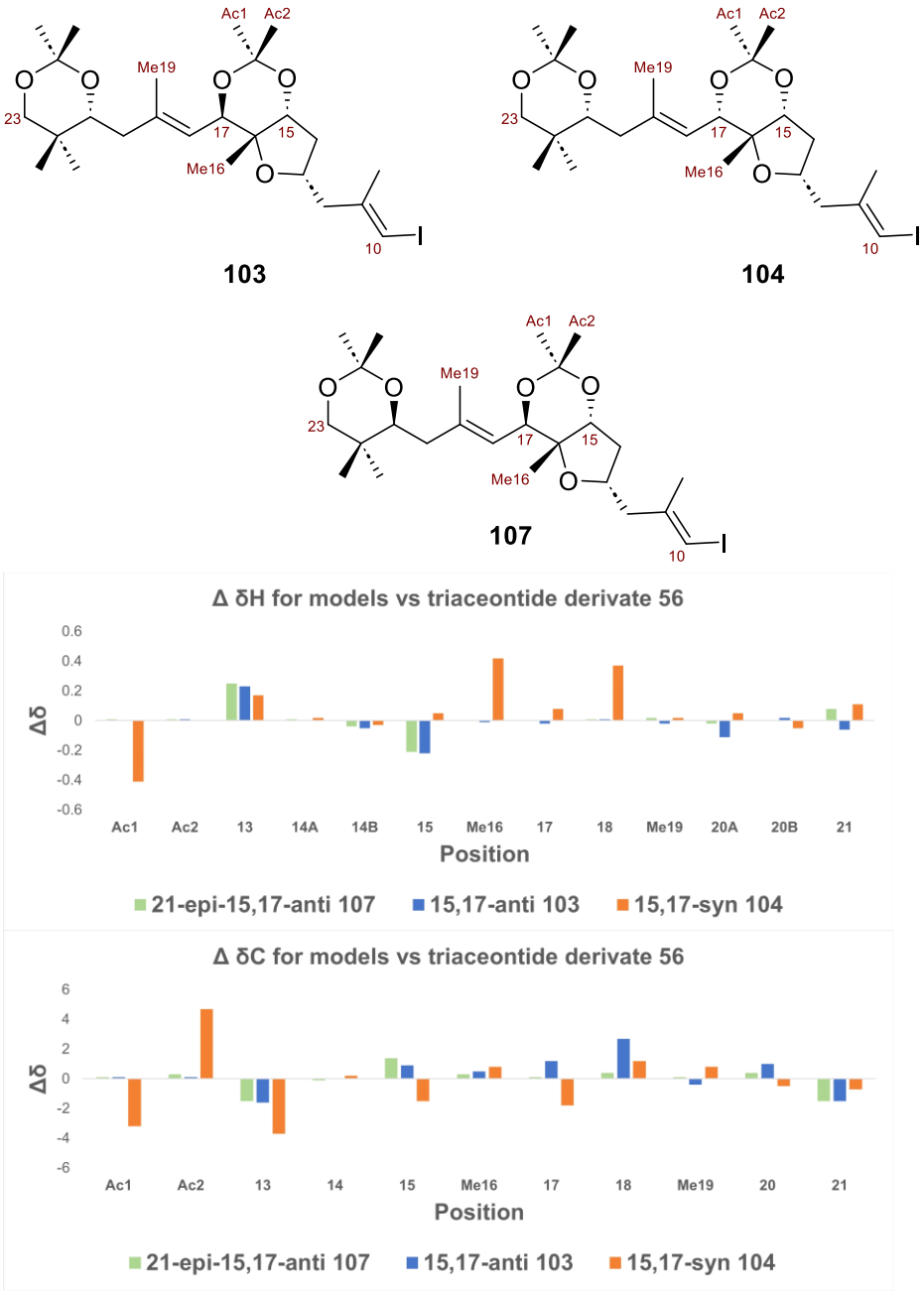

Figure 2.6. **The difference in proton chemical shifts and carbon chemical shifts of models 103, 104, and 107 *versus* the data for the natural product. Graphs are plotted as position *versus* difference in chemical shift.**

2.4.2. Stereochemical Reassignment of Phormidolide A Based On TransATor

Shortly after we published the stereochemical reassignment of phormidolide A based on comparison with model structures, Jörn Piel and co-workers published a

stereochemical reassignment proposal for phormidolide A based on results obtained from an automated structure prediction software they had developed, named TransATor. TransATor is a program that predicts the structure of polyketide NP products based on an organism's genome. This program is specific to *trans*-acyltransferase polyketide synthases (*trans*AT PKSs), which is one type of PKS that is responsible for polyketide NP synthesis.[56]

As highlighted in Chapter 1, PKSs are large, multi-enzyme complexes which contain a variety of enzymes to construct polyketide NPs. One key enzyme in this process is the acyltransferase (AT), which is responsible for transferring and loading the substrate onto the next suite of enzymes which can impart further modifications.[90] What distinguishes *trans*AT PKSs from their counterpart *cis*AT PKSs is that *trans*AT PKSs contain one AT that is distinct from the rest of the enzymatic cluster (or a small number of ATs compared to the rest of the enzymatic cluster) which is used at each point where that enzymatic function is required. *Cis*AT PKSs instead have a separate AT at each point where that enzymatic function is required.[90,91]

While NP structures constructed by *cis*AT PKSs can be fairly easily predicted, structural prediction from *trans*AT PKS is more challenging since they can have a much more diverse array of enzymes than *cis*AT PKSs.[56,90,92] However, the Piel group was able to correlate structural features in *trans*AT-type polyketide NPs with specific genome sequences and develop a database that could predict structural features of polyketide NPs synthesized from *trans*AT-type pathways based on the organism's whole genome. To make this process user-friendly, they developed the program TransATor which can automatically predict NP structures from PKS sequences.[56]

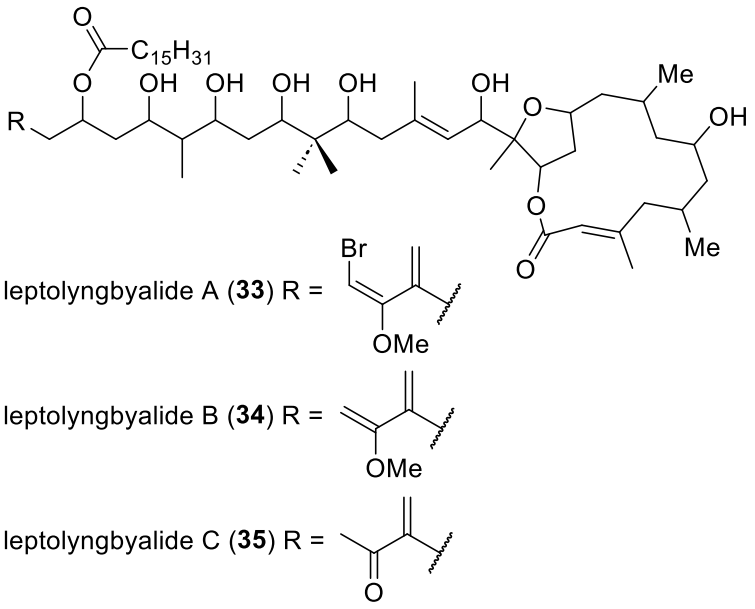

Figure 2.7. Leptolyngbyalides A, B, and C.

Using this program, the Piel group analyzed the genome of the bacterium from which phormidolide A was isolated, *Leptolyngbya* sp. PCC 7375.[52,62] The software predicted that the bacterium would produce several other NPs, similar to phormidolide A. An isolation campaign by the Piel group led to the isolation of leptolyngbyalides A-C (**33-35**, **Figure 2.7**). However, due to the limited amounts isolated, they could not determine the stereochemistry of these compounds. Instead, they elected to use TransATor to predict the stereochemistry of the leptolyngbyalides. They tested the accuracy of the software's stereochemical prediction against the proposed structure for phormidolide A to see if there was reasonable confidence and found that the software predicted the opposite stereochemistry for each position in phormidolide A. Noting that the Mosher's ester analysis had been interpreted incorrectly,[62,67] they proposed a stereochemical reassignment of phormidolide A to **108** shown in **Figure 2.8**.[56]

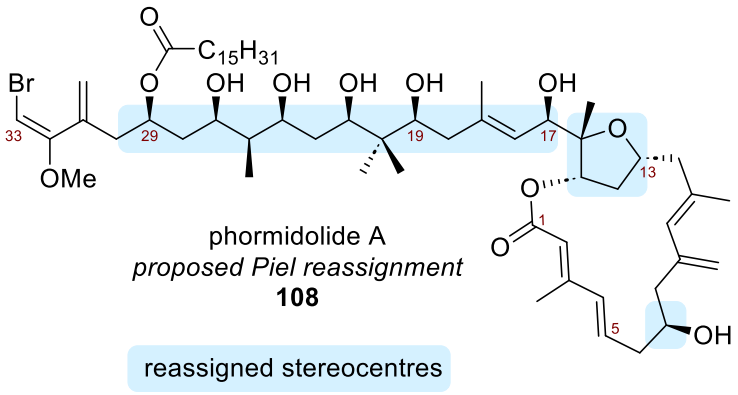

Figure 2.8. Piel's proposed reassignment of phormidolide A.

2.4.3. The Collective Final Proposal of the Phormidolide A Stereochemical Reassignment

Noting the stereochemical ambiguities with the original assignment and two different stereochemical reassignments proposed, **91** and **108**, our group and collaborators: the Piel group, and the groups of the original isolation team came together to propose **109** as the correct and reassigned structure (**Figure 2.9**). To support this reassignment, a combination of anisotropic and computation NMR spectroscopic analysis was undertaken.[93]

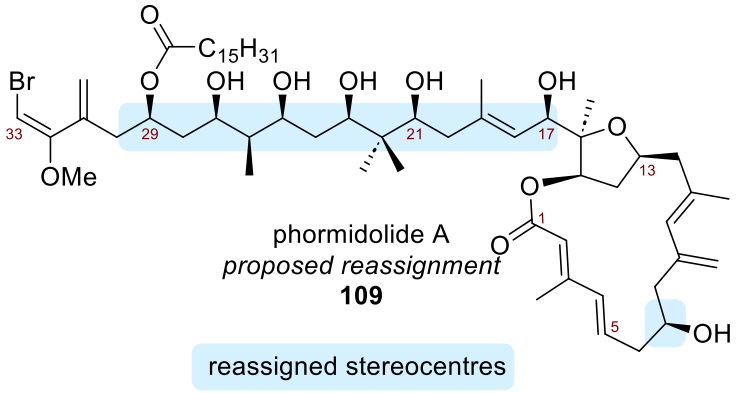

Figure 2.9. The collective proposed reassiged structure of phormidolide A.

The first step in supporting the stereochemical reassignment was to confirm the reassignment of the C17 position through density functional theorem (DFT) coupling constant calculations. The homonuclear and heteronuclear coupling constants of two C17 epimers of a C20-truncated fragment of phormidolide A, **110** and **111** (**Figure 2.10**), were calculated. The H17 to C37 $^{3}J_{CH}$ coupling constant was calculated to be 4.1 Hz in **110**, the

C17 *R* epimer, which matched that found for the NP, while other epimer was calculated to have a H17 to C37 $^{3}J_{CH}$ coupling constant of 3.3 Hz, which supports the proposed reassignment to **109**.

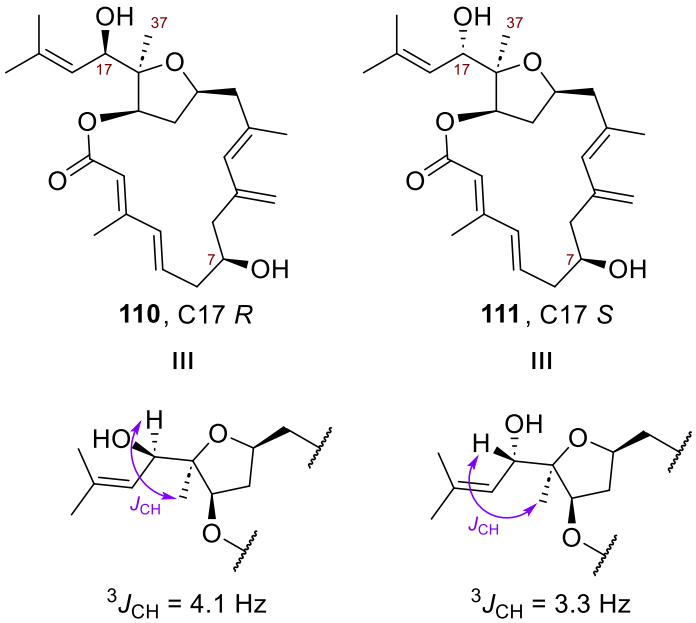

Figure 2.10. The truncated models of phormidolide A 110 and 111 for computational analysis along with the predicted $^{3}J_{CH}$ coupling constants between H17 and C37.

To further investigate the stereochemical reassignment, DP4 analysis was used, which can quantify the agreement between experimental and calculated NMR chemical shifts. For each structure calculated, the DP4 program analyzes the likelihood of the calculated NMR data matching the experimental data and outputs that likelihood as a percentage. A higher percentage for a given calculated structure means that it is more likely correct.[94] The calculated chemical shifts for **110** and **111**, along with the C7 epimers for each compound, were compared with the experimental values derived from the NP using DP4 analysis.[56] This analysis gave 100% confidence for the stereochemistry displayed in **110**, further supporting the proposed reassignment to **109**.

In addition, the $^{3}J_{HH}$, $^{2}J_{CH}$, and $^{3}J_{CH}$ coupling constants and ^{13}CNMR shifts were calculated for a C24 truncated fragment of phormidolide A, **112** (**Figure 2.11**). All possible diastereomers at C7, C17, and C21 were considered, along with C23 being set *syn* to C21, resulting in 8 total structures. Determining the C21 stereochemistry would inform on the stereochemistry of the polyol chain, as the relative configuration of the side chain was

relayed back to C21 *via J*-based analysis and analysis of the acetonide derivative of phormidolide A. Based on the mean absolute error of experimental *versus* calculated coupling and chemical shift values, the C24 truncated 21(*S*),17(*R*),7(*S*)-fragment of phormidolide A, **113** (**Figure 2.11**), had the closest match to the experimental data. This result again supports the proposed reassignment to **109**.

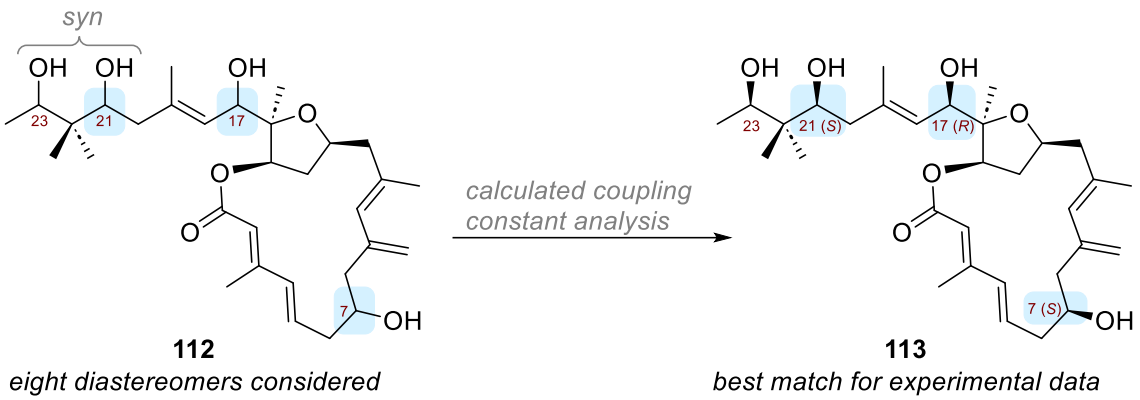

112
eight diastereomers considered

113
best match for experimental data

Figure 2.11. The fragment of phormidolide A, 112, for which 8 diastereomers were considered for coupling constant analysis to reveal fragment 113 as the closest matching diastereomer.

Finally, the stereochemical reassignment was evaluated by an orthogonal assessment of anisotropic NMR parameters. Anisotropic NMR assessment uses two parameters to assess the structure and configuration of a molecule: residual dipolar coupling (RDC) and residual chemical shift anisotropy (RCSA).[95] These parameters are small positive or negative changes to coupling constants and chemical shifts when a molecule is constrained in an alignment media, such as a polymeric gel. In this assessment, RDC values are the differences between $^{1}J_{CH}$ coupling in the constrained and unconstrained material and report on the relative configuration around particular carbons. Analogously, RCSA values are the difference in ^{13}C chemical shift between the constrained and unconstrained material, which also report relative configuration, but can inform on carbons without bonded hydrogen. These observed RDC and RCSA values can then be compared with the corresponding computationally predicted values for a certain structure and plotted. A Q-factor is generated from this plot which reports on the similarity between the experimental and computational factors. Generally, a Q-factor between 0.1 and 0.2 indicates a high confidence in the structural assignment.[95]

The same 8 diastereomers of **112** were considered in this anisotropic NMR analysis, which was compared to experimental values of phormidolide A obtained from the NP suspended in a poly-γ-benzyl-L-glutamate gel. When the anisotropic NMR values derived from the suspended NP were compared with the values for all 8 computationally generated diastereomers, it was again observed that the configuration shown in **113**, the 21(*S*), 17(*R*), 7(*S*) fragment of phormidolide A, best matched the data for the NP, with a Q-factor of 0.190. This analysis indicates a strong correlation between the structure shown in **113** with the structure of the NP, supporting the stereochemical reassignment of phormidolide A to **109**.[93]

2.5. Conclusion

Noting several ambiguities with the original stereochemical assignment of phormidolide A, we embarked on a stereochemical reassignment. Comparing the spectral data derived from phormidolide A with spectral data from model C10-C23 fragments of phormidolide A suggested a reassignment of the C17 and C21 positions and, since the stereochemistry of the rest of the polyol chain was relayed back to the C21 position, a reassignment at each position on the side chain. Independently, the Piel group developed structural prediction software which suggested a reassignment to the enantiomer of the proposed structure.

To finalize the stereochemical reassignment, all interested groups collaborated to propose stereostructure **109** (**Figure 2.9**). Computational comparison with NMR data from the NP and anisotropic NMR data supported the reassignment of phormidolide A as **109**. Notably, this stereochemical reassignment addresses all ambiguities from the original isolation paper. A reassignment of C7 aligns with a correct Mosher's ester analysis, a C17 reassignment explains the data from an acetonide analysis, which suggested an *anti*-relationship between the C17 and C15 positions, and a reassignment of the side chain supports the prediction of the stereochemistry based on the biosynthetic enzymes. From this collective evidence, we were confident in the structural reassignment and **109** became the synthetic target for the total synthesis of phormidolide A.

Chapter 3. Synthesis of the Macrocycle of Phormidolide A

The work contained in this chapter was performed in collaboration with Dr. Nelson Lam. Dr. Lam was responsible for the assessment of the macrocyclization reactions covered in subchapters 3.3 and 3.5-3.8, while the synthesis of the intermediates in these subchapters was a collaborative effort between the author and Dr. Lam. All other work reported is the authors unless otherwise stated.

3.1. Introduction

Phormidolide A (**28**, **Figure 3.1**) is a natural product (NP) isolated from a marine cyanobacterium. It was shown to be toxic towards brine shrimp with an LC_{50} of 1.5 μM but was found to be inactive against the 60 different clinically relevant cancer cell lines, in a screen by the National Cancer Institute (NCI).[52] However, several structurally related members of the phormidolide family of NPs have shown anti-cancer and anti-fouling activity. For example, phormidolides B and C (**29** and **30, Figure 3.1**) have shown activity against three different cancer cell lines that were present in the same NCI screen.[53,55] Notably, the macrocyclic phormidolide fragment **114** was inactive in the same screen, highlighting the importance of the side chain for anti-cancer activity.

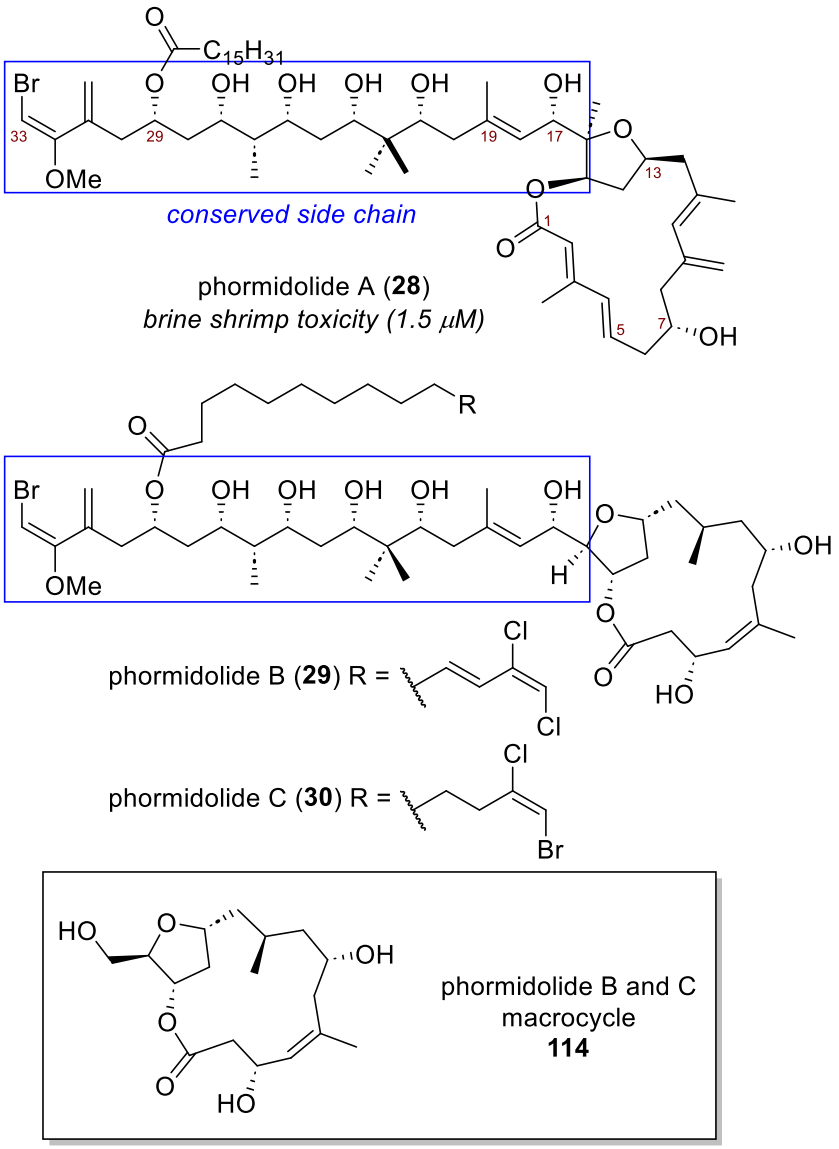

Compound	Lung (A-549)	Colon (HT-29)	Breast (MDA-MB-231)
29	1.4 μM	1.3 μM	1.0 μM
30	1.3 μM	0.8 μM	0.5 μM
114		No activity observed	

Figure 3.1. Phormidolide A, B and C with the reported activity (IC_{50}) of phormidolides B and C against 3 human cancer cell lines.

The Gerwick group originally proposed a structural assignment for phormidolide A (**28**) based on data from the NP and derivates.[52,62] As detailed in Chapter 2, A reassessment of data derived from a Mosher's ester derivative at C7 and from an acetonide derivative along with biosynthetic studies by the Gerwick and Piel groups suggested that the stereocenters at C7 and from C17 to C29 should be the opposite of

that originally proposed. Additionally, based on the comparison of spectral data derived from the NP with synthetic model compounds, along with anisotropic NMR spectroscopic analysis and computational prediction of chemical shifts, a stereochemical reassignment of the NP to **109** (**Figure 3.2**) has been proposed.[93,96] Drawn to the complex and interesting structure of the NP, we embarked on a total synthesis of phormidolide A in collaboration with the Paterson group to confirm the structural assignment and provide material for further biological assessment, targeting the reassigned structure **109**.

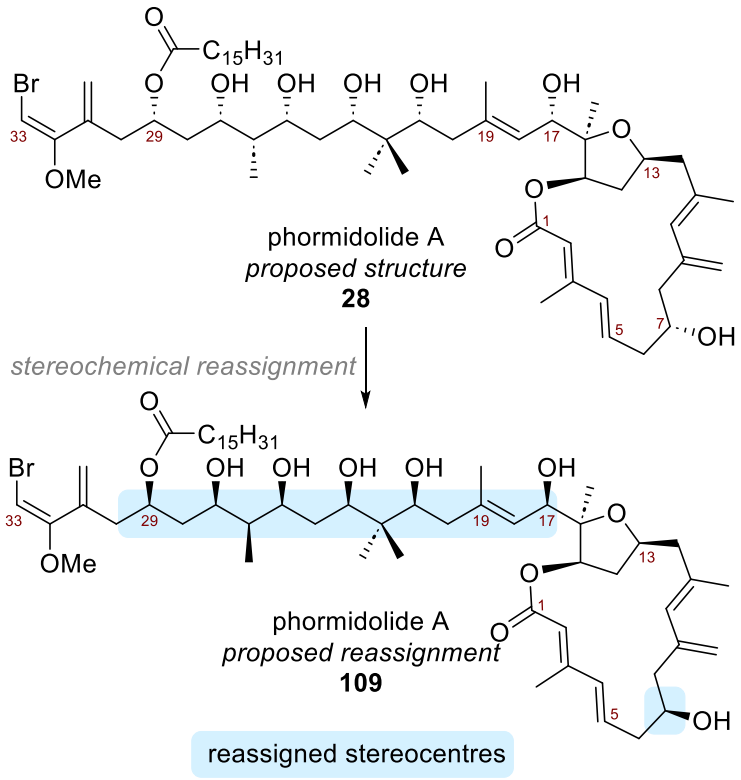

Figure 3.2. The proposed stereochemical reassignment of phormidolide A.

3.2. Retrosynthetic Analysis

A retrosynthetic analysis for phormidolide A is shown in **Scheme 3.1**. As depicted, we planned to prepare the side chain **115** and the macrocycle **116** independently and connect both *via* a vinyl metal addition, such as a Nozaki-Hiyama-Kishi (NHK) or a Grignard addition. Given the Paterson lab's expertise in synthesizing polyketides,[28,97–100] their focus became the synthesis of the side chain **115**, while our focus was the synthesis of the macrocycle **116**, based on our lab's expertise in the synthesis of THF-containing

NPs. This chapter will cover our efforts directed towards the synthesis of the macrocycle of phormidolide A.

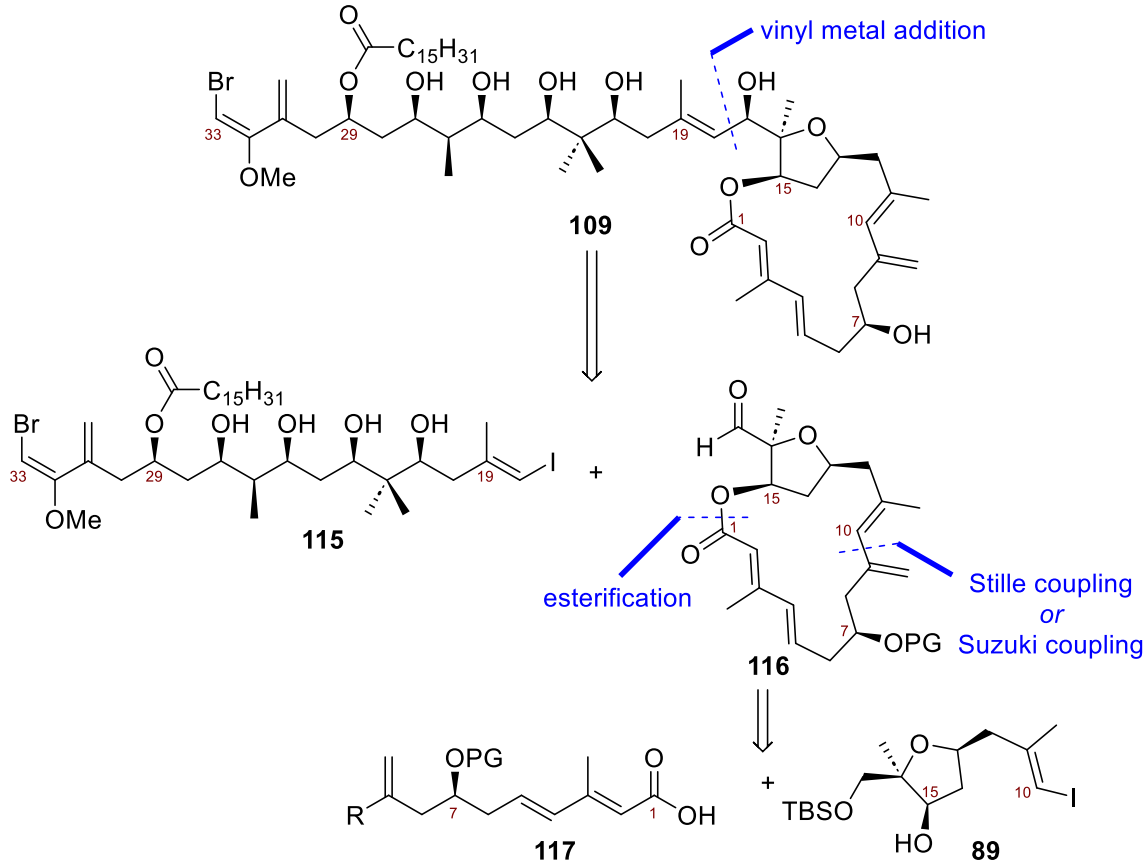

Scheme 3.1. Retrosynthetic Analysis for 109.
PG = protecting group

Macrocycle **116** could be constructed based on two key retrosynthetic disconnections at the C1-C15 alcohol and across the C9-C10 bond. Specifically, these bonds could be formed by an esterification reaction and a Stille or Suzuki coupling, respectively. The coupling partners for these reactions would be the C1-C9 moiety **117**, where R represents a suitable functional group for a Stille or Suzuki coupling, and THF **89**. The synthesis of THF **89** had been developed both for the stereochemical reassignment and the total synthesis of phormidolide A (Section 2.3). With this THF core in hand, we began efforts to prepare precursors for the macrocyclization studies.

3.3. First Generation Macrolactonization

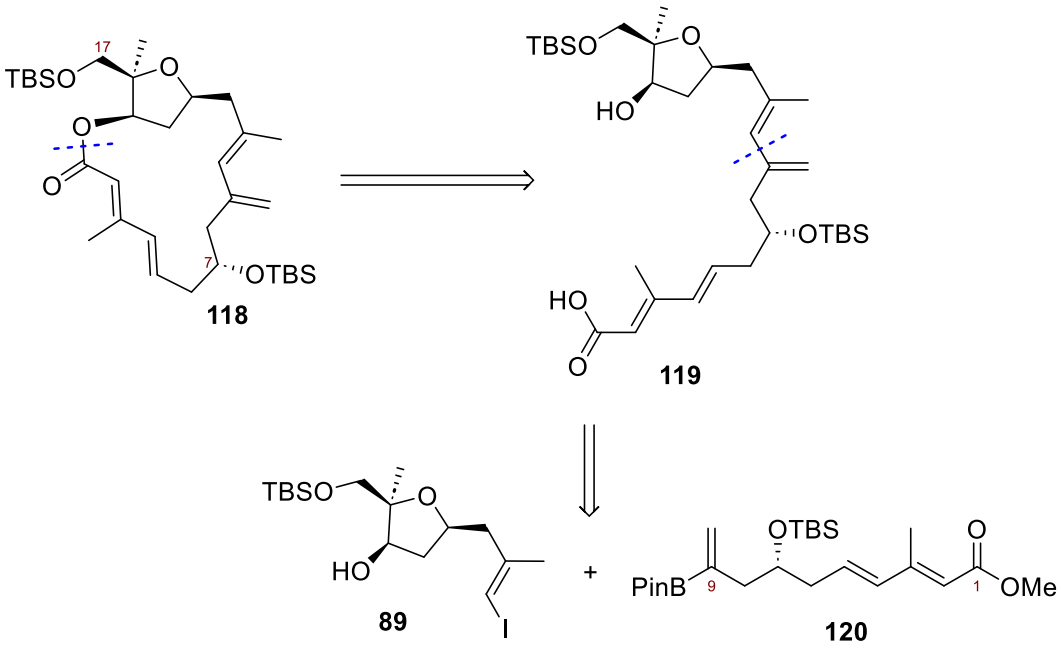

Scheme 3.2. Retrosynthetic Analysis for the First-Generation Macrolactonization Approach.

As highlighted in **Scheme 3.2**, our initial macrocycle target was compound **118,** which contains TBS protecting groups for both the C7 and C17 alcohol. We envisioned a selective deprotection of the less hindered C17 primary alcohol would allow further elaboration of the NP. Notably, this work was designed and executed before our reassignment of the stereochemistry of the NP and therefore the macrocycle **118** incorporates the originally proposed (*R*)-stereochemistry at C7. From a retrosynthetic perspective, this macrolactonization approach required the preparation of seco acid **119**, which we envisioned could be constructed *via* Suzuki coupling to form the C9-C10 bond from THF **89** and vinyl boronate **120**.[101]

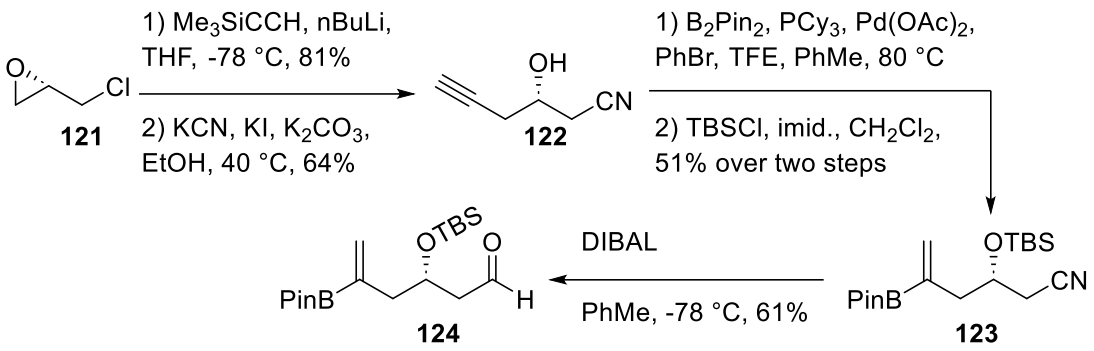

Scheme 3.3. Preparation of Vinyl Boronate 124.

Construction of vinyl boronate **124** (**Scheme 3.3**) began with the conversion of (*S*)-epichlorohydrin **121** into alcohol **122**, a process that involves sequential alkyne and cyanide addition steps.[102] Palladium-catalyzed hydroborylation[103] then TBS protection afforded **123** in 51% yield over two steps. Finally, the aldehyde **124** was accessed via DIBAL reduction of the nitrile function. Critical to the DIBAL reduction was the use of 10% citric acid solution as an aqueous work-up to hydrolyze the intermediate imine, as standard work-up conditions using Rochelle's salt did not result in imine hydrolysis.

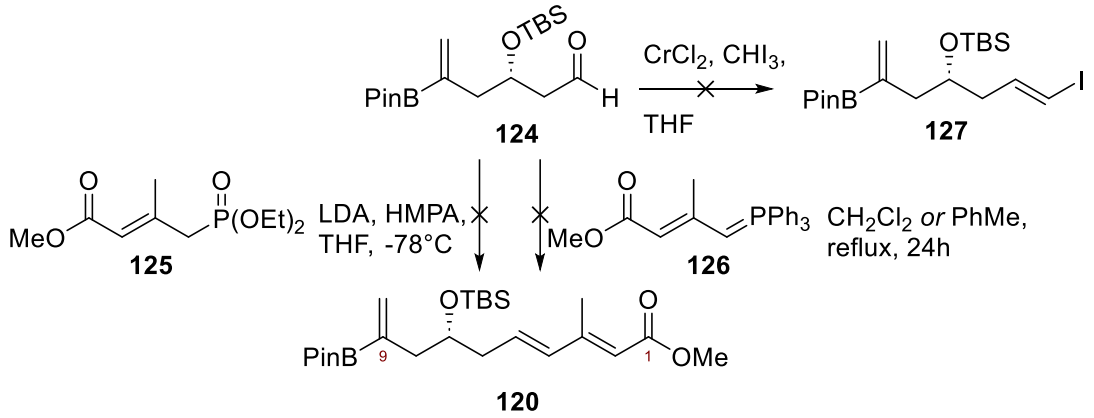

Scheme 3.4. Efforts Towards the Preparation of Vinyl Boronate 120.

Our next goal then became the preparation of the C1-C9 fragment **120** from the aldehyde **124** (**Scheme 3.4**). Unfortunately, the Horner-Wadsworth-Emmons (HWE) reaction of aldehyde **124** with phosphonate **125** resulted in degradation of the vinyl boronate and no reaction was observed using Wittig reagent **126**.[104] Attempts to convert **124** into vinyl iodide **127** for Stille coupling also led to degradation. We attributed these issues to the instability of the vinyl boronate function and to avoid these challenges we

converted the aldehyde **124** into alcohol **128** (**scheme 3.5**) and resolved to further elaborate this fragment of the macrocycle after coupling to the THF core.

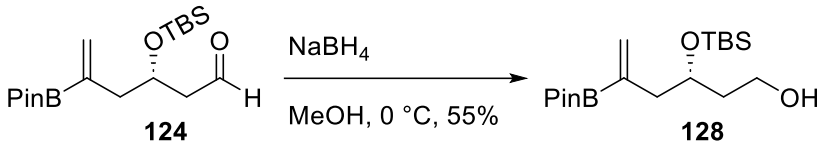

Scheme 3.5. Preparation of Alcohol 128.

With the vinyl boronate **128** in hand, we protected the alcohol function in THF **89** with dimethylacrylic acid (**98**), affording ester **99** (**Scheme 3.6**), an intermediate used in the stereochemical reassignment proposal (Section 2.4.1). To prepare the target seco acid **119**, the two fragments vinyl boronate **128** and THF **99** were coupled using Suzuki conditions (**Scheme 3.6**). This step proved challenging, and after careful optimization, we found that 2.5 equivalents of the vinyl boronate and thallium(I) ethoxide as a base were required to afford the coupling product in reproducibly good yield, especially upon scale-up of the reaction. Thallium (I) ethoxide was chosen as it has been shown to accelerate the rate of Suzuki reactions and allow these reactions to be run at lower temperatures.[105] As the resulting product could not be fully separated from residual boronate using flash column chromatography, the crude material was carried through to the oxidation step. Fortunately, this next reaction cleanly oxidized the material while removing the boronate impurity, affording aldehyde **129** in an 89% yield over two steps.

From here, Takai olefination[106] afforded vinyl iodide **130** in a 71% yield with an *E*/*Z* selectivity of 3:1. Despite optimization of this reaction by varying the solvent and temperature, the *E*/*Z* selectivity could not be improved. Finally, vinyl iodide **130** was coupled to the known vinyl stannane **131**[107] under palladium conditions with a copper thiophene-2-carboxylate (CuTC) additive,[108] followed by $Ba(OH)_2$ hydrolysis to furnish seco acid **119** in good yields (**Scheme 3.6**).

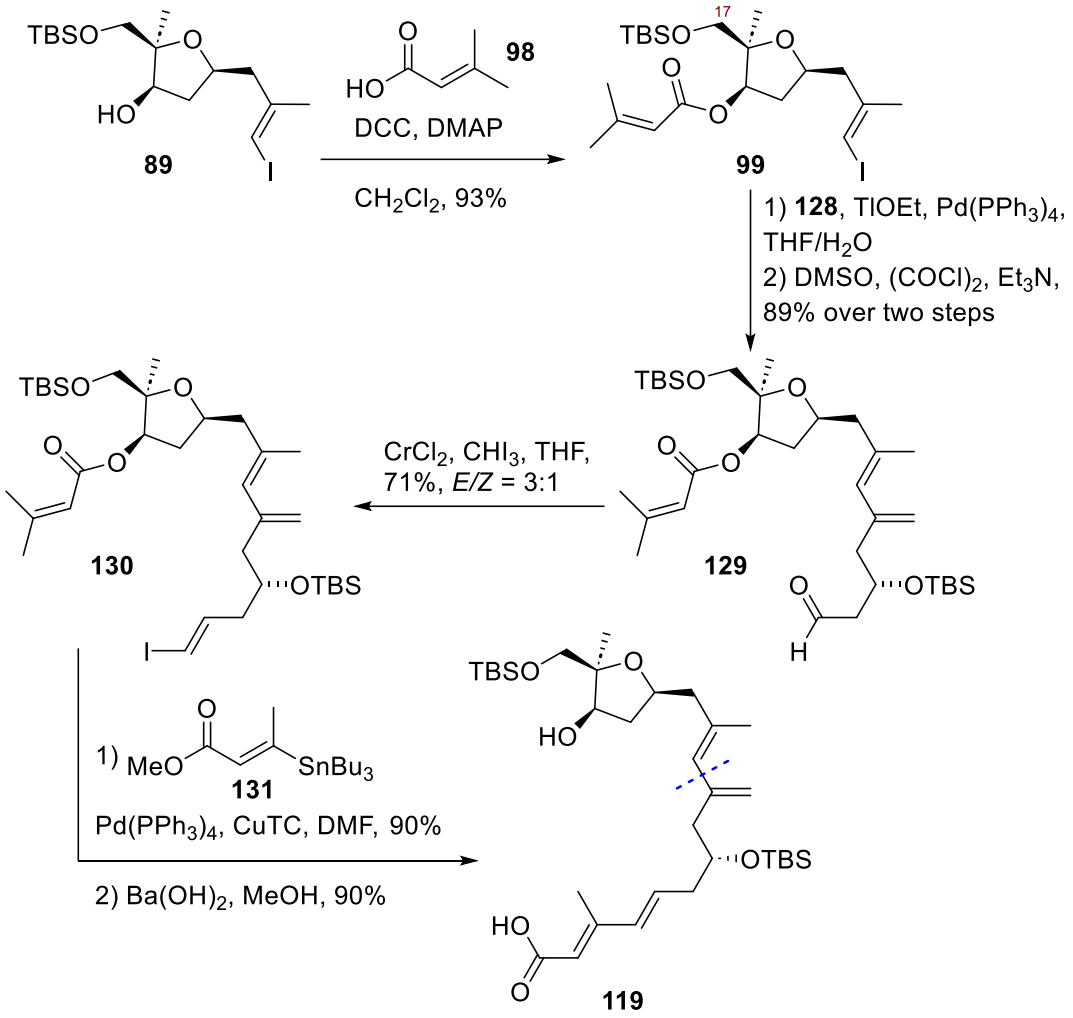

Scheme 3.6. Preparation of Seco Acid 119 for Macrolactonization Assessment.

With **119** in hand, we began to explore macrolactonization conditions. Unfortunately, all attempts to affect the formation of the macrocycle from **119** failed. Yamaguchi macrolactonization conditions, reported for the synthesis of phormidolides B and C,[53,58] afforded complex mixtures of inseparable products despite efforts to optimize the reaction by adjusting the temperature, dilution, or using slow addition of the starting material. Shiina macrolactonization conditions[109–111] afforded the expected mixed anhydride, but would not undergo macrolactonization. We attributed the failure of this reaction to steric congestion around the neopentyl C15 alcohol. Given the observed issues, we decided to explore a macro-Stille cyclization,[98] where bond formation occurs distal to the steric congestion around the THF ring.

3.4. C3-C4 Macro-Stille

Noting our success in forming the C3-C4 bond via Stille coupling during the preparation of seco acid **119**, we reasoned that macrocyclization using a similar reaction may prove successful. While less common than macrolactonization, macro-Stille cyclization reactions have been used in several NP total syntheses.[112,113] We envisioned two possible macro-Stille precursors: the first with a vinyl bromide at C3 and vinyl stannane at C4, **132**, and the second containing a vinyl stannane at C3 and a vinyl iodide at C4, **133** (**Scheme 3.7**). With the goal of preparing macrocyclic precursor **132**, we aimed to construct a key fragment of this precursor, vinyl bromide **134**. Unfortunately, **134** was found to be highly unstable to work-up conditions and solid phase purification media, rendering us unable to proceed with the synthesis of **132**. Therefore, we turned our efforts towards the synthesis of the alternative macrocyclic precursor, **133** (**Scheme 3.8**).

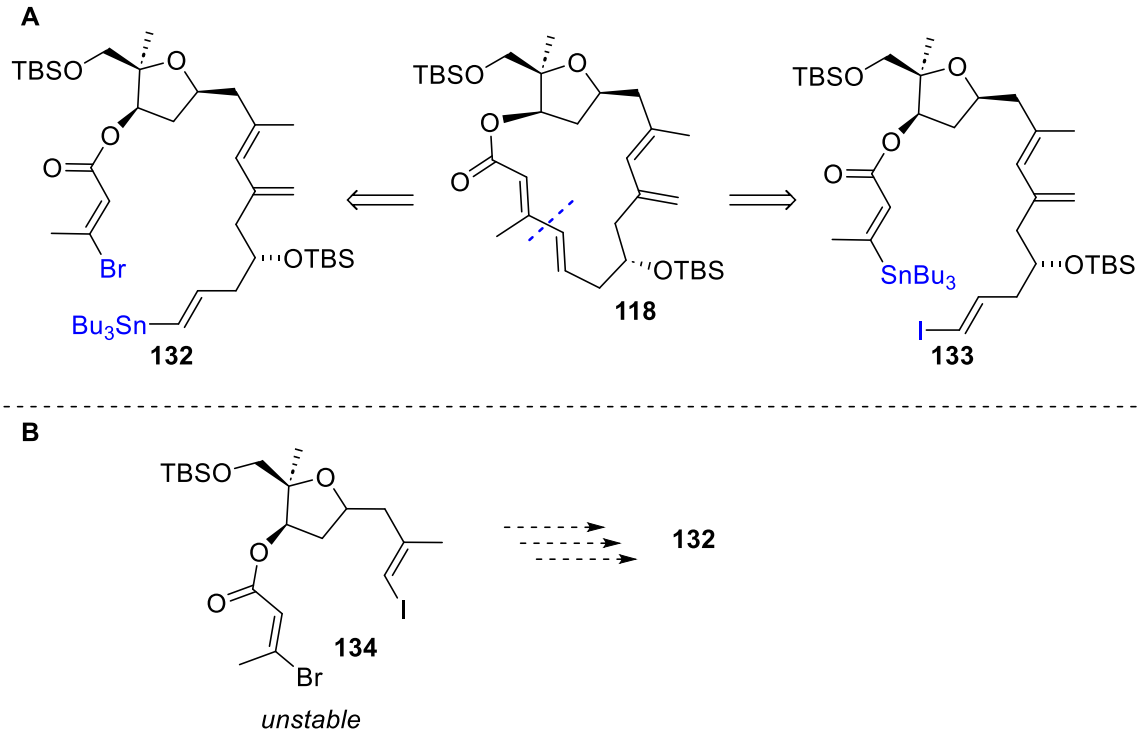

Scheme 3.7. A: Retrosynthetic Analysis for the C3-C4 Macro-Stille Assessment. B: Vinyl Bromide 134 Which Proved Too Unstable for Synthetic Use.

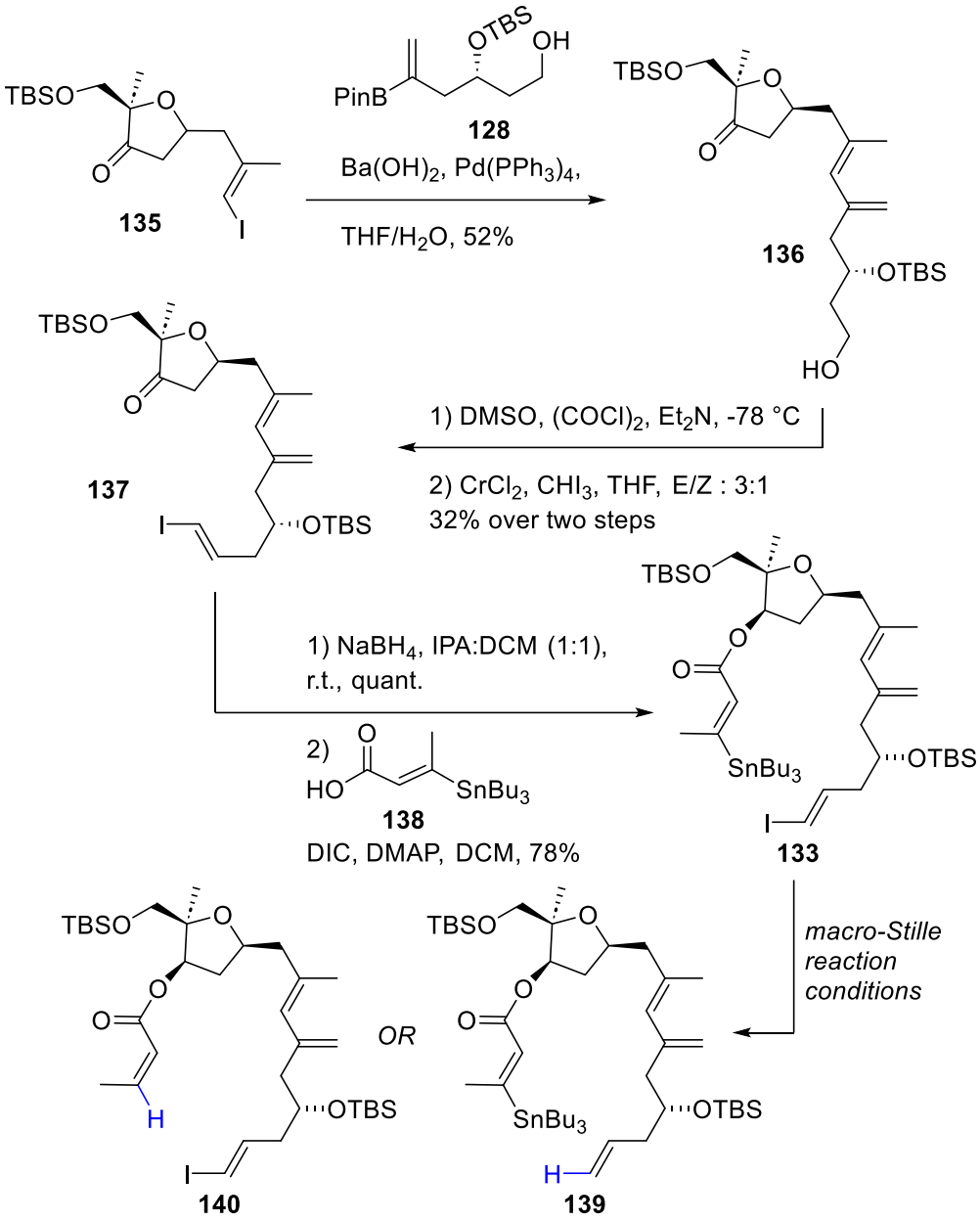

Scheme 3.8. Preparation of Vinyl Stannane 133 and Protodeiodinated and Protodestannylated Products 139 and 140 Resulting from Certain Macro-Stille Conditions.

The construction of macro-Stille precursor **133** began with the Suzuki coupling of vinyl boronate **128** with THF **135** to afford alcohol **136**. Elaboration of **136** to the vinyl iodide **137**, followed by reduction and esterification with known carboxylic acid **138**[114] afforded macro-Stille precursor **133** in good yields for the assessment of the macrocyclization strategy (**Scheme 3.8**).

Unfortunately, none of our efforts to affect the macrocyclization to **118** were successful. Outlined in **Table 2.1**, we assessed several conditions with three different palladium catalysts, $Pd_2(dba)_3$, $Pd(PPh_3)_4$, and $Pd(dppf)Cl_2$. Macro-Stille precursor **133** proved unreactive at room temperature with $Pd_2(dba)_3$ (entry 1) and only degradation of the material was observed upon heating with or without Cu(I) additives (entries 2 and 3). Using DMSO as the solvent resulted in no change in the outcome (entry 4). Similarly, no reaction was observed at room temperature with a change in catalyst to $Pd(PPh_3)_4$ and LiCl (entry 5), while heating under these same conditions resulted in the protodeiodinated product **139** (entry 6, **Scheme 3.8**). When changing the additive to a Cu(I) salt with $Pd(PPh_3)_4$, no reaction occurred at room temperature and, similarly, heating only resulted in degradation (entries 7-10). **107** again proved unreactive at room temperature with $Pd(dppf)Cl_2$ (entry 11) and upon heating to 60 °C, only the protodestannylated product **140** was recovered (entry 12, **Scheme 3.8**). Increasing the temperature further resulted in the degradation of the material (entry 13). Pd-free conditions using a Cu(I) salt resulted in solely the protodestannylated product **140** being recovered (entry 14, **Scheme 3.8**). Given that we were unable to affect C3-C4 macro-Stille cyclization, we chose to evaluate an alternative macro-Stille cyclization.

Table 3.1. Optimization Conditions for the C3-C4 Macro-Stille Reaction

Entry	Pd source	Additive	Temperature	Reaction Outcome
1	$Pd_2(dba)_3$	CuTc	20 °C	NR
2	$Pd_2(dba)_3$	CuTc	40 °C	Degradation
3	$Pd_2(dba)_3$	none	40 °C	Partial degradation
4 [a]	$Pd_2(dba)_3$	CuTc	40 °C	Degradation
5	$Pd(PPh_3)_4$	LiCl	20 °C	NR
6	$Pd(PPh_3)_4$	LiCl	40 °C	Protodeiodination, **139**
7	$Pd(PPh_3)_4$	CuTc	20 °C	NR
8	$Pd(PPh_3)_4$	CuTc	40 °C	Degradation
9	$Pd(PPh_3)_4$	CuCl	20 °C	NR
10	$Pd(PPh_3)_4$	CuCl	40 °C	Degradation
11	$Pd(dppf)Cl_2$	CuTc	20 °C	NR
12	$Pd(dppf)Cl_2$	CuTc	60 °C	Protodestannylation, **140**
13	$Pd(dppf)Cl_2$	CuTc	80 °C	Degradation
14	none	CuTc	100 °C	Protodestannylation, **140**
15	$Pd_2(dba)_3$	CuTc	40 °C	Degradation

[a]reaction run in dry DMSO, dba = dibenzylideneacetone, dppf = 1,1'-bis(diphenylphosphino)ferrocene, NR = No reaction

3.5. First Generation C9-C10 Macro-Stille

Following our failure to affect Stille-macrocyclization, we turned our attention to forming the C9-C10 bond. To this end, we elected to employ a related C9-10 macro-Stille cyclization strategy. Here, we targeted macrocycle **140**, containing a TIPS protecting group at the C7 position, which should allow for selective removal of the C17 TBS protecting group. This strategy required the preparation of macrocyclic precursor **141** (**Scheme 3.9**), which we envisioned could arise from the esterification of THF **142** and carboxylic acid **143**.

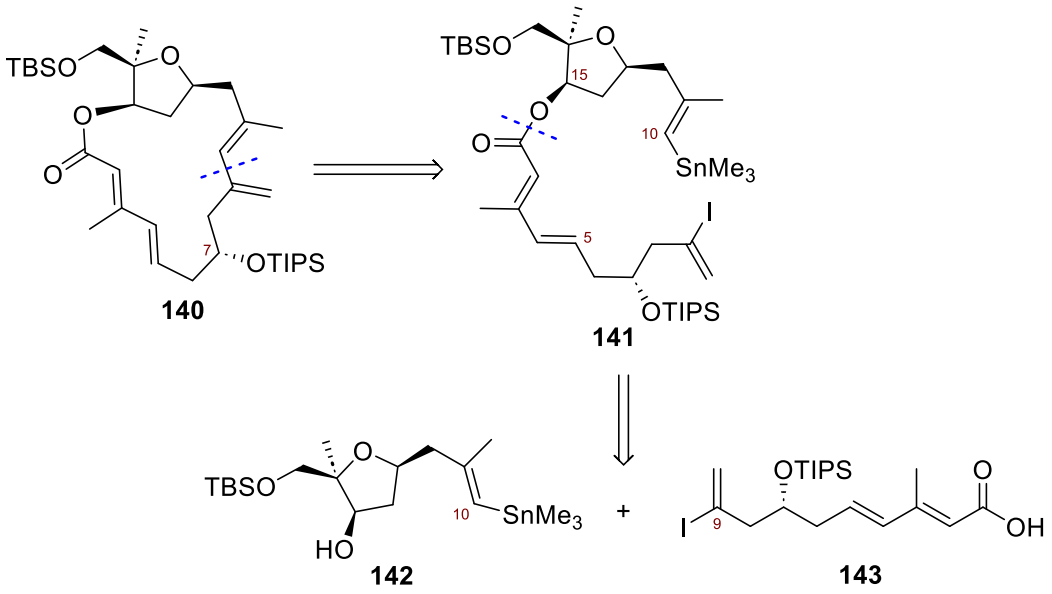

Scheme 3.9. Retrosynthetic Analysis for the First Generation C9-C10 Macro-Stille Assessment.

As highlighted in **Scheme 2.11**, TIPS protection of **122** followed by iodoborylation and acidic work-up[115] afforded vinyl iodide **144** which was converted to aldehyde **145** via DIBAL reduction. The C1-C9 fragment was then prepared by an HWE reaction between aldehyde **145** and known phosphonate **125**,[104] followed by hydrolysis of the methyl ester to afford **146**. Critical to the HWE reaction was the use of HMPA as a cosolvent, which prevented otherwise significant isomerization of the C3-C4 olefin.[104,116] Separately, THF **89** was converted to the C10 vinyl stannane **142** with Wulff-Stille conditions[117] and appended to **146** under Yamaguchi conditions to construct macrocyclic precursor **141** in excellent yields (**Scheme 3.10**).[44]

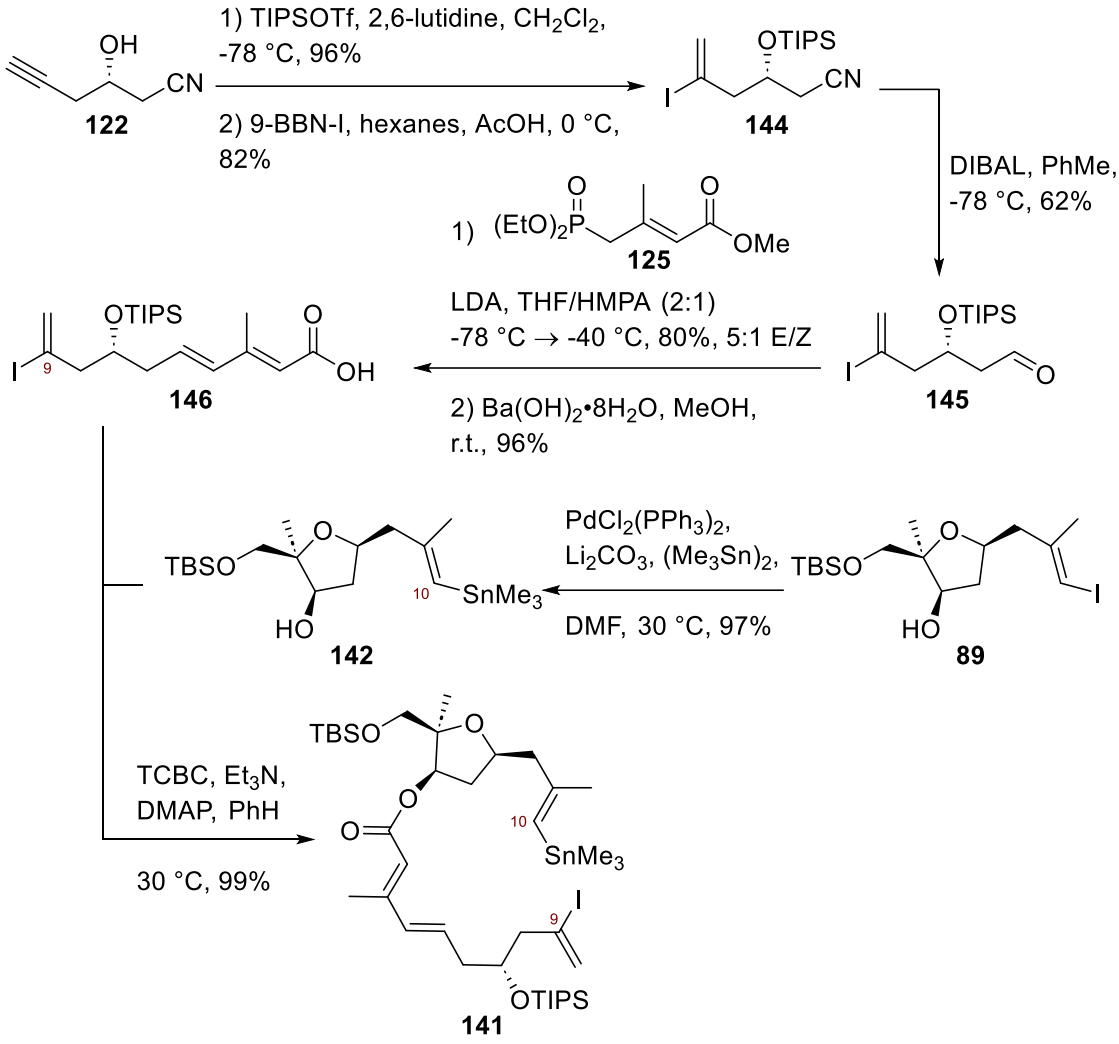

Scheme 3.10. Preparation of Macro-Stille Precursor 141.

Unfortunately, and despite considerable experimentation, we were not able to access **140** from the macro-Stille precursor **141**. The use of palladium catalysis, based on the Paterson synthesis of chivosazole F,[98] resulted in protodestannylation at room temperature and increasing the reaction temperature resulted in degradation of the starting material. The same result was observed if either a copper or arsine additive was used.[98,118] Use of Cu(I)-mediated Stille cross-coupling conditions[119] led to the C9 homocoupled product and dilution afforded only the protodestannylated product. Based on these disappointing results, and cognizant of our goal to form the macrocycle at a position remote from the THF ring we decided to assess alternative and potentially more mild macrocyclization conditions, starting with a macro-HWE approach.

3.6. C2-C3 Macro-HWE

It is important to note that at this point in our efforts, the stereochemical reassignment of phormidolide A was proposed, which included a reassignment of the C7 alcohol, as detailed in Chapter 2. Therefore, from this point, all intermediates and targets contained the newly proposed stereochemistry at this centre. As noted above, we envisioned a macrocyclization strategy utilizing an HWE reaction to form the C2-C3 alkene. HWE macrocyclizations often involve mild reaction conditions and,[120–122] given the sensitivity observed during attempted Stille reactions discussed above, we theorized that the use of an HWE macrocyclization may avoid degradation. We thus targeted phosphonate **148** (**Scheme 3.11**), which we envisioned forming by Stille coupling between THF **89** and vinyl stannane **149**, followed by esterification with carboxylic acid **150**.

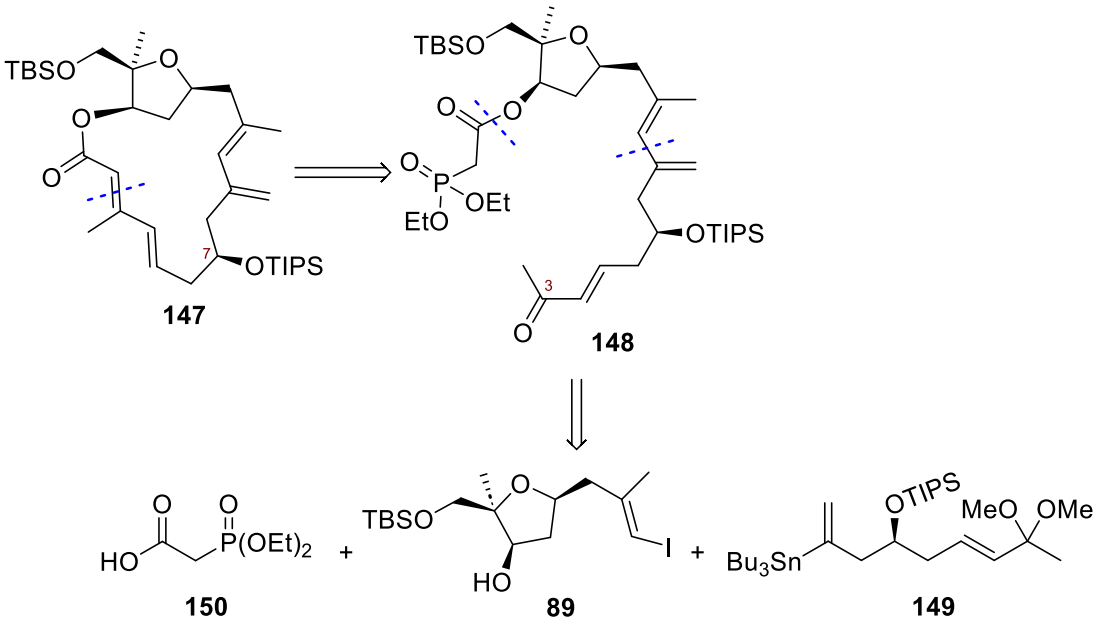

Scheme 3.11. Retrosynthetic Analysis for the C2-C3 Macro-HWE Approach.

Construction of **148** began with iodoborylation and acidic work-up[115] of known alkyne **151**,[123] affording vinyl iodide **152** (**Scheme 3.12**). This later material was elaborated to aldehyde **153** under reductive DIBAL conditions and vinyl iodide **155** was prepared via a HWE reaction between aldehyde **153** and commercially available phosphonate **154**.[124] Protection of **155** as a dimethyl acetal was necessary for I/Sn exchange. This process afforded **149** which was then coupled to THF **89**. Treatment of the crude material under acidic conditions quantitatively afforded ketone **156**. Esterification with commercially

available diethylphosphonoacetic acid (**150**) then gave phosphonate **148** for evaluation of the C2-C3 HWE macrocyclization.

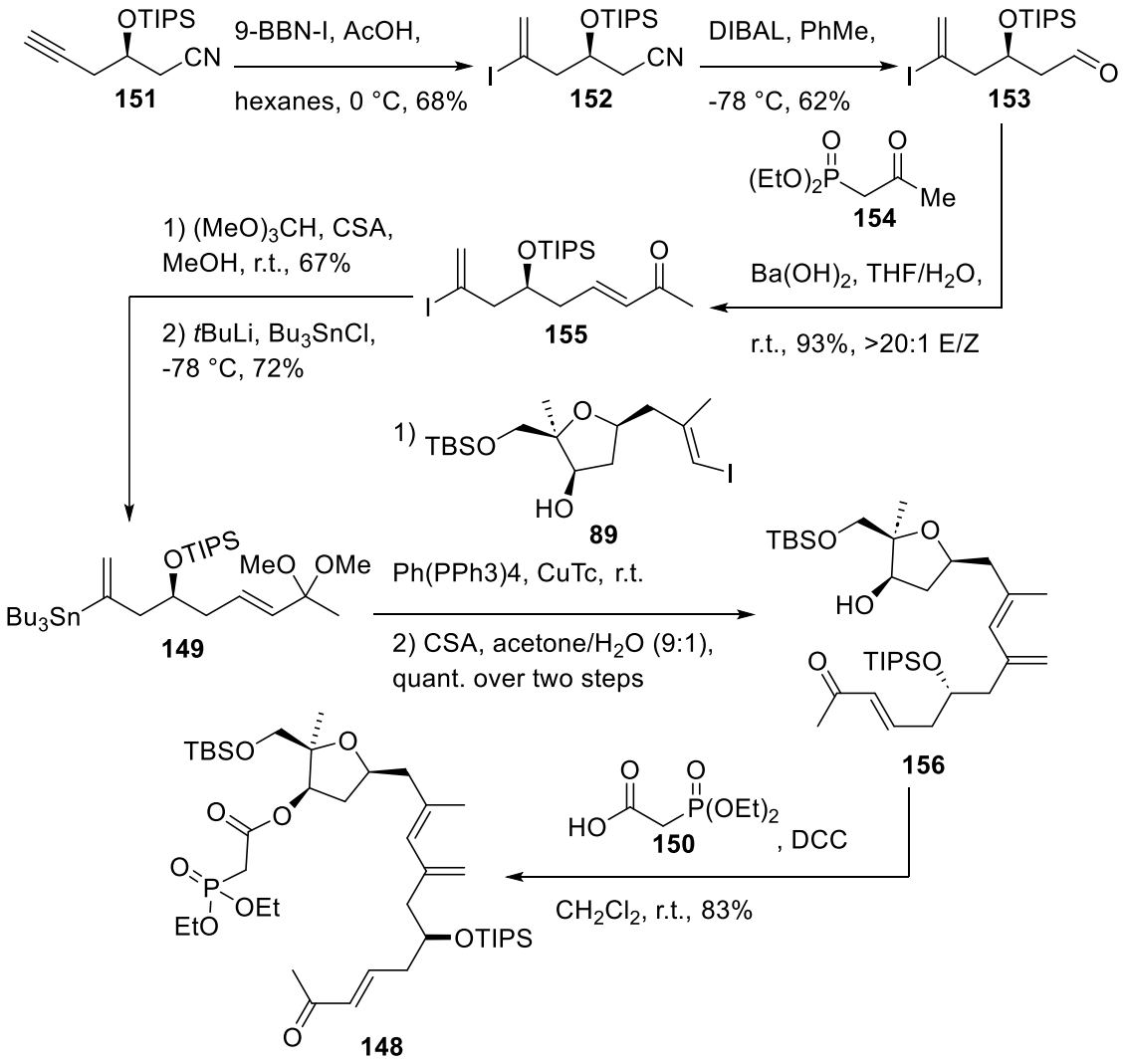

Scheme 3.12. Preparation of C2-C3 Macro-HWE Precursor 148.

Unfortunately, all attempts at C2-C3 bond formation and macrocycle construction were unsuccessful. Using Masamune-Roush conditions[125] or using lithium diisopropyl amine (LDA) as a base led to ester cleavage, while NaH conditions caused significant degradation of the substrate. We hypothesized that this was due to a lack of reactivity of the C3 ketone. While this strategy failed, it inspired us to explore the equivalent bond formation using a macrocyclic Reformatsky reaction.

3.7. C2-C3 Macro-Reformatsky

Given the manifold difficulties noted above in macrocycle formation, we surmised that alleviating the strain the in macrocycle with one less alkene in the macrocyclic precursor might improve the outcome of the macrocyclization reaction. Macrocyclic Reformatsky cyclization reactions have been used in NP synthesis and this strategy was recently demonstrated by our group in the synthesis of biselide A, a THF-containing marine macrolide.[37,126] Esterification of **156** with commercially available bromoacetyl bromide (**157**) afforded α-bromoester **158** (**Scheme 3.13**). However, upon treatment of **158** with SmI_2 at 0 °C by slow addition,[127,128] only degradation was observed. With both the C2-C3 macro-HWE and macro-Reformatsky reactions unviable, we decided to pursue a ring-closing metathesis (RCM) strategy.

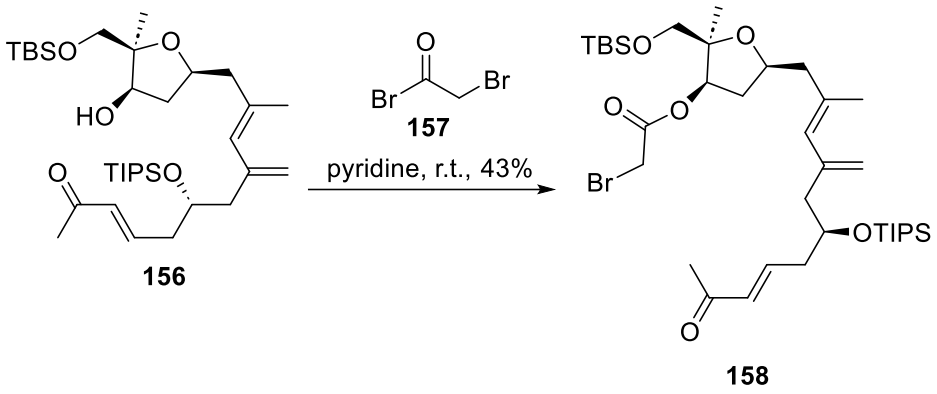

Scheme 3.13. Preparation of Bromoester 158.

3.8. C4-C5 Ring Closing Metathesis

RCM reactions have been used extensively in NP synthesis and are often uniquely useful due to the high functional group compatibility.[129] Preparation of the RCM precursor **162** (**Scheme 3.14**) began with the conversion of aldehyde **153** to vinyl stannane **159**, which proceeded in good yield. Vinyl stannane **159** was then coupled to THF **89** and esterification of known alkene **161**[114] afforded **162**. Unfortunately, treatment of **162** with the Hoveyda-Grubbs II catalyst led to the exclusive formation of the 5-membered ring product **163**, suggesting the reactivity of the C9 alkene was significantly higher than that of the C4 alkene. Further model studies on ester derivatives of diene **161** indicated the dienoate was particularly unreactive under RCM conditions. With RCM also unsuccessful, we next decided to assess an HWE macrocyclization, but now involving the C4-C5 alkene.

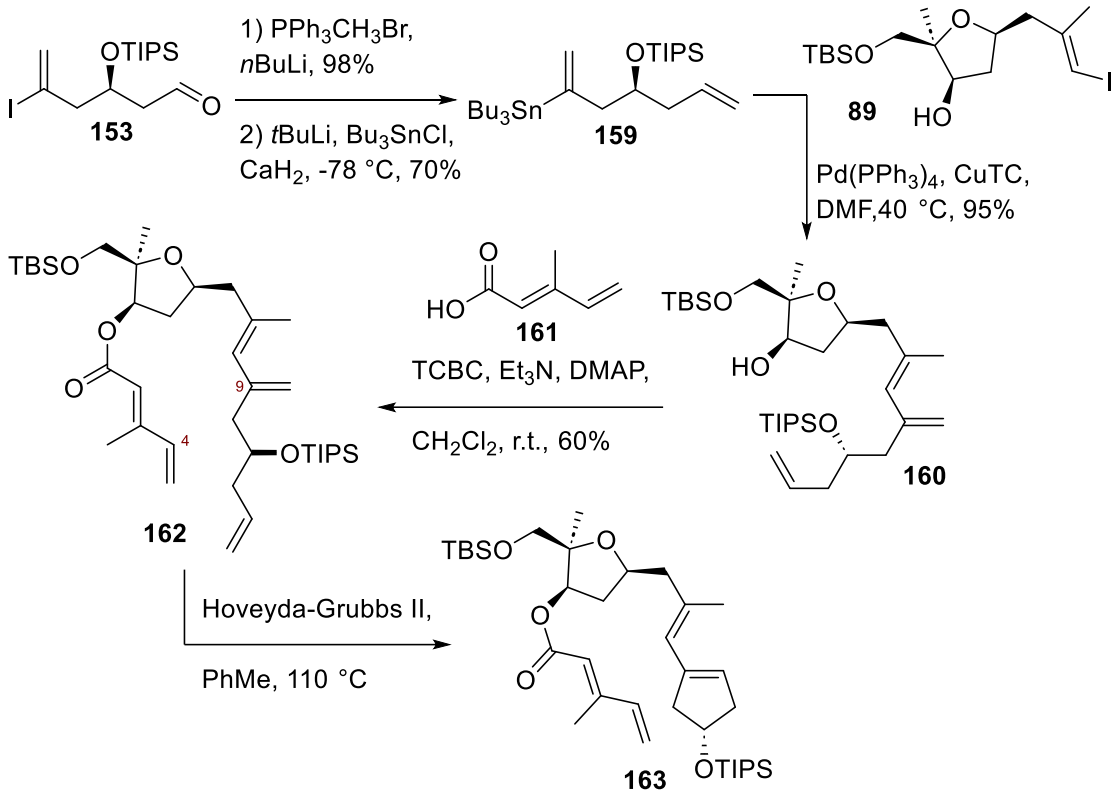

Scheme 3.14. Preparation of Diene 162 and Cyclization to Cyclopentene 163.

3.9. C4-C5 Macro-HWE

While we were unable to form the C2-C3 bond using a macro-HWE approach (see above), we felt that a macrocyclic HWE that formed the C4-C5 bond may still provide access to the desired macrocycle. As noted above, these reactions rely on mild conditions and have been used in late-stage macrocyclization strategies for the synthesis of several complex NPs.[120–122] Thus, we envisioned phosphonate **164** as the macrocyclic precursor (**Scheme 3.15**), which could be accessed *via* esterification of THF **89** with carboxylic acid **165** and Stille-coupling of vinyl stannane **166**.

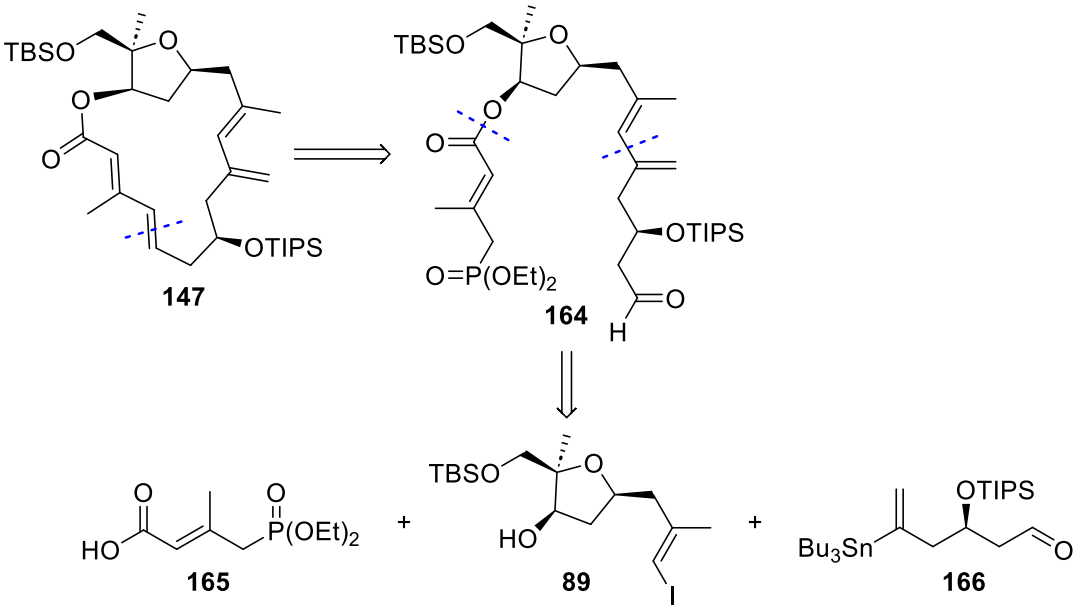

Scheme 3.15. Retrosynthetic Analysis for the C4-C5 Macro-HWE.

In the event, preparation of carboxylic acid **165** proved challenging. Hydrolysis of the methyl ester in **125** led to the degradation of the material and direct conversion of known allylic bromide **167** into phosphonate **165**[130] using standard Arbuzov conditions caused significant *E*/*Z* isomerization. Fortunately, *t*-butyl ester formation could be affected by treatment with *t*-butyltrichloroacetimidate (TBTA), and a subsequent Arbuzov reaction and acidic deprotection afforded **165** (**Scheme 3.16**).

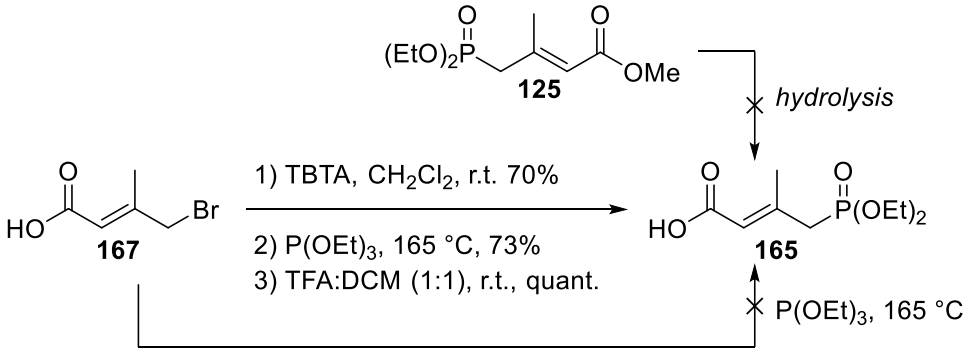

Scheme 3.16. Preparation of Carboxylic Acid 165.

To access **166,** aldehyde **153** was converted into the corresponding dimethyl acetal **168**. I/Sn exchange proceeded smoothly on this substrate, affording vinyl stannane **169**. Unfortunately, the deprotection of **169** presented significant challenges. Brønsted acid conditions caused protodestannylation, while Lewis acidic conditions resulted in

complete degradation. Fortunately, the use of trimethyl silyl triflate/2,6-lutidine, reported by others for the deprotection of acetals,[131,132] afforded the deprotected product **166** in moderate yields (**Scheme 3.17**).

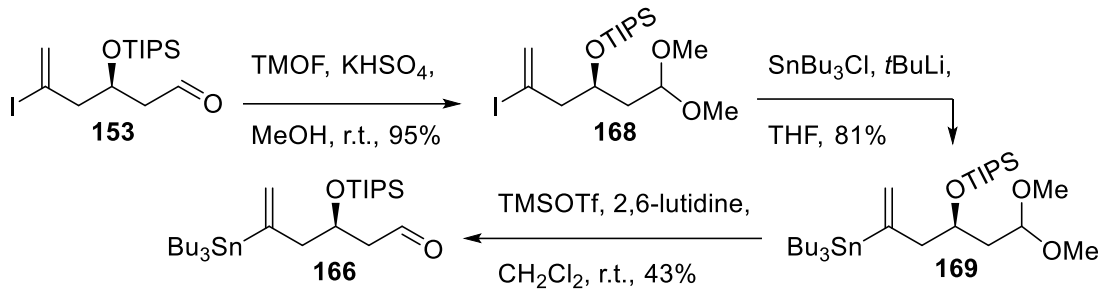

Scheme 3.17. Preparation of Aldehyde 166.

With the coupling partners in hand, the final construction of **164** began (**Scheme 3.18**) with the esterification of carboxylic acid **165** using tetrahydrofuranol **89**. A screen of reaction conditions revealed that Shiina conditions[109–111] caused silyl deprotection, while Steglich[133] and HOBt esterification[134] conditions caused significant C2-*E*/*Z* isomerization of the resulting ester. Mukaiyama esterification conditions[135] only resulted in degradation of the phosphonate and no reaction was observed with the corresponding acetyl chloride. Fortunately, optimized Yamaguchi esterification[44] afforded the ester product **170** with minimal C2-*E*/*Z* isomerization, resulting in a 2.5:1 ratio of *E* and *Z* isomers. Vinyl stannane **166** was then coupled to **170** using Stille conditions to afford phosphonate **164**. Phosphonate **164** proved non-trivial to purify due to its instability on silica, alumina, and C2-modified silica. However, prior treatment of the silica gel with triethyl amine allowed for the purification of this compound with minimal degradation.

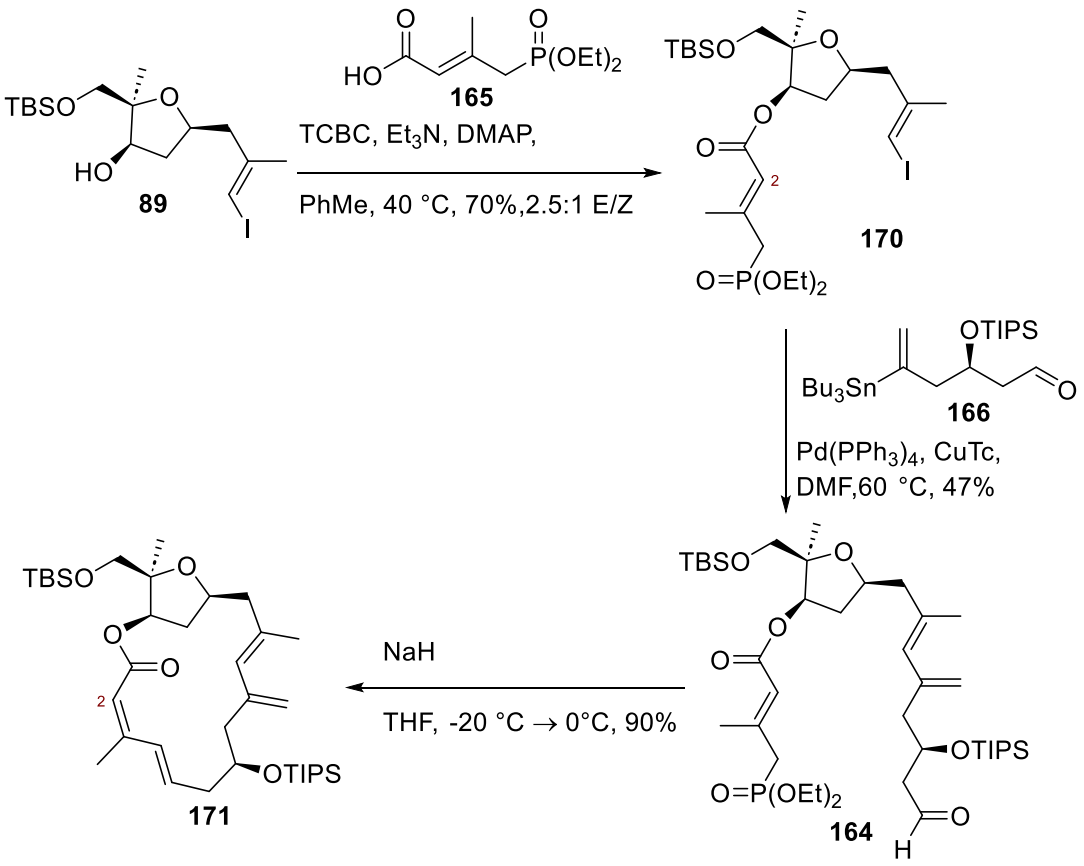

Scheme 3.18. Preparation of Phosphonate 164 and Macrocyclization to Form C2-*Z* Macrocycle 171.

With the synthesis of **164** completed, we assessed the key macrocyclization reaction. Initially, the first conditions evaluated (NaH, THF, -20 °C → 0 °C, entry 1, **Table 3.2**) cleanly afforded the C2-C3 *Z*-macrocycle **171** in >90% yield. The *Z*-macrocycle was presumed to form due to the isomerization of the intermediate anion before ring-closing, which had been observed in analogous esters of this phosphonate.[104] While we were excited to have accessed the macrocycle, extensive efforts to avoid isomerization failed to provide the desired *E,E*- macrocyclic dienoate in appreciable amounts as highlighted in **Table 3.2**. In addition, all attempts to isomerize macrocycle **171** to the target C2 *E*-macrocycle under chemical or photochemical conditions failed.

Table 3.2. Optimization Conditions for the C4-C5 Macro-HWE Reaction

Entry	Base	Solvent	Temperature	Ratio of C2 *Z*/*E*-macrocycle (171:147)
1	NaH	THF	-20 °C → 0 °C	9:1
2	NaH	THF:HMPA (2:1)	-78 °C	NR
3	NaH	THF:HMPA (2:1)	-20 °C → 0 °C	9:1
4	NaH	THF	-50 °C	NR
5	NaH	THF	-30 °C	NR
6	KH	THF	-20 °C → 0 °C	9:1
7[a]	NaH	THF	-20 °C → 0 °C	9:1
8	NaH	THF	40 °C	> 20:1
9	NaH	THF	reflux	> 20:1
10	LiHMDS	THF	-20 °C → 0 °C	8:1
11	LDA	THF	-20 °C → 0 °C	8:1
12	NaH	DMF	-20 °C → 0 °C	> 20:1

[a]addition of 15-crown-5; LiHMDS = Lithium bis(trimethylsilyl)amide, LDA = Lithium diisopropylamine, THF= tettrahysdrofuran, HMPA = Hexamethylphosphoramide, DMF = Dimethylformamide, NR = No reaction

As summarized in **Table 3.2**, the use of HMPA as a cosolvent, which we had used previously to limit the isomerization of the phosphonate during intermolecular HWE reactions, proved ineffective at avoiding isomerization in this case (entries 2 and 3). Model studies suggested that the isomerization of the phosphonate was suppressed at temperatures below -50 °C. However, a careful temperature screen revealed that ring closure only occurred at -20 °C or above (entries 4 and 5). Changing or coordinating the counterion (entries 6 and 7) did not prevent isomerization and raising the temperature above room temperature (entries 8 and 9) enhanced it. Changing the base to LiHMDS or LDA slightly limited the isomerization, affording the products in an 8:1 *Z*/*E* ratio, but also caused significant degradation (entries 10-11). Finally, changing the solvent to DMF resulted in only *Z*-isomer formation (entry 12). These results indicate that the formation of the *Z*-isomer is significantly favoured over the formation of the *E*-isomer. We also assessed a screen of conditions to isomerize *Z*-macrocycle **171** to the desired *E*-macrocycle **147**, however, this strategy proved ineffective. With these disappointing results and the challenges faced in the preparation of the material, we turned back to a C9-C10 macro-Stille strategy to better understand the reactivity of the macrocycle with the goal of limiting the previously observed degradation regularly present in our previous macro-Stille efforts.

3.10. Second Generation C9-C10 Macro-Stille

Noting that we observed the formation of the C2-C3 *Z*-macrocycle at -20 °C in the C4-C5 macro-HWE approach, we theorized that it may be possible to close the ring with macrocyclization reactions other than a macro-HWE at room temperature or below. In the previous macro-Stille efforts (Sections 3.5 and 3.6), we generally observed no reaction at room temperature and degradation once the reaction mixture was heated. However, we hypothesized that if a macro-Stille cyclization could be performed at room temperature, we would avoid the degradation observed at higher temperatures. We decided to explore these prospects for the formation of the C9-C10 bond. The C9-C10 macro-Stille precursor **172a** was easily accessed from a simple revision in the order of the steps of the preparation of macro-HWE precursor **170**. Thus, coupling aldehyde **166** to phosphonate **170** under HWE conditions afforded the macro-Stille precursor **172a** (**Scheme 3.19**). Despite extensive optimization, the C2-*E*/*Z* selectivity of this reaction could not be improved beyond 1.3:1 C2-*E*/*Z*. Despite this, the two isomers, C2-*E*, **172a**, and C2-*Z*, **172b**, were readily separable by column chromatography, and a sufficient amount of material was prepared for the assessment of the macro-Stille cyclization.

Surprisingly, the C2 *Z*-isomer, **172b,** formed the corresponding Z-macrocycle **171** under palladium-catalyzed conditions ($Pd(dppf)Cl_2$, CuTc, DMF, 60 °C) in moderate yields (**Scheme 3.19**). However, treatment of the *E*-isomer **172a** with the same conditions resulted in degradation. **172a** proved unreactive under Stille conditions at room temperature and the evaluation of several reaction temperatures indicated that elevating the temperature only caused degradation, as previously observed. Changing the Pd catalyst or reaction time resulted in either no reaction or degradation. The examination of the compatibility of each reagent with **172a** while heating suggested that the degradation resulted from a Pd(0) species. Therefore, Pd-free, Cu(I) and Ni(II) systems were assessed, but only protodestannylation was observed.

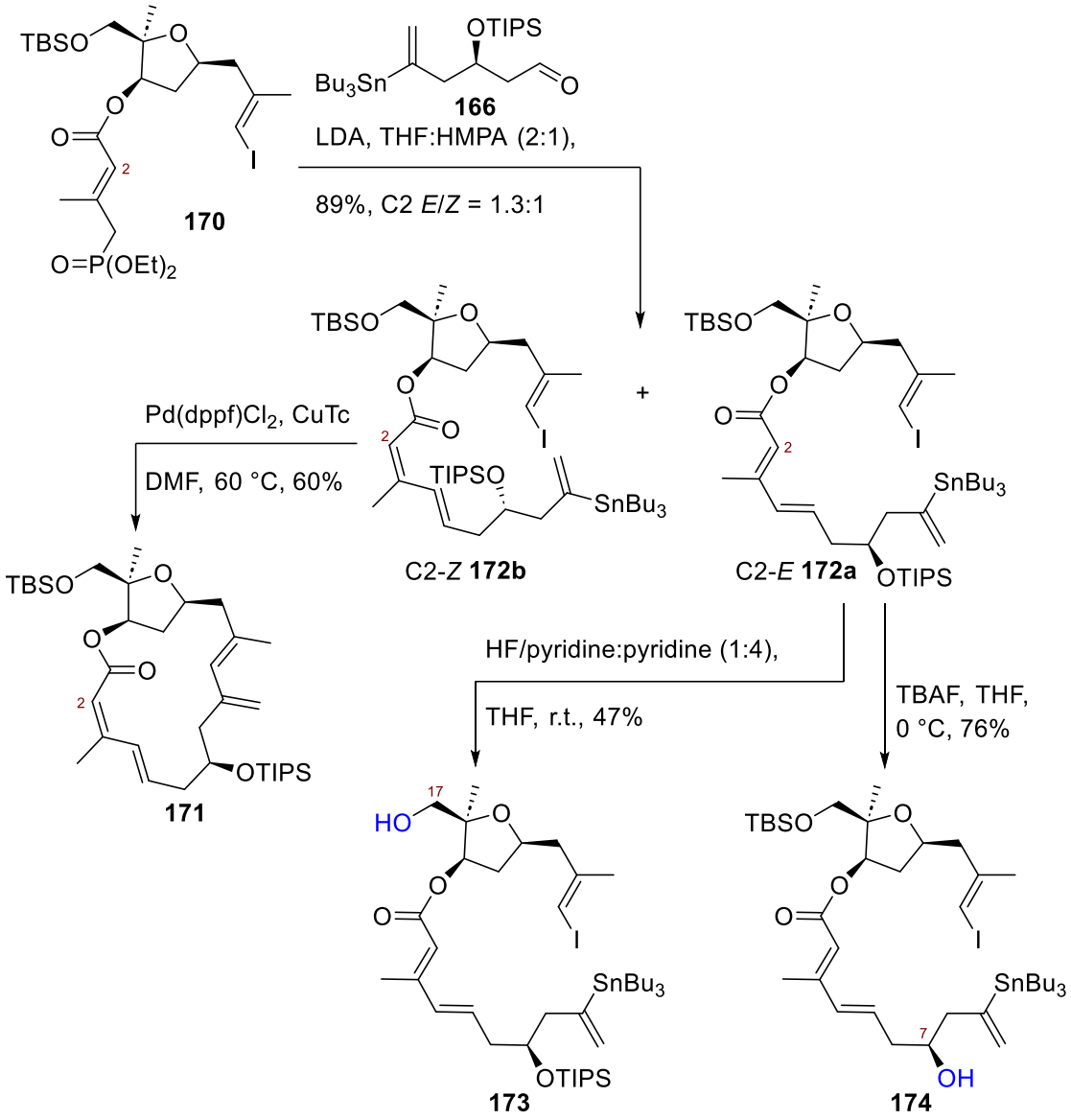

Scheme 3.19. Preparation of Vinyl Stannanes 172a, 172b and Deprotected Vinyl Stannanes 173 and 174.

As **172a** was unreactive at room temperature, we theorized that if we were able to increase the reactivity of the substrate, we may achieve a macro-Stille reaction at room temperature and avoid degradation. A change in silyl protecting groups can have a significant impact on the reactivity in complex molecule synthesis,[37] and it was deemed appropriate to assess analogues of **172a** that lack bulky silyl protecting groups. Towards this goal, we examined the deprotection of **172a**. Here we found that HF/pyridine with added pyridine allowed for selective deprotection of the C17 TBS silyl ether to afford **173**

(**Scheme 3.19**) while, surprisingly, cold (0 °C) TBAF deprotection conditions enabled selective deprotection of the C7 TIPS silyl ether to afford **174** (**Scheme 3.19**).

With **173** and **174** in hand, we assessed room-temperature macro-Stille cyclization conditions on both substrates. Treatment of both substrates with Pd(0) and Pd(II) catalysts at room temperature resulted in protodestannylation and degradation, while the use of only Cu(I) at room temperature resulted in protodestannylation. While we could not form the desired macrocycle, this change in the protection of the substrate revealed that the reactivity increased if the silyl-protecting groups were removed, as mono-protected **173** and **174** underwent degradation at room temperature while the silyl-protected variant **172a** proved unreactive under the same conditions. Based on these results, we decided to return to the original macrolactonization strategy with a change in the protecting groups.

3.11. Second Generation Macrolacontization

In the original macrolactonization approach (Section 3.4), we noted a lack of reactivity of the seco acid and attributed this to steric congestion around the THF ring. Therefore, we theorized that a change in the protecting group at C17, adjacent to the THF ring, may increase the reactivity of the seco acid and facilitate macrocyclization. As a proof-of-concept experiment, we prepared the C17-OMe seco acid **178**, as a representative less bulky C17 protecting group (**Scheme 3.20**). The C17 OMe-protected THF **176** was prepared by methylation of THF **175**. The reaction of aldehyde **166** and phosphonate **125** under HWE conditions, afforded vinyl stannane **178**. Stille reaction of **177** and **178** followed by hydrolysis of the methyl ester afforded seco acid **175** in a 3:1 mixture of the *E*/*Z* isomers of the C2 alkene.

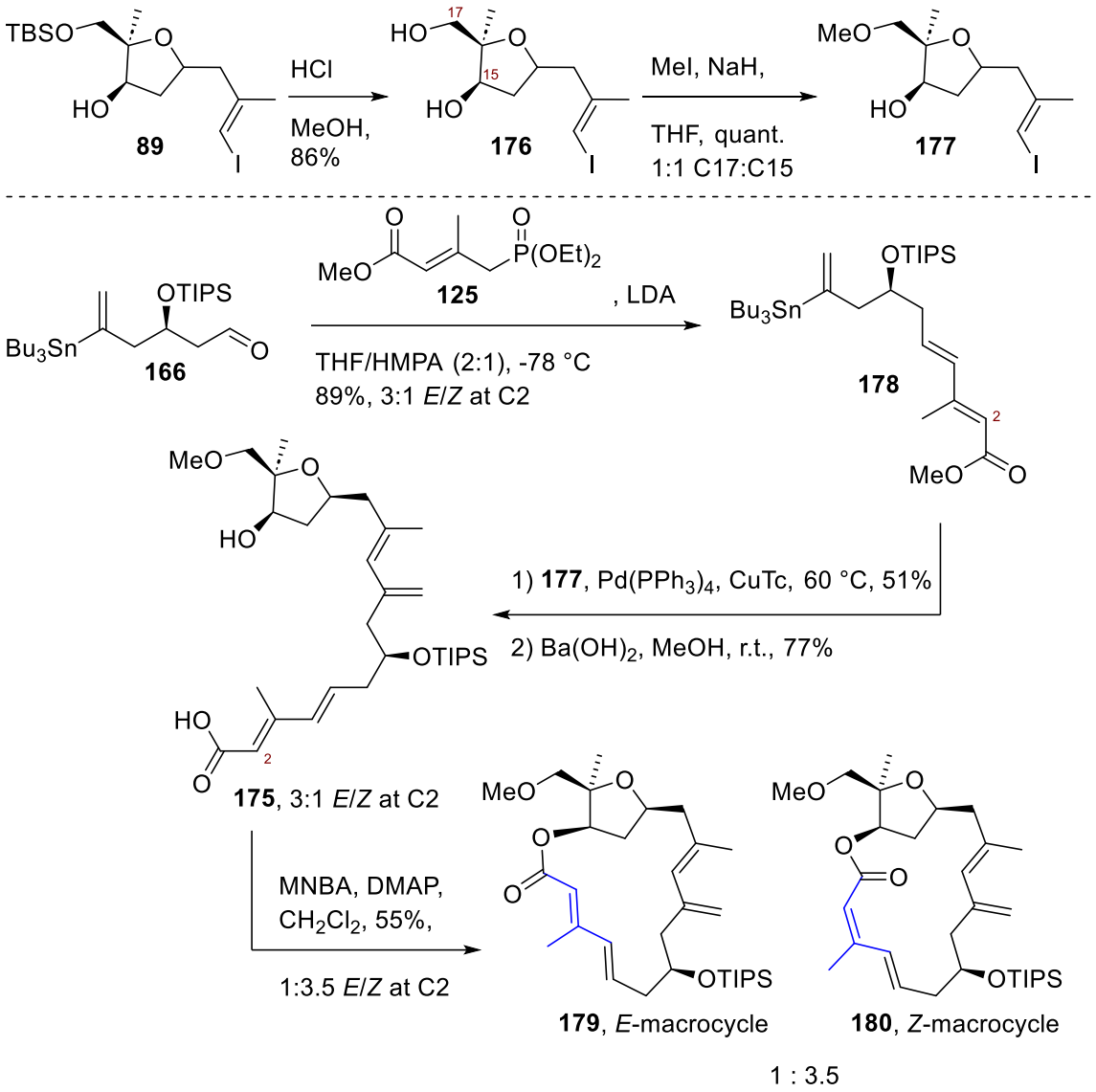

Scheme 3.20. Preparation of Proof-Of-Concept Seco Acid 175 and Cyclization to a 1:3.5 Mixture of *E*- and *Z*-macrocycles 179 and 180.

Excitingly, under Shiina macrolactonization conditions,[109] **175** closed to afford a 1:3.5 ratio of the desired C2-*E*macrocycle **179** to the C2-*Z* macrocycle **180** in a 55% overall yield (**Scheme 3.20**, ^{1}HNMR spectrum of both products mixed shown in **Figure 3.3**). This represents approximately 50% *E/Z* isomerization from the starting material, which was a 3:1 mixture of *E*/*Z* isomers and is significantly less than the >90% isomerization observed in the C4-C5 macro-HWE assessment. This proof-of-concept experiment was critical in showing that a less hindered protecting group at the C17 position may allow for a successful macrolactonization. Therefore, we set out to find a suitable protecting group

that would be compatible with macrolactonization. Notably, we also assessed a macrolactonization strategy without a C17 protecting group, but this resulted in the exclusive formation of a lactone at the C17 position rather than the desired C15 position.

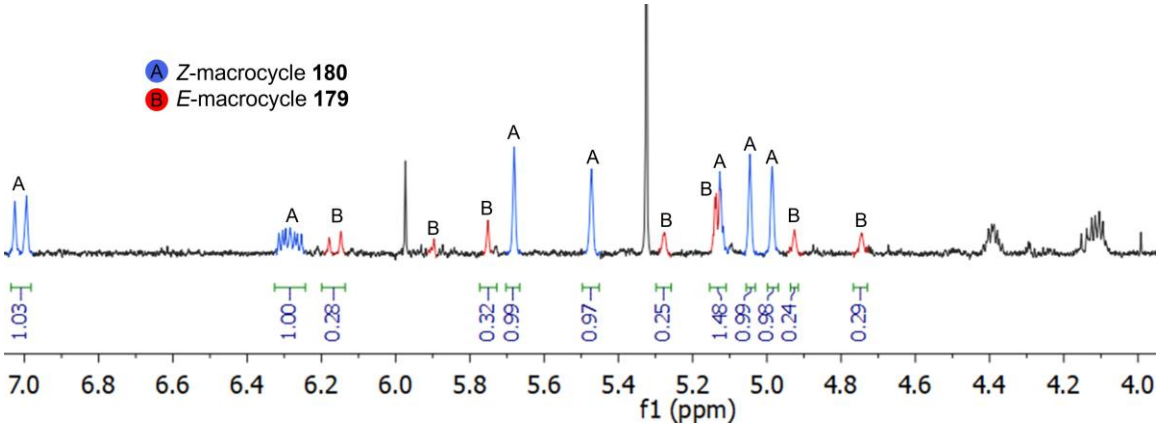

Figure 3.3. The ^{1}HNMR spectrum of a mixture of the *E*- and *Z*-macrocycles 179 and 180 from 4.0 to 7.0 ppm. Peaks associated with 180 are marked in blue and with an A. Peaks associated with 179 are marked in red and with a B.

Moving forward, there were two key considerations when deciding which protecting group to use at the C17 position: i) the protecting group should be smaller than a TBS group and stable to basic conditions and palladium-based coupling conditions; and, ii) mild deprotection conditions would be required due to the observed sensitivity of the macrocyclic precursors. Based on these requirements we opted to first assess the macrolactonization with a trimethylsilylethoxymethyl (SEM) protection. This group has been reported to be removed under mild Lewis acidic or fluoride conditions.[136,137]

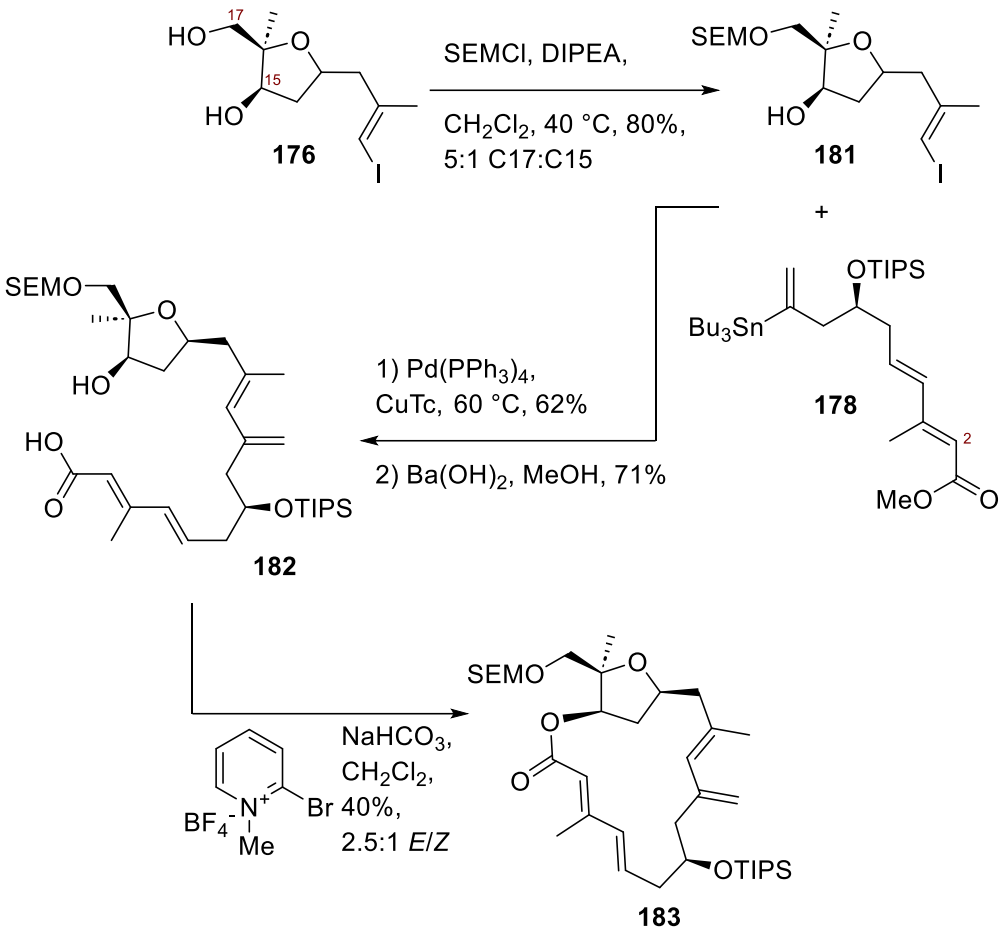

Scheme 3.21. Preparation of Seco Acid 183 and Cyclization to Macrocycle 184.

THF **176** was converted to the SEM-protected THF **181**, which was then coupled with vinyl stannane **178** and treated with base to afford seco acid **182**. With **182** in hand, we began optimization of the macrolactonization to form macrocycle **183** (**Scheme 3.21**) without significant E/Z isomerization. As highlighted in **Table 3.3**, the previously used Shiina macrolactonization conditions afforded the same mixture of C2 *E*- and *Z*-macrocycles as previously observed. A careful assessment of the equivalents of 4-dimethylaminopyridine (DMAP) made it clear that at least 1 equivalent of DMAP was required but was likely also the main source of *E*/*Z* isomerization (entries 1 and 2). Therefore, we assessed several conditions that did not require DMAP. The use of 4-(trifluoromethyl)benzoic anhydride (TFBA), catalyzed by $TiCl_2(ClO_4)_2$,[111] led to the degradation of the material (entry 3). We observed no reaction under the Corey-Nicolaou macrolactonization conditions (entry 4),[138] but the Trost macrocyclization conditions[47] afforded the desired *E*-macrocycle as the major product. However, the yield of this

reaction could not be improved beyond 21% (entry 5). Inspired by Smith and coworker's synthesis of sorangicin A,[139] we assessed the Evans-modified Mukaiyama conditions.[135,140] These conditions, which use the reagent 2-chloro-1-methyl pyridinium iodide, led to a yield of 33% of the desired macrocycle, though still with significant isomerization (entry 6). Noting that Smith *et al.* had observed the iodide anion from the reagent causing isomerization and their use of the tetrafluoroborate (BF_4^-) counterion to prevent this isomerization,[139] we prepared the corresponding Mukaiyama reagent with a BF_4^- counterion. The reaction of the seco acid with this prepared reagent led to a significant reduction in isomerization, affording an *E*/*Z* ratio of 2.5:1 from a 3:1 *E*/*Z* of the starting material. However, the yield dropped significantly to 8% (entry 7). Fortunately, the use of the commercially available 2-bromo-1-methyl pyridinium tetrafluoroborate led to the formation of macrocycle **183** with an *E*/*Z* ratio of 2.5:1 in a 40% yield (entry 8, **Scheme 3.21**).[139]

Table 3.3. Macrolactonization Optimization Conditions

Entry	Conditions	C2-*E*/*Z* ratio (yield)
1	MNBA, DMAP (1 eq.), CH_2Cl_2	1:3.5 (55% of C2-*Z*)
2	MNBA, DMAP (0.1-0.5 eq.), CH_2Cl_2	NR
3	TFBA, $TiCl_2(ClO_4)_2$, CH_2Cl_2	NA
4	2,2'-dipyridal disulfide, PPh_3, PhMe	NR
5	Ethyl ethynyl ether, $[RuCl_2(p\text{-cymene})]_2$, CSA	2:1 (21%)
6	2-chloro-1-methyl pyridinium iodide, $NaHCO_3$, CH_2Cl_2	1:1 (33%)
7	2-chloro-1-methyl pyridinium tetrafluoroborate, $NaHCO_3$, CH_2Cl_2	2.5:1 (8%)
8	2-bromo-1-methyl pyridinium tetrafluoroborate, $NaHCO_3$, CH_2Cl_2	2.5:1 (40%)

MNBA = meta-nitrobenzoic anhydride, TFBA = 4-trifluoromethylbenzoic anhydride, NR = No reaction

At this point, it was quite disheartening to find that the SEM protecting group could not be removed. No reaction of the SEM-protected **183** was observed under mild Lewis acidic conditions or buffered fluoride conditions. Mild Brønsted acidic conditions led to TIPS deprotection while non-buffered fluoride, Lewis acidic, or Brønsted acidic conditions led to degradation. Despite our failure to remove the SEM group, this study highlighted that the use of a smaller C17-protecting group would allow for macrolactonization. Thus, undaunted, we decided to explore this chemistry using a *p*-methoxybenzyloxymethyl (PMBM) protecting group at C17, which has been shown to undergo mild oxidative deprotection (**Scheme 3.22**).[141]

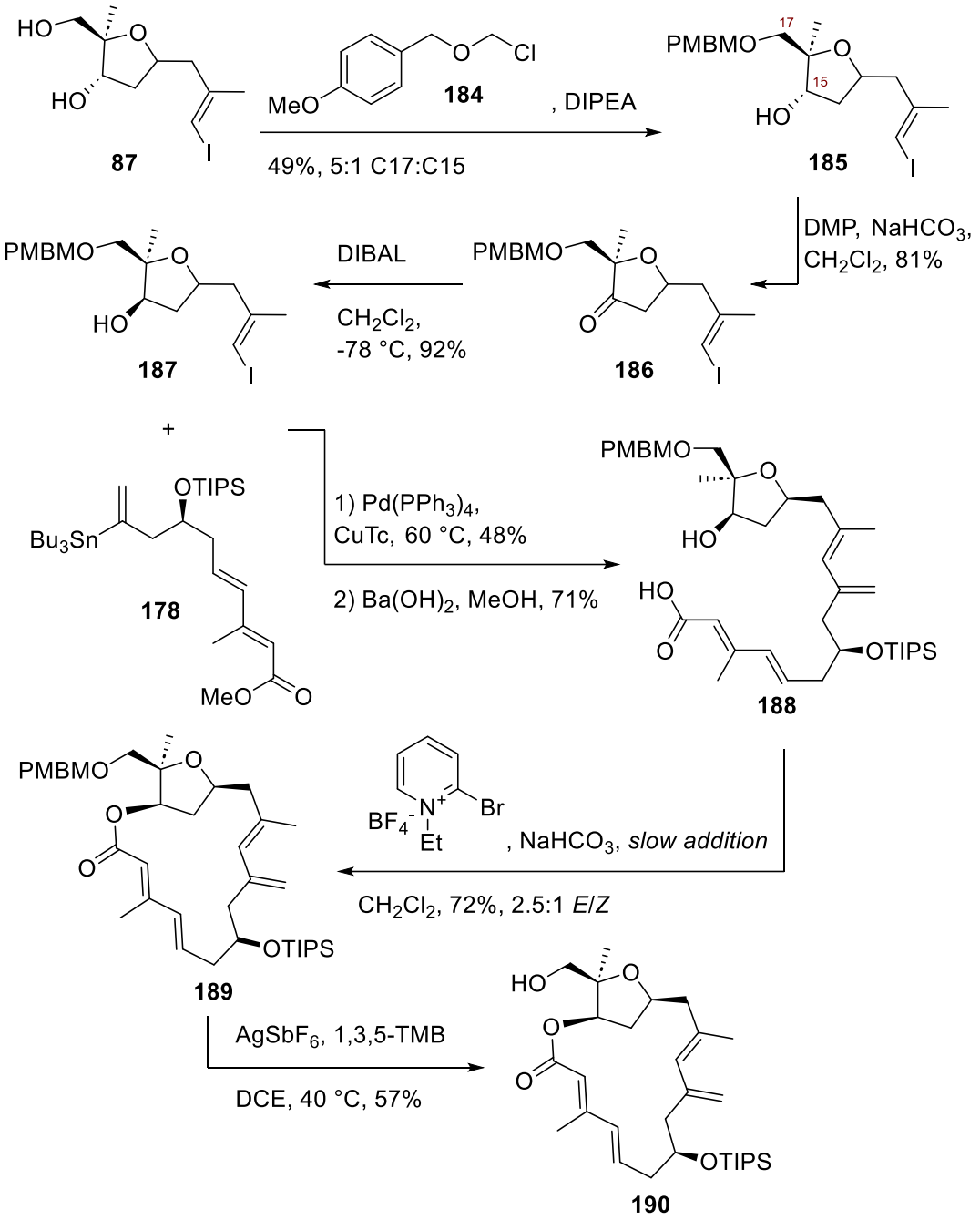

Scheme 3.22. Preparation of PMBM-protected Macrocycle 189 and Deprotection to Afford Macrocycle 190.

Conversion of THF **87** into the PMBM-protected THF **185** using the reported reagent PMBMCl (**184**)[142] and inversion of the C15 alcohol *via* DMP oxidation to **186** and DIBAL reduction afforded THF **187**. Coupling of this product to **178** followed by ester hydrolysis afforded PMBM-protected seco acid **188** (**Scheme 3.22**). From here, we reassessed our macrolactonization conditions and found that the use of the modified

Mukaiyama reagent, 2-bromo-1-methyl pyridinium tetrafluoroborate, gave similar results as observed in the SEM-protected system, affording macrocycle **189** in a 41% yield. Noting the major by-product in the crude reaction mixture was the acid anhydride from the homocoupling of 2 equivalents of the seco acid, we examined further dilution of the reaction and added the seco acid v*ia* slow addition. These modifications afforded the macrocycle **189** in 72% yield with an E/Z ratio of 2.5:1 at the C2 alkene position. After considerable effort to reach this point, this was an outstanding result.

Disappointingly, deprotection of the PMBM group using standard DDQ conditions led to complete degradation. Optimizing for temperature, time, equivalents of DDQ or the pH of the buffer used in the reaction led to no change in this outcome. Cerium ammonium nitrate[143] and $AlCl_3$ conditions[144] also led to degradation, while no reaction was observed under $MgBr_2$ conditions.[145] However, the use of $AgSbF_6$ along with 1,3,5-trimethoxybenzene (1,3,5-TMB), reported for the deprotection of PMB protecting groups,[146] afforded deprotected macrocycle **190** in a 57% yield.

3.12. Comparison of Synthetic Products with Phormidolide A

Comparison of NMR spectral data derived from macrocycle **190** with that from the NP showed a close similarity between the synthetic material and the macrocyclic portion of the NP. The comparison of the ^{1}H NMR spectroscopic data derived from the synthetic macrocycle **190** and the macrocyclic portion of phormidolide A is highlighted in **Table 3.4**, with the numeric labelling of both compounds and ^{1}HNMR spectrum of **190** presented in **Figure 3.4**.

Table 3.4. Comparison of ^{1}HNMR Values for the Macrocyclic Portion of Phormidolide A (28) and the Synthetic Macrocycle, 190.

Position	δH Phormidolide A (28)	δH synthetic macrocycle (190)	|Δ| of δH values
2	5.80	5.72	0.08
4	6.20	6.14	0.06
5	5.88	5.87	0.01
6	2.85	2.82	0.03
	2.13	2.15	0.02
7	4.05	4.11	0.06
8	2.46	2.47	0.01
	1.81	1.83	0.02
10	5.28	5.25	0.03
12	2.33	2.30	0.03
	2.58	2.57	0.01
13	4.48	4.50	0.02
14	1.57	1.58	0.01
	2.33	2.30	0.03
15	5.15	5.13	0.01
34	2.07	2.08	0.01
35	4.76	4.73	0.03
	4.98	4.91	0.07
36	1.58	1.59	0.01
37	1.19	1.26	0.07

As summarized in Table 2.4, the difference between all δ_H values is in all cases less than 0.08 ppm, indicating that the synthetic macrocycle shares significant similarity with the NP. The largest differences in δ_H values are seen near the silylated C7 alcohol and near the C17 alcohol where the side chain connects in the NP, supporting the stereochemical assignment around the THF ring and the reassignment of the C7 position.

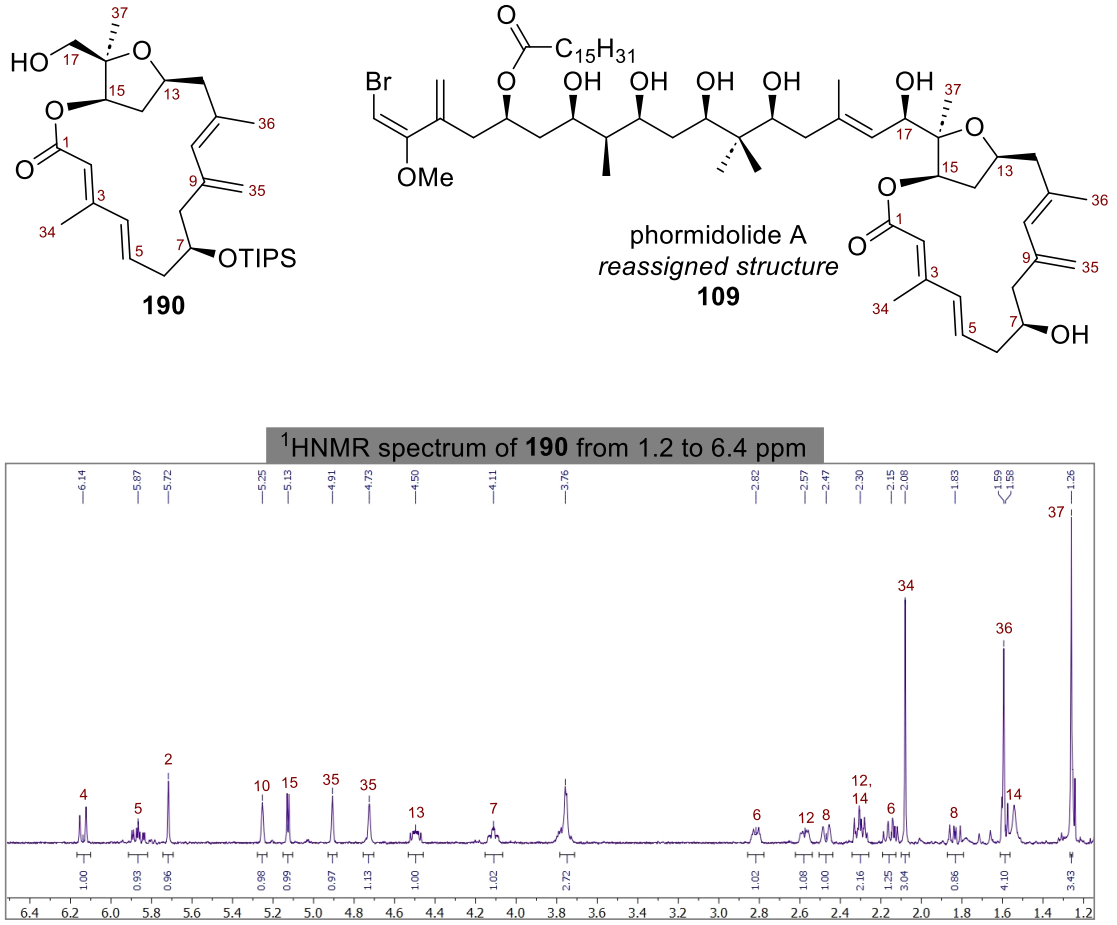

Figure 3.4. The numeric labelling for macrocycle 190 and the structure of the proposed stereochemical reassignment of phormidolide A, 109 along with the ^{1}HNMR spectrum for 190 in $CDCl_3$ from 1.2 to 6.4 ppm with relevant peaks labelled.

3.13. Summary

In conclusion, the synthesis of the phormidolide A macrocycle has been completed. Assessment of several macrolactonization efforts revealed that i) macro-Stille conditions generally cause degradation before cyclization, ii) formation of the C2-C3 or C4-C5 bond is not possible via macro-HWE type conditions, and iii) large protecting groups on the C17 alcohol prevent macrolactonization and limit the reactivity of macrocyclic precursors.

Based on these insights, we reassessed macrolactonization efforts with smaller protecting groups. Importantly use of a C17 methyl ether as an alcohol protecting group revealed that the macrocycle could be formed under relatively mild conditions, though

significant C2-C3 alkene *E*/*Z* isomerization was observed. Ultimately, both the SEM and PMBM protection allowed for the ring formation using a modified Mukaiyama reagent with minimal C2-C3 alkene *E*/*Z* isomerization. Finally, we found that the PMBM group could be removed without causing degradation of the macrocycle, affording the desired deprotected macrocycle **190**. Comparison of the data derived from macrocycle **190** with that of the NP revealed close similarities between both materials, supporting the proposed structural assignment for **109**. With macrocycle **190** in hand and confidence in the stereochemical assignment of the phormidolide A macrocycle, we turned to completing the total synthesis of phormidolide A by linking the side chain to the macrocycle, the efforts of which are outlined in Chapter 4.

Chapter 4. Studies Towards the Completion of the Total Synthesis of Phormidolide A

4.1. Introduction

Many naturally occurring THF-containing macrolides contain side chains that are attached to the THF ring and extend out from the macrocyclic core.[33] As detailed by Whitty *et al.*,[147] often the binding mode of these macrolides involves the side- or face-on binding of the macrolide to protein surface along with the insertion of the side chain into clefts or pockets adjacent to the macrocycle binding location on the protein. Thus, the side chain plays a critical role in protein binding and ultimately the biological activity of the natural product (NP). This is evidenced in both the haterumalide (**10**) and phormidolide (**29** and **30**) family of NPs where a significant reduction in biological activity was observed for synthetic macrocycles that lacked the natural side chain.[53,58,148]

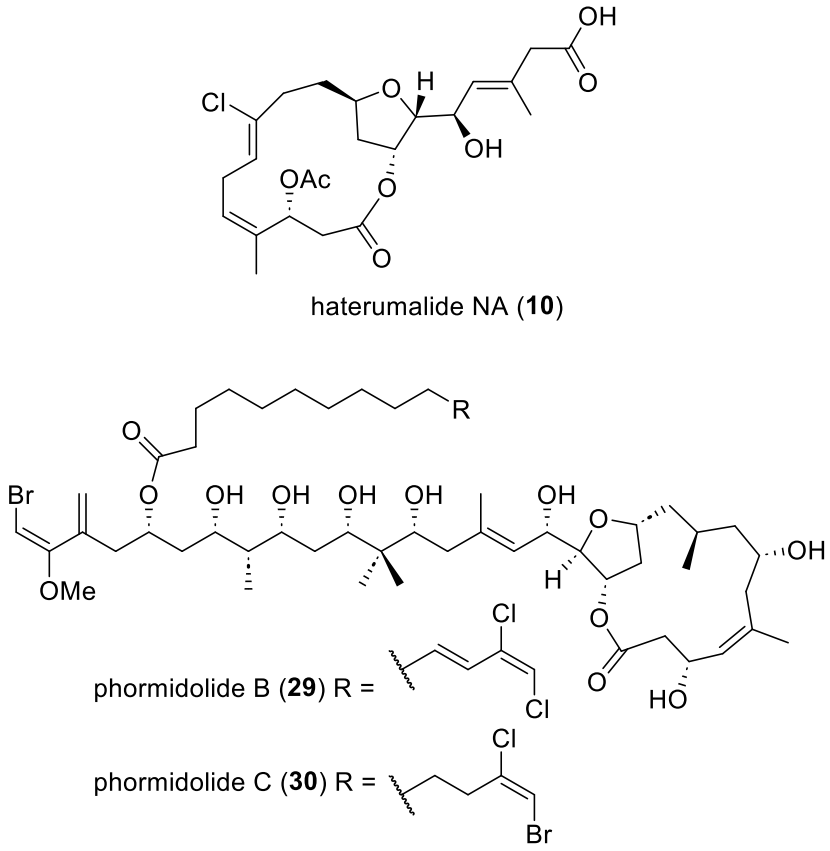

Figure 4.1. Haterumalide NA (10) and phormidolides B and C (29 and 30).

From the reported syntheses of THF-containing macrolides, several strategies have been used to append the side chain.[33,149–151] The most common approach is to attach the side chain after macrocyclization through the use of a Nozaki–Hiyama–Kishi (NHK) coupling,[152–154] which is a mild chromium-mediated coupling between a vinyl halide and an aldehyde. For example, Álvarez *et al.* employed this strategy in their efforts towards the synthesis of phormidolides B-D. As discussed in Chapter 1 (**Scheme 1.10**), this group prepared macrocycle **54**[58] *via* a Shiina macrolactonization and, following deprotection and oxidation, accessed macrocycle **191**. Vinyl iodide **194** was prepared in 7 steps from vinyl iodide **192** and silyl enol ether **193**. Coupling of vinyl iodide **194** to macrocyclic aldehyde **191** using NHK conditions unfortunately only afforded the undesired diastereomer **195** in low yield (**Scheme 4.1**). Elaboration of **195** to the NP proved unsuccessful in this case.[54]

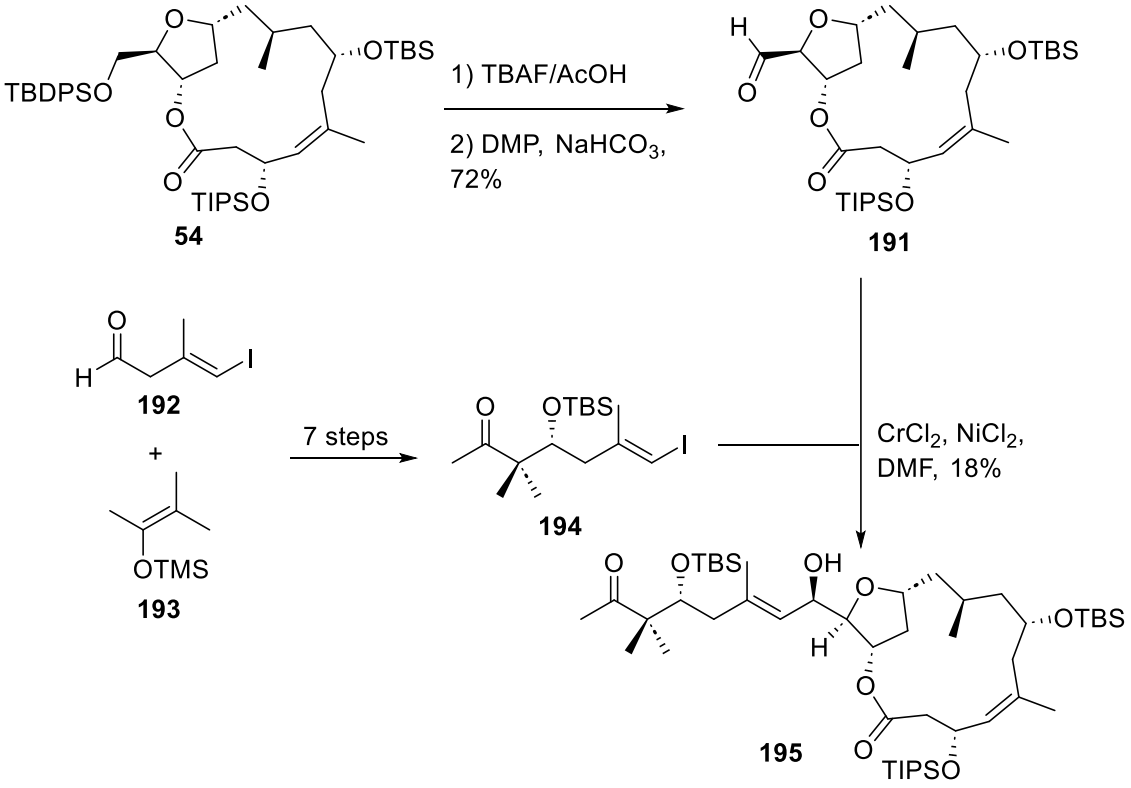

Scheme 4.1. Coupling of Side Chain 194 to the Macrocyclic Aldehyde 191 in the Efforts Towards the Synthesis of Phormidolide B and C.

As presented in Chapters 2 and 3, in our studies towards the total synthesis of phormidolide A, we prepared segments of the phormidolide A side chain and, in collaboration with several other research groups, proposed a stereochemical reassignment of phormidolide A.[93] In addition, we completed the synthesis of the

macrocyclic fragment of phormidolide A, **190**. With the macrocycle in hand, and targeting a completed synthesis of the NP, we set out to assess the coupling of the side chain to the macrocyclic core.

4.2. Linking the Side Chain to the Macrocycle of Phormidolide A

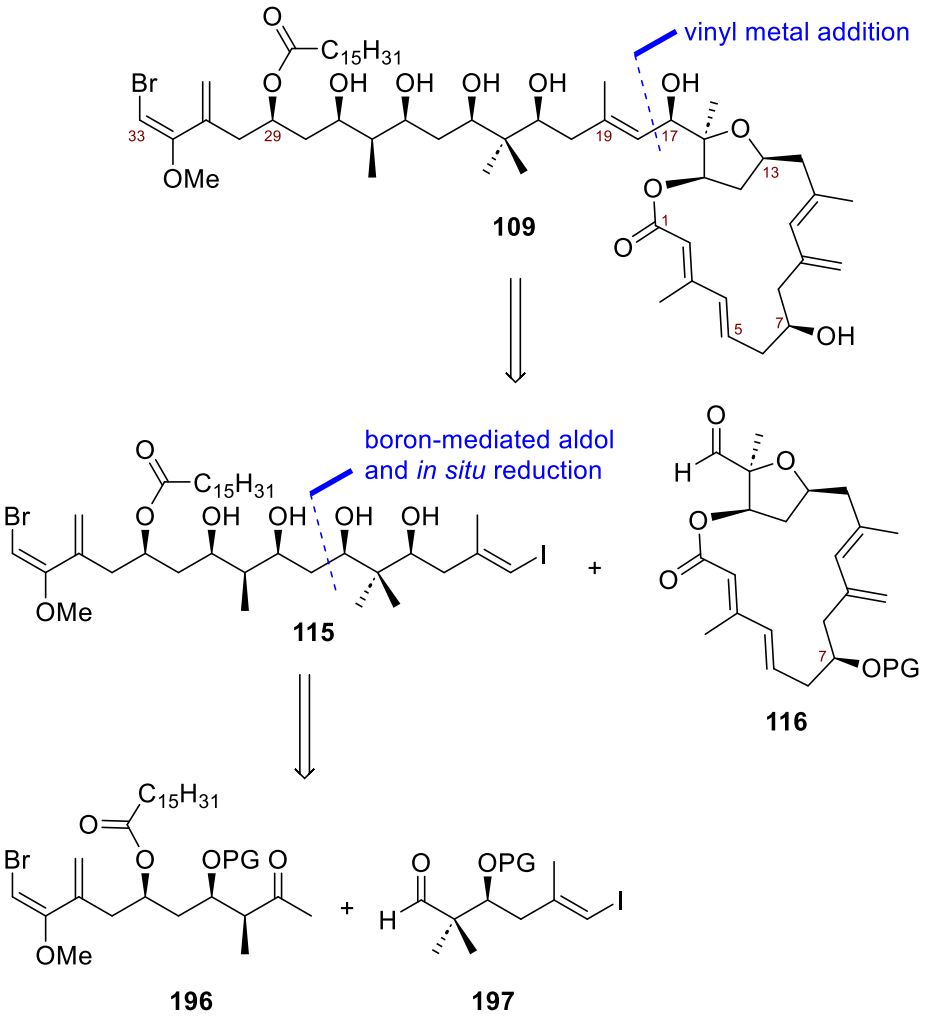

Scheme 4.2. Retrosynthetic Analysis of Phormidolide A and Side Chain 115.
PG = protecting group

Based on the initial retrosynthetic analysis of phormidolide A (**109**, **Scheme 4.2**), we envisioned two key synthetic targets, side chain **115**, to be constructed by the Paterson group, and macrocycle **116**, to be constructed by the Britton group. Furthermore, we

envisioned side chain **115** could be prepared *via* a boron-mediated aldol reaction[99,155] between methyl ketone **196** and aldehyde **197** (**Scheme 4.2**).

4.2.1. Macrocyclic Oxidation

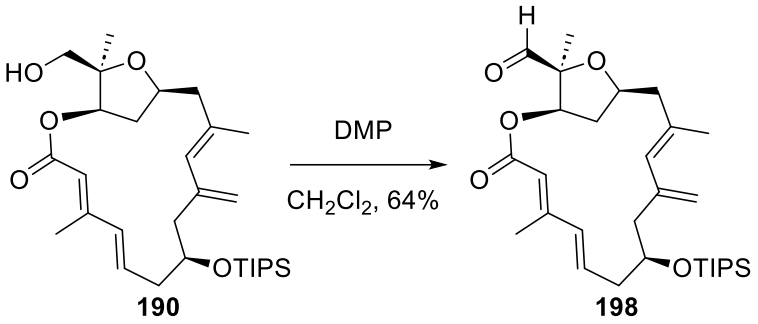

190 **198**

Scheme 4.3. Oxidation of Macrocycle 162.

With our successful synthesis of macrocycle **190** (Chapter 3), we envisioned coupling the side chain to this macrocycle, which could be accomplished *via* 1,2-addition of a suitable organometallic to macrocyclic aldehyde **198** (**Scheme 4.3**). To access the aldehyde, several oxidation reactions were explored and are summarized in **Table 4.1**. Swern oxidation conditions[156] (entry 1) afforded the desired aldehyde in 41% yield but also caused *E*/*Z* isomerization of the C2-C3 alkene. TEMPO/BAIB oxidation conditions afforded aldehyde **198** in a 38% yield (entry 2) and PDC conditions caused significant degradation (entry 3). While the Ley oxidation[157] provided the desired aldehyde with the least amount of by-products, the isolated yield of **198** was still less than 50% (entry 4).

Dess–Martin periodinane (DMP) oxidation using commercial DMP only afforded degradation products and no formation of **198** was observed. However, analysis of the commercial reagent by ^{1}H NMR spectroscopy indicated that it contained several unknown contaminants. Treatment of the commercial DMP with acetic anhydride and acetic acid at 85 °C and recrystallization of the product[158] afforded a much cleaner reagent by ^{1}H NMR spectroscopic analysis. With recrystallized DMP, treatment of macrocycle **190** with 2 equivalents of DMP resulted in 50% conversion at which point the reaction failed to progress further (entry 5). The use of 4 equivalents of DMP, buffered by $NaHCO_3$, afforded aldehyde **198** in 46% yield (entry 6) and switching to pyridine as a base lowered the yield to 30% (entry 7). The use of unbuffered DMP afforded the highest yield of 64% (entry 8). Notably, any attempt to purify aldehyde **198** by column chromatography led to partial

degradation and loss of material. However, dilution of the reaction with a 1:1:1 mixture of saturated aqueous $NaHCO_3$ to saturated aqueous $Na_2S_2O_3$ solution to water followed by vigorous stirring resulted in the removal of all by-products and reagents from the DMP oxidation procedure without the need for column chromatography. With **198** in hand, we assessed the coupling of the C18-C23 side fragment **199**, prepared similarly to the C18-C23 fragments outlined in Chapter 2 (**Scheme 2.2**).

Table 4.1. Oxidation Optimization of Macrocycle 190

Entry	Conditions	Yield (%)
1	DMSO (4 eq), $(COCl)_2$ (3 eq), Et_3N (6 eq), CH_2Cl_2 -78 °C	41%[a]
2	TEMPO, BAIB, CH_2Cl_2, r.t.	38%
3	PDC, CH_2Cl_2, r.t.	NA
4	TPAP, NMO, MeCN, r.t.	45%
5	DMP (2 eq), $NaHCO_3$, CH_2Cl_2, r.t.	NA[b]
6	DMP (4 eq), $NaHCO_3$, CH_2Cl_2, r.t.	46%
7	DMP (4 eq), pyridine, CH_2Cl_2, r.t.	30%
8	DMP (4 eq), CH_2Cl_2, r.t.	64%

[a]13% C2 *E*/*Z* isomerization; [b]50% conversion; Eq = equivalents, TEMPO = (2,2,6,6-Tetramethylpiperidin-1-yl)oxyl, BAIB = (Diacetoxyiodo)benzene, PDC = pyridinium dichromate, TPAP = tetrapropylammonium perruthenate, NMO = N-Methylmorpholine N-oxide, DMP = Dess–Martin periodinane

4.2.2. NHK Addition

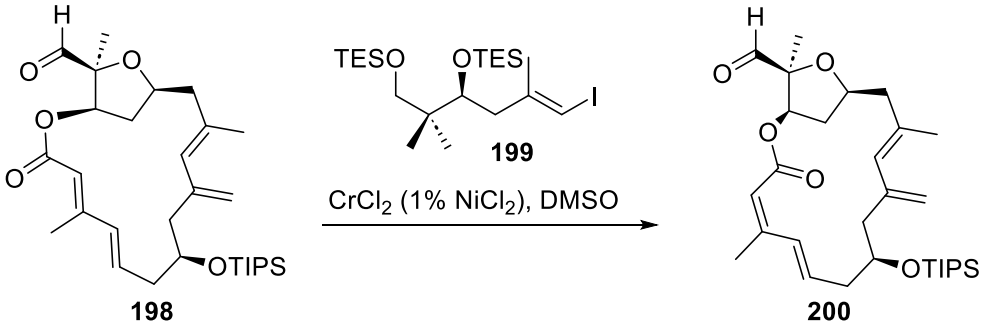

Scheme 4.4. Addition of C18-C23 Side Chain Fragment 199 to Macrocyclic Aldehyde 198 Using NHK Conditions.

Noting that the NHK reaction has often been used to attach side chains to macrocyclic aldehydes,[33] we assessed these conditions to attach side chain fragment **199** to macrocyclic aldehyde **198** (**Scheme 4.4**). However, the major product recovered from this reaction was the C2-C3 *E*/*Z* isomerized macrocyclic aldehyde **200**. The observed

isomerization may be due to free chloride ions in solution, as we previously observed iodide ions caused C2 *E*/*Z*-isomerization during the previous macrocyclization studies.

4.2.3. Vinyl Lithium Addition

In our efforts outlined in Chapter 2, we were able to successfully append a C18-C23 side chain fragment to a tetrahydrofurfural fragment through vinyl lithium and vinyl magnesium addition (**Scheme 2.4**).[81,96] Thus, we set out to examine this strategy for the preparation of **201** from side chain fragment **199** and macrocyclic aldehyde **198** (**Scheme 4.5**). Unfortunately, generating a vinyl lithium species by treatment of **199** with *t*BuLi and subsequent reaction with aldehyde **198** at -78 °C resulted in complete degradation of the macrocyclic aldehyde **198**. Therefore, we turned to assessing the related vinyl magnesium reaction with **198**.

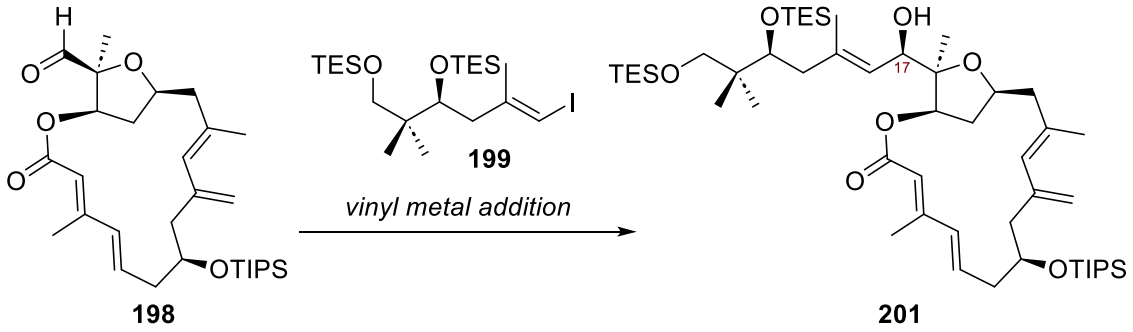

Scheme 4.5. Addition of C18-C23 Side Chain Fragment 199 to Macrocyclic Aldehyde 198 to form 201.

4.2.4. Initial Vinyl Magnesium Addition with Lithium-Magnesium Exchange

Vinyl magnesium reagents can be prepared from the corresponding vinyl lithium species through a transmetallation with $MgBr_2$ at -78 °C.[81,159–162] Following this protocol, we were delighted to find that the addition of the corresponding vinyl magnesium reagent afforded the 1,2-addition product **201** (**Scheme 4.5**) in approximately 70% yield, the ^{1}HNMR spectrum of which is shown in **Figure 4.2**. Moreover, a comparison of this NMR spectral data derived from **201** with that derived from the NP showed a close match, especially around the C17 position, which supported our stereochemical reassignment. However, to our dismay, while this reaction successfully afforded **201** two times, all further attempts to repeat this reaction resulted in the degradation of macrocycle **201**.

Furthermore, we were unable to determine what aspect of the reaction was responsible for this new outcome. For example, increasing the equivalents of vinyl magnesium species relative to the macrocyclic aldehyde **198** led to the formation of the desired product **201** in 5% yield but both significant degradation and C2-C3 alkene isomerization were also observed. No change in these results was observed when different oxidation conditions were used to form **198**, when $MgBr_2$ was added portion-wise, or when the reaction time for the 1,2- addition was increased. In our initial efforts, the ratio of $MgBr_2$ relative to the vinyl iodide was 2.5:1. Lowering this ratio to 1:1 led to yields between 5-20%, however, significant degradation of starting material and or product was observed. With our inability to replicate the 1,2-addition reaction that was so critical to the success of the planned total synthesis, we set out to better understand this process.

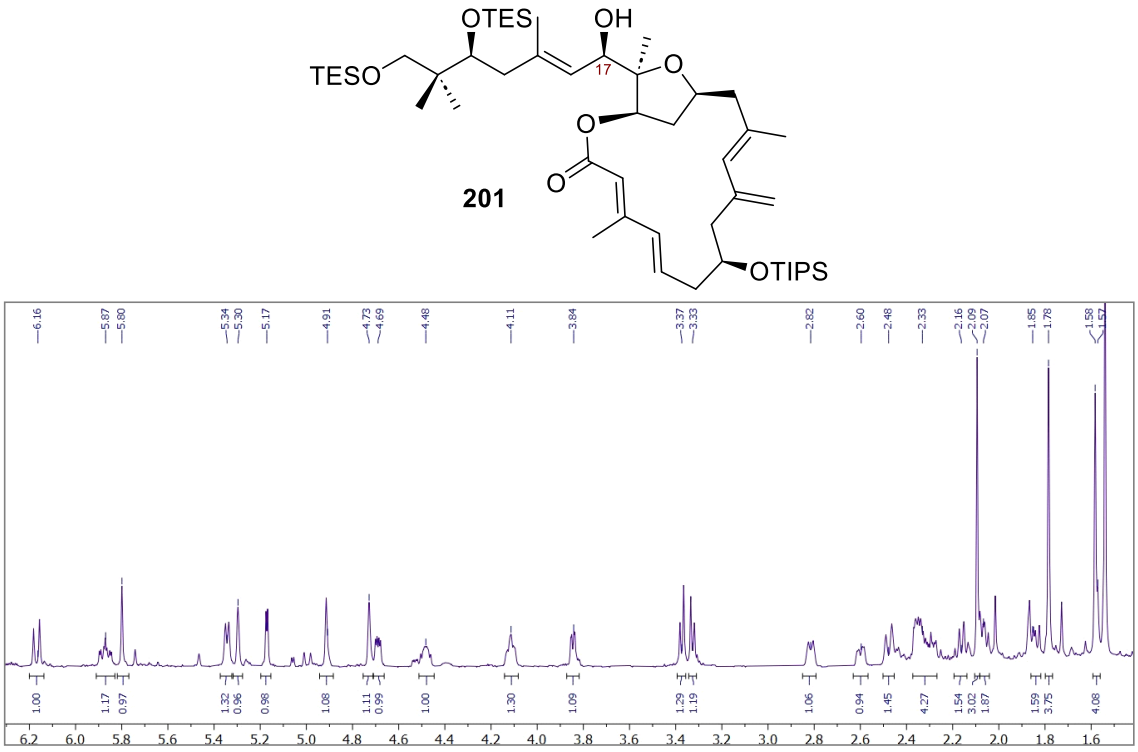

Figure 4.2. The ^{1}HNMR spectrum of C1-C23 fragment 201 from 1.4 to 6.3 ppm.

4.2.5. Studies Into the Vinyl Magnesium Addition

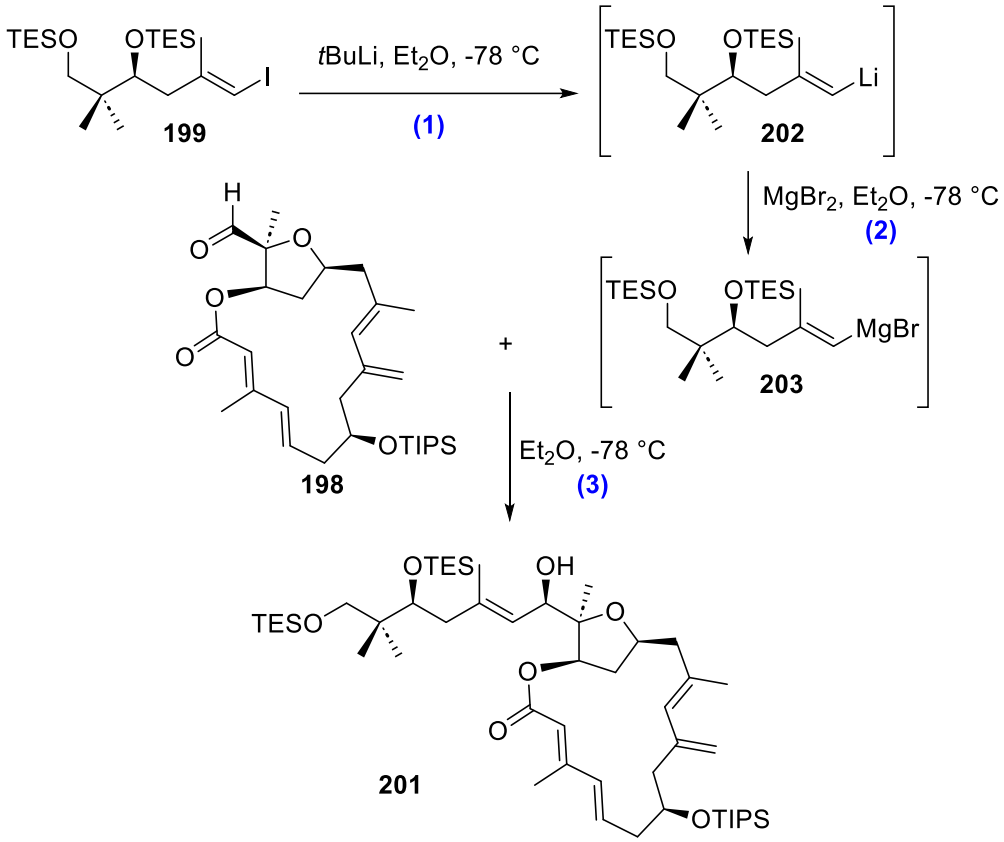

Scheme 4.6. Breakdown of the 3 Different Steps in the Vinyl Metal Addition of 199 to Macrocyclic Aldehyde 198.

In the addition of vinyl magnesium halide reagent **199** to the macrocyclic aldehyde **198** there are 3 key steps to consider (**Scheme 4.6**). The first step is the iodine lithium exchange to form **202**, followed by a lithium magnesium transmetallation to form vinyl magnesium **203**, and finally, a 1,2-addition of the organometallic reagent to the macrocyclic aldehyde **198**.[81,161] To better understand where the problems were occurring we set out to examine each step individually.

We first examined step 1: the preparation of the vinyl lithium species **202** (**Scheme 4.6**). While this is a well-established process for generating vinyl lithium species,[163] we assessed this step by forming the vinyl lithium species and subsequently quenching the reaction with a deuterium source. The ratio of starting material **199** to the deuterodeiodinated product, **204**, would provide insight into the production of the vinyl lithium species while the ratio of protodeiodinated product **205** would inform on any

unintentional quenching of the vinyl lithium species (**Scheme 4.7**). This model study revealed several crucial factors, namely that the solvent used had to be dried *via* distillation, that extending this reaction past 10 minutes or increasing the temperature above -78 °C (the standard temperature for this conversion)[163] resulted in quenching of the vinyl anion, and that *t*BuLi afforded the fastest and cleanest iodine-lithium exchange. Based on these results, we were able to form the vinyl lithium species **202** cleanly and reproducibly with over 95% conversion. The use of these optimized conditions, however, did not affect the outcomes of the 1,2-addition reaction.

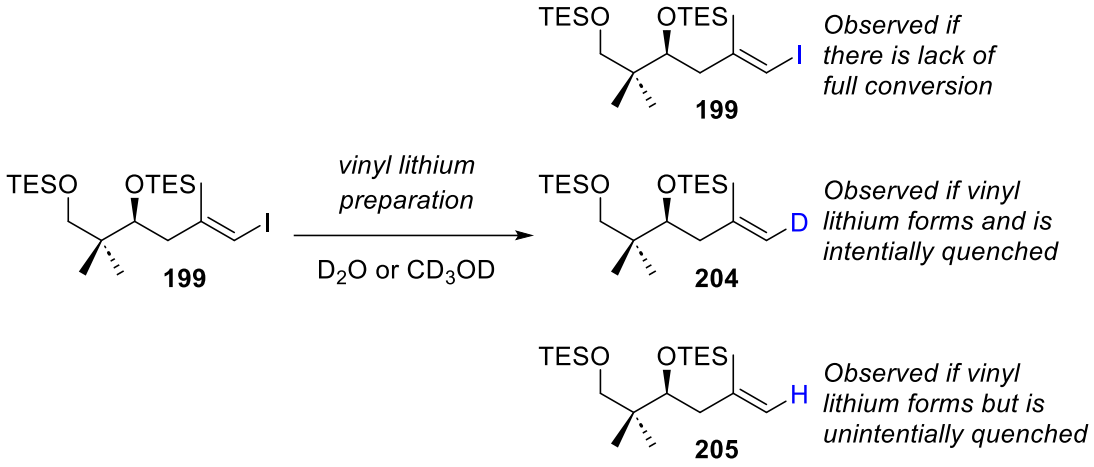

Scheme 4.7. Possible Products 199, 204, or 205 Observed in Model Quenching Studies of Vinyl Lithium Formation.

We next examined step 3: the 1,2-addition (**Scheme 4.6**). No reaction was observed when the reaction was executed at -100 °C and no significant change in yield was noted when reaction time at -78 °C was varied from 15 minutes to 2 hours. Assessing equivalents of the vinyl metal species showed that 2 equivalents resulted in no reaction while anywhere between 3 to 7 equivalents resulted primarily in degradation with no yield above 10%. Further, the yield was not improved if the addition order was changed, the method for purification of the macrocyclic aldehyde was modified, or if the aldehyde was prepared using a Swern oxidation. Since we were unable to realize an increase in yield, we reasoned the issue was likely occurring in the second step.

The second step of this reaction involves a transmetallation of the vinyl lithium to a vinyl magnesium substrate, **203**. Notably, if this transmetallation does not occur, based on our previous observations of the reaction of macrocyclic aldehyde **198** with the prepared vinyl lithium species, the residual vinyl lithium **202** would cause significant

degradation of the macrocycle. Suspecting this may be the cause of our problems, we used a model system to assess this transmetallation (**Scheme 4.8**). Notably, the addition of commercial vinyl magnesium bromide to macrocyclic aldehyde **198** afforded the 1,2-addition product **206** as a mixture of alcohols in 49% yield, while the addition of vinyl lithium only caused degradation. These results further confirmed that we were most likely not achieving full conversion to the vinyl magnesium species and that the transmetallation step was the problem.

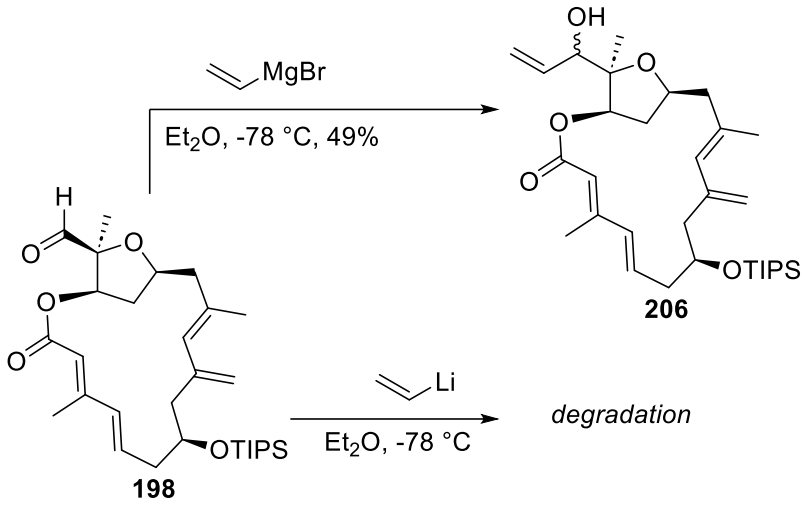

Scheme 4.8. Model Addition of Vinyl Lithium and Vinyl Magnesium Bromide to Macrocyclic Aldehyde 198.

Based on the above results, we explored several factors to try and improve the transmetallation step and reduce the observed degradation. No reduction in degradation or increase in yield was observed when THF, Et_2O, or Et_2O/benzene mixtures were used to prepare the $MgBr_2$ solution. Similarly, no change in reaction outcome was observed when the $MgBr_2$ solution was made using either commercial $MgBr_2 \bullet OEt_2$, or prepared from the reaction of magnesium and dibromoethane.[164] Complete degradation of the macrocyclic material was noted when solid $MgBr_2 \bullet OEt_2$ was added to the vinyl lithium species. Increasing the reaction time or the temperature of the transmetallation only resulted in partial or complete quenching of the vinyl metal species. In addition, increasing the equivalents of $MgBr_2$ relative to the vinyl iodide **199** had a detrimental effect on the yield.

We also attempted to quantify the amount of vinyl lithium and vinyl magnesium species formed *in situ* in a model system by quenching with deuterated dichloromethane,

which should selectively react with the vinyl lithium species and not the vinyl magnesium species. Notably, reactions between organolithium species and dichloromethane have been reported,[165] while Grignard reactions can be carried out in dichloromethane without issue.[166] However, this strategy also caused partial degradation of the side chain, rendering it challenging to assess reaction outcomes. Based on these results, we theorized that if the vinyl magnesium could be generated without the vinyl lithium intermediate, the following 1,2-addition may be successful. Therefore, we assessed the preparation of the vinyl magnesium compound directly from the vinyl iodide **199**.

4.2.6. Vinyl Magnesium Addition with Direct Iodide Magnesium Exchange

Often Grignard reagents are prepared by the direct insertion of magnesium into organohalides, however, for vinyl bromides and iodides, this insertion process is both challenging and non-stereoselective, rendering it unsuitable for our purposes.[167,168] We were encouraged by a report from Knochel *et al.* detailing the conversion of monosubstituted vinyl iodides into the corresponding vinyl Grignard reagent with the use of the "turbo" Grignard reagent, *i*PrMgCl•LiCl.[167] Although **199** contains a disubstituted vinyl iodide, we thought it worthwhile to assess this methodology on **199** as it would provide a direct conversion to the necessary vinyl magnesium species, **207** (**Scheme 4.11**). Repeating the reported procedure (*i*PrMgCl•LiCl, THF, -40 °C, 12h) showed no reaction with vinyl iodide **199**. Thus, a large screen of reaction conditions was undertaken that revealed that vinyl iodide **199** could undergo 70% conversion to the vinyl magnesium species **207** when treated with *i*PrMgCl•LiCl at room temperature for 6 hours. This process afforded a 5:2 mixture of the vinyl magnesium species **207** to the *i*PrMgCl•LiCl reagent. Critical to this preparation was the use of a Schlenk flask, which minimized inadvertent quenching by moisture in the air.

Unfortunately, when the macrocyclic aldehyde **198** (**Scheme 4.9**) was treated with 3 equivalents of prepared vinyl magnesium reagent **207**, no reaction was observed. Furthermore, only degradation was observed when 7 equivalents of **207** were used. The observed degradation may be due to the presence of magnesium salts, which had caused degradation of the material in other earlier studies, and which are formed in this reaction. Nevertheless, all these efforts show that the 1,2-addition of a vinyl magnesium, lithium, or

chromium species is unfeasible and an alternative method for appending the side chain to the macrocyclic core will have to be devised.

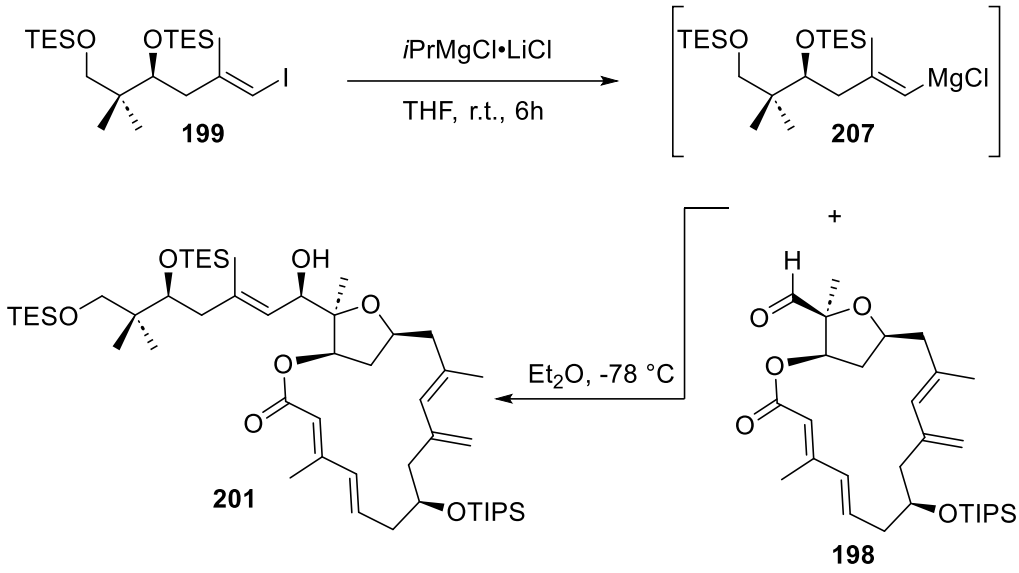

Scheme 4.9. Direct Preparation of Vinyl Magnesium Species 207 and Addition to Macrocyclic Aldehyde 198.

4.3. End-Game Synthetic Studies

Despite our failure to append the side chain to the macrocycle with repeatable and high yields, we were still able to produce a small amount of material for evaluation of the rest of the late-stage strategy. The first step involved selective TES deprotection of **226**. Due to the lack of material, this selective deprotection was first assessed on **199** as a model for the real system (**Scheme 4.10**) and results are summarized in **Table 4.2**. No reaction was observed upon treating **199** with pyridinium p-toluenesulfonate in a CH_2Cl_2:MeOH solution at 0 °C or room temperature for 6 hours (entries 1 and 2). After leaving the reaction for 18 hours, the alcohol **208** was produced in a 3:2 ratio to diol **209** with 50% conversion (entry 3). Switching from MeOH to EtOH and repeating the reaction at 0 °C improved this ratio to 4:1 but gave poor conversion (entry 4). No reaction was observed when **199** was treated with TBAF at -20 °C (entry 5) and at 0 °C the reaction afforded a 1:2 ratio of **208** to **209** (entry 6). Use of HF/pyridine buffered with pyridine in a 1:3 ratio by volume afforded **208** in a 5.6:1 with **209** (entry 7), which was improved to 6.7:1 when the ratio of HF/pyridine to pyridine was increased to 1:4 ratio by volume (entry 8).

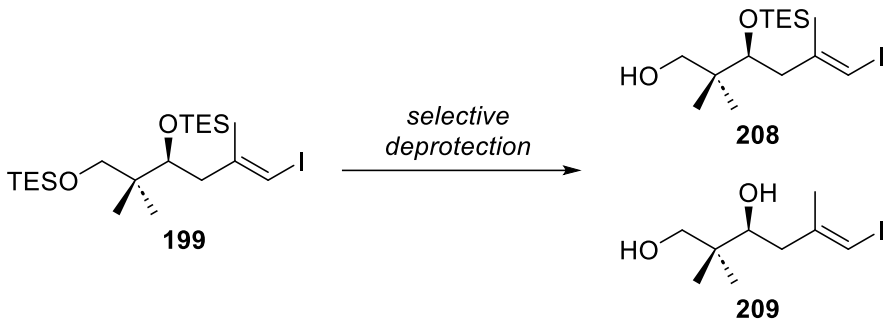

Scheme 4.10. Selective Deprotection of 199.

Table 4.2. Conditions For the Deprotection of Bis-Silyl Ether 199 to Alcohol 208 and Diol 209.

Entry	Reagent	Temperature	Solvent	Conversion	Ratio of 208:209
1	PPTS	0 °C	CH_2Cl_2:MeOH (5:1)	0%	NA
2	PPTS	r.t.	CH_2Cl_2:MeOH (3:1)	0%	NA
3	PPTS	r.t.	CH_2Cl_2:MeOH (3:1)	50%	3:2
4	PPTS	0 °C	CH_2Cl_2:EtOH (3:1),	40%	4:1
5	TBAF	-20 °C	THF	0%	NA
6	TBAF	0 °C	THF	100%	1:2
7	HF/py:py (1:3)	r.t.	THF	80%	5.6:1
8	HF/py:py (1:4)	r.t.	THF	80%	6.7:1

PPTS = pyridinium p-toluenesulfonate, r.t. = room temperature, TBAF = tetra-n-butylammonium fluoride, py = pyridine

When 1,2-addition product **201** was treated with the optimized conditions from the model study, **210** was afforded in 50% yield, with a 4:1 ratio of the C23 alcohol to the C23/C21 diol (**Scheme 4.11**). The next step involved selective oxidation of the primary C23 alcohol. TEMPO/BAIB oxidations have been used for selective primary alcohol oxidations to aldehydes on complex substrates.[100] Initially, TEMPO/BAIB oxidation conditions resulted in the degradation of **210**, but optimization of the reaction by reducing the amount of TEMPO and reaction concentration afforded aldehyde **211** in 67% yield (**Scheme 4.11**).

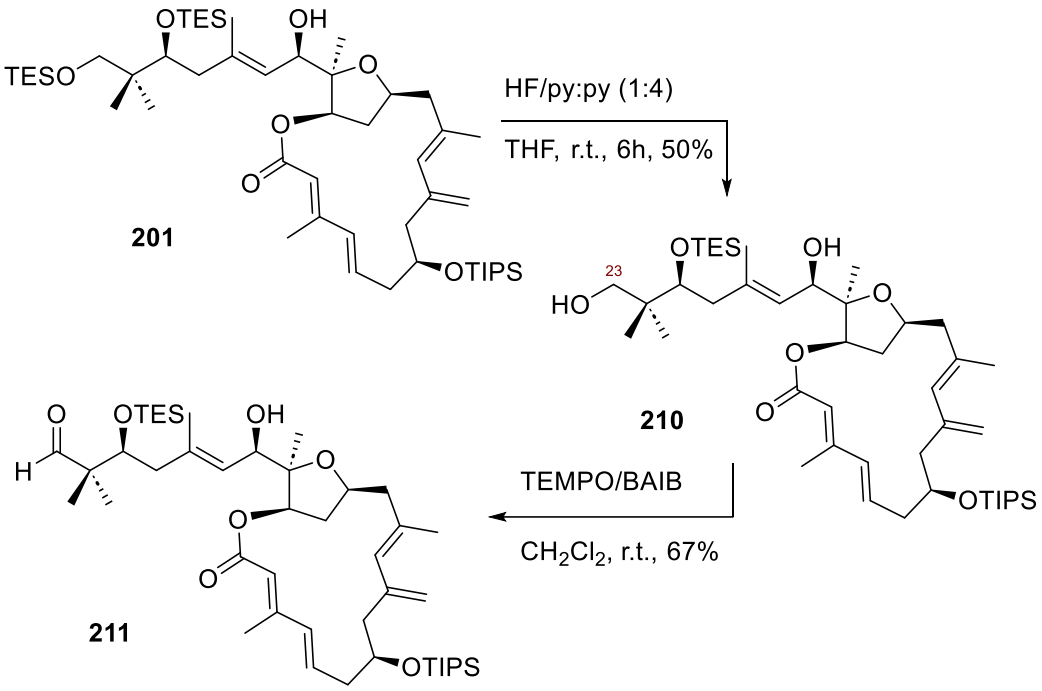

Scheme 4.11. Preparation of C23 Aldehyde 211.

At this point, we envisioned forming the C23-C24 bond *via* a boron-mediated aldol reaction[99] between **211** and methyl ketone **212**. The synthesis of methyl ketone **212** was developed by Dr. Nelson Lam and then carried out by the author for these studies and is not presented in this thesis. From the above work, we produced enough of the aldehyde **211** to assess 3 attempts of the planned boron-mediated aldol reaction (**Scheme 4.12**).

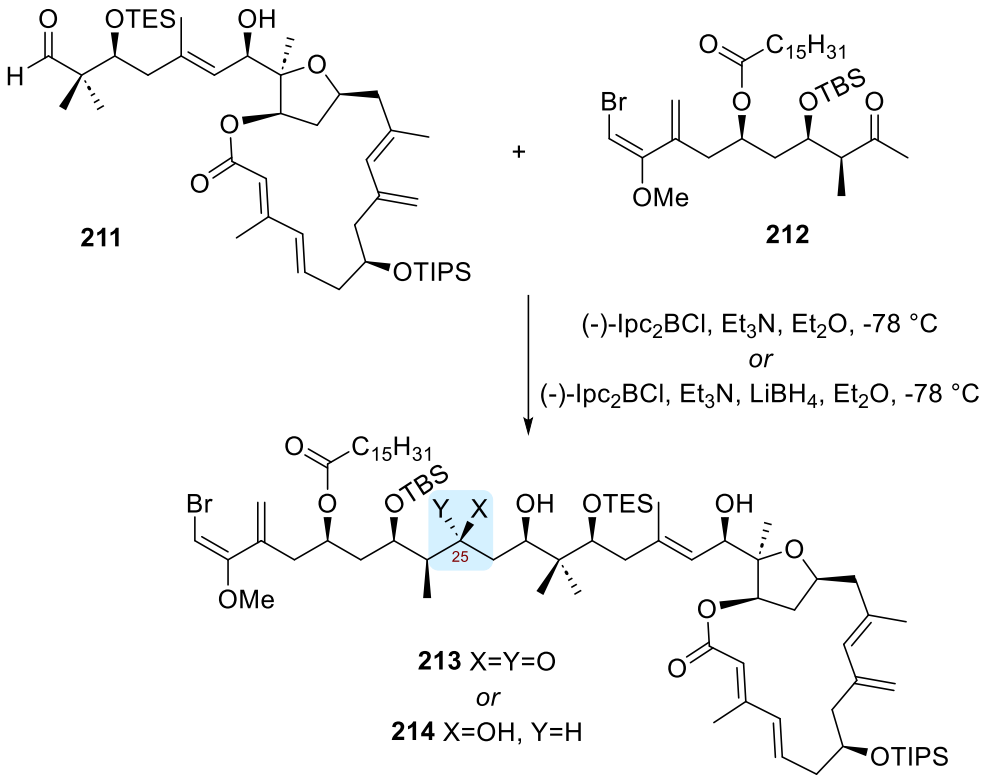

Scheme 4.12. Studies on the Boron-Mediated Aldol Coupling of 211 and 212.

In the first attempt at the boron aldol reaction, on a 0.4 mg scale of aldehyde **211**, we used reported literature conditions.[99] However, on this scale, we observed no product formation and only partial degradation of the macrocycle. Repeating these conditions on a 1.0 mg scale of **211** we observed the loss of the starting material and the formation of a new product that closely resembled the NMR spectral data reported for phormidolide A in the ^{1}H NMR spectrum recorded on the crude reaction product. MS analysis of the crude material was inconclusive as to whether **213** had been formed. However, upon column chromatographic purification of the crude product on Flourosil, only the starting material was recovered. This observation was at odds with the NMR spectral data that had indicated no starting material was present in the crude reaction mixture. Recovery of the starting material from the column chromatographic purification suggests the product underwent a retro-aldol reaction during purification. Based on this observation we next attempted an *in situ* reduction coupled with the boron-mediated aldol reaction to afford the C25 alcohol product **214**,[99] as **214** would not be able to undergo retro aldol reactions during purification using column chromatography. Assessment of the previous conditions on 0.7 mg of **211** followed by the addition of $LiBH_4$ for the *in situ* reduction only afforded the C23 alcohol product **210**. The recovery of **210** suggests that, in this case, the boron-

mediated aldol reaction did not occur and instead, **211** was reduced by $LiBH_4$. It is likely that our inability to affect a boron-mediated aldol reaction and *in situ* reduction is due to the reaction scale. At this point, we had exhausted our supply of material for assessing this strategy and therefore concluded the efforts towards the total synthesis of phormidolide A.

4.4. Conclusion

We assessed several strategies involving appending the C18-C23 side chain after macrocyclization had been completed. These studies showed that NHK conditions and vinyl lithium addition did not form the product, but our first two attempts at the vinyl magnesium addition were successful. However, efforts to repeat these conditions failed. Examination of the reaction through a systematic study revealed that a lack of a Li/Mg transmetallation was likely the culprit of this failure. However, our efforts to overcome this transmetallation issue were not successful.

Despite our inability to develop a reproducible method to append the side chain to the macrocycle, we still were able to gain insight into the end-game strategy of linking the C24-C33 side chain to the rest of the molecule *via* a boron-mediated aldol strategy. Selective TES deprotection and TEMPO/BAIB oxidation afforded the C23 aldehyde. Assessment of the boron-mediated aldol reaction showed that, while the aldol reaction was likely successful, the β-hydroxy ketone product undergoes retro-aldol upon column purification. Therefore, if the boron-mediated aldol reaction could be accomplished with an *in-situ* reduction to afford the *syn*-diol product, the retro-aldol would be avoided and global deprotection should afford phormidolide A. From these results, it is recognizable that if a robust and repeatable synthesis of **201** can be developed, then this late-stage methodology can be explored and the total synthesis of phormidolide A completed. Several different proposed methods to complete the total synthesis are outlined in Chapter 5.

Chapter 5. Future Work Towards the Synthesis of Phormidolide A

5.1. Introduction

In our efforts to complete the total synthesis of phormidolide A, we successfully synthesized the macrocycle **190**, the C18-C23 side chain **199** and the C24-C33 side chain **212** in collaboration with the Paterson group (**Scheme 5.1**). Scale-up of these syntheses should allow for sufficient quantities to be prepared for completion of the total synthesis. To complete the total synthesis, the coupling of each fragment needs to be addressed.

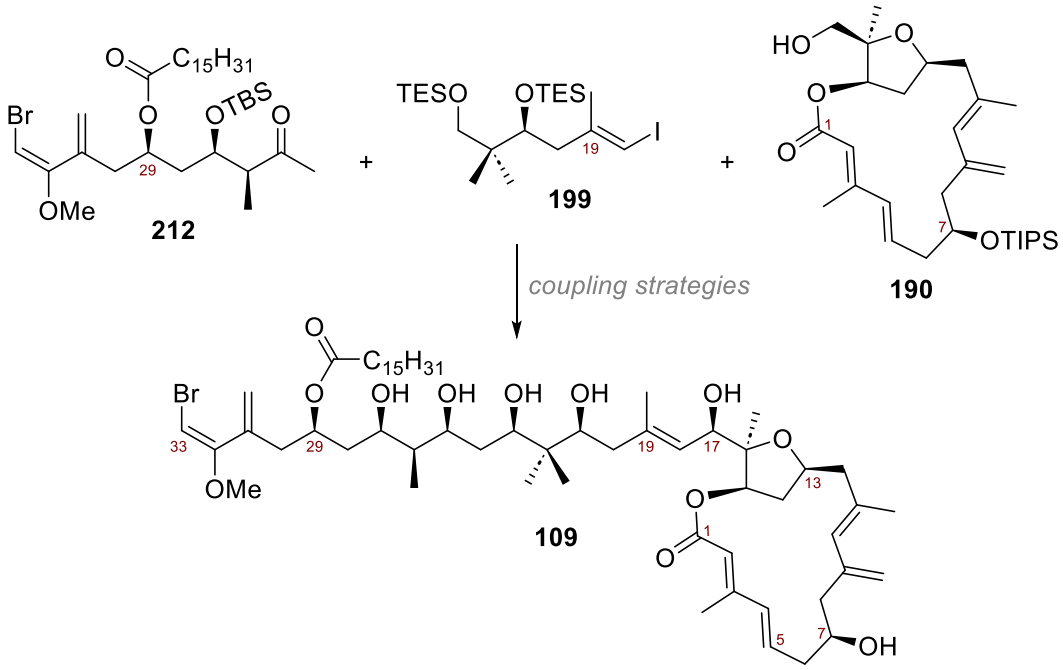

Scheme 5.1. Outline for the Final Construction of Phormidolide A.

As outlined in Chapter 4, attaching the side chain fragment **199** to the macrocycle core through the use of the use of NHK conditions or a vinyl lithium addition proved unsuccessful. Attaching the side chain *via* 1,2-addition of a vinyl magnesium species has been exhaustively explored and, while two successful examples of this coupling have been achieved, the irreproducible yields and significant degradation observed for this coupling render it unusable for this synthesis. Additionally, the coupling of side chain fragment **212** to a C1-C23 fragment of phormidolide A has been initially explored on a small scale. Here, potential strategies for completing the total synthesis are outlined.

5.2. Coupling of the C18-C23 Side Chain

5.2.1. Vinyl Metal Addition Strategies

Based on an extensive study of the coupling between the macrocyclic aldehyde **198** and C18-C23 side chain **199**, we theorized that the addition failed because the vinyl lithium derivative of **199** was not completely converted into the vinyl magnesium derivative (**Scheme 5.2**). One way to address this issue may be to identify conditions that ensure full transmetallation and develop a system to assess whether any vinyl lithium species is present. As studies with the vinyl metal species suggest it needs to be used in at least 6 equivalents, partial conversion to the vinyl magnesium species would be insufficient as the residual vinyl lithium would still exist in sufficient quantities to cause degradation.

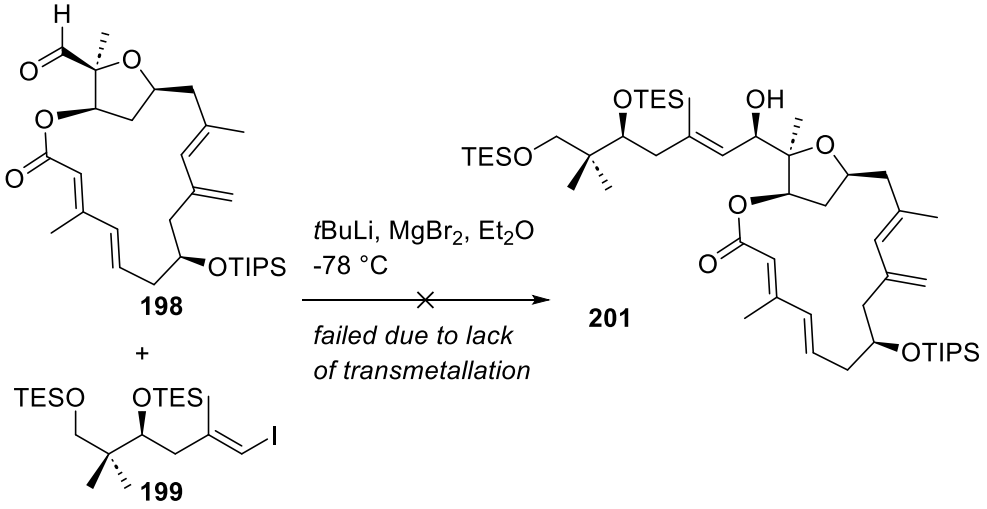

Scheme 5.2. Coupling of Macrocycle Aldehyde 198 and C18-C23 Side Chain Fragment 199.

An alternative strategy that was not investigated by the author is to use an additive that would selectively react with, and quench, the vinyl lithium species. This additive would have to be inert towards vinyl magnesium species and therefore the selectivity for vinyl lithium species could be easily assessed by model systems. An example of one option for an additive may be 1,2-dibromoethane (**215**), which undergoes reactions with organolithium compounds[169] and has been used in reactions with hindered Grignard reagents without causing quenching of the Grignard reagent.[170] However, an additive of this type may cause further issues as there is no guarantee that the vinyl bromide by-product **216** would be inert in the overall process and the LiBr produced in the vinyl lithium

quench may cause C2 *E*/*Z* isomerization of the macrocycle (**Scheme 5.3**). Finally, this strategy is contingent on at least a partial conversion to the vinyl magnesium species so there is sufficient vinyl magnesium material available to react with **225**.

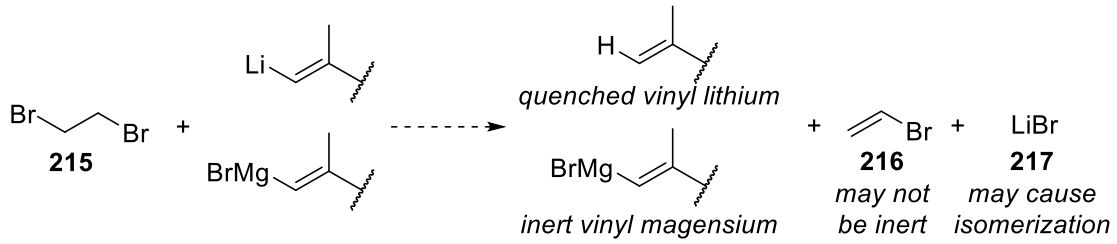

Scheme 5.3. Potential Products from Quenching a Mixture of Vinyl Lithium and Vinyl Magnesium Species.

A second strategy would be to prepare the zincate species **218** from the C18-C23 vinyl lithium intermediate **202** (**Scheme 5.4**). Vinyl zincates have been easily prepared from vinyl lithium intermediates and used in complex NP synthesis for the addition of the zincate species to aldehydes.[171–174] Notably, some of these examples include sensitive dienoates in the reacting structures, which suggests that these compounds are relatively mild and unlikely to cause any degradation. Additionally, transmetallation of organolithiums to organozinc species has been documented[175] and could be further explored for this coupling.

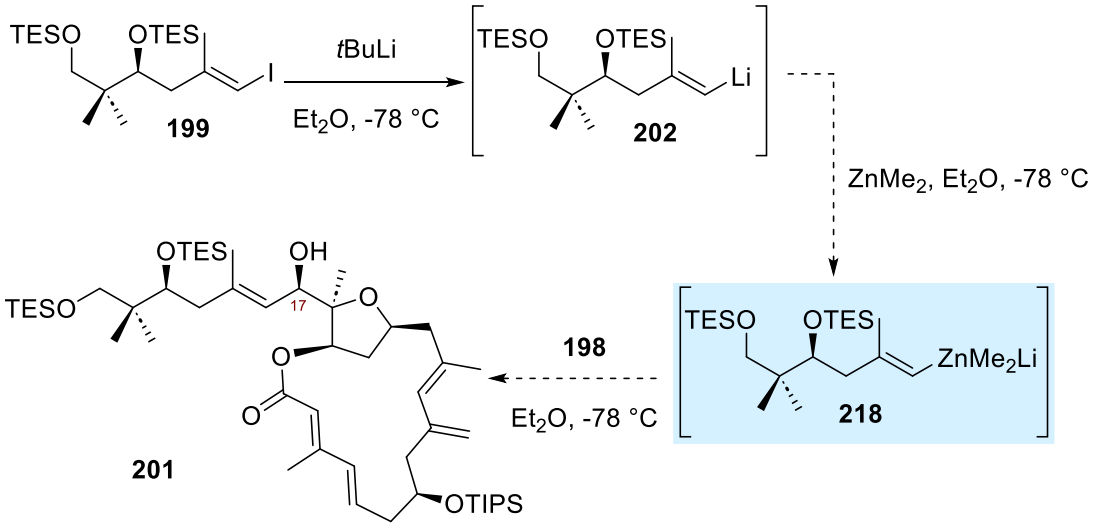

Scheme 5.4. A Potential Strategy for Coupling the C18-C23 Side Chain Fragment to the Macrocycle Core Through Organozinc Generation.

5.2.2. Alkyne Addition

Strategies for adding other side chain fragments than **199** to the macrocyclic aldehyde **198** could also be explored. One example of this could involve the addition of alkyne fragment **219** (**Scheme 5.5**). The generation of Grignard reagents directly from alkynes has been reported[176] and therefore the Grignard derivate **220** could be generated directly from alkyne **219** and reacted with **198** to form the propargylic alcohol **221**, avoiding detrimental organolithium intermediates. Elaboration to the vinyl methyl **201** could be accomplished by an aluminum-mediated reduction/iodination of the alkyne and a suitable coupling of a methyl group, such as a palladium-based coupling.[177,178] Other strategies for the formation of methyl-substituted *trans*-alkenes from alkynes are known, such as through the use of ruthenium-catalyzed hydrosilylation methodology followed by a rearrangement/cross-coupling strategy to afford the desired vinyl substitution.[179,180]

In addition, Álvarez *et al.* have studied the organometallic addition of side chain fragments to tetrahydrofurfural species as part of their efforts towards the synthesis of phormidolides B-D. They assessed a carboalumination of an alkyne followed by the *in situ* addition to a tetrahydrofurfural, which afforded products in moderate yields and diastereoselectivity.[181] A similar strategy could be envisioned with the carboalumination of alkyne **219** to generate the vinyl aluminum species **222** *in situ*. Treatment of macrocyclic aldehyde **198** with **222** could form the desired **201** product, though the resulting diastereoselectivity may need further optimization.

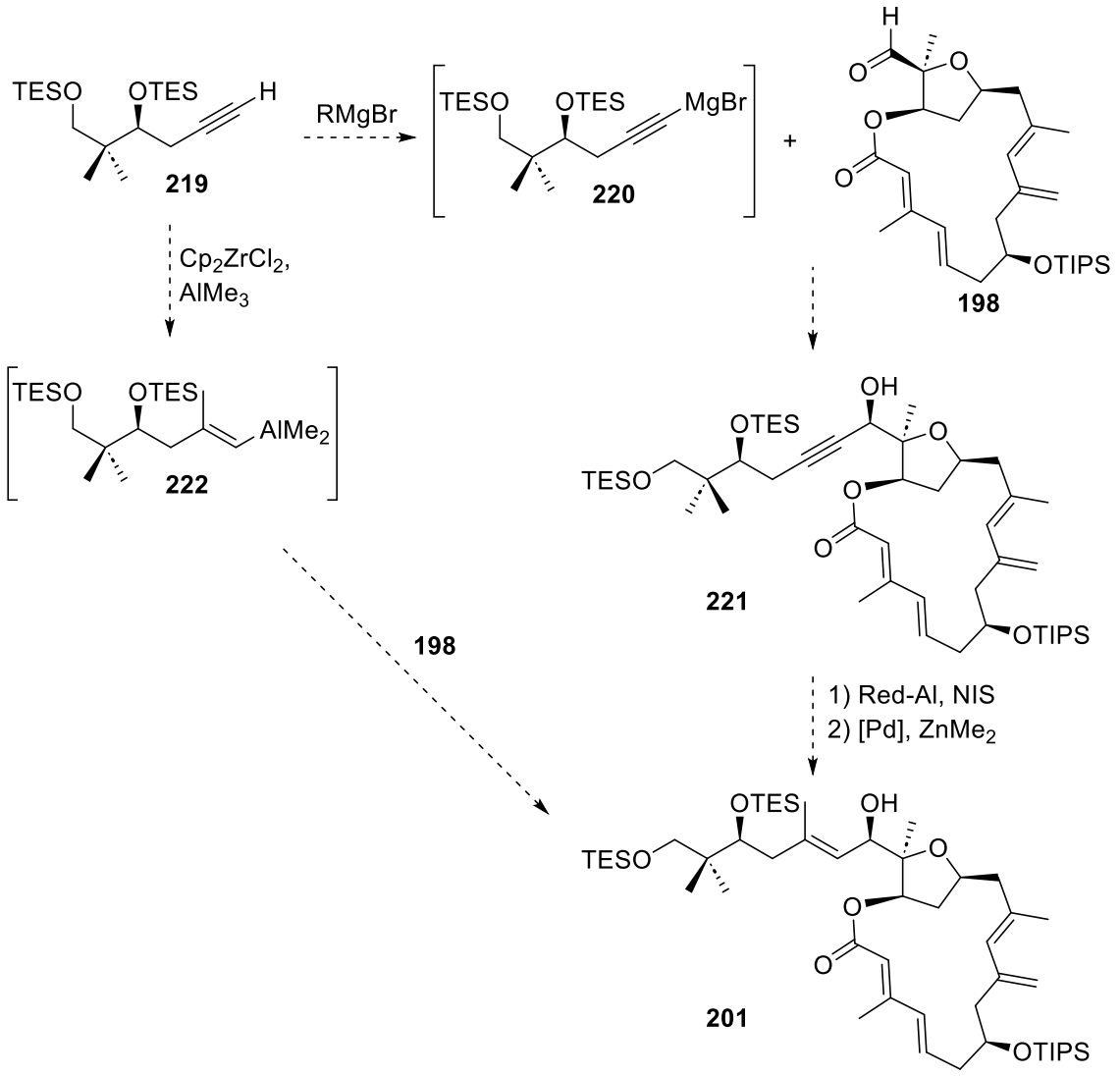

Scheme 5.5. Potential Strategies to Couple Alkyne Side Chain Fragment 219 to Macrocyclic Aldehyde 198.

The goal of these various 1,2-addition strategies is to eventually form C1-C23 fragment **201** since synthetic methodology to form phormidolide A has been developed from this structure. Once **201** is in hand and a robust strategy has been developed to provide material, further end-game studies can progress.

5.3. Elaboration of the C18-C23 Side Chain

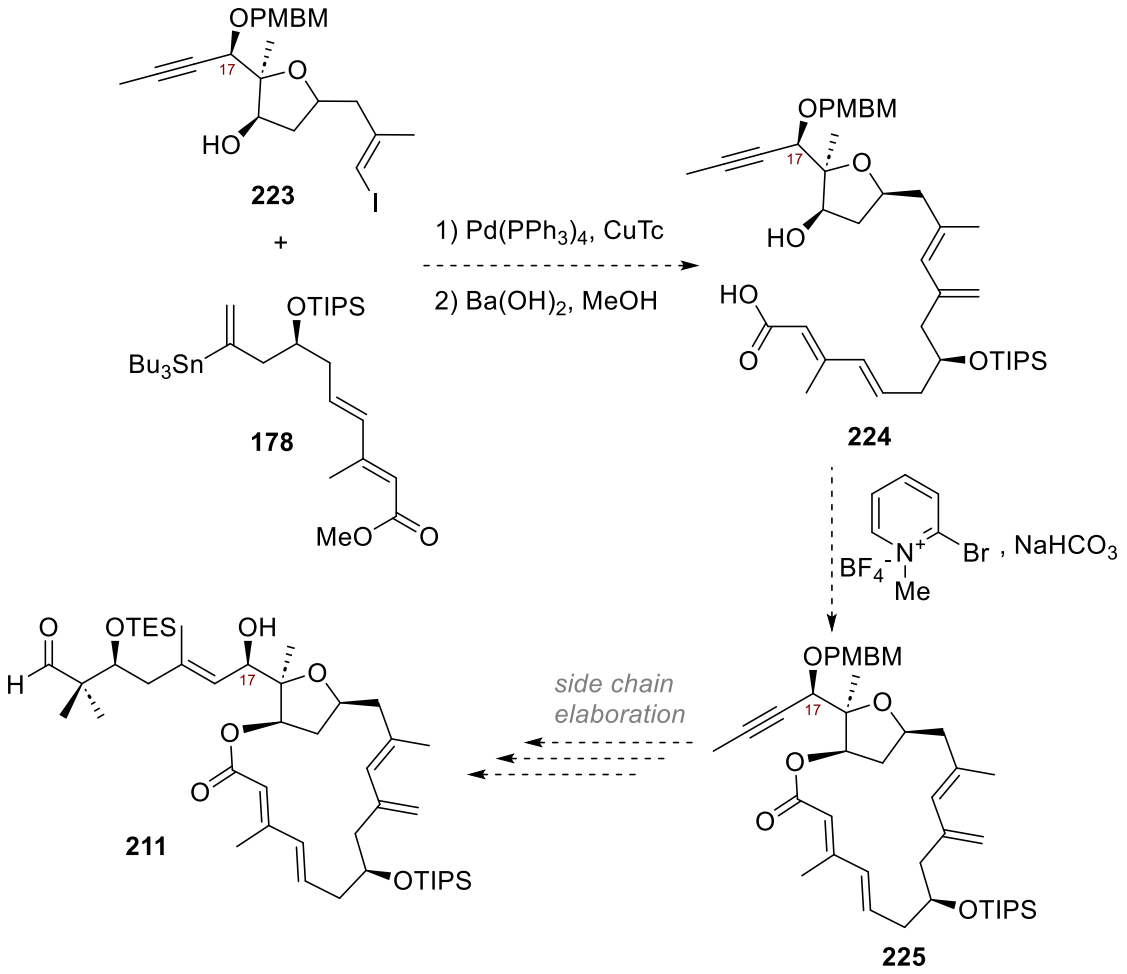

Scheme 5.6. An Example of a Potential Strategy for Forming 211 by Introducing an Alkyne Functional Handle at C17 Before Macrocyclization.

As an alternative approach, and to avoid organometallic addition to macrocycle aldehyde **198**, a small function group could be incorporated at C17 before macrocyclization. **Scheme 5.6** outlines an example of this with an alkynyl functional group at C17. If THF **223** could be prepared, an analogous methodology as that outlined in Chapter 3 could be used to prepare seco acid **224** and then form macrocycle **225**. From here, side chain elaboration through the use of mild and selective reactions, such as alkyne metathesis,[182] could be accomplished to form aldehyde **211** for use in the late-stage boron-mediated aldol strategy. While the C17 functional group, protecting groups, and reactions should be carefully selected to avoid reactions with the sensitive

macrocycle, this strategy would avoid all the various issues observed with 1,2-addition to the macrocyclic aldehyde.

5.4. Coupling of the C24-C33 Side Chain

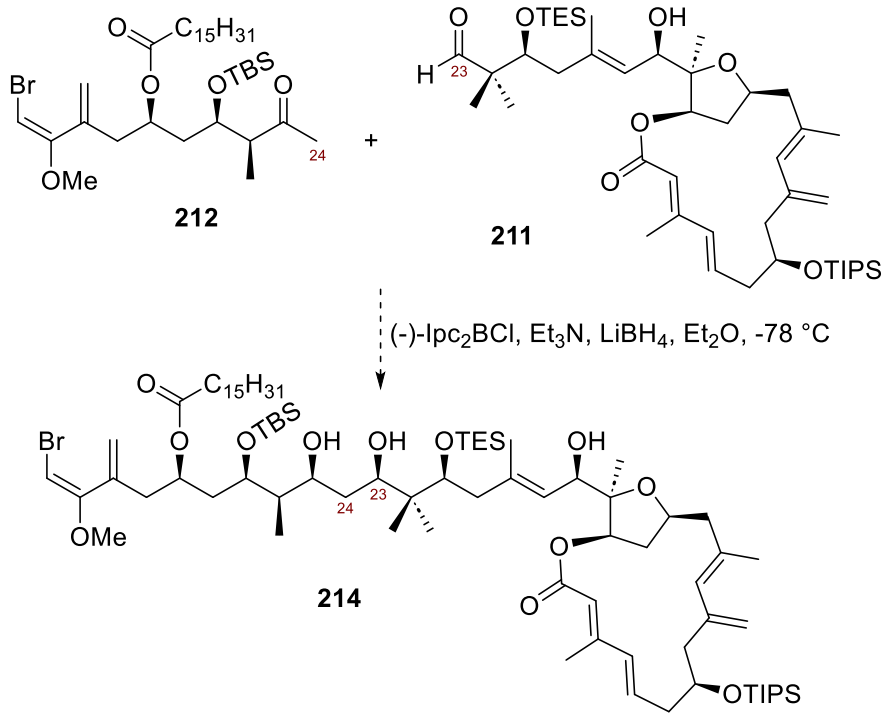

Scheme 5.7. Coupling of Aldehyde 211 and Methyl ketone 212 to Form the Protected Phormidolide A, 214.

Previous efforts described in Chapter 4 include the transformation of **201** to aldehyde **211** (**Scheme 5.7**). Our synthetic plan called for the use of a boron-mediated aldol coupling to form the C23-C24 bond. The original efforts revealed that the use of a boron-mediated aldol with an *in situ* reduction[99] could potentially form this C23-C24 bond, affording the protected NP. Based on these results, there is still confidence in the boron-mediated aldol strategy, and we, therefore, theorize that if conditions can be found to repeatably form **211**, there will be sufficient material to assess this boron-mediated aldol. Care should be taken for both the hydrolysis of the resulting C23,C25 boronic ester from the reduction reaction and the final purification of this substrate.

5.5. Global Deprotection

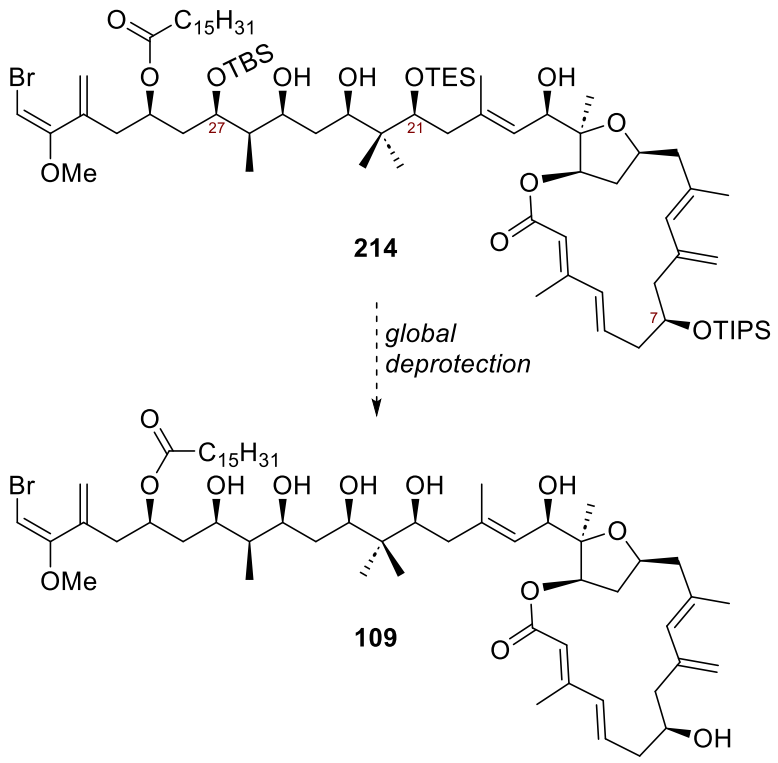

Scheme 5.8. Global Deprotection of 214 to 109, the Stereochemically Reassigned Phormidolide A.

Upon completion of the synthesis of **240**, the NP can be revealed by global deprotection, that is, desilylation of the C7 TIPS group, C21 TES group, and C27 TBS group (**Scheme 5.8**). While previous studies suggested that the C7 TIPS group can be removed *via* catalytic camphorsulfonic acid (CSA), the bromomethoxydiene unit has shown significant sensitivity to acidic conditions and therefore the use of acidic deprotection conditions is not recommended. Preliminary studies on macrocycle **190** have shown that the TIPS group can be effectively removed through the use of HF/pyridine buffered further with pyridine (1:1 v/v).[183] Given that the TIPS group will likely be the most challenging protecting group of the three to remove,[183] it is expected that HF/pyridine conditions buffered by pyridine can affect global deprotection of **214**. Successful global deprotection will afford the NP and spectral comparison with the data derived from the NP will inform on the stereochemical reassignment of phormidolide A.

5.6. Conclusion

While several strategies for appending side chain fragments to the macrocycle were explored, a methodology to reproducible form quantities of late-stage intermediates to ultimately construct the NP was not realized. However, as outlined in this chapter, there are many other options for constructing the NP. Selective vinyl lithium quenching or the addition of a vinyl zincate species or alkyne side chain fragment may allow for the addition of the C18-C23 side chain fragment to the macrocycle core while avoiding the highly variable yields and significant degradation observed using Grignard reagents. Alternatively, if a suitable sterically 'small' functional handle could be installed at C17 before macrocyclization, this functional handle could be elaborated to form the side chain and avoid the problematic organometallic addition to the macrocyclic aldehyde.

A robust synthesis of the C1-C23 fragment of the NP should allow for further exploration of the end-game strategies of the total synthesis of phormidolide A. A boron-mediated aldol strategy should allow for attachment of the C24-C33 side chain fragment and subsequent desilylation of the product would then finally allow for the completion of the total synthesis of phormidolide A.

Chapter 6. Halide Effects in Diastereoselective Grignard Reactions: An Enabling Tool for C4'-Modified Nucleoside Synthesis

6.1. Introduction

The Grignard reaction is a prototypical carbon-carbon bond-forming reaction and has been widely exploited by organic chemists for more than a century.[184,185] In addition to 1,2-addition reactions, Grignard reagents undergo radical[186–188] and cross-coupling reactions,[189,190] and can be exploited as strong bases in a variety of scenarios.[191] Transmetalation to other organometal species also engenders a suite of complimentary reactivities.[185,192,193]

$$2\mathrm{RMgX} \rightleftharpoons \mathrm{MgR_2} + \mathrm{MgX_2}$$

While Grignard reagents are commonly represented as "RMgX", their actual structure is understood to be far more complex. First, an equilibrium (Schlenk) exists between the diorganomagnesium (MgR_2), organomagneisum halide (RMgX) and dihalomagnesium (MgX_2) species.[184,194] Second, these individual species can exist as monomers or as dimeric or polymeric aggregates depending on concentration, choice of solvent, and the nature of the halide.[187,195] Third, temperature also impacts reagent composition and reactivity.[87,196] Recent computational studies have helped shed additional light on these complex processes.[197] Thus, the solvent, R group, and temperature all impact reagent composition, reaction mechanism, and outcomes.[87,188,194,197] For example, the distinct reactivity of MgR_2 and RMgX has been discussed in detail.[196,198]

The diastereoselective addition of Grignard reagents to prochiral ketones[87,199,200] has been studied extensively by Ashby[187,194] and others[201,202] and often involves coordination to proximal functional groups (e.g., alkoxy[166,203–205] and amino[206–208], **Figure 6.1**) and can differ in selectivity from other organometallic reagents (e.g., Cu, Al, Li).[209–212] In the specific case of β–hydroxy ketones, the formation of an intermediate magnesium alkoxide can rigidify acyclic systems and impart further control of the diastereochemical outcome of reactions.

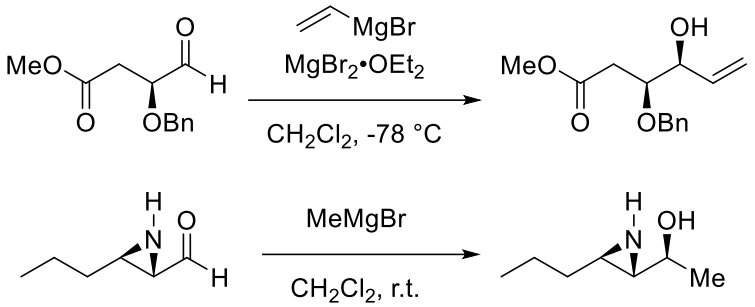

Figure 6.1. Examples of chelation-controlled addition through coordination to proximal functional groups.

Previous work from our groups demonstrated that the addition of Grignard reagents to ketofluorohydrins of general structure **226** provided a direct route to C4'-modified L-configured α- and β-nucleoside analogues (NAs, **227a**) (**Figure 6.2**).[70] We were interested in exploring the chelation of Grignard reagents to **226** to change the diastereoselectivity of addition and access D-configured β-nucleoside analogues.

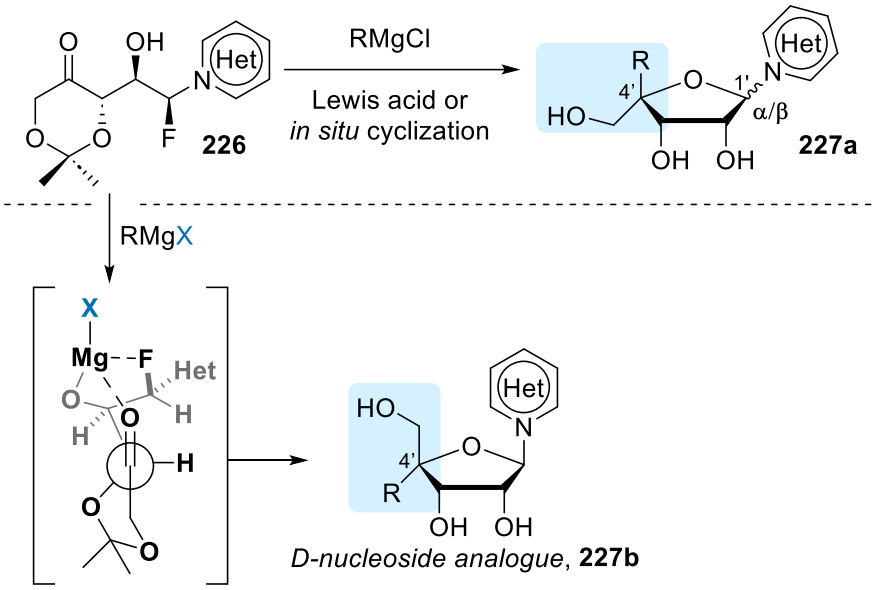

Figure 6.2. Previous work to prepare L-configured C4'-modified nucleoside analogues and the current work to access the D-configured C4'-modified nucleoside analogues.

Our interest in this process derives from the significant role C4'-nucleoside modification plays in modulating the conformation (sugar pucker) of the furanose and consequently interactions with biological targets.[213–215] As a result, C4'-modified NAs play an important role as antiviral agents,[214,216–218] lead cancer treatments,[219] and core

structural components of antisense oligonucleotides.[220–222] Examples of these include ALS-8112 (**228**), an anti-RSV agent, 4'-cyano-2'-deoxyguanosine (**229**), an anti-HBV agent, and islatravir (**230**), developed by Merck for the treatment of HIV (**Figure 6.3**). Despite the simplicity of our approach, this work was largely limited to the production of unnaturally configured L-NAs, which were produced as both α- and β-anomers, which are less suitable for supporting medicinal chemistry campaigns. To better understand the observed diastereoselectivity of these processes and access the complimentary suite of naturally configured D-NAs, we initiated a detailed study of this 1,2-additon reaction. Unexpectedly, we discovered a unique halide effect that controls the diastereoselectivity of reactions between Grignard reagents and β–hydroxy ketones. To the best of our knowledge, this halide effect has not been previously described. Here, we report the discovery of the halide effect, its impact on the stereochemical outcome of Grignard reactions, and its application in the rapid production of C4'-modified D-configured Nas.

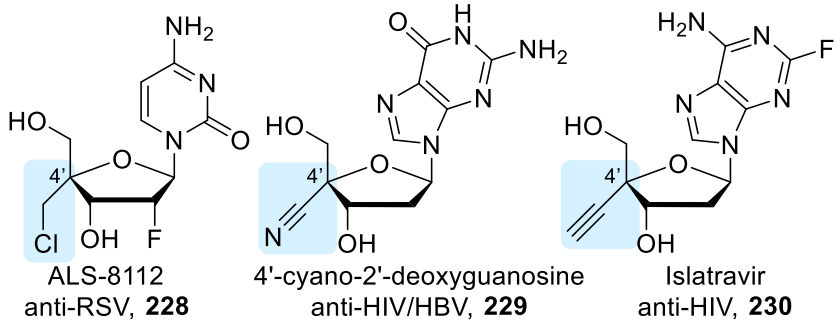

Figure 6.3. Examples of medicinally-relevant C4'-modified nucleoside analogues.

6.2. Grignard additions to β-hydroxyketones

Considering the potential for multiple chelation modes in the Grignard reactions discussed above (**Figure 6.2**), we prepared the hydroxy ketones **231**-**234**,[68,69,223] with and without a Cl or F substituent, and lacking the nucleobase function to better understand the influence of individual functional groups on diastereoselectivity (**Scheme 6.1**). From a panel of organometallic reagents, we found that Grignard reagents generally gave the cleanest reaction profile.

The addition of various organometallic reagents to the corresponding silyl ethers (e.g., **231**, **Table 6.1**, entry 1) gave exclusively the 1,3-*anti* product **238**. This result confirmed the importance of the β-hydroxy function for the formation of the desired 1,3-

syn diol. Furthermore, while the reaction of the β-hydroxyketone **232** with MeMgCl in THF gave a 1:1 mixture of diastereomeric diols (entry 2), the equivalent reaction in non-coordinating CH_2Cl_2 improved selectivity for the *syn* diol **5** (entry 3), highlighting the importance of chelation.[166] Surprisingly, the use of MeMgBr led to a significant increase in diastereoselectivity (~6:1 d.r.) that was also observed with MeMgI (entries 4 and 5), though in CH_2Cl_2 only (entry 6). To assess the role of the fluorine atom in these processes, we prepared the corresponding chlorohydrin **233** and carried out a similar suite of reactions (entries 8-10). Here, we observed a ~5-fold increase in diastereoselectivity on switching from MeMgCl to MeMgI. Finally, we examined the dehalogenated analogue **234** and found that the diastereoselectivity increased ~2.5-fold on switching from MeMgCl to MeMgI (entries 11 and 12), suggesting that the halide effect was perhaps more general.

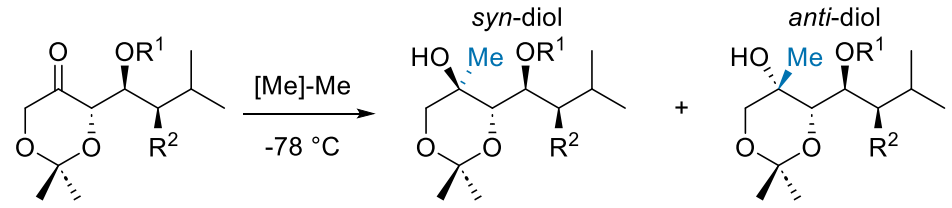

231 - R^1 = TBS, R^2 = Cl
232 - R^1 = H, R^2 = F
233 - R^1 = H, R^2 = Cl
234 - R^1 = H, R^2 = H

235a - R^1 = H, R^2 = F
236a - R^1 = H, R^2 = Cl
237a - R^1 = H, R^2 = H

235b - R^1 = H, R^2 = F
236b - R^1 = H, R^2 = Cl
237b - R^1 = H, R^2 = H
238 - R^1 = TBS, R^2 = Cl

Scheme 6.1. Addition of Methyl Grignard Reagents to Model Hydroxyketones.

Table 6.1. Addition of [M]-Me to β-hydroxyketones Shown in Scheme 6.1.

Entry	Compound	[M]-Me	Solvent	Product (ratio)[a]	Yield *syn*-diol
1	**231**	MeMgCl	THF	**238**[b]	53%
2	**232**	MeMgCl	THF	**235a**:**235b** (1.1:1)	33%
3	**232**	MeMgCl	CH_2Cl_2	**235a**:**235b** (2.2:1)	48%
4	**232**	MeMgBr	CH_2Cl_2	**235a**:**235b** (6:1)	45%
5	**232**	MeMgI	CH_2Cl_2	**235a**:**235b** (7.8:1)	72%
6	**232**	MeMgI	THF	**235a**:**235b** (0.8:1)	17%
7	**232**	Me_2Mg	CH_2Cl_2	**235a**:**235b** (1:1)	ND[c]
8	**233**	MeMgCl	CH_2Cl_2	**236a**:**236b** (1:1)	43%
9	**233**	MeMgBr	CH_2Cl_2	**236a**:**236b** (2.5:1)	56%
10	**233**	MeMgI	CH_2Cl_2	**236a**:**236b** (5.5:1)	78%
11	**233**	MeMgCl	CH_2Cl_2	**237a**:**237b** (0.7:1)	21%
12	**233**	MeMgI	CH_2Cl_2	**237a**:**237b** (1.8:1)	58%

[a] As determined by analysis of ^{1}HNMR spectra recorded on the crude reaction mixture; [b] Only product produced; [c] Not determined; THF = tetrahydrofuran.

6.3. NMR Spectral Assessment of Grignard Reagents

To assess whether the Schlenk equilibrium played a role in this process, the dialkyl magnesium reagent Me_2Mg was also reacted with ketone **232**, which gave a 1:1 mixture of diols (entry 7). This result prompted us to confirm that a MeMgX-Me_2Mg equilibrium was not complicating the reactions presented in Table 1. To do so, we analyzed each commercial Grignard reagent in CD_2Cl_2 by NMR spectroscopy at both room temperature and -58 °C (**Figure 6.4**) and found that i) the reagents were distinguishable by carbon chemical shift, and ii) the MeMgX reagents were free of Me_2Mg at these temperatures. Additionally, we ensured that the observed halide effect was not due to unexpected aggregates of the Grignard reagents by ensuring reactions were executed at concentrations shown to prevent the formation of aggregates.[187]

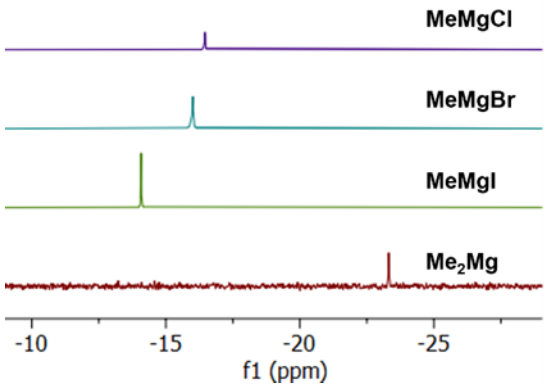

Figure 6.4. The -58 °C ^{13}CNMR spectral assessment of MeMgCl, MeMgBr, and MeMgI as compared to Me_2Mg.

Collectively, these results indicate that changes in diastereoselectivity can be attributed to the halide "X" in MeMgX. Notably, the very few examples of halide effects on reactions of Grignard reagents include impact on regioselectivity,[224,225] yields,[226] and diastereoselectivity (in ethereal solvents).[227–229] The most similar finding to that presented in Table 1 was a small increase in diastereoselectivity reported in a table of data describing the addition of MeMgBr vs MeMgCl to a 2′-oxouridine derivative.[230] Beyond this observation and to the best of our knowledge, the halide effect on diastereoselective addition reactions of Grignard reagents has not been discussed or exploited in a unified way.

We also observed that the halide in the ketohalohydrins played a role in increasing the diastereoselectivity, under the optimal conditions, for the *syn*-diol. When the substrate did not contain a halogen, there was a 2.6-fold increase in selectivity for the *syn*-diol between the chloro-Grignard and iodo-Grignard reagents. However, when the substrate contained a fluoro- or chlorohydrin, the difference in selectivity for the *syn*-diol 3.5-fold and 5.5-fold respectively. The halogen in these privileged halohydrin structures imparts increased selectivity in this chelation-driven addition.

6.4. Grignard Additions to Nucleobase-Containing Ketofluorohydrins

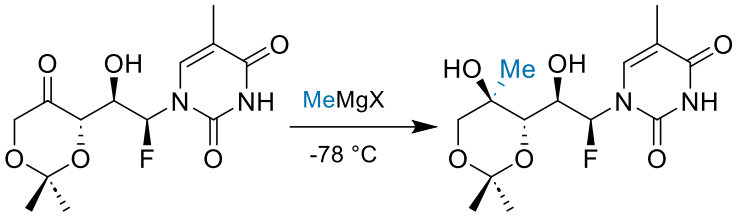

239 **240**

Scheme 6.2. Reaction of Ketofluorohydrin 239 with Methyl Grignard Reagents to Form 240.

Having identified conditions for the selective formation of *syn* diol **235a** (Table 1, entry 5), we turned to the more complicated ketofluorohydrin **239**, incorporating the unprotected nucleobase thymine (**Scheme 6.2**). As summarized in Table 2, we observed a similar trend in diastereoselectivity, indicating that the nucleobase had minimal effect on the diastereochemical outcome of these reactions. For example, using MeMgCl in CH_2Cl_2 led to a 2.3:1 diastereomeric ratio favouring the *syn* diol **240** (entry 1), while MeMgI favoured the *syn* diol **240** with a 6:1 d.r. (entry 3). Again, the use of THF as the solvent or Me_2Mg as the Grignard reagent led to a 1:1 mixture of diastereomers (entries 4 and 5).

Table 6.2. Addition of MeMgX to Ketofluorohydrin 239, Shown in Scheme 6.2.

Entry	X	solvent	*syn:anti*[a] (yield 240)
1	Cl	CH_2Cl_2	2.3:1 (41%)
2	Br	CH_2Cl_2	3.2:1 (38%)
3	I	CH_2Cl_2	6.0:1 (61%)
4	I	THF	1:1 (22%)
5	Me	CH_2Cl_2	1:1[b]

[a] As determined by analysis of 1HNMR spectra recorded on the crude reaction mixture; [b] Yield not recorded.

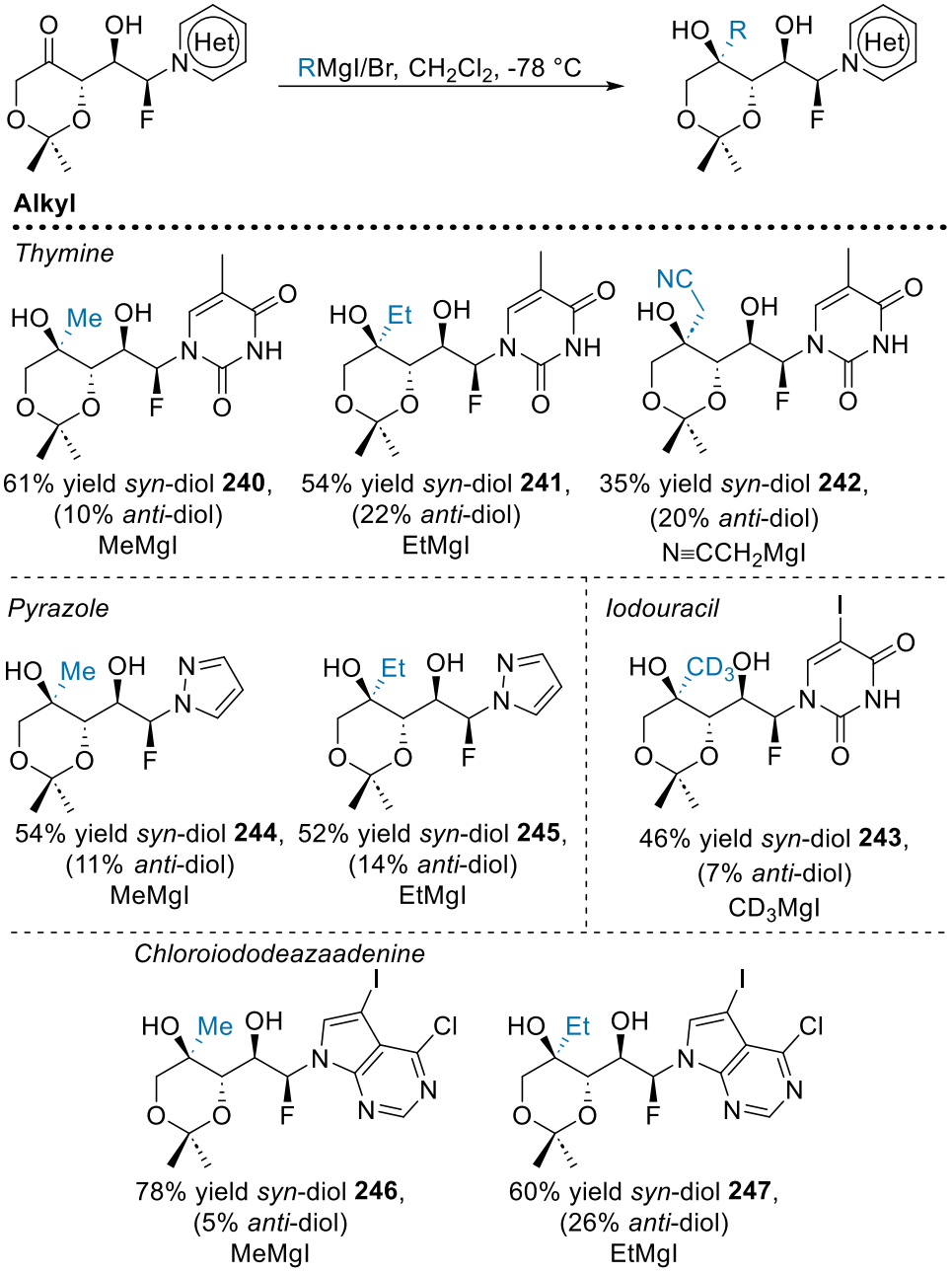

Figure 6.5. The scope of the 1,2-addition of alkyl reagents to ketofluorohydrins.

Figures 6.5 and **6.6** summarize our efforts to explore the broader scope of this reaction and, more specifically, target 1,2-addition products that could be useful for the synthesis of C4'-modified nucleoside analogues. As indicated, for alkyl Grignard reagents the trends identified above translated to the addition of ethyl and cyclopropyl Grignard reagents with the thymine derivative **239**. Several additional nucleobases, including 5-

iodouracil, pyrazole and a chloro-iododeazadenine also proved compatible with this process. While the magnitude of diastereoselectivity varied slightly based on the combination of the alkyl group and nucleobase, the simple modification of solvent (CH_2Cl_2) and halide (I or Br) led to the preferred formation of the desired 1,3-*syn* diol in all cases, providing a collection of 9 distinct 1,2-addition products **240**-**247** (**Figure 6.5**). In contrast, the addition of alkenyl or alkynyl Grignard reagents was not improved by the use of the corresponding MgI or MgBr reagent, and the alkene **248** and alkyne **249** were formed as the minor diastereomer or in equal amounts to the corresponding 1,3-*anti*-diol (**Figure 6.6**).

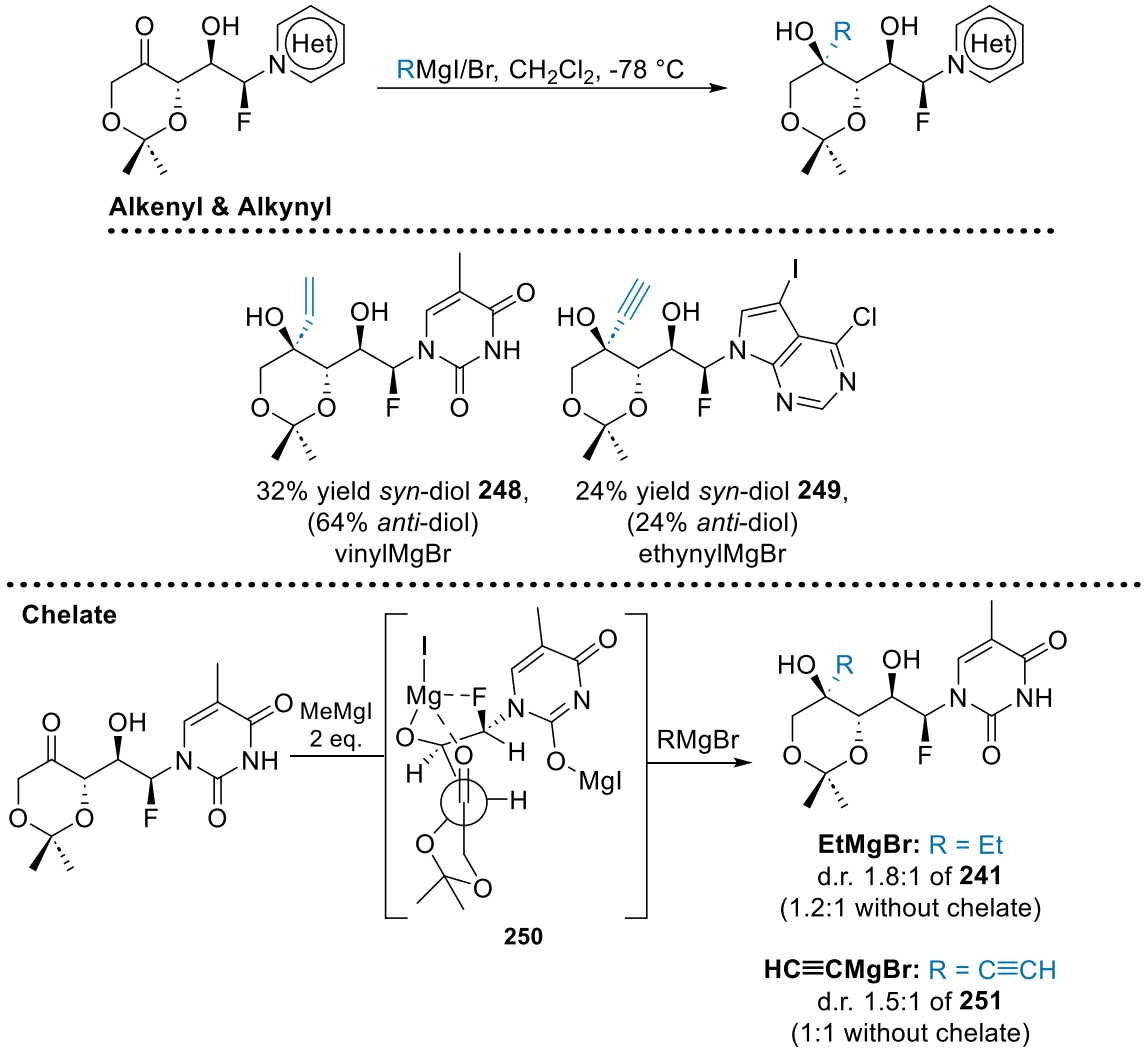

Figure 6.6. The scope of addition of vinyl and alkynyl addition of ketofluorohydrins and model studies on chelate formation showing enhancement of diastereoselectivity.

Notably, each of the reactions required an excess (typically 5-8 equivalents) of RMgX to ensure completion. In the case of thymine derivative **239**, it is reasonable that the first two equivalents of Grignard reagent are consumed through the deprotonation of the thymine NH and hydroxyl functions. It is then expected that the reaction proceeds via a chelate structure (e.g. **250**) and that the halide in this chelate structure (Br or I) plays a central role in determining the diastereoselectivity. To probe this hypothesis, we also examined the addition of 2 equivalents of MeMgI to thymine derivative **239**, which proved insufficient to generate any of the 1,2-adduct **240** but should produce Mg chelate **250**. We then examined the addition of RMgCl reagents and found that this simple modification was sufficient to recapitulate the use of a RMgBr/I reagent. For example, the addition of 2 equivalents of MeMgI to thymine derivative **239** followed by EtMgBr gave the 1,2-addition product **241** in improved diastereoselectivty. Likewise, the addition of 2 equivalents of MeMgI followed by HC≡CMgBr gave the 1,2-addition product **251** in improved diastereoselectivity (**Figure 6.6**).

6.5. Computational Calculations for Mechanistic Insight

The following subchapter was performed in collaboration with Dr. Guillermo Caballero-García. Dr. Caballero-García was responsible for all computational modelling of ground state intermediates and transition states.

To better understand this unusual halide effect on diastereoselectivity, we conducted density functional theory (DFT) calculations (**Figure 6.7**). Full details are provided in the Supplementary Information. Considering that the nucleobase had little impact on diastereoselectivity, we used the simplified model system **252** in which the nucleobase is replaced by a methyl group for all calculations. As noted above, we hypothesized that deprotonation of the alcohol function in **252** would lead to a Mg chelate **253**.[198] Due to the non-coordinating nature of the solvent CH_2Cl_2 and the tendency for Mg to be tetracoordinated in solution, the fluorine atom was also expected to serve as an additional Lewis donor.[231,232] In the appropriate conformation, *(Re)*-addition of a second equivalent of the Grignard reagent would yield ***anti*-254**. On the other hand, *(Si)*-addition would form the desired diastereoisomer ***syn*-254**.

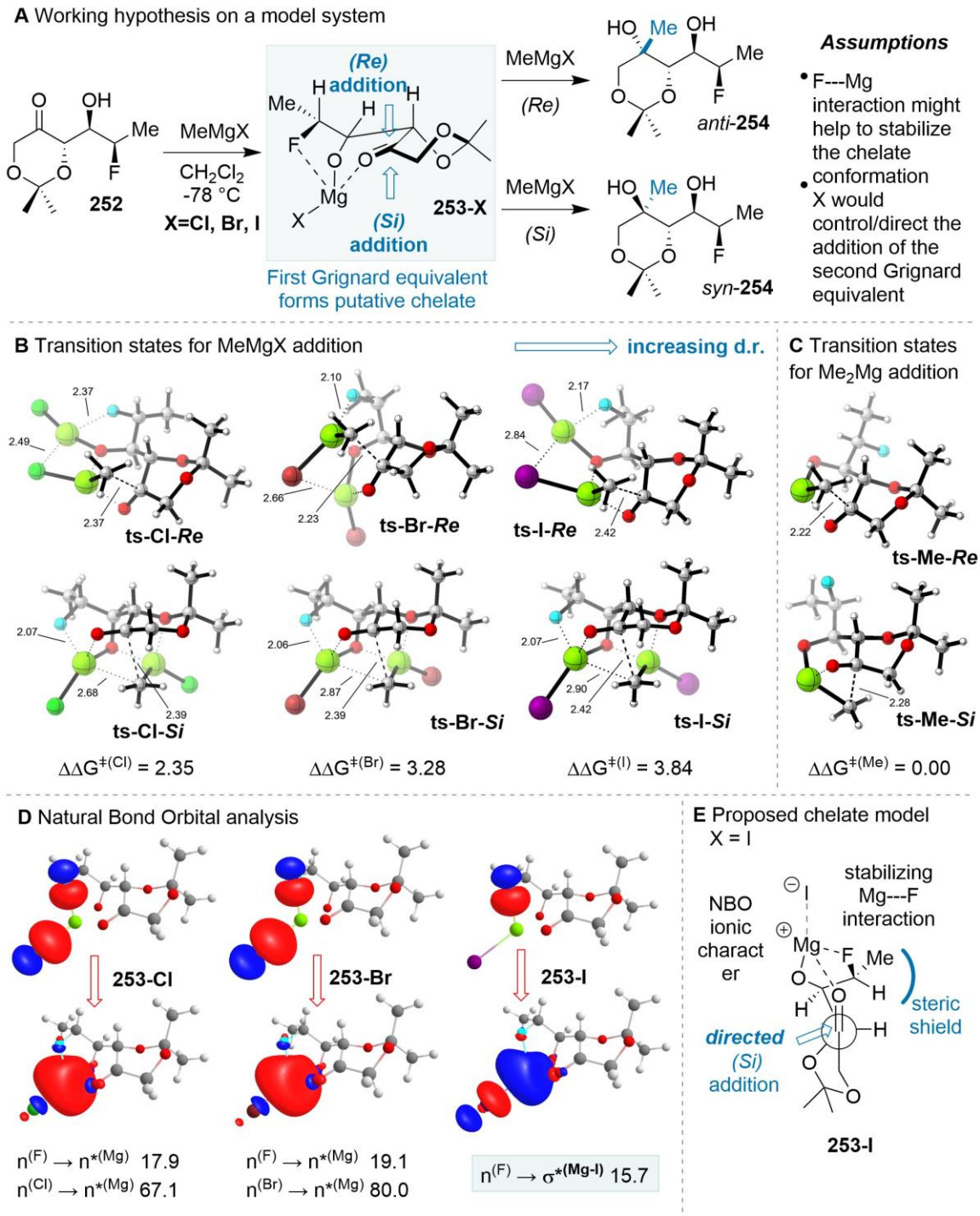

Figure 6.7. **A) The mechanistic hypothesis through chelate 253-X (X=Cl, Br, I). B) The calculated TSs for the Grignard addition of MeMgCl, MeMgBr, MeMgI (left to right). Bottom: *(Si)*-addition. Top: *(Re)*-addition. C) the calculated TSs for the addition of Me_2Mg, *(Si)*-addition on the bottom, *(Re)*-addition on top. D) The NBO analysis showing donor orbitals (top) and acceptor orbitals (bottom). E) The proposed chelate model.**

With chelate **253** in mind, we located the corresponding transition states (TSs) for the *(Si)* and *(Re)*-additions of MeMgCl, MeMgBr and MeMgI (Figure 4B). Computationally, we can interpret d.r. as the difference of differences of energies ($\Delta\Delta G^{\ddagger}$) for two competing diastereoisomeric TSs.[233] Gratifyingly, the observed experimental trends (Tables 1 and 2) were reproduced through calculations, which show an increasing $\Delta\Delta G^{\ddagger}$ throughout the halide series Cl→Br→I ($\Delta\Delta G^{\ddagger(Cl)}$=2.35 kcal mol^{-1} for **TS-Cl-*Si*/*Re***, $\Delta\Delta G^{\ddagger(Br)}$=3.28 kcal mol^{-1} for **TS-Br-*Si*/*Re***, and $\Delta\Delta G^{\ddagger(I)}$=3.84 kcal mol^{-1} for **TS-I-*Si*/*Re***). Here, all (*Si*)-additions include a chair conformation of the dioxanone and are favoured over the corresponding twist-boat-TSs for the *(Re)*-additions. Throughout the *(Si)*-TS series, the Mg-F interaction further enforces a chair conformation and the Mg-F distance is 2.07 Å for each of **TS-Cl-*Si***, **TS-Br-*Si*** and **TS-I-*Si*** (Figure 4B). In contrast, in the *(Re)*-addition TSs, the Mg-F distances are longer and show more variation: **TS-Cl-*Re*** (2.37 Å), **TS-Br-*Re*** (2.10 Å) and **TS-I-*Re*** (2.17 Å). As an additional point of interest, the terminal methyl group in model system **252** is directed away from the reacting carbonyl in all TSs. This observation is consistent with experimental results, where the diastereoselectivity is not greatly influenced by the terminal group (nucleobase or *i*-Pr group).

In addition to the TSs discussed above, we also located TSs **TS-Me-*Si*** and **TS-Me-*Re***, derived from the equivalent reaction with Me_2Mg (Figure 4C). For these two TSs a $\Delta\Delta G^{\ddagger(Me)}$=0.00 kcal mol^{-1} was calculated, which is consistent with the low observed diastereoselectivity for the reaction Me_2Mg with both the fluorohydrin **2** (Table 1, entry 7) and **9** (Table 2, entry 5).

Geometrically, the TSs **TS-Cl-*Si***, **TS-Br-*Si*** and **TS-I-*Si*** show little structural difference. Each TS includes the aforementioned Mg-F interaction, a chair conformation in the dioxanone scaffold, and a bridging nucleophilic methyl group between the two magnesium atoms. Observing these transition states suggests that the magnesium atom from the intermediate chelate **253** could be directing the (*Si*)-facial addition of the second equivalent of MeMgX. These observations suggest that the halide effect may not be the controlling feature of a TS but one of a ground-state conformation instead.[228] Notably, the halides in each of the (*Si*)-TSs are directed away from the reacting center, indicating that the halide size is not a factor in diastereoselection.

To gain further insight we turned to Natural Bond Orbital (NBO) analysis of the corresponding chelates, **253-Cl**, **253-Br** and **253-I** (Figure 4D). Herein we looked at the

orbital delocalizations, from donor to acceptor, and their energies, with emphasis on the orbitals on the Mg atom as a Lewis acceptor (Figure 4D, bottom row structures). As for the donor orbitals, particular attention was paid to the lone pairs on the F atom and the halides Cl, Br or I (Figure 4D, top structures).

For **253-Cl** and **253-Br**, the Mg-F interaction results from an electron donation from a lone pair in the F atom to a non-bonding orbital in the Mg atom ($n^{(F)} \rightarrow n^{*(Mg)}$). This electron donation is slightly stronger in **253-Br** (19.1 kcal mol^{-1}) than in **253-Cl** (17.9 kcal mol^{-1}). This electron donation may further restrict the conformation allowing the Mg atom to direct the second equivalent of MeMgBr more easily. Likewise, the Cl atom in both **253-Cl** and the Br atom in **253-Br** donate electron density from a lone-pair to the same empty orbital on the Mg atom ($n^{(Cl)} \rightarrow n^{*(Mg)}$, 67.1 kcal mol^{-1} and $n^{(Br)} \rightarrow n^{*(Mg)}$, 80.0 kcal mol^{-1}. These $n \rightarrow n^*$ donations suggest that the halides are more associated in chelates **253-Cl** and **253-Br** as it is known that the bonding strength of the Mg atom can have variable effects in diastereoselection.[234] The case is different for **253-I**. Here, no donations from the iodine atom were found to the Mg non-bonding orbitals. However, the electron donation from the F atom ends up in the Mg-I anti-bonding orbital ($n^{(F)} \rightarrow \sigma^{*(Mg\text{-}I)}$, 15.7 kcal mol^{-1}). This suggests that in chelate **253-I**, the iodine atom is more dissociated when compared to the bromine and chlorine counterparts, thus increasing the Lewis acidity on the Mg center, which would help direct the addition of an incoming nucleophile to the *(Si)*-face of the carbonyl.

While magnesium chelation has been exploited to influence diastereoselectivity in Grignard reactions,[166] the effect of the halide in these intermediate chelates has not been thoroughly studied. Generally, a chelating magnesium is thought to lock the substrate in a conformation that biases the addition of a nucleophilic reagent to a particular face of the carbonyl.[166,235,236] Here, we propose that the chelating magnesium can take on a second role; the coordination to, and directing of, the next equivalent of the Grignard reagent. In turn, the halide already bound to the chelating magnesium can influence the metal's ability to act as this guiding center.

6.6. Cyclization of 1,2-diols to access C4'-modified nucleoside analogues

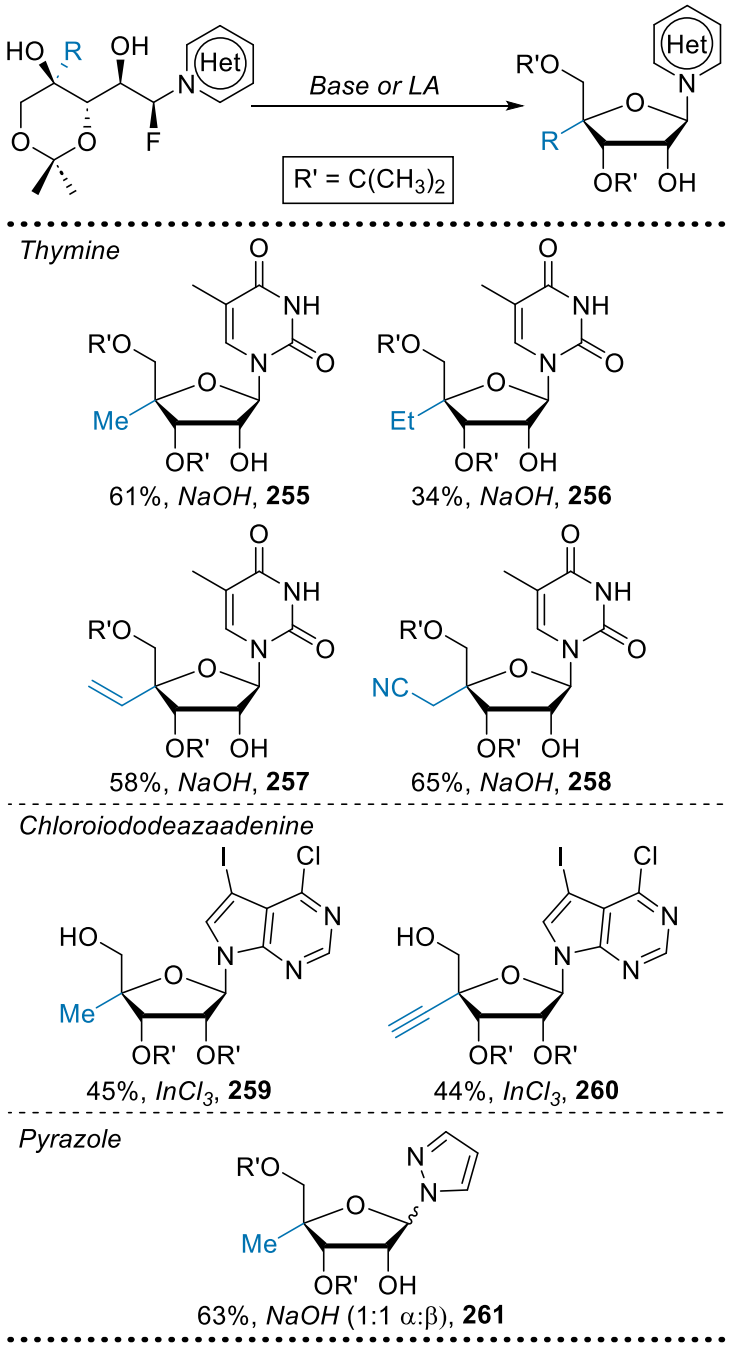

Figure 6.8. The scope of 1,2-diol cyclization to form C4'-modified nucleoside analogues.

Finally, with a collection of *syn*-diols made accessible using RMgI reagents, we demonstrated that these compounds could be readily converted into C4'-modified

nucleoside analogues (**Figure 6.8**). Notably, the sequence of reactions required to access these compounds requires only alkylation of the heterocycle,[237] an α-fluorination/aldol reaction,[70,72] addition of RMgI and cyclization. Thus, this 4-step *de novo* synthesis of naturally or D-configured nucleoside analogues provides an incredibly convenient and diversifiable route to these high-value targets for medicinal chemists. Several thymine, 5-iodouracil, deazadenine and pyrazole-containing nucleoside analogues were prepared in good yield through either base or Lewis-acid promoted annulative fluoride displacement[70] reactions. Notably, using basic cyclization conditions with heat, the nitrile containing nucleoside analogue **258** underwent hydrolysis to give the corresponding carboxylic acid (not shown). Executing this reaction at room temperature, the desired nucleoside **258** was produced in good yield. Importantly, all cyclization reactions yielded the β,D-nucleosides. The methyl and ethynyl chloroiododeazaadenine substrates were also cyclized to their corresponding nucleoside analogues using the previously reported Lewis acidic cyclization conditions (**259**-**260**).[70]

6.7. Conclusion

In conclusion, we describe a remarkable halide effect on the diastereoselectivity of 1,2-addition reactions to β-hydroxy ketones involving Grignard reagents. Through experimental and computational studies, we show that changing the halide tunes the electronic properties of the intermediate magnesium chelate and in turn its ability to direct the reaction with a second equivalent of Grignard reagent. This process now serves as a foundation for the rapid production of C4'-modified nucleosides with diversifiable positions at the nucleobase and C4'. We expect these results will inspire the synthesis of a wide range of nucleoside analogues and accelerate drug discovery efforts in this area.

References

(1) Dewick, P. M. *Medicinal Natural Products: A Biosynthetic Approach 3rd Edition*; John Wiley & Sons, Ltd: West Sussex, England, 2009.

(2) Hanson, J. R., Ed.; 2007; pp 1–34.

(3) Maplestone, R. A.; Stone, M. J.; Williams, D. H. *Gene* **1992**, *115*, 151–157.

(4) Dias, D. A.; Urban, S.; Roessner, U. *Metabolites* **2012**, *2* (2), 303–336.

(5) Haefner, B. *Drug Discov. Today* **2003**, *8* (12), 536–544.

(6) Barbosa, F.; Pinto, E.; Kijjoa, A.; Pinto, M.; Sousa, E. *Int. J. Antimicrob. Agents* **2020**, *56* (1).

(7) Proksch, P.; Edrada, R. A.; Ebel, R. *Appl. Microbiol. Biotechnol.* **2002**, *59* (2–3), 125–134.

(8) Jensen, P. R.; Fenical, W. *Annu. Rev. Microbiol.* **1994**, *48*, 559–584.

(9) Leal, M. C.; Puga, J.; Serôdio, J.; Gomes, N. C. M.; Calado, R. *PLoS One* **2012**, *7* (1).

(10) Gerwick, W. H.; Moore, B. S. *Chem. Biol.* **2012**, *19* (1), 85–98.

(11) Papon, N.; Copp, B. R.; Courdavault, V. *Biotechnol. Adv.* **2022**, *54* (November 2021), 107871.

(12) Stincone, P.; Brandelli, A. *Crit. Rev. Biotechnol.* **2020**, *40* (3), 306–319.

(13) Nweze, J. A.; Mbaoji, F. N.; Huang, G.; Li, Y.; Yang, L.; Zhang, Y.; Huang, S.; Pan, L.; Yang, D. *Mar. Drugs* **2020**, *18* (3).

(14) Ruggieri, G. D. *Science (80-.).* **1976**, *194* (4264), 491–497.

(15) Newman, D. J.; Cragg, G. M. *Planta Med.* **2016**, *82* (9–10), 775–789.

(16) Almaliti, J.; Gerwick, W. H. *Expert Opin. Drug Discov.* **2023**, *18* (7), 687–691.

(17) Haque, N.; Parveen, S.; Tang, T.; Wei, J.; Huang, Z. *Mar. Drugs* **2022**, *20* (8).

(18) Dyshlovoy, S. A.; Honecker, F. *Mar. Drugs* **2020**, *18* (1), 18–21.

(19) Altmann, K. H. *Chimia (Aarau).* **2017**, *71* (10), 646–651.

(20) Montaser, R.; Luesch, H. *Futur. Med Chem* **2012**, *3* (12), 1475–1489.

(21) Molinski, T. F.; Dalisay, D. S.; Lievens, S. L.; Saludes, J. P. *Nat. Rev. Drug Discov.* **2009**, *8* (1), 69–85.

(22) Aicher, T. D.; Buszek, K. R.; Fang, F. G.; Forsyth, C. J.; Jung, S. H.; Kishi, Y.; Matelich, M. C.; Scola, P. M.; Spero, D. M.; Yoon, S. K. *J. Am. Chem. Soc.* **1992**, *114* (8), 3162–3164.

(23) Kaghad, A.; Panagopoulos, D.; Caballero-García, G.; Zhai, H.; Britton, R. *Nat.*

Commun. **2023**, *14* (1), 1904.

(24) Paterson, I.; Anderson, E. a. *Science (80-.).* **2005**, *310* (5747), 451–453.

(25) Hunziker, J.; Koch, G.; Press, N. J. *Chem* **2016**, *1* (3), 336–338.

(26) Smith, A. B.; Beauchamp, T. J.; Lamarche, M. J.; Kaufman, M. D.; Qiu, Y.; Arimoto, H.; Jones, D. R.; Kobayashi, K. *J. Am. Chem. Soc.* **2000**, *122* (36), 8654–8664.

(27) Paterson, I.; Florence, G. J.; Gerlach, K.; Scott, J. P. *Angew. Chemie - Int. Ed.* **2000**, *39* (2), 377–380.

(28) Paterson, I.; Florence, G. J.; Gerlach, K.; Scott, J. P.; Sereinig, N. *J. Am. Chem. Soc.* **2001**, *123* (39), 9535–9544.

(29) Paterson, I.; Florence, G. J. 2008; pp 73–119.

(30) Yu, M. J.; Kishi, Y.; Littlefield, B. A. *Anticancer Agents from Nat. Prod.* **2005**, 241–266.

(31) Nicolaou, K. C.; Snyder, S. A. *Angew. Chemie - Int. Ed.* **2005**, *44* (7), 1012–1044.

(32) Suyama, T. L.; Gerwick, W. H.; McPhail, K. L. *Bioorganic Med. Chem.* **2011**, *19* (22), 6675–6701.

(33) Lorente, A.; Lamariano-Merketegi, J.; Albericio, F.; Álvarez, M. *Chem. Rev.* **2013**, *113* (7), 4567–4610.

(34) Fernández-Peña, L.; Díez-Poza, C.; González-Andrés, P.; Barbero, A. *Mar. Drugs* **2022**, *20* (2), 120.

(35) Bauer, I.; Maranda, L.; Young, K. A.; Shimizu, Y.; Fairchild, C.; Cornell, L.; Macbeth, J.; Huang, S. *J. Org. Chem.* **1995**, *60* (4), 1084–1086.

(36) Teruya, T.; Suenaga, K.; Maruyama, S.; Kurotaki, M.; Kigoshi, H. *Tetrahedron* **2005**, *61* (27), 6561–6567.

(37) Challa, V. R.; Kwon, D.; Taron, M.; Fan, H.; Kang, B.; Wilson, D.; Haeckl, F. P. J.; Keerthisinghe, S.; Linington, R. G.; Britton, R. *Chem. Sci.* **2021**, *12* (15), 5534–5543.

(38) Vidal, J. P.; Escale, R.; Girard, J. P.; Rossi, J. C.; Chantraine, J. M.; Aumelas, A. *J. Org. Chem.* **1992**, *57* (22), 5857–5860.

(39) Smith, A. B.; Duffey, M. O.; Basu, K.; Walsh, S. P.; Suennemann, H. W.; Frohn, M. *J. Am. Chem. Soc.* **2008**, *130* (2), 422–423.

(40) Smith, S.; Tsai, S. C. *Nat. Prod. Rep.* **2007**, *24* (5), 1041–1072.

(41) Staunton, J.; Weissman, K. J. *Nat. Prod. Rep.* **2001**, *18* (4), 380–416.

(42) Kopp, F.; Marahiel, M. A. *Nat. Prod. Rep.* **2007**, *24* (4), 735–749.

(43) Matilla, M. A.; Stöckmann, H.; Leeper, F. J.; Salmond, G. P. C. *J. Biol. Chem.* **2012**, *287* (46), 39125–39138.

(44) Inanaga, J.; Hirata, K.; Saeki, H.; Katsuki, T.; Yamaguchi, M. *Bulletin of the Chemical Society of Japan*. 1979, pp 1989–1993.

(45) Nicolaou, K. C.; Bulger, P. G.; Brenzovich, W. E. *Org. Biomol. Chem.* **2006**, *4* (11), 2158–2183.

(46) Kita, Y.; Maeda, H.; Omori, K.; Okuno, T.; Tamura, Y. *J. Chem. Soc., Perkin Trans. 1* **1993**, No. 23, 2999–3005.

(47) Trost, B. M.; Chisholm, J. D. *Org. Lett.* **2002**, *4* (21), 3743–3745.

(48) Kim, C. H.; An, H. J.; Shin, W. K.; Yu, W.; Woo, S. K.; Jung, S. K.; Lee, E. *Angew. Chemie* **2006**, *118* (47), 8187–8189.

(49) Klüppel, A.; Gille, A.; Karayel, C. E.; Hiersemann, M. *Org. Lett.* **2019**, *21* (7), 2421–2425.

(50) Schomaker, J. M.; Borhan, B. *J. Am. Chem. Soc.* **2008**, *130* (37), 12228–12229.

(51) Murakami, M.; Matsuda, H.; Makabe, K.; Yamaguchi, K. *Tetrahedron Lett.* **1991**, *32* (21), 2391–2394.

(52) Williamson, R. T.; Boulanger, A.; Vulpanovici, A.; Roberts, M. A.; Gerwick, W. H. *J. Org. Chem.* **2002**, *67* (23), 7927–7936.

(53) Lorente, A.; Gil, A.; Fernández, R.; Cuevas, C.; Albericio, F.; Álvarez, M. *Chem. - A Eur. J.* **2015**, *21* (1), 150–156.

(54) Gil, A.; Giarrusso, M.; Lamariano-Merketegi, J.; Lorente, A.; Albericio, F.; Álvarez, M. *ACS Omega* **2018**, *3* (2), 2351–2362.

(55) Alves Reis, M.; Reis Almeida, J.; Vasconcelos, V.; Pereira Morais, J. C.; Ferreria, L.; Pereira, S.; Gonçalves, C.; Neves, J. BIOACTIVE COMPOUNDS OBTAINED FROM CYANOBACTERA LEPTOTHOE SP. LEGE 181152. EP4233857A1, 2023.

(56) Helfrich, E. J. N.; Ueoka, R.; Dolev, A.; Rust, M.; Meoded, R. A.; Bhushan, A.; Califano, G.; Costa, R.; Gugger, M.; Steinbeck, C.; Moreno, P.; Piel, J. *Nat. Chem. Biol.* **2019**, *15* (August), 813–821.

(57) Murata, K.; Mori, H.; Fuwa, H. *Bull. Chem. Soc. Jpn.* **2022**, *95* (12), 1775–1785.

(58) Gil, A.; Lorente, A.; Albericio, F.; Alvarez, M. *Org. Lett.* **2015**, *17* (24), 6246–6249.

(59) Blakemore, P. R.; Cole, W. J.; Kocieński, P. J.; Morley, A. *Synlett* **1998**, No. 1, 26–28.

(60) Kocienski, P. J.; Bell, A.; Blakemore, P. R. *Synlett* **2000**, No. 3, 365–366.

(61) Carey, J. S.; MacCormick, S.; Stanway, S. J.; Teerawutgulrag, A.; Thomas, E. J.

Org. Biomol. Chem. **2011**, *9* (10), 3896–3919.

(62) Bertin, M. J.; Vulpanovici, A.; Monroe, E. A.; Korobeynikov, A.; Sherman, D. H.; Gerwick, L.; Gerwick, W. H. *ChemBioChem* **2016**, *17* (2), 164–173.

(63) Williamson, R. T.; Marquez, B. L.; Gerwick, W. H.; Koehn, F. E. *Magn. Reson. Chem.* **2001**, *39* (9), 544–548.

(64) Rychnovsky, S. D.; Skalitzky, D. J. *Tetrahedron Lett.* **1990**, *31* (7), 945–948.

(65) Matsumori, N.; Kaneno, D.; Murata, M.; Nakamura, H.; Tachibana, K. *J. Org. Chem.* **1999**, *64* (3), 866–876.

(66) Latypov, S. K.; Seco, J. M.; Quinoa, E.; Riguera, R. *J. Am. Chem. Soc.* **1998**, *120* (5), 877–882.

(67) Hoye, T. R.; Jeffrey, C. S.; Shao, F. *Nat. Protoc.* **2007**, *2* (10), 2451–2458.

(68) Bergeron-Brlek, M.; Teoh, T.; Britton, R. *Org. Lett.* **2013**, *15* (14), 3554–3557.

(69) Meanwell, M.; Fehr, G.; Ren, W.; Adluri, B.; Rose, V.; Lehmann, J.; Silverman, S. M.; Rowshanpour, R.; Adamson, C.; Bergeron-Brlek, M.; Foy, H.; Challa, V. R.; Campeau, L. C.; Dudding, T.; Britton, R. *Commun. Chem.* **2021**, *4* (1), 1–9.

(70) Meanwell, M.; Silverman, S. M.; Lehmann, J.; Adluri, B.; Wang, Y.; Cohen, R.; Campeau, L.-C.; Britton, R. *Science (80-.).* **2020**, *369* (6504), 725–730.

(71) Meanwell, M.; Sutherland, M.; Britton, R. *Can. J. Chem.* **2018**, *96* (2), 144–147.

(72) Davison, E. K.; Petrone, D. A.; Meanwell, M.; Nodwell, M. B.; Silverman, S. M.; Campeau, L. C.; Britton, R. *Nat. Protoc.* **2022**, *17* (9), 2008–2024.

(73) Bergeron-Brlek, M.; Meanwell, M.; Britton, R. *Nat. Commun.* **2015**, *6*, 1–6.

(74) Bergeron-Brlek, M.; Goodwin-Tindall, J.; Cekic, N.; Roth, C.; Zandberg, W. F.; Shan, X.; Varghese, V.; Chan, S.; Davies, G. J.; Vocadlo, D. J.; Britton, R. *Angew. Chemie - Int. Ed.* **2015**, *54* (51), 15429–15433.

(75) Ashmus, R. A.; Wang, Y.; González-Cuesta, M.; King, D. T.; Tiet, B.; Gilormini, P. A.; García Fernández, J. M.; Ortiz Mellet, C.; Britton, R.; Vocadlo, D. J. *Org. Biomol. Chem.* **2021**, *19* (37), 8057–8062.

(76) Ren, W.; Farren-Dai, M.; Sannikova, N.; Świderek, K.; Wang, Y.; Akintola, O.; Britton, R.; Moliner, V.; Bennet, A. J. *Chem. Sci.* **2020**, *11* (38), 10488–10495.

(77) Ren, W.; Pengelly, R.; Farren-Dai, M.; Shamsi Kazem Abadi, S.; Oehler, V.; Akintola, O.; Draper, J.; Meanwell, M.; Chakladar, S.; Świderek, K.; Moliner, V.; Britton, R.; Gloster, T. M.; Bennet, A. J. *Nat. Commun.* **2018**, *9* (1), 1–12.

(78) Fuwa, H. *Org. Chem. Front.* **2021**, *8* (14), 3990–4023.

(79) Paul, D.; Kundu, A.; Saha, S.; Goswami, R. K. *Chem. Commun.* **2021**, *57* (27),

3307–3322.

(80) Fletcher, S. *Org. Chem. Front.* **2015**, *2*, 739–752.

(81) Evans, D. A.; Fitch, D. M.; Smith, T. E.; Cee, V. J. *J. Am. Chem. Soc.* **2000**, *122* (41), 10033–10046.

(82) Negishi, E.; Van Horn, D. E.; Yoshida, T. *J. Am. Chem. Soc.* **1985**, *107* (23), 6639–6647.

(83) Kan, S. B. J.; Ng, K. K. H.; Paterson, I. *Angew. Chemie - Int. Ed.* **2013**, *52* (35), 9097–9108.

(84) Kiyooka, S.; Hena, M. A. *J. Org. Chem.* **1999**, *64* (15), 5511–5523.

(85) Boden, E. P.; Keck, G. E. *J. Org. Chem.* **1985**, *50* (13), 2394–2395.

(86) Rychnovsky, S. D.; Rogers, B.; Yang, G. *J. Org. Chem.* **1993**, *58* (13), 3511–3515.

(87) Mowat, J.; Kang, B.; Fonovic, B.; Dudding, T.; Britton, R. *Org. Lett.* **2009**, *11* (10), 2057–2060.

(88) Bonnett, S. A.; Whicher, J. R.; Papireddy, K.; Florova, G.; Smith, J. L.; Reynolds, K. A. *Chem. Biol.* **2013**, *20* (6), 772–783.

(89) Reid, R.; Piagentini, M.; Rodriguez, E.; Ashley, G.; Viswanathan, N.; Carney, J.; Santi, D. V.; Richard Hutchinson, C.; McDaniel, R. *Biochemistry* **2003**, *42* (1), 72–79.

(90) Helfrich, E. J. N.; Piel, J. *Nat. Prod. Rep.* **2016**, *33* (2), 231–316.

(91) Miyanaga, A.; Ouchi, R.; Ishikawa, F.; Goto, E.; Tanabe, G.; Kudo, F.; Eguchi, T. *J. Am. Chem. Soc.* **2018**, *140* (25), 7970–7978.

(92) Hertweck, C. *Angew. Chemie - Int. Ed.* **2009**, *48* (26), 4688–4716.

(93) Ndukwe, I. E.; Wang, X.; Lam, N. Y. S.; Ermanis, K.; Alexander, K. L.; Bertin, M. J.; Martin, G. E.; Muir, G.; Paterson, I.; Britton, R.; Goodman, J. M.; Helfrich, E. J. N.; Piel, J.; Gerwick, W. H.; Williamson, R. T. *Chem. Commun.* **2020**, *56* (55), 7565–7568.

(94) Smith, S. G.; Goodman, J. M. *J. Am. Chem. Soc.* **2010**, *132* (37), 12946–12959.

(95) Liu, Y.; Saurí, J.; Mevers, E.; Peczuh, M. W.; Hiemstra, H.; Clardy, J.; Martin, G. E.; Williamson, R. T. *Science (80-.).* **2017**, *356* (6333).

(96) Lam, N. Y. S.; Muir, G.; Challa, R.; Paterson, I.; Britton, R. *Chem. Commun.* **2019**, *55*, 9717–9720.

(97) Paterson, I.; Maltas, P.; Dalby, S. M.; Lim, J. H.; Anderson, E. A. *Angew. Chemie - Int. Ed.* **2012**, *51* (11), 2749–2753.

(98) Williams, S.; Jin, J.; Kan, S. B. J.; Li, M.; Gibson, L. J.; Paterson, I. *Angew. Chemie - Int. Ed.* **2017**, *56* (2), 645–649.

(99) Paterson, I.; Ashton, K.; Britton, R.; Cecere, G.; Chouraqui, G.; Florence, G. J.; Stafford, J. *Angew. Chemie - Int. Ed.* **2007**, *46* (32), 6167–6171.

(100) Paterson, I.; Britton, R.; Delgado, O.; Meyer, A.; Poullennec, K. G. *Angew. Chemie - Int. Ed.* **2004**, *43* (35), 4629–4633.

(101) Gopalarathnam, A.; Nelson, S. G. *Org. Lett.* **2006**, *8* (1), 7–10.

(102) Herb, C.; Dettner, F.; Maier, M. E. *European J. Org. Chem.* **2005**, No. 4, 728–739.

(103) Ojha, D. P.; Prabhu, K. R. *Org. Lett.* **2016**, *18* (3), 432–435.

(104) Corey, E. J.; Erickson, B. W. *J. Org. Chem.* **1974**, *39* (6), 821–825.

(105) Frank, S. A.; Chen, H.; Kunz, R. K.; Schnaderbeck, M. J.; Roush, W. R. *Org. Lett.* **2000**, *2* (17), 2691–2694.

(106) Takai, K.; Nitta, K.; Utimoto, K. *J. Am. Chem. Soc.* **1986**, *108* (23), 7408–7410.

(107) Schmidt-Leithoff, J.; Brückner, R. *Helv. Chim. Acta* **2005**, *88* (7), 1943–1959.

(108) Fürstner, A.; Funel, J. A.; Tremblay, M.; Bouchez, L. C.; Nevado, C.; Waser, M.; Ackerstaff, J.; Stimson, C. C. *Chem. Commun.* **2008**, No. 25, 2873–2875.

(109) Shiina, I.; Kubota, M.; Ibuka, R. *Tetrahedron Lett.* **2002**, *43* (42), 7535–7539.

(110) Shiina, I.; Kubota, M.; Oshiumi, H.; Hashizume, M. *J. Org. Chem.* **2004**, *69* (6), 1822–1830.

(111) Shiina, I. *Tetrahedron* **2004**, *60* (7), 1587–1599.

(112) Duncton, M. A. J.; Pattenden, G. *J. Chem. Soc. - Perkin Trans. 1* **1999**, No. 10, 1235–1246.

(113) Smith, A. B.; Ott, G. R. *J. Am. Chem. Soc.* **1998**, *120* (16), 3935–3948.

(114) Abarbri, M.; Parrain, J. L.; Duchêne, A.; Thibonnet, J. *Synthesis (Stuttg).* **2006**, *38* (17), 2951–2970.

(115) Ali, G.; Cuny, G. D. *J. Org. Chem.* **2021**, *86* (15), 10517–10525.

(116) Yanovskaya, L. A.; Shakhidayatov, K. *Russ. Chem. Rev.* **1970**, *39* (10), 859–874.

(117) Wulff, W. D.; Peterson, G. A.; Bauta, W. E.; Chan, K.-S.; Faron, K. L.; Gilbertson, S. R.; Kaesler, R. W.; Yang, D. C.; Murray, C. K. *J. Org. Chem.* **1986**, *51* (2), 277–279.

(118) Nicolaou, K. C.; Murphy, F.; Barluenga, S.; Ohshima, T.; Wei, H.; Xu, J.; Gray, D. L. F.; Baudoin, O. *J. Am. Chem. Soc.* **2000**, *122* (16), 3830–3838.

(119) Allred, G. D.; Liebeskind, L. S. *J. Am. Chem. Soc.* **1996**, *118* (11), 2748–2749.

(120) Smith, A. B.; Rano, T. A.; Chida, N.; Sulikowski, G. A. *J. Org. Chem.* **1990**, *55* (4),

1136–1138.

(121) Smith, A. B.; Safonov, I. G.; Corbett, R. M. *J. Am. Chem. Soc.* **2002**, *124* (37), 11102–11113.

(122) Keck, G. E.; Wager, C. A.; Wager, T. T.; Savin, K. A.; Covel, J. A.; McLaws, M. D.; Krishnamurthy, D.; Cee, V. J. *Angew. Chemie - Int. Ed.* **2001**, *40* (1), 231–234.

(123) Tseng, C. C.; Ding, H.; Li, A.; Guan, Y.; Chen, D. Y. K. *Org. Lett.* **2011**, *13* (16), 4410–4413.

(124) Beszant, S.; Giannini, E.; Zanoni, G.; Vidari, G. *European J. Org. Chem.* **2003**, No. 20, 3958–3968.

(125) Blanchette, M. A.; Choy, W.; Davis, J. T.; Essenfeld, A. P.; Masamune, S.; Roush, W. R.; Sakai, T. *Tetrahedron Lett.* **1984**, *25* (21), 2183–2186.

(126) Pellissier, H. *Beilstein J. Org. Chem.* **2018**, *14*, 325–344.

(127) Sparling, B. A.; Moslin, R. M.; Jamison, T. F. *Org. Lett.* **2008**, *10* (6), 1291–1294.

(128) Edmonds, D. J.; Johnston, D.; Procter, D. J. *Chem. Rev.* **2004**, *104* (7), 3371–3403.

(129) Gradillas, A.; Pérez-Castells, J. *Angew. Chemie - Int. Ed.* **2006**, *45* (37), 6086–6101.

(130) Jeon, H. S.; Yeo, J. E.; Jeong, Y. C.; Koo, S. *Synthesis (Stuttg).* **2004**, No. 17, 2813–2820.

(131) Fujioka, H.; Okitsu, T.; Sawama, Y.; Murata, N.; Li, R.; Kita, Y. *J. Am. Chem. Soc.* **2006**, *128* (17), 5930–5938.

(132) Fujioka, H.; Sawama, Y.; Murata, N.; Okitsu, T.; Kubo, O.; Matsuda, S.; Kita, Y. *J. Am. Chem. Soc.* **2004**, *126* (38), 11800–11801.

(133) Neises, B.; Steglich, W. *Angew. Chemie Int. Ed. English* **1978**, *17* (7), 522–524.

(134) Tsakos, M.; Schaffert, E. S.; Clement, L. L.; Villadsen, N. L.; Poulsen, T. B. *Nat. Prod. Rep.* **2015**, *32* (4), 605–632.

(135) Mukaiyama, T.; Usui, M.; Shimada, E.; Saigo, K. *Chem. Lett.* **1975**, *4* (10), 1045–1048.

(136) Saito, A.; Higgins, M.; Zheng, S.; Li, W.; Ojima, I.; Dinkova-Kostova, A. T.; Honda, T. *Bioorganic Med. Chem. Lett.* **2013**, *23* (20), 5540–5543.

(137) Piccinini, P.; Vidari, G.; Zanoni, G. *J. Am. Chem. Soc.* **2004**, *126* (16), 5088–5089.

(138) Corey, E. J.; Nicolaou, K. C. *J. Am. Chem. Soc.* **1974**, *96* (17), 5614–5616.

(139) Smith, A. B.; Dong, S.; Brenneman, J. B.; Fox, R. J. *J. Am. Chem. Soc.* **2009**, *131* (34), 12109–12111.

(140) Evans, D. A.; Starr, J. T. *J. Am. Chem. Soc.* **2003**, *125* (44), 13531–13540.
(141) Trost, B. M.; Haffner, C. D.; Jebaratnam, D. J.; Krische, M. J.; Thomas, A. P. *J. Am. Chem. Soc.* **1999**, *121* (26), 6183–6192.
(142) Gómez, C.; Maciá, B.; Lillo, V. J.; Yus, M. *Tetrahedron* **2006**, *62* (42), 9832–9839.
(143) Jaracz, S.; Nakanishi, K.; Jensen, A. A.; Strømgaard, K. *Chem. - A Eur. J.* **2004**, *10* (6), 1507–1518.
(144) Kuntiyong, P.; Lee, T. H.; Kranemann, C. L.; White, J. D. *Org. Biomol. Chem.* **2012**, *10* (39), 7884–7899.
(145) Onoda, T.; Shirai, R.; Iwasaki, S. *Tetrahedron Lett.* **1997**, *38* (8), 1443–1446.
(146) Kern, N.; Dombray, T.; Blanc, A.; Weibel, J. M.; Pale, P. *J. Org. Chem.* **2012**, *77* (20), 9227–9235.
(147) Villar, E. A.; Beglov, D.; Chennamadhavuni, S.; Porco, J. A.; Kozakov, D.; Vajda, S.; Whitty, A. *Nat. Chem. Biol.* **2014**, *10* (9), 723–731.
(148) Ueda, M.; Yamaura, M.; Ikeda, Y.; Suzuki, Y.; Yoshizato, K.; Hayakawa, I.; Kigoshi, H. *J. Org. Chem.* **2009**, *74* (9), 3370–3377.
(149) Hayakawa, I.; Ueda, M.; Yamaura, M.; Ikeda, Y.; Suzuki, Y.; Yoshizato, K.; Kigoshi, H. *Org. Lett.* **2008**, *10* (1), 1859–1862.
(150) Hayakawa, I.; Okamura, M.; Suzuki, K.; Shimanuki, M.; Kimura, K.; Yamada, T.; Ohyoshi, T.; Kigoshi, H. *Synth.* **2017**, *49* (13), 2958–2970.
(151) Schulthoff, S.; Hamilton, J. Y.; Heinrich, M.; Kwon, Y.; Wirtz, C.; Fürstner, A. *Angew. Chemie - Int. Ed.* **2021**, *60* (1), 446–454.
(152) Okude, Y.; Hirano, S.; Hiyama, T.; Nozaki, H. *J. Am. Chem. Soc.* **1977**, *99* (9), 3179–3181.
(153) Jin, H.; Uenishi, J.; Christ, W. J.; Kishi, Y. *J. Am. Chem. Soc.* **1986**, *108* (18), 5644–5646.
(154) Takai, K.; Tagashira, M.; Kuroda, T.; Oshima, K.; Utimoto, K.; Nozaki, H. *J. Am. Chem. Soc.* **1986**, *108* (19), 6048–6050.
(155) Paterson, I.; Goodman, J. M.; Anne Lister, M.; Schumann, R. C.; McClure, C. K.; Norcross, R. D. *Tetrahedron* **1990**, *46* (13–14), 4663–4684.
(156) Omura, K.; Swern, D. *Tetrahedron* **1978**, *34* (11), 1651–1660.
(157) Ley, S. V.; Norman, J.; Griffith, W. P.; Marsden, S. P. *Synthesis (Stuttg).* **1994**, *1994* (07), 639–666.
(158) Boeckman, R. K.; Shao, P.; Mullins, J. J.; Minbiole, K. P.; Smith, A. B. *Org. Synth.* **2000**, *77* (September), 141.

(159) Carpenter, J.; Northrup, A. B.; Chung, D. M.; Wiener, J. J. M.; Kim, S. G.; MacMillan, D. W. C. *Angew. Chemie - Int. Ed.* **2008**, *47* (19), 3568–3572.

(160) Scheerer, J. R.; Lawrence, J. F.; Wang, G. C.; Evans, D. A. *J. Am. Chem. Soc.* **2007**, *129* (29), 8968–8969.

(161) Dhakal, R. C.; Dieter, R. K. *Org. Lett.* **2014**, *16* (5), 1362–1365.

(162) Rychnovsky, S. D.; Khire, U. R.; Yang, G. *J. Am. Chem. Soc.* **1997**, *119* (8), 2058–2059.

(163) Leroux, F.; Schlosser, M.; Zohar, E.; Marek, I. *The Preparation of Organolithium Reagents and Intermediates*; 2009.

(164) Nakatsuka, M.; Ragan, J. A.; Sammakia, T.; Smith, D. B.; Uehling, D. E.; Schreiber, S. L. *J. Am. Chem. Soc.* **1990**, *112* (14), 5583–5601.

(165) Matteson, D. S. *Chem. Rev.* **1989**, *89* (7), 1535–1551.

(166) Keck, G. E.; Andrus, M. B.; Romer, D. R. *Journal of Organic Chemistry*. January 1, 1991, pp 417–420.

(167) Ren, H.; Krasovskiy, A.; Knochel, P. *Org. Lett.* **2004**, *6* (23), 4215–4217.

(168) Knochel, P.; Nonnant, J. F. *Tetrahedron Lett.* **1986**, *27* (37), 4431–4434.

(169) Gilman, H.; Cartledge, F. K. *J. Organomet. Chem.* **1964**, *2* (6), 447–454.

(170) Dong, C. G.; Yeung, P.; Hu, Q. S. *Org. Lett.* **2007**, *9* (2), 363–366.

(171) Williams, D. R.; Kissel, W. S. *J. Am. Chem. Soc.* **1998**, *120* (43), 11198–11199.

(172) Zanato, C.; Pignataro, L.; Ambrosi, A.; Hao, Z.; Gennari, C. *European J. Org. Chem.* **2010**, No. 30, 5767–5771.

(173) Boer, R. E.; Giménez-Bastida, J. A.; Boutaud, O.; Jana, S.; Schneider, C.; Sulikowski, G. A. *Org. Lett.* **2018**, *20* (13), 4020–4022.

(174) Crimmins, M. T.; Haley, M. W.; O'Bryan, E. A. *Org. Lett.* **2011**, *13* (17), 4712–4715.

(175) Rio, J.; Perrin, L.; Payard, P. *European J. Org. Chem.* **2022**, *2022* (44).

(176) Butkevich, A. N.; Meerpoel, L.; Stansfield, I.; Angibaud, P.; Corbu, A.; Cossy, J. *Org. Lett.* **2013**, *15* (15), 3840–3843.

(177) Kobayashi, Y.; Saeki, R.; Nanba, Y.; Suganuma, Y.; Morita, M.; Nishimura, K. *Synlett* **2017**, *28* (19), 2655–2659.

(178) Kawai, N.; Lagrange, J. M.; Uenishi, J. *European J. Org. Chem.* **2007**, No. 17, 2808–2814.

(179) Trost, B. M.; Ball, Z. T. *J. Am. Chem. Soc.* **2005**, *127* (50), 17644–17655.

(180) Smith, A. B.; Kim, W. S.; Tong, R. *Org. Lett.* **2010**, *12* (3), 588–591.

(181) Lamariano-Merketegi, J.; Lorente, A.; Gil, A.; Albericio, F.; Álvarez, M. *European J. Org. Chem.* **2015**, *2015* (1), 235–241.
(182) Fürstner, A. *J. Am. Chem. Soc.* **2021**, *143* (38), 15538–15555.
(183) Crouch, R. D. *Tetrahedron* **2013**, *69* (11), 2383–2417.
(184) Seyferth, D. *Organometallics* **2009**, *28* (6), 1598–1605.
(185) Knochel, P.; Dohle, W.; Gommermann, N.; Kneisel, F. F.; Kopp, F.; Korn, T.; Sapountzis, I.; Vu, V. A. *Angew. Chemie - Int. Ed.* **2003**, *42* (36), 4302–4320.
(186) Hoffmann, R. W. *Chem. Soc. Rev.* **2003**, *32* (4), 225–230.
(187) Ashby, E. C. *Pure Appl. Chem.* **1980**, *52* (3), 545–569.
(188) Ashby, E. C.; Bowers, J. R. *J. Am. Chem. Soc.* **1981**, *103* (9), 2242–2250.
(189) Legros, J.; Figadère, B. *Phys. Sci. Rev.* **2017**, *3* (3), 1–27.
(190) Zeng, X.; Cong, X. *Org. Chem. Front.* **2015**, *2* (1), 69–72.
(191) Samineni, R.; Eda, V.; Rao, P.; Sen, S.; Oruganti, S. *ChemistrySelect* **2022**, *7* (5), 1–12.
(192) Hoffmann, R. W.; Hölzer, B. *J. Am. Chem. Soc.* **2002**, *124* (16), 4204–4205.
(193) Matsuzawa, S.; Horiguchi, Y.; Nakamura, E.; Kuwajima, I. *Tetrahedron* **1989**, *45* (2), 349–362.
(194) Ashby, E. C.; Laemmle, J.; Neumann, H. M. *Acc. Chem. Res.* **1974**, *7* (8), 272–280.
(195) Walker, F. W.; Ashby, E. C. *J. Am. Chem. Soc.* **1969**, *91* (14), 3845–3850.
(196) Parris, G. E.; Ashby, E. C. *J. Am. Chem. Soc.* **1971**, *93* (5), 1206–1213.
(197) Peltzer, R. M.; Gauss, J.; Eisenstein, O.; Cascella, M. *J. Am. Chem. Soc.* **2020**.
(198) French, W.; Wright, G. F. *Can. J. Chem.* **1964**, *42* (11), 2474–2479.
(199) Carreira, E. M.; Bois, J. Du. *J. Am. Chem. Soc.* **1995**, *117* (31), 8106–8125.
(200) Nicolaou, K. C.; Claremon, D. A.; Barnette, W. E. *J. Am. Chem. Soc.* **1980**, *102* (21), 6611–6612.
(201) Roberts, J. T. In *Handbook of Grignard Reagents*; Silverman, G. S., Akita, P. E., Eds.; CRC Press, 1996; pp 557–575.
(202) Bartolo, N. D.; Read, J. A.; Valentín, E. M.; Woerpel, K. A. *Chem. Rev.* **2020**, *120* (3), 1513–1619.
(203) Trost, B. M.; Frederiksen, M. U.; Papillon, J. P. N.; Harrington, P. E.; Shin, S.; Shireman, B. T. *J. Am. Chem. Soc.* **2005**, *127* (11), 3666–3667.
(204) Ais, V. D.; Hall, M. J.; Corsi, C.; Wendeborn, S. V.; Meyer, C.; Cossy, J. *Org. Lett.* **2009**, *11* (4), 935–938.

(205) Bai, X.; Eliel, E. L. *J. Org. Chem.* **1992**, *57* (19), 5166–5172.
(206) Righi, G.; Pietrantonio, S.; Bonini, C. *Tetrahedron* **2001**, *57* (50), 10039–10046.
(207) Deng, W.; Overman, L. E. *J. Am. Chem. Soc.* **1994**, *116* (25), 11241–11250.
(208) Liang, X.; Lee, C. J.; Zhao, J.; Toone, E. J.; Zhou, P. *J. Med. Chem.* **2013**, *56* (17), 6954–6966.
(209) Takahashi, S.; Nakata, T. *J. Org. Chem.* **2002**, *67* (16), 5739–5752.
(210) Bailey, W. F.; Reed, D. P.; Clark, D. R.; Kapur, G. N. *Org. Lett.* **2001**, *3* (12), 1865–1867.
(211) Takahashi, S.; Kuzuhara, H. *J. Chem. Soc. - Perkin Trans. 1* **1997**, No. 5, 607–612.
(212) Kim, K. S.; Ahn, Y. H.; Bong Park, S.; Hacng Chc, I.; Joo, Y. H.; Youn, B. H. *J. Carbohydr. Chem.* **1991**, *10* (5), 911–915.
(213) Malek-Adamian, E.; Patrascu, M. B.; Jana, S. K.; Martínez-Montero, S.; Moitessier, N.; Damha, M. J. *J. Org. Chem.* **2018**, *83* (17), 9839–9849.
(214) Yates, M. K.; Seley-Radtke, K. L. *Antiviral Res.* **2019**, *162* (November 2018), 5–21.
(215) Nikam, R. R.; Harikrishna, S.; Gore, K. R. *European J. Org. Chem.* **2021**, *2021* (6), 924–932.
(216) Kirby, K. A.; Michailidis, E.; Fetterly, T. L.; Steinbach, M. A.; Singh, K.; Marchand, B.; Leslie, M. D.; Hagedorn, A. N.; Kodama, E. N.; Marquez, V. E.; Hughes, S. H.; Mitsuya, H.; Parniak, M. A.; Sarafianos, S. G. *Antimicrob. Agents Chemother.* **2013**, *57* (12), 6254–6264.
(217) McLaughlin, M.; Kong, J.; Belyk, K. M.; Chen, B.; Gibson, A. W.; Keen, S. P.; Lieberman, D. R.; Milczek, E. M.; Moore, J. C.; Murray, D.; Peng, F.; Qi, J.; Reamer, R. A.; Song, Z. J.; Tan, L.; Wang, L.; Williams, M. J. *Org. Lett.* **2017**, *19* (4), 926–929.
(218) Wang, G.; Dyatkina, N.; Prhavc, M.; Williams, C.; Serebryany, V.; Hu, Y.; Huang, Y.; Wan, J.; Wu, X.; Deval, J.; Fung, A.; Jin, Z.; Tan, H.; Shaw, K.; Kang, H.; Zhang, Q.; Tam, Y.; Stoycheva, A.; Jekle, A.; Smith, D. B.; Beigelman, L. *J. Med. Chem.* **2019**, *62* (9), 4555–4570.
(219) Guinan, M.; Benckendorff, C.; Smith, M.; Miller, G. J. *Molecules* **2020**, *25* (9), 2050.
(220) Zhou, Y.; Zang, C.; Wang, H.; Li, J.; Cui, Z.; Li, Q.; Guo, F.; Yan, Z.; Wen, X.; Xi, Z.; Zhou, C. *Org. Biomol. Chem.* **2019**, *17* (22), 5550–5560.

(221) Liboska, R.; Snášel, J.; Barvík, I.; Buděšínský, M.; Pohl, R.; Toík, Z.; Páv, O.; Rejman, D.; Novák, P.; Rosenberg, I. *Org. Biomol. Chem.* **2011**, *9* (24), 8261–8267.

(222) Wang, G.; Middleton, P. J.; Lin, C.; Pietrzkowski, Z. *Bioorg. Med. Chem. Lett.* **1999**, *9* (6), 885–890.

(223) Suri, J. T.; Ramachary, D. B.; Barbas, C. F. *Org. Lett.* **2005**, *7* (7), 1383–1385.

(224) Crotti, S.; Bertolini, F.; Bussolo, V. Di; Pineschi, M. *Org. Lett.* **2010**, *12* (8), 1828–1830.

(225) Kobayashi, Y.; Nakata, K.; Ainai, T. *Org. Lett.* **2005**, *7* (2), 183–186.

(226) Li, S.; Miao, B.; Yuan, W.; Ma, S. *Org. Lett.* **2013**, *15* (5), 977–979.

(227) Fuji, K.; Tanaka, K.; Ahn, M.; Mizuchi, M. *Chem. Pharm. Bull.* **1994**, *42* (4), 957–959.

(228) Bartolo, N. D.; Demkiw, K. M.; Valentín, E. M.; Hu, C. T.; Arabi, A. A.; Woerpel, K. A. *J. Org. Chem.* **2021**, *86* (10), 7203–7217.

(229) Giuliano, R. M.; Villani, F. J. *J. Org. Chem.* **1995**, *60* (1), 202–211.

(230) Chung, J. Y. L.; Kassim, A. M.; Simmons, B.; Davis, T. A.; Song, Z. J.; Limanto, J.; Dalby, S. M.; He, C. Q.; Calabria, R.; Wright, T. J.; Campeau, L. C. *Org. Process Res. Dev.* **2022**, *26* (3), 698–709.

(231) Mori, T.; Kato, S. *Chem. Phys. Lett.* **2007**, *437* (1–3), 159–163.

(232) Tuulmets, A.; Pällin, V.; Tammiku-Taul, J.; Burk, P.; Raie, K. *J. Phys. Org. Chem.* **2002**, *15* (10), 701–705.

(233) Peng, Q.; Duarte, F.; Paton, R. S. *Chem. Soc. Rev.* **2016**, *45* (22), 6093–6107.

(234) Mulzer, J.; Pietschmann, C.; Buschmann, J.; Luger, P. *J. Org. Chem.* **1997**, *62* (12), 3938–3943.

(235) Yadav, J. S.; Swamy, T.; Subba Reddy, B. V.; Ravinder, V. *Tetrahedron Lett.* **2014**, *55* (30), 4054–4056.

(236) Cleator, E.; McCusker, C. F.; Steltzer, F.; Ley, S. V. *Tetrahedron Lett.* **2004**, *45* (15), 3077–3080.

(237) Huxley, C.; Lucas, C.; Bruno, J. M. M.; Anketell, M. J.; Davison, E. K.; Muir, G.; Nodwell, M. B.; Meanwell, M.; Silverman, S. M.; Britton, R.; Campeau, L.-C. *Can. J. Chem.* **2023**, No. Chart 1, 1–4.

(238) Clausen, D. J.; Wan, S.; Floreancig, P. E. **2011**, 5178–5181.

(239) Waga, T.; Nishizaki, T.; Miyakawa, I.; Ohrui, H.; Meguro, H. *Biosci. Biotechnol. Biochem.* **1993**, *57* (9), 1433–1438.

Appendix A. Supplementary Information

A.1. General Information

All reactions were performed at ambient temperature and atmosphere unless otherwise specified. Flash chromatography was performed using 230-400 mesh silica gel (Merck, Silica Gel 60). Concentration of solutions and removal of solvents was done via a Büchi rotary evaporator using an acetone/dry ice condenser and vacuum applied from an Emerson vacuum pump.

All reagents, solvents, and starting materials were purchased from Sigma Aldrich, Fisher, Alfa Aesar, Oakwood Chemicals, TCI America or AK Scientific and were used without further purification or were prepared according to literature preparations where applicable. Dry dichloromethane (CH_2Cl_2) was obtained by freshly distilling over calcium hydride each time before use. Tetrahydrofuran (THF) was freshly distilled over sodium metal/benzophenone each time before use. Deuterodichloromethane (CD_2Cl_2) was freshly distilled over calcium hydride each time before use. All other dry solvents were obtained by treatment with 4Å molecular sieves for 48h before use or purchased from as the dry solvent. -78 °C bath temperatures were maintained using an acetone/dry ice bath.

Nuclear magnetic resonance (NMR) spectra were recorded using deuterochloroform ($CDCl_3$) or deuteroacetonitrile (CD_3CN) as the solvent.. Signal positions (δ) are given in parts per million from tetramethylsilane (δ 0) and were measured relative to the signal of the solvent (^{1}HNMR: $CDCl_3$: δ 7.26, CD_3CN: δ 1.94, $(CD_3)_2SO$: δ 2.50; ^{13}CNMR: $CDCl_3$: δ 77.16, CD_3CN: δ 118.26, $(CD_3)_2SO$: δ 39.52).). Coupling constants (*J*) are given in Hertz (Hz) and are reported to the nearest 0.1Hz. 1H NMR spectral data are tabulated in the order: multiplicity (s, singlet; bs, broad singlet; d, doublet; t, triplet; q, quartet; hept, heptet; m, multiplet), coupling constants, number of protons. NMR spectra were recorded on a Bruker Advance II or III 600 equipped with a QNP or QCI cryoprobe (600 MHz), Bruker Advance III 400 (400 MHz), Bruker Advance III 500 (500 MHz), or Bruker Advance III 400_Solids (400 MHz). Diastereomeric ratios (dr) was determined by analysis of crude ^{1}HNMR. Stereochemical assignments of compounds and signal assignments of ^{1}HNMR and ^{13}CNMR was based on analysis of COSY, HSQC, HMBC, and 2D NOESY spectra and comparison to literature spectra, where applicable.

Optical rotation was measured on a Perkin Elmer 341 Polarimeter at 589 nm. Infrared (IR) spectra were recorded on a Thermo Nicolet Nexus 670 FTIR with neat samples. Only selected, characteristic absorption data are provided for each compound. High resolution mass spectrometry was performed on an Agilent 6210 TOF LC/MS using ESI-MS or a Bruker Maxis Impact using ESI-MS. High performance liquid chromatography (HPLC) analysis was performed on an Agilent 1290 Affinity II HPLC or an Agilent 1100 Series HPLC, equipped with a variable wavelength UV-Vis and mass spectrometry detector.

The data presented in this appendix has been reported in part, see:

Lam, N. Y. S.; Muir, G.; Challa, R.; Paterson, I.; Britton, R. Chem. Commun. **2019**, 55, 9717–9720.

Edits to compound numbering and formatting of analytical data titles are used for clarity.

A.2. Experimental procedures and characterization data

A.2.1. Preparation of Reagents

Synthesis of thioether S1

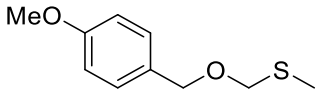

To a room temperature stirred solution of sodium iodide (5.40 g, 36.0 mmol, 1 eq.) and sodium hydride (60% w/w suspension in mineral oil, 2.88 g, 72.0 mmol, 2 eq.) in THF (72 mL) under N_2 was added *para*-methoxybenzel alcohol (4.47 mL, 36.0 mmol, 1 eq.) dropwise. The resulting mixture was cooled to 0 °C and chloromethyl methyl sulfide (3.0 mL, 36 mmol, 1 eq.) was added. The resulting mixture was stirred at 0 °C for 2 hours and then warmed to room temperature and stirred for 18 hours. The reaction mixture was diluted with H_2O (70 mL) and Et_2O (70 mL) and the phases separated. The aqueous phase was then washed with Et_2O (3 x 50 mL). The organic layers were combined, and

washed with brine, dried with $MgSO_4$, filtered, and concentrated under reduced pressure. The resulting oil was purified by flash chromatography (gradient of EtOAc:hexanes 1:9) to afford the thioether S1 as a clear oil (4.84 g, 68%). This material was stored long-term and transformed to the chloromethyl ether as required.

Data in agreement with that presented in the literature.[142]

Synthesis of PMBMCl 184

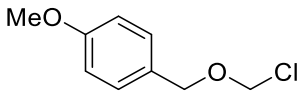

To a cold, -78 °C, stirred solution of sulfide S1 (462 mg, 3.43 mmol, 1.0 eq.) in DCM under N_2 was added sulfuryl chloride (0.29 mL, 3.43 mmol, 1.0 eq.) dropwise. The resulting mixture was stirred at -78 °C for 30 min and then warmed to room temperature. The resulting mixture was concentrated under reduced pressure to afford PMBCl 184 as a yellow oil (639 mg, 99%) that was used without further purification.

Data in agreement with that presented in the literature.[142]

Preparation of $MgBr_2$ solution

To a room temperature stirred mixture of magnesium (30 mg, 1.2 mmol, 1.0 eq.) under N_2 in Et_2O (2.5 mL) and benzene (1.6 mL) was added 1,2-dibromoethane (0.11 mL, 1.2 mmol, 1.0 eq). The level of the solvent was marked on the flask and the resulting mixture heated to reflux and stirred until all the magnesium was observed to have dissolved, approximately 3 hours. Et_2O was added over the course of this reflux to maintain the concentration. The solution was then allowed to cool to room temperature and used without further handling.

A.2.2. Experimental Procedures for the Preparation of Substrates for Stereochemical Reassignment

Synthesis of vinyl iodide 78

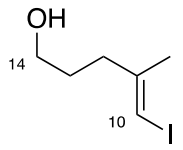

$AlMe_3$ (89 mL, 178 mmol, 2.0 M solution in hexane) was added dropwise to a stirred solution of Cp_2ZrCl_2 (5.20 g, 17.8 mmol) in dichloroethane (200 mL) at –30 °C. The solution was stirred at –30 °C for 5 min before the dropwise addition of H_2O (535 μL, 29.7 mmol) into the reaction mixture. The resultant mixture was allowed to warm to r.t. over 10 min before cooling to –30 °C. A solution of 4-pentyn-1-ol (5.53 ml, 59.4 mmol) in dichloroethane (97 mL) was added dropwise *via* cannula to the reaction mixture at –30 °C. The reaction mixture was allowed to warm to r.t. and stirred at r.t. for 20 h before cooling to– 30°C. A solution of I_2 (30.1 g, 119 mmol) in THF (59 mL) was added dropwise *via* cannula to the reaction mixture. The resulting mixture was stirred at – 30°C for a further 2 h before quenching with Na/K tartrate (200 mL), warming to r.t. and stirred for 16 h at r.t.. The resulting suspension was filtered to remove excess salts and the layers were separated. The aqueous layer was extracted with dichloromethane (3 × 100mL) and the combined organic phases were washed with brine (300 mL), dried ($MgSO_4$), and the solvent removed under reduced pressure. Purification by flash chromatography (EtOAc/hexanes: 30% → 50%) gave the vinyl iodide 78 as an orange oil (11.72 g, 51.8 mmol, 87%).

R_f (EtOAc/hexanes: 50%) = 0.40; **^{1}H NMR** (400 MHz, $CDCl_3$) δ_H 5.94 (1H, q, *J* = 1.2 Hz, H10), 3.65 (2H, t, *J* = 6.4 Hz, H14), 2.32 (2H, td, *J* = 7.5, 1.1 Hz, H12), 1.87 (3H, d, *J* = 1.2 Hz, Me11), 1.76-1.68 (2H, m, H13).

Data in agreement as presented in the literature.[238]

Synthesis of chlorohydrin 82

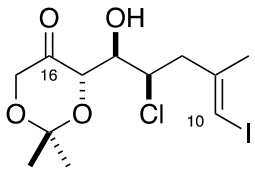

Dess-Martin Periodinane (18.87 g, 44.5 mmol) was added to a stirred suspension of alcohol 8a (8.40 g, 37.1 mmol), $NaHCO_3$ (9.33 g, 111.0 mmol) in dichloromethane (123 mL). The reaction mixture was stirred at r.t. for 1 h before quenching with the addition of $NaHCO_3$ (50 mL), $Na_2S_2O_3$ (50 mL) and H_2O (50 mL). The mixture was stirred for 2 h before the layers were separated. The aqueous layer was extracted with dichloromethane (3 × 100 mL). The combined organic phases were washed with brine (300 mL), dried ($MgSO_4$), and the solvent removed under reduced pressure to afford the crude aldehyde 80 (8.04 g, 35.9 mmol, 95%), which was used directly in subsequent steps without purification.

NCS (4.31 g, 32.3 mmol) was added to a stirred solution of aldehyde 80 (8.04 g, 35.9 mmol), L-proline (3.72 g, 32.3 mmol) in dichloromethane (120 mL). The reaction was stirred at r.t. until complete chlorination of the aldehyde was observed by NMR (*ca.* 2 h). At this point, 2,2-dimethyl-1,3-dioxan-5-one, 81, (5.62 g, 43.1 mmol) was added and the reaction mixture was stirred at r.t. for 24 h. The reaction was quenched by addition of brine (100 mL) and the layers separated. The organic phase was washed with brine (100 mL) and the combined aqueous phases were extracted with dichloromethane (3 × 150 mL). The combined organic phases were dried ($MgSO_4$), and the solvent removed under reduced pressure. Purification by flash chromatography (EtOAc/hexanes: 10% → 25%) afforded chlorohydrin 82 as a yellow oil (6.56 g, 16.9 mmol, 47%, 98% *ee*) as a separable 5.3:1 mixture of diastereomers.

R_f (EtOAc/hexanes: 20%) = 0.35; **^{1}H NMR** (600 MHz, $CDCl_3$) δ_H 6.15 (1H, q, *J* = 1.2 Hz, H10), 4.39 (1H, dd, *J* = 8.9, 1.5 Hz, H15), 4.33–4.26 (2H, m, H13, H17a), 4.08 (1H, d, *J* = 17.6 Hz, H17b), 3.88 (1H, ddd, *J* = 8.9, 3.0, 1.7 Hz, H14), 3.39 (1H, dd, J = 3.0, 1.4 Hz, OH), 2.80 (2H, dt, *J* = 7.7, 1.3 Hz, H12), 1.88 (3H, d, *J* = 1.1 Hz, Me11), 1.51 (3H, s, $\underline{Me}_AMe_BCO_2$), 1.43 (s, 3H, $Me_A\underline{Me}_BCO_2$); **^{13}C NMR** (150 MHz, CDCl3) δ_c 212.4, 143.2,

101.8, 79.5, 72.8, 70.6, 66.5, 58.6, 43.8, 24.0, 23.9, 23.5; **IR** (neat): ν_{max} (cm^{-1}) = 3513, 2987, 1738, 1376, 1222, 1086, 863; $[\alpha]_D^{20}$ –68.2 (*c* 1.54, $CHCl_3$); **Chiral HPLC** (Chiralpak® IG, *i*PrOH : *n*-hexane: 1%) R_T (major) 3.47 min, R_T (minor) 2.98 min; **HRMS** (ESI^+) calculated for $C_{12}H_{18}ClIO_4Na$ $[M+Na]^+$ 410.9830, found 410.9841.

Synthesis of alcohol 83

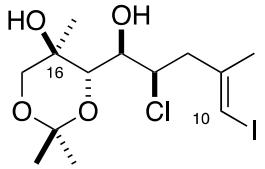

MeMgI (27.6 mL, 82.8 mmol, 3.0 M solution in Et_2O) was added dropwise to a stirred solution of chlorohydrin 9 (9.17 g, 23.6 mmol) in dichloromethane (79 mL) at –78 °C. The reaction was stirred at –78 °C for 24 h before quenching with HCl (100 mL, 1.0 M solution in H_2O) and warmed to r.t.. The layers were separated, and the aqueous phase was extracted with dichloromethane (3 × 100 mL). The combined organic phases were washed with brine (300 mL), dried ($MgSO_4$), and the solvent removed under reduced pressure to afford the crude alcohol as a 6:1 mixture of diastereomers at C16. Purification by flash chromatography (EtOAc/PE 40-60: 20% → 30%) afforded alcohol 83 as an off-white solid (4.69 g, 11.6 mmol, 49%) as a single diastereomer.

R_f (EtOAc/PE 40-60: 30%) = 0.39; **^{1}H NMR** (600 MHz, $CDCl_3$) δ_H 6.14 (1H, q, *J* = 1.2 Hz, H10), 4.41 (1H, ddd, *J* = 9.0, 6.1, 1.4 Hz, H13), 3.79 (1H, d, *J* = 9.2 Hz, H15), 3.74-3.69 (2H, m, H14, H17a), 3.49 (1H, d, *J* = 11.3 Hz, H17b), 2.76 (1H, ddd, *J* = 14.3, 9.0, 1.0 Hz, H12a), 2.74 (1H, s, OH16), 2.70 (1H, ddd, *J* = 14.3, 6.1, 1.2 Hz, H12b), 2.47 (1H, d, *J* = 8.6 Hz, OH14), 1.89 (3H, d, *J* = 1.1 Hz, Me11), 1.47 (3H, s, $\underline{Me}_AMe_BCO_2$), 1.41 (3H, s, Me16), 1.38 (s, 3H, $Me_A\underline{Me}_BCO_2$).; **^{13}C NMR** (150 MHz, $CDCl_3$) δ_c 143.2, 99.7, 79.3, 73.6, 72.9, 70.3, 68.2, 60.8, 44.3, 28.9, 23.8, 20.5, 19.2.; **IR** (neat): ν_{max} (cm^{-1}) = 3397, 3320, 2998, 2876, 1377, 1146, 1080, 1043, 860, 519; $[\alpha]_D^{20}$ –8.7 (*c* 1.3, $CHCl_3$); **HRMS** (ESI^+) calculated for $C_{13}H_{22}ClIO_4Na$ $[M+Na]^+$ 427.0149, found 427.0155.

The absolute configuration of the C15 center was determined using a Mosher ester analysis.[67]

Mosher esters – (*R*)-MTPA-90 and (*S*)-MTPA-90

(R)-Mosher ester – (*R*)-MTPA-90

A stock solution of DMAP (1.2 mg) in CH_2Cl_2 (1 mL) was separately prepared (0.01M). DIC (5.7 μL, 37 μmol) was added in portion to a stirred solution of *(R)*-MTPA (8.7 mg, 37 μmol) in the DMAP/CH_2Cl_2 solution (250 μL). Alcohol 83 (10.0 mg, 24.7 μmol) was added to this solution. The mixture was stirred for 24 h at r.t, to the point when product was observed by TLC. The solution was diluted with CH_2Cl_2 (1 mL) and sat. $NaHCO_3$ (1 mL) was added. The layers were separated, and the aqueous phase was extracted with CH_2Cl_2 (2 x 2 mL) The organic layers were combined, washed with brine (5 mL), dried (Na_2SO_4), and concentrated. Purification by flash chromatography (EtOAc/hexanes: 10% → 20%) afforded the product (*R*)-MTPA-90 as a colourless oil.

R_f (EtOAc/hexanes: 30%) = 0.48; **^{1}H NMR** (601 MHz, Chloroform-d) δ 7.65 (dd, J = 7.1, 2.8 Hz, 2H, ArH), 7.47 – 7.42 (m, 3H, ArH), 6.03 (q, J = 1.1 Hz, 1H, H10), 5.19 (dd, J = 9.1, 1.4 Hz, 1H, H10), 4.43 (ddd, J = 10.4, 4.3, 1.3 Hz, 1H, H13), 4.11 (d, J = 9.1 Hz, 1H, H15), 3.65 (s, 3H, OMe), 3.60 (d, J = 11.8 Hz, 1H, H17a), 3.34 (d, J = 11.4 Hz, 1H, H17b), 2.60 (m, 1H, H12a), 2.40 (ddd, J = 14.6, 10.4, 0.8 Hz, 1H, H12b), 1.86 (d, J = 1.0 Hz, 3H, Me11), 1.46 (s, 3H, $\underline{Me}_AMe_BCO_2$), 1.38 (s, 3H, $Me_A\underline{Me}_BCO_2$), 1.14 (s, 3H, Me16).

(S)-Mosher ester – (*S*)-MTPA-90

DIC (122 μL, 0.79 mmol) was added to a stirred solution of *(S)*-MTPA (92.5 mg, 0.395 mol) and DMAP (96.5 mg, 0.79 mmol) in CH_2Cl_2 (400 μL). Alcohol 83 (16 mg, 39.5 μmol) was added to this solution. The mixture was stirred for 5h at r.t., to the point when product was observed by TLC. The solution was diluted with CH_2Cl_2 (1 mL) and sat. $NaHCO_3$ (1 mL) was added. The layers were separated, and the aqueous phase was extracted with CH_2Cl_2 (2 x 2 mL) The organic layers were combined, washed with brine (5 mL), dried (Na_2SO_4), and concentrated. Purification by flash chromatography (EtOAc/hexanes: 10%) afforded the product (*S*)-MTPA-90 as a colourless oil.

R_f (EtOAc/hexanes: 30%) = 0.70; **^{1}H NMR** (500 MHz, Chloroform-d) δ 7.69 – 7.64 (m, 2H, ArH), 7.46 – 7.40 (m, 3H, ArH), 5.82 (q, J = 1.1 Hz, 1H, H10), 5.16 (dd, J = 9.2, 1.4 Hz, 1H, H14), 4.37 (ddd, J = 10.8, 3.9, 1.4 Hz, 1H, H13), 4.20 (d, J = 9.1 Hz, 1H, H15), 3.70 (d, J = 11.5 Hz, 1H, 17a), 3.47 (d, J = 1.3 Hz, 3H, OMe), 3.45 (d, J = 11.5 Hz, 1H,

17b), 2.48 (ddd, J = 14.7, 4.0, 1.3 Hz, 1H, 12a), 2.11 (dd, J = 14.5, 10.8 Hz, 1H, 12b), 1.80 (d, J = 1.1 Hz, 3H, Me11), 1.48 (s, 3H, $\underline{Me}_A Me_B CO_2$), 1.40 (s, 3H, $Me_A \underline{Me}_B CO_2$), 1.29 (s, 3H, Me16).

Following the Mosher's ester described by Hoye *et al.*,[67] the C15 centre arising from the enantioselective Mukaiyama aldol reaction was assigned as 15*R*.

Synthesis of triol 84

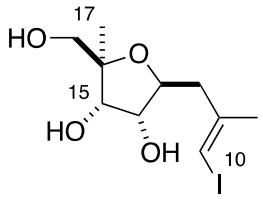

Alcohol 83 (1.48 g, 3.66 mmol) was dissolved in MeOH (50 mL) in a pressurized vessel and heated to 120 ˚C over 15 minutes in a microwave, reaching a pressure of 250 psi. The reaction was maintained at 120 ˚C at 250 psi for 110 minutes before cooling to r.t.. The solvent was removed under reduced pressure and the product was purified by flash chromatography (EtOAc: 100%) to afford triol 84 as an off-white solid (0.804 g, 2.45 mmol, 67%).

R_f (CH_2Cl_2/MeOH: 10%) = 0.42; **^{1}H NMR** (600 MHz, $CDCl_3$) δ_H 6.05 (1H, q, *J* = 1.2 Hz, H10), 4.09 (1H, d, *J* = 6.3 Hz, H15), 3.96 (1H, ddd, *J* = 7.5, 6.1, 5.3 Hz, H13), 3.83 (1H, t, *J* = 6.2 Hz, H14), 3.49 (1H, d, *J* = 11.6 Hz, H17a), 3.44 (1H, d, *J* = 11.6 Hz, H17b), 2.52 (1H, ddd, *J* = 14.5, 5.3, 1.2 Hz, H12a), 2.44 (1H, ddd, *J* = 14.5, 7.5, 1.2 Hz, H12b), 1.90 (3H, d, *J* = 1.1 Hz, Me11), 1.19 (3H, s, Me16). **^{13}C NMR** (150 MHz, $CDCl_3$) δ_c 144.7, 84.8, 79.6, 77.3, 75.4, 72.2, 67.8, 43.3, 24.8, 17.3; **IR** (neat): ν_{max} (cm^{-1}) = 3301, 2924, 1105, 1045, 1023, 761, 676, 574, 558; $[\alpha]_D^{20}$ -22.1 (*c* 1.63, MeOH); **HRMS** (ESI^+) calculated for $C_{10}H_{17}IO_4Na$ $[M+Na]^+$ 351.0063, found 351.0078.

The relative configuration in triol 12 was confirmed by observing a NOE enhancement between H13 and Me16, placing H13 and Me16 in a *syn* configuration. This supports that H13, OH14, OH15 and Me16 are in a *syn* relationship around the THF ring.

Synthesis of alcohol 85

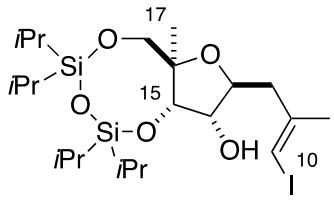

1,3-Dichloro-1,1,3,3-tetraisopropyldisiloxane (1.88 mL, 5.88 mmol) was added dropwise to a stirred solution of triol 12 (1.607 g, 4.90 mmol) in dichloromethane (18 mL) and pyridine (6 mL) at 0 °C. The solution was allowed to warm to r.t. and stirred for 48 h at r.t. before quenching with NH_4Cl (25 mL). The layers were separated, and the organic phase was washed with NH_4Cl (25 mL). The combined aqueous phase was extracted with dichloromethane (2 × 50 mL) and the combined organic phases were washed with brine (50 mL), dried ($MgSO_4$) and concentrated under reduced pressure. Purification by flash chromatography (EtOAc/hexanes: 5% → 10%) afforded alcohol 85 as a yellow oil (2.49 g, 4.36 mmol, 89%).

R_f (EtOAc/hexanes: 20%) = 0.72; **^{1}H NMR** (600 MHz, $CDCl_3$) δ_H 6.02 (1H, q, *J* = 1.2 Hz, H10), 4.13-4.07 (2H, m, H13, H15), 3.80 (1H, dd, *J* = 6.9, 2.9 Hz, H14), 3.66 (2H, d, *J* = 2.3 Hz, H17), 2.86 (1H, s, OH), 2.47-2.39 (2H, m, H12), 1.90 (3H, d, *J* = 1.1 Hz, Me11), 1.24 (3H, s, Me16), 1.12-0.97 (24H, m, *i*PrSi).; **^{13}C NMR** (150 MHz, $CDCl_3$) δ_c 144.5, 83.1, 81.1, 77.4, 75.0, 74.8, 69.8, 44.0, 25.0, 17.6, 17.7, 17.6, 17.5, 17.4, 17.3, 17.3, 17.2, 17.1, 13.5, 13.0, 13.0, 12.8; **IR** (neat): ν_{max} (cm^{-1}) = 2944, 2867, 1464, 1113, 1035, 885, 867, 692; $[\alpha]_D^{20}$ –10.6 (*c* 0.82, $CHCl_3$); **HRMS** (ESI^+) calculated for $C_{22}H_{43}IO_5Si_2H$ $[M+H]^+$ 571.1766, found 571.1776.

Synthesis of Disiloxane 86

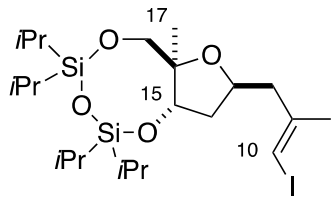

Pyridine (3.03 mL, 37.5 mmol) was added to a solution of alcohol 86 (4.28 g, 7.50 mmol) in dichloromethane (75.0 mL) and the solution was cooled to 0 °C, to which Tf_2O (3.14 mL, 18.8 mmol) was added dropwise to the stirred solution at 0 °C. Upon completion, the stirred solution was allowed to warm to r.t. over 1 h before quenching with $NaHCO_3$ (75 mL). The layers were separated, and the aqueous layer was extracted with CH_2Cl_2 (3 × 75 mL). The organic layers were combined, washed with brine (100 mL), dried ($MgSO_4$), and the solvent removed under reduced pressure. The crude product was filtered over a plug of silica, eluting with EtOAc/hex (1:4) and the solvent removed under reduced pressure to afford 5.27g of crude material. Owing to the instability of the product, the material was used immediately in the subsequent step without further purification.

$NaBH_4$ (0.56 g, 14.9 mmol) was added to a stirred solution of the crude material (5.27g) in DMF (75 mL) at r.t.. The mixture was heated to 50 °C and stirred for 45 minutes before the addition of NH_4Cl (75 mL) and allowing the mixture to cool to r.t.. The layers were separated, and the aqueous phase extracted with CH_2Cl_2 (3 × 75 mL). The combined organic phases were washed with brine (100 mL), dried ($MgSO_4$), and the solvent removed under reduced pressure. Purification by flash chromatography (EtOAc/hexanes: 2% → 5%) afforded siloxane 86 as a clear oil (2.97 g, 5.35 mmol, 72% over two steps).

R_f (EtOAc/hexanes: 10%) = 0.53; **^{1}H NMR** (600 MHz, $CDCl_3$) δ_H 5.94 (1H, q, *J* = 1.1 Hz, H10), 4.29 (1H, t, *J* = 8.8 Hz, H15), 4.19 (1H, dddd, *J* = 9.2, 6.9, 5.9, 3.6 Hz, H13), 3.69 (1H, d, *J* = 11.7 Hz, H17a), 3.64 (1H, d, *J* = 11.7 Hz, H17b), 2.43 (1H, ddd, *J* = 14.0, 5.9, 1.2 Hz, H12a), 2.28 (1H, ddd, J = 14.0, 7.0, 1.0 Hz, H12b), 2.13-2.04 (1H, m, H14a), 1.94-1.84 (1H, m, H14b), 1.86 (3H, d, J = 1.1 Hz, Me11), 1.11 (3Hm s, 3H, Me16), 1.13-1.01 (28H, m, *i*PrSi).; **^{13}C NMR** (150 MHz, $CDCl_3$) δ_c 145.0, 83.1, 77.1, 73.0, 72.0, 68.4, 46.8, 37.3, 24.9, 17.7, 17.6, 17.6, 17.6, 17.6, 17.5, 17.4, 17.3, 17.3, 17.2, 16.4, 13.6, 13.2, 12.8, 12.8; **IR** (neat): ν_{max} (cm^{-1}) = 2943, 2867, 1464, 1105, 1032, 885, 692; $[\alpha]_D^{20}$ –

7.2 (*c* 0.93, $CHCl_3$); **HRMS** (ESI^+) calculated for $C_{22}H_{43}IO_4Si_2H$ $[M+H]^+$ 555.1817, found 555.1803.

Synthesis of diol 87

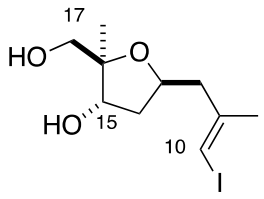

Siloxane 86 (1.16 g, 2.09 mmol) was dissolved in a solution of HCl in MeOH (21 mL, 21.0 mmol, 0.1 M) and stirred at 50 °C for 7 h. The reaction was quenched by the addition of solid $NaHCO_3$ (*ca.* 3 g) and the mixture diluted with CH_2Cl_2 (60 mL). The solids were filtered off, the filtrate collected, and the solvents removed under reduced pressure. Purification by flash chromatography (EtOAc/hexanes: 80%) afforded diol 87 as clear oil (548 mg, 1.75 mmol, 84%).

R_f (EtOAc)= 0.52; **^{1}H NMR** (600 MHz, $CDCl_3$) δ_H 5.99 (1H, q, *J* = 1.0 Hz, H10), 4.31 (1H, qn, *J* = 6.8 Hz, H13), 4.25 (1Hm, dd, *J* = 6.8, 4.6 Hz, H15), 3.45 (1H, d, *J* = 11.2 Hz, H17a), 3.41 (1H, d, *J* = 11.3 Hz, H17b), 2.46 (1H, dd, *J* = 14.1, 6.8 Hz, H12a), 2.33 (1H, dd, *J* = 14.1, 6.2 Hz, H12b), 2.09-1.96 (3H, m, H14a, OH, OH), 1.89 (1H, dd, *J* = 13.7, 6.5 Hz, H14b), 1.86 (3H, d, *J* = 1.0 Hz, Me11), 1.16 (3H, s, Me16).; **^{13}C NMR** (150 MHz, $CDCl_3$) δ_C 144.8, 85.5, 77.2, 74.1, 73.4, 67.8, 46.1, 40.2, 24.6, 17.1.; **IR** (neat): ν_{max} (cm^{-1}) = 3377, 2933, 1376, 1274, 1044, 769, 669; $[\alpha]_D^{20}$ +6.5 (*c* 1.0, MeOH); **HRMS** (ESI^+) calculated for $C_{10}H_{17}IO_3NH_4$ $[M+NH_4]^+$ 330.0566, found 330.0526.

Synthesis of TBS ether 88

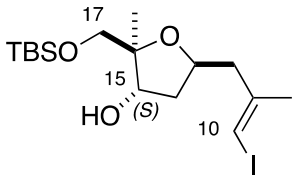

Diol 87 (707 mg, 2.26 mmol) and imidazole (462 mg, 6.78 mmol) were dissolved in CH_2Cl_2 (23 mL) and cooled to 0 °C. TBSCl (406 mg, 2.71 mmol) was added and the solution was allowed to warm to r.t. over 2 h before quenching with NH_4Cl (20 mL). The layers were separated, and the aqueous layer was extracted with CH_2Cl_2 (3 × 20 mL). The organic layers were combined, washed with brine (60 mL), dried ($MgSO_4$), and the solvent removed under reduced pressure. Purification by flash chromatography (EtOAc/hexanes: 10% → 30%) afforded TBS ether 88 as a clear oil (802 mg, 1.88 mmol, 83%).

R_f (EtOAc/hexanes: 20%) = 0.53; **^{1}H NMR** (500 MHz, $CDCl_3$) δ_H 5.96 (1H, q, *J* = 1.0 Hz, H10), 4.29 (1H, ddd, *J* = 13.0, 7.3, 6.6 Hz, H13), 4.24 (1H, dt, *J* = 6.4, 4.0 Hz, H15), 3.47 (1H, d, *J* = 9.8 Hz, H17a), 3.36 (1H, d, *J* = 9.8 Hz, H17b), 2.48 (1H, dd, *J* = 13.9, 6.4 Hz, H12a), 2.31 (1H, dd, *J* = 13.9, 6.7 Hz, H12b), 1.95* (1H, ddd, *J* = 13.0, 6.5, 4.2 Hz, H14a), 1.92-1.87* (1H, m, H14b), 1.86 (3H, d, *J* = 1.0 Hz, Me11), 1.65 (1H, d, *J* = 4.3 Hz, OH), 1.19 (3H, s, Me16), 0.89 (9H, s, $SiMe_2tBu$), 0.06 (6H, s, $SiMe_2tBu$); **^{13}C NMR** (125 MHz, $CDCl_3$) δ_C 144.9, 83.4, 79.3, 74.1, 67.9, 46.0, 41.0, 25.7, 24.3, 22.5, 18.0, –5.5, –5.8; **IR** (neat): ν_{max} (cm^{-1}) = 3439, 2928, 2857, 1463, 1258, 1088 779; $[\alpha]_D^{20}$ –1.7 (*c* 0.24, $CHCl_3$); **HRMS** (ESI^+) calculated for $C_{16}H_{31}O_3SiIH$ $[M+H]^+$ 427.1165, found 427.1162.

Synthesis of ketone 135

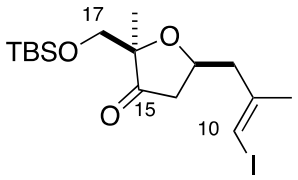

Dess-Martin Periodinane (311 mg, 733 μmol) was added to a stirred suspension of alcohol 88 (125 mg, 293 μmol) and $NaHCO_3$ (100 mg, 1.17 mmol) in wet CH_2Cl_2 (4 mL). The reaction mixture was stirred at r.t. until TLC monitoring indicated full consumption of the starting material (ca. 30 min). The reaction mixture was quenched by the addition of $NaHCO_3$ (2 mL) and $Na_2S_2O_3$ solution (2 mL) and stirred at r.t. for 30 min. The layers were separated, and the aqueous phase was extracted with CH_2Cl_2 (3 × 2 mL). The combined organic phases were dried ($MgSO_4$) and concentrated under reduced pressure. Purification by flash column chromatography (EtOAc/PE 40-60: 0% → 5%) afforded the product 135 as a colourless oil (123 mg, 290 μmol, 99%).

R_f (EtOAc/PE 40-60: 20%) = 0.71; **^{1}H NMR** (500 MHz, $CDCl_3$) δ_H 6.03 (1H, q, *J* = 0.9 Hz, H10), 4.33 (1H, app dq, *J* = 10.5, 6.1 Hz, H13), 3.64 (1H, d, *J* = 10.5 Hz, H17a), 3.53 (1H, d, *J* = 10.5 Hz, H17b), 2.71 (1H, dd, *J* = 14.3, 6.1 Hz, H14a), 2.55 (1H, dd, *J* = 14.3, 6.1 Hz, H14b), 2.48 (1H, dd, *J* = 17.4, 5.8 Hz, H12a), 2.19 (1H, dd, *J* = 17.4, 10.5 Hz, H12b), 1.92, (3H, d, *J* = 0.9 Hz, Me11), 1.09 (3H, s, Me16), 0.87 (9H, s, $SiMe_2tBu$), 0.05 (3H, s, $SiMe_2tBu$), 0.02 (3H, s, $SiMe_2tBu$); **^{13}C NMR** (125 MHz, $CDCl_3$) δ_C 216.2, 144.1, 84.8, 77.5, 71.6, 67.3, 45.6, 43.3, 25.9, 24.6, 18.3, 17.7, –5.3, –5.6; **IR** (neat): ν_{max} (cm^{-1}) = 2948, 2867, 1762, 1454, 1253, 1098, 898; $[\alpha]_D^{20}$ +16.3 (*c* 0.95, $CHCl_3$); **HRMS** (ESI^+) calculated for $C_{16}H_{29}O_3SiIH$ $[M+H]^+$ 425.1009, found 425.1006.

Synthesis of alcohol 89

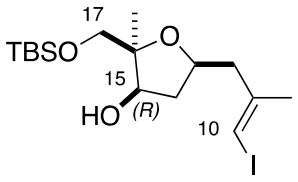

DIBAL (1.69 mL, 1.69 mmol, 1 M solution in hexanes) was added dropwise to a stirred solution of ketone 135 (239 mg, 563 μmol) in dichloromethane (6 mL) at –78 °C. The reaction mixture was stirred at –78 °C for 1 h before quenching with MeOH (500 μL), Na/K tartrate (5 mL) and the stirred mixture allowed to warm to r.t. over 3 h. The layers were separated, and the aqueous phase was extracted with CH_2Cl_2 (3 × 5 mL). The combined organic phases were dried ($MgSO_4$) and concentrated under reduced pressure. Purification by flash column chromatography (EtOAc/PE 40-60: 2%) afforded the product 89 as a colourless oil (238 mg, 559 μmol, 99%) as a single diastereomer.

R_f (EtOAc/PE 40-60: 20%) = 0.53; **^{1}H NMR** (500 MHz, $CDCl_3$) δ_H 5.99 (1H, s, H10), 4.14-4.11 (2H, m, H13, H15), 3.76 (1H, d, *J* = 10.3 Hz, H17a), 3.67 (1H, d, *J* = 10.3 Hz, H17b), 3.55 (1H, d, *J* = 6.2 Hz, OH15), 2.59 (1H, dd, *J* = 13.9, 6.8 Hz, H12a), 2.43 (1H, dd, *J* = 13.9, 6.3 Hz, H12b), 2.39-2.32* (1H, m, H14a), 1.88 (3H, s, Me11), 1.70-1.64* (1H, m, H14b), 1.15 (3H, s, Me16), 0.93 (9H, s, $SiMe_2$*t*Bu), 0.13 (3H, s, $SiMe_2$*t*Bu), 0.12 (3H, s, $SiMe_2$*t*Bu); **^{13}C NMR** (125 MHz, $CDCl_3$) δ_C 144.9, 83.4, 79.3, 74.1, 67.9, 46.0, 41.0, 25.7, 24.3, 22.5, 18.0, –5.5, –5.8; **IR** (neat): ν_{max} (cm^{-1}) = 3439, 2928, 2857, 1463, 1258, 1088 779; $[\alpha]_D^{20}$ –1.7 (*c* 0.24, $CHCl_3$); **HRMS** (ESI^+) calculated for $C_{16}H_{31}O_3SiIH$ $[M+H]^+$ 427.1165, found 427.1162.

Synthesis of ester 99

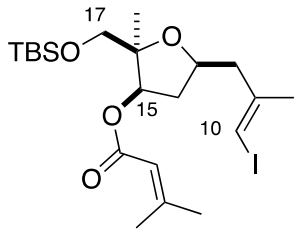

DCC (2.27 mL, 2.27 mmol, 1 M solution in dichloromethane) was added in one portion to a stirred solution of alcohol 89 (160 mg, 378 μmol), dimethylacrylic acid (227 mg, 2.27 mmol), DMAP (277 mg, 2.27 mmol) and DMAP·HCl (359 mg, 2.27 mmol) in dichloromethane (4 mL) at r.t.. The cloudy white suspension was stirred at r.t. for 24 h before quenching with NH_4Cl (5 mL). The layers were separated, and the aqueous phase was extracted with Et_2O (3 × 5 mL). The combined organic phases were dried ($MgSO_4$) and concentrated under reduced pressure. Purification by flash column chromatography (EtOAc/PE 40-60: 0% → 5%) afforded the product 99 as a colourless oil (178 mg, 350 μmol, 93%).

R_f (EtOAc/PE 40-60: 20%) = 0.72; **^{1}H NMR** (500 MHz, $CDCl_3$) δ_H 5.94 (1H, d, *J* = 1.0 Hz, H10), 5.66 (1H, sept, *J* = 1.2 Hz, =CH), 5.10 (1H, dd, *J* = 6.4, 3.9 Hz, H15), 4.22 (1H, ddt, *J* = 7.5, 6.8, 6.5 Hz, H13), 3.70 (1H, d, *J* = 9.7 Hz, H17a), 3.50 (1H, d, *J* = 9.7 Hz, H17b), 2.56 (1H, dd, *J* = 13.9, 6.8 Hz, H12a), 2.46 (1H, ddd, *J* = 13.8, 7.5, 6.6 Hz, H14a), 2.38 (1H, dd, *J* = 13.9, 6.6 Hz, H12b), 2.17 (3H, d, *J* = 1.7 Hz, $=CMe_aMe_b$), 1.91 (3H, d, *J* = 1.2 Hz, $=CMe_a\underline{Me}_b$), 1.85 (3H, d, *J* = 1.0 Hz, Me11), 1.70 (1H, ddd, *J* = 13.9, 6.4, 3.9 Hz, H14b), 1.20 (3H, s, Me16), 0.86 (9H, s, $SiMe_2tBu$), 0.03 (3H, s, $SiMe_2tBu$), 0.01 (3H, s, $SiMe_2tBu$); **^{13}C NMR** (125 MHz, $CDCl_3$) δ_C 165.7, 157.4, 144.9, 116.0, 84.5, 77.2, 74.5, 66.0, 46.3, 37.6, 27.4, 25.8, 24.5, 21.7, 20.3, 18.2, –5.5, –5.6; **IR** (neat): ν_{max} (cm^{-1}) = 2927, 2853, 1723, 1561, 1444, 1144,1103; $[\alpha]_D^{20}$ –13.0 (*c* 0.30, $CHCl_3$); **HRMS** (ESI^+) calculated for $C_{21}H_{37}O_4SiIH$ $[M+H]^+$ 509.1579, found 509.1572.

Synthesis of alcohol S2

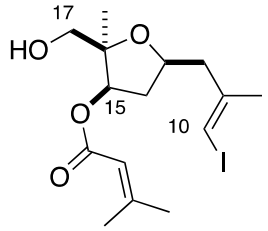

$TsOH \cdot H_2O$ (3.5 mg, 20.3 μmol) was added to a stirred solution of TBS ether 99 (103 mg, 203 μmol) in MeOH (1 mL) and dichloromethane (1 mL) at r.t.. The reaction mixture was stirred for 3 h at r.t., after which it was diluted with dichloromethane (5 mL) and quenched by the addition of $NaHCO_3$ (10 mL). The layers were separated, and the aqueous phase was extracted with dichloromethane (3 × 5 mL). The combined organic phases were dried ($MgSO_4$) and concentrated under reduced pressure. Purification by flash column chromatography (EtOAc/PE 40-60: 20%) afforded the product S2 as a colourless oil (54.6 mg, 138 μmol, 68%).

R_f (EtOAc/PE 40-60: 20%) = 0.23; **^{1}H NMR** (400 MHz, $CDCl_3$) δ_H 5.99 (1H, s, H10), 5.70 (1H, s, =CH), 5.08 (1H, dd, *J* = 6.8, 4.9 Hz, H15), 4.22 (1H, app qn, *J* = 6.8 Hz, H13), 3.57 (1H, dd, *J* = 11.8, 6.3 Hz, H17a), 3.51 (1H, dd, *J* = 11.8, 6.2 Hz, H17b), 2.57 (1H, dd, *J* = 13.9, 6.4 Hz, H12a), 2.52 (1H, ddd, *J* = 13.6, 6.8, 6.8 Hz, H14a), 2.42 (1H, dd, *J* = 13.9, 6.3 Hz, H12b), 2.18 (3H, s, $=CMe_aMe_b$), 1.93 (3H, s, $=CMe_a\underline{Me}_b$), 1.87 (3H, s, Me11), 1.72 (1H, ddd, *J* = 13.5, 7.1, 4.9 Hz, H14b), 1.26 (3H, s, Me16); ^{13}C NMR (100 MHz, $CDCl_3$) δ_C 166.4, 159.1 144.6, 115.3, 84.1, 78.1, 77.2, 74.1, 65.8, 46.0, 37.7, 27.6, 24.5, 21.7, 20.4; **IR** (thin film): ν_{max} (cm^{-1}) = 3511, 2919, 1717, 1649, 1377, 1228, 1145, 1008; $[\alpha]_D^{20}$ +2.2 (*c* 0.19, $CHCl_3$); **HRMS** (ESI^+) calculated for $C_{15}H_{23}O_4INa$ $[M+Na]^+$ 417.0539, found 417.0535.

Synthesis of C10-C17 aldehyde 100

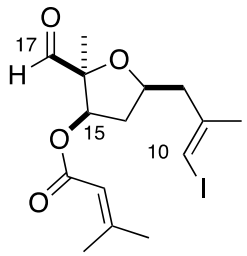

Dess-Martin Periodinane (250 mg, 583 μmol) was added to a stirred suspension of alcohol S2 (46.0 mg, 117 μmol) and $NaHCO_3$ (48 mg, 1.17 mmol) in wet CH_2Cl_2 (2 mL). The reaction mixture was stirred at r.t. for 30 min before quenching by the addition of $NaHCO_3$ (2 mL) and $Na_2S_2O_3$ solution (2 mL) and stirred at r.t. for 30 min. The layers were separated, and the aqueous phase was extracted with CH_2Cl_2 (3 × 2 mL). The combined organic phases were dried ($MgSO_4$) and concentrated under reduced pressure. Purification by flash column chromatography (EtOAc/PE 40-60: 0% → 5%) afforded the product 100 as a colourless oil (30.3 mg, 77.2 μmol, 86% brsm), alongside with 20-30% of the C10 protodeiodinated product that is inseperable at this stage.

R_f (EtOAc/PE 40-60: 20%) = 0.35; **^{1}H NMR** (500 MHz, $CDCl_3$) δ_H 9.63 (1H, s, H17), 6.03 (1H, q, *J* = 1.1 Hz, H10), 5.59 (1H, s, =CH), 5.19 (1H, dd, *J* = 6.4, 4.1 Hz, H15), 4.41 (1H, dt, *J* = 13.7, 6.6 Hz, H13), 2.70 (1H, dd, *J* = 14.0, 6.7 Hz, H12a), 2.55 (1H, ddd, *J* = 13.7, 7.2, 6.4 Hz, H14a), 2.50 (1H, dd, *J* = 14.0, 6.4 Hz, H12b), 2.15 (3H, d, *J* = 1.3 Hz, =C$\underline{Me}_a$Me$_b$), 1.90 (6H, s, Me11, =CMe$_a$$\underline{Me}_b$), 1.79 (1H, ddd, *J* = 13.7, 6.2, 4.1 Hz, H14b), 1.31 (3H, s, Me16); **^{13}C NMR** (125 MHz, $CDCl_3$) δ_C 201.0, 165.1, 159.3, 144.4, 114.9, 87.6, 79.7, 77.6, 76.8, 45.9, 37.7, 27.5, 24.4, 20.4, 19.6; **IR** (thin film): ν_{max} (cm^{-1}) = 2918, 1738, 1723, 1649, 1443, 1377, 1224, 1138, 1076; $[\alpha]_D^{20}$ –3.4 (*c* 0.29, $CHCl_3$); **HRMS** (ESI$^+$) calculated for $C_{15}H_{21}IO_4Na$ $[M+Na]^+$ 415.0382, found 415.0373.

General procedure for the 1,2-addition of vinyl iodide 97 or 105 to aldehyde 100

*t*BuLi (13 eq., molarity in pentane titrated before use) was added dropwise (down the side of the flask) to a stirred solution of vinyl iodide 97 or 105 (6.5 eq., dried by azeotroping with PhH and over CaH_2) in Et_2O (0.1 M relative to vinyl iodide) at –78 °C,

taking care that the reaction temperature does not exceed –78 °C. The solution was stirred for 30 seconds before the dropwise addition of a freshly prepared solution of $MgBr_2 \cdot OEt_2$ (19 eq., 0.6 M in Et_2O) into the reaction mixture at –78 °C. The mixture was stirred for 5 min at –78 °C before the dropwise addition of aldehyde 3 (1 eq., dried by azeotroping with PhH × 3) in dichloromethane (0.1 M relative to aldehyde) *via* cannula (down the side of the flask). The pale-yellow reaction mixture was stirred at –78 °C for 1 h before quenching with NH_4Cl (3 mL) and warmed to r.t.. The layers were separated, and the aqueous phase was extracted with CH_2Cl_2. The combined organic phases were dried ($MgSO_4$) and concentrated under reduced pressure. Purification by flash column chromatography (Et_2O/PE 40-60: 0% → 5%) afforded the crude product as a colourless oil as an inseparable mixture of diastereomers, alongside with their C10 protodeiodinated counterparts. The crude product mixture was subjected to the acetonide formation sequence outlined below.

General procedure for the synthesis of diacetonides 103, 104 and 107

PPTS (one crystal) was added to a stirred solution of *bis*-silyl ethers 101, 102 or 106 (1 eq.) in dichloromethane (100 μL) and methanol (100 μL) at r.t.. The reaction mixture was stirred for 16 h at r.t. before quenching with $NaHCO_3$ and diluting with EtOAc. The layers were separated, and the aqueous phase was extracted with EtOAc. The combined organic phases were dried ($MgSO_4$) and concentrated under reduced pressure. The crude triol was dissolved in MeOH (150 μL) and K_2CO_3 (6 mg, ca. 10 eq.) was added. The pale-yellow mixture was stirred overnight at r.t. before quenching with NH_4Cl and diluted with EtOAc. The layers were separated, and the aqueous phase was extracted with EtOAc. The combined organic phases were dried ($MgSO_4$) and concentrated under reduced pressure. The crude tetraol was redissolved in dichloromethane (100 μL) and 2,2-dimethoxypropane (100 μL) and PPTS (one crystal) was added. The solution was stirred for a further 16 h before quenching with $NaHCO_3$ and diluting with EtOAc. The layers were separated, and the aqueous phase was extracted with EtOAc. The combined organic phases were dried ($MgSO_4$) and concentrated under reduced pressure. Purification by preparative thin layer chromatography (EtOAc/PE 40-60: 20%) afforded the diacetonide as a colourless oil.

Synthesis of Alcohol 101 and 15,17-anti acetonide 103

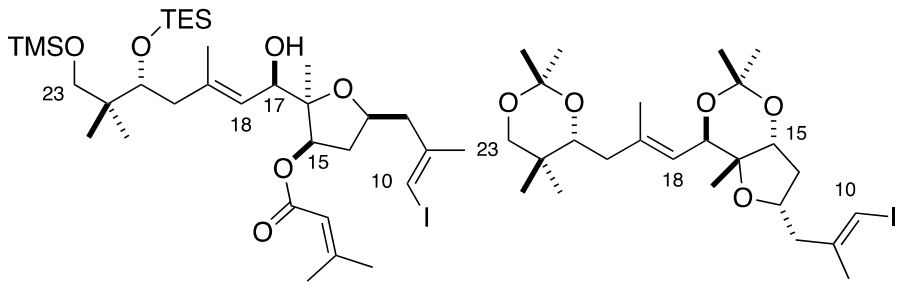

The addition reaction was performed according to the general procedure described above, using vinyl iodide 97 (42.0 mg, 88.9 μmol), *t*BuLi (120 μL, 185 μmol, 1.5 M in pentane), $MgBr_2 \cdot OEt_2$ (381 μL, 229 μmol, 0.6 M solution in Et_2O), and aldehyde 3 (4.9 mg, 12.7 μmol) to afford the crude product 101 (7.2 mg, 9.78 μmol, 77%), a colourless oil as an inseparable 5:1 mixture of diastereomers at C17 alongside with the C10 protodeiodinated material.

The crude product was transformed to the corresponding acetonide 103 according to the general procedure described above to afford the pure diacetonide 103 as a colourless oil (1.3 mg, 2.37 mmol, 24% over three steps)

R_f (EtOAc/PE 40-60: 20%) = 0.85; **^{1}H NMR** (500 MHz, $CDCl_3$) δ_H 5.97 (1H, q, *J* = 0.9 Hz, H10), 5.19 (1H, dq, *J* = 8.6, 1.0 Hz, H18), 4.40 (1H, d, *J* = 8.6 Hz, H17), 4.21-4.14 (1H, m, H13), 3.94 (1H, dd, *J* = 7.0, 2.1 Hz, H15), 3.64 (1H, dd, *J* = 9.0, 2.7 Hz, H21), 3.61 (1H, d, *J* = 11.4 Hz, H23a), 3.28 (1H, d, *J* = 11.4 Hz, H23b), 2.63 (1H, dd, *J* = 13.9, 7.7 Hz, H12a), 2.48 (1H, dd, *J* = 13.9, 5.5 Hz, H12b), 2.32 (1H, app dt, *J* = 13.9, 7.0 Hz, H14a), 2.11-2.01 (2H, m, H20), 1.85 (3H, d, *J* = 0.9 Hz, Me11), 1.73-1.65 (4H, m, H14b, Me19), 1.39 (3H, s, $\underline{Me}_A Me_B CO(O))^A$, 1.38 (3H, s, $\underline{Me}_A Me_B CO(O))^B$, 1.36 (3H, s, $Me_A \underline{Me}_B CO(O))^B$, 1.34 (3H, s, $Me_A \underline{Me}_B CO(O))^A$, 1.06 (3H, s, Me16), 1.01 (3H, s, Me22a), 0.74 (3H, s, Me22b); **^{13}C NMR** (125 MHz, $CDCl_3$) δ_C 145.3, 137.6, 123.0, 100.3^A, 98.6^B, 87.0, 77.7, 76.6, 76.1, 75.5, 73.0, 46.4, 39.9, 38.7, 36.7, 32.9, 31.9, 29.7^B, 25.4^A, 24.2, 23.8^A, 21.8, 18.9^B, 18.5, 18.0, 17.8; **IR** (thin film): ν_{max} (cm^{-1}) = 2925, 1460, 1375, 1223, 1100; $[\alpha]_D^{20}$ +19.5 (*c* 0.06, $CHCl_3$); **HRMS** (ESI^+) calculated for $C_{25}H_{41}O_5IH$ $[M+H]^+$ 549.2077, found 549.2082.

[A]Signals attributed to the C15,C17 acetonide [B]Signals attributed to the C21,C23 acetonide

Alcohol 102 and 15,17-*syn* acetonide 104

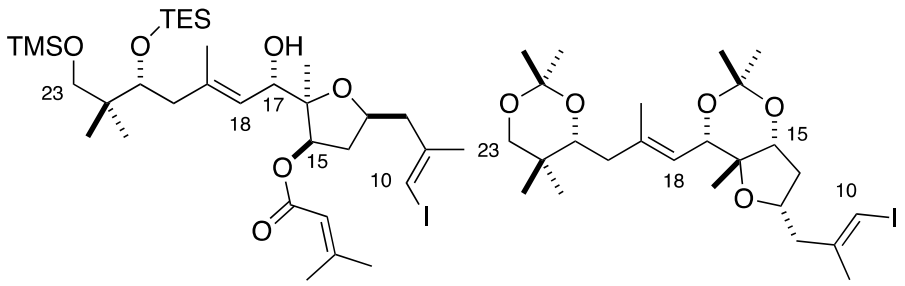

The addition reaction was performed according to the general procedure described above except omitting the addition of $MgBr_2OEt_2$, using vinyl iodide 97 (42.0 mg, 88.9 μmol), *t*BuLi (97 μL, 185 μmol, 1.9 M in pentane), and aldehyde 100 (4.9 mg, 12.7 μmol) to afford the crude product 17b (3.5 mg, 4.74 μmol, 37%), a colourless oil as an inseperable 4 : 1 mixture of diastereomers at C17, alongside with the C10 protodeiodinated material.

The crude product was transformed to the corresponding acetonide 104 according to the general procedure described above to afford the pure diacetonide as a colourless oil (1.8 mg, 3.28 mmol, 69% over three steps). Owing to competing lithium/iodine exchange at C10 from the formed vinyllithium species in the previous step, the product acetonide contains a 1:1 mixture of the C10 protodeiodinated species that was inseparable.

R_f (EtOAc/PE 40-60: 20%) = 0.87; **^{1}H NMR** (500 MHz, $CDCl_3$) δ_H 5.98 (1H, s, H10), 5.55 (1H, d, *J* = 8.6 Hz, H18), 4.50 (1H, d, *J* = 8.6 Hz, H17), 4.22-4.19 (1H, m, H13), 4.11 (1H, app d, *J* = 4.5 Hz, H15), 3.81 (1H, dd, *J* = 7.0, 2.2 Hz, H21), 3.66 (1H, d, *J* = 11.6 Hz, H23a), 3.27 (1H, d, *J* = 11.5 Hz, H23b), 2.73 (1H, dd, *J* = 13.5, 7.8 Hz, H12a), 2.44 (1H, dd, *J* = 13.5, 5.8 Hz, H12b), 2.38-2.30 (1H, m, H14a), 2.25 (1H, dd, *J* = 15.5 Hz, 7.0 Hz, H20a), 1.98-1.93 (1H, m, H20b), 1.88 (3H, d, *J* = 1.0 Hz, Me11), 1.76 (3H, s, Me19), 1.74-1.66 (1H, m, H14b), 1.49 (3H, s, $\underline{Me}_A Me_B CO(O))^A$, 1.42 (3H, s, $\underline{Me}_A Me_B CO(O))^A$, 1.42 (3H, s, $\underline{Me}_A Me_B CO(O))^B$, 1.37 (3H, s, $\underline{Me}_A Me_B CO(O))^B$, 1.03 (3H, s, Me22a), 0.93 (3H, s, Me16), 0.74 (3H, s, Me22b); **^{13}C NMR** (125 MHz, $CDCl_3$) δ_C 145.6, 140.2, 121.3,

98.5[B], 97.4[A], 78.8, 76.9, 75.3, 74.5, 72.3, 69.7, 46.8, 38.5, 36.9, 32.9, 30.0[A], 29.9[B], 24.4, 21.8, 20.6, 19.2[A], 19.0, 18.8[B], 18.1; **IR** (thin film): ν_{max} (cm^{-1}) = 2928, 1464, 1377, 1261, 1129, 1098; $[\alpha]_D^{20}$ +17.9 (*c* 0.08, $CHCl_3$); **HRMS** (ESI^+) calculated for $C_{25}H_{41}O_5IH$ $[M+H]^+$ 549.2077, found 549.2078.

[A]Signals attributed to the C15,C17 acetonide [B]Signals attributed to the C21,C23 acetonide

Preparation of Mosher's ester derivative of 102, S3

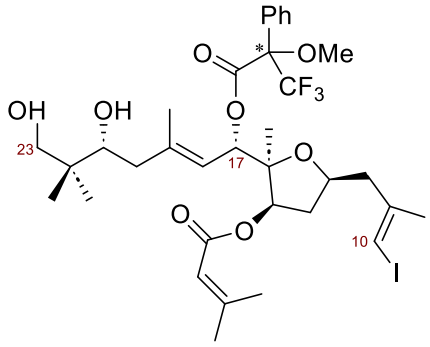

(*R*)- or (*S*)-S3

The assigned configuration at C17 was confirmed by forming the diastereomeric MTPA esters of alcohol 102 described below: DCC (15 μL, 14.9 μmol, 1 M in dichloromethane) was added dropwise to a stirred solution of alcohol 102 (2.75 mg, 3.73 μmol), (*R*) or (*S*)-MTPA (3.5 mg, 14.9 μmol) and DMAP (one crystal) in dichloromethane (50 μL). The reaction mixture was stirred at r.t. for 16 h before filtering through a pad of silica The crude product was dissolved in MeOH (25 μL) and dichloromethane (25 μL) and PPTS (one crystal) was added. The solution was stirred at r.t. for 24 h before quenching with $NaHCO_3$ (one drop), dried ($MgSO_4$), filtered and the solvent removed under reduced pressure to afford the (*S*)-MTPA ester diols [(*S*)-MTPA-S3, 1.0 mg, 1.30 mmol, 46% over two steps] or (*R*)-MTPA ester diols [(*R*)-MTPA-S3, 1.0 mg, 1.30 mmol, 46% over two steps] as a colourless oil.

(*S*)-MTPA-S3

R_f (EtOAc/PE 40-60: 20%) = 0.25; **^{1}H NMR** (500 MHz, $CDCl_3$) δ_H 5.81 (1H, d, *J* = 10.0 Hz, H17), 5.79 (1H, s, H10), 5.66 (1H, s, =CH), 5.14 (1H, d, *J* = 10.0 Hz, H18), 5.04 (1H, dd, *J* = 7.0, 5.8 Hz, H15), 4.40 (1H, d, *J* = 10.8 Hz, H23a), 4.18 (1H, m, H13), 4.01 (1H, d, *J* = 10.8 Hz, H23b), 3.48 (1H, m, H21), 2.43 (1H, m, H14a), 2.41 (1H, m, H12a), 2.26 (1H, m, H12b), 2.19 (3H, s, =C$\underline{Me}_a$Me$_b$), 2.11 (1H, m, H20a), 1.94 (1H, m, H20b), 1.93 (3H, s, =CMe$_a$$\underline{Me}_b$), 1.82 (3H, s, Me11), 1.75 (3H, s, Me19), 1.65 (1H, m, H14b), 1.17 (3H, s, Me16), 0.92 (3H, s, Me22a), 0.88 (3H, s, Me22b)

(*R*)-MTPA-S3

R_f (EtOAc/PE 40-60: 20%) = 0.22; **^{1}H NMR** (500 MHz, $CDCl_3$) δ_H 5.88 (1H, s, H10), 5.73 (2H, m, =CH, H17), 5.33 (1H, s, H18), 4.95 (1H, dd, *J* = 7.8, 7.0 Hz, H15), 4.29 (1H, d, *J* = 10.4 Hz, H23a), 4.09 (1H, d, *J* = 10.4 Hz, H23b), 4.09 (1H, m, H13), 2.52 (1H, m, H12a), 3.50 (1H, m, H21), 2.51 (1H, m, H20a), 2.32 (1H, m, H12b), 2.25 (1H, m, H20b), 2.21 (3H, s, =C$\underline{Me}_a$Me$_b$), 2.13 (1H, m, H14a), 1.98 (3H, s, =CMe$_a$$\underline{Me}_b$), 1.81 (3H, s, Me11), 1.76 (3H, s, Me19), 1.14 (3H, s, Me16), 1.10 (1H, m, H14b), 0.92 (3H, s, Me22a), 0.88 (3H, s, Me22b)

Following the Mosher's ester analysis described by Hoye *et al.*,[67] the C17 stereocentre was assigned as *S*.

<u>Alcohol 106 and 21-epi-anti acetonide 107</u>

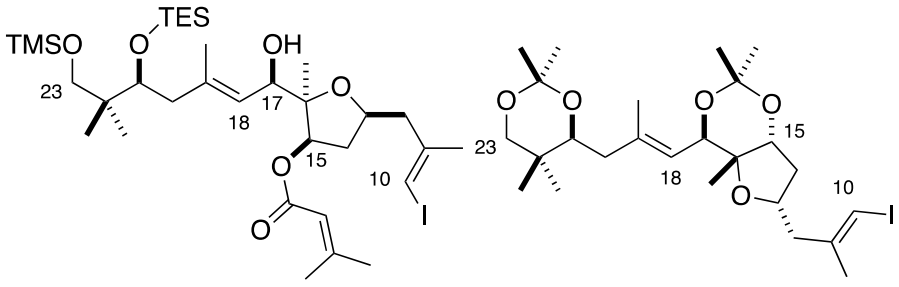

The addition reaction was performed according to the general procedure described above, using vinyl iodide 105 (42.0 mg, 88.9 μmol), *t*BuLi (97 μL, 185 μmol, 1.9 M in pentane), $MgBr_2 \cdot OEt_2$ (381 μL, 229 μmol, 0.6 M solution in Et_2O), and aldehyde 100 (4.9

mg, 12.7 μmol) to afford the crude product 106 (5.0 mg, 6.78 μmol, 53%), a colourless oil as an inseparable 5:1 mixture of diastereomers at C17, alongside with the C10 protodeiodinated material.

The crude product was transformed to the corresponding acetonide 107 according to the general procedure described above to afford the pure diacetonide 107 as a colourless oil (1.8 mg, 3.28 mmol, 48% over three steps)

R_f (EtOAc/PE 40-60: 20%) = 0.83; **^{1}H NMR** (500 MHz, $CDCl_3$) δ_H 5.98 (1H, q, *J* = 0.8 Hz, H10), 5.19 (1H, dq, *J* = 8.6, 1.2 Hz, H18), 4.42 (1H, d, *J* = 8.6 Hz, H17), 4.22-4.16 (1H, m, H13), 3.95 (1H, dd, *J* = 6.9, 1.9 Hz, H15), 3.77 (1H, dd, *J* = 9.2, 2.4 Hz, H21), 3.62 (1H, d, *J* = 11.4 Hz, H23a), 3.27 (1H, d, *J* = 11.4 Hz, H23b), 2.64 (1H, dd, *J* = 13.8, 7.8 Hz, H12a), 2.49 (1H, dd, *J* = 13.9, 6.2 Hz, H12b), 2.33 (1H, app dt, *J* = 14.0, 6.2 Hz, H14a), 2.21-2.18 (1H, m, H20a), 2.03-1.97 (1H, m, H20b), 1.86 (3H, d, *J* = 0.9 Hz, Me11), 1.76 (3H, d, *J* = 1.0 Hz, Me19), 1.75-1.68 (1H, m, H14b), 1.42 (3H, s, $\underline{Me}_A Me_B CO(O))^B$, 1.39 (3H, s, $\underline{Me}_A Me_B CO(O))^A$, 1.38 (3H, s, $Me_A \underline{Me}_B CO(O))^B$, 1.35 (3H, s, $Me_A \underline{Me}_B CO(O))^A$, 1.07 (3H, s, Me16), 1.02 (3H, s, Me22a), 0.73 (3H, s, Me22b); **^{13}C NMR** (125 MHz, $CDCl_3$) δ_C 145.3, 138.9, 120.7, 100.4^A, 98.5^B, 86.9, 78.2, 76.7, 76.1, 71.9, 71.0, 46.5, 39.4, 36.6, 32.9, 30.9, 29.8^B, 25.3^A, 24.2, 23.6^A, 18.8^B, 18.7, 18.3, 18.1 ; **IR** (thin film): ν_{max} (cm^{-1}) = 2928, 2857, 1465, 1377, 1222, 1090, 1021; $[\alpha]_D^{20}$ –22.9 (*c* 0.05, $CHCl_3$); **HRMS** (ESI^+) calculated for $C_{25}H_{41}O_5INa$ $[M+Na]^+$ 571.1891, found 571.1885.

^{A}Signals attributed to the C15,C17 acetonide ^{B}Signals attributed to the C21,C23 acetonide

A.2.3. Experimental Procedures for the Preparation of the Phormidolide A Macrocycle

Synthesis of PMBM ether 185

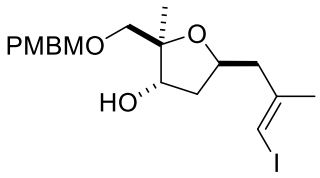

To a room temperature, stirred solution of THF 87 (1.07 g, 3.43 mmol, 1.0 eq.) in 1,2-dichloroethane (20.0 mL) under N_2 was added DIPEA (1.80 mL, 10.3 mmol, 3.0 eq.) and freshly prepared PMBMCl 184 in dichloroethane (14.3 mL) in two washes. The resulting mixture was heated to 40 °C and stirred for 18 hours until bis-protected by-product material was observed by TLC analysis. The reaction mixture was diluted with sat. NH_4Cl (30 mL) and the phases were separated. The aqueous phase was then washed with DCM (3 x 30 mL). The organic layers were combined, and washed with brine, dried with $MgSO_4$, filtered, and concentrated under reduced pressure. The resulting oil was purified by flash chromatography (gradient of EtOAc:hexanes 1:4 to 1:3 then EtOAc:hexanes 1:1) to afford PMBM ether 185 as a clear oil (775 mg, 49%, 63% based on recovered starting material).

^{1}H NMR (500 MHz, $CDCl_3$) δ 7.29 – 7.25 (m, 2H), 6.92 – 6.86 (m, 2H), 5.96 (q, *J* = 1.1 Hz, 1H), 4.73 (s, 2H), 4.54 (d, *J* = 11.4 Hz, 1H), 4.51 (d, *J* = 11.4 Hz, 1H), 4.30 (dq, *J* = 8.1, 6.5 Hz, 1H), 4.20 (dt, *J* = 6.3, 4.0 Hz, 1H), 3.81 (s, 3H), 3.46 (d, *J* = 9.6 Hz, 1H), 3.38 (d, *J* = 9.7 Hz, 1H), 2.49 (ddd, *J* = 13.9, 6.3, 1.2 Hz, 1H), 2.31 (ddd, *J* = 13.9, 6.6, 1.0 Hz, 1H), 1.96 (ddd, *J* = 13.0, 6.5, 4.0 Hz, 1H), 1.92 – 1.87 (m, 1H), 1.85 (d, *J* = 1.1 Hz, 3H), 1.77 (d, *J* = 4.1 Hz, 1H), 1.24 (s, 3H). **^{13}C NMR** (126 MHz, $CDCl_3$) δ 159.45, 144.91, 129.86, 129.66, 114.02, 94.90, 84.50, 77.15, 75.08, 74.64, 74.18, 69.41, 55.44, 46.15, 39.67, 24.74, 17.85. **IR** (neat): ν_{max} (cm^{-1}) = 3439, 2933, 1513, 1248, 1108, 1036, 819, 736. $[\alpha]_D^{20}$= -0.6 (*c* 0.93 in CH_2Cl_2). **HRMS** (ESI^+) calc. for $C_{19}H_{27}INaO_5$ $[M+Na]^+$ 485.0795, found 485.0797.

Synthesis of ketone 186

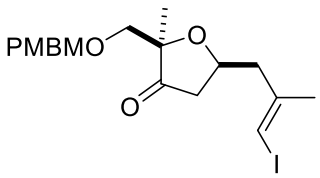

To a room temperature, stirred solution of PMBM ether 185 (789 mg, 1.71 mmol, 1.0 eq.) and NaHCO3 (1.43 g, 17.1 mmol, 10 eq.) in DCM (17.1 mL) was added Dess–Martin periodinane (2.90 mL, 6.83 mmol, 4.0 eq). The resulting mixture was stirred for 1 hour after which complete consumption of the PMBM ether was observed by TLC analysis. The reaction mixture was diluted with a solution of sat. $NaHCO_3$: sat $Na_2S_2O_3$: H_2O (1:1:1, 20 mL) and stirred vigorously for 2 hours. The phases were separated, and the aqueous phase was then washed with DCM (3 x 20 mL). The organic layers were combined, and washed with brine, dried with $MgSO_4$, filtered, and concentrated under reduced pressure. The resulting oil was purified by flash chromatography (EtOAc:hexanes 1:4) to afford ketone 186 as a clear oil (632 mg, 81%).

^{1}H NMR (500 MHz, $CDCl_3$) δ 7.31 – 7.25 (m, 2H), 6.92 – 6.85 (m, 2H), 6.07 (q, *J* = 1.2 Hz, 1H), 4.69 (s, 2H), 4.48 (d, *J* = 11.1 Hz, 1H), 4.45 (d, *J* = 11.2 Hz, 1H), 4.38 (dq, *J* = 10.2, 6.1 Hz, 1H), 3.81 (s, 3H), 3.67 (d, *J* = 10.4 Hz, 1H), 3.55 (d, *J* = 10.5 Hz, 1H), 2.71 (ddd, *J* = 14.2, 6.3, 1.2 Hz, 1H), 2.57 (dd, *J* = 14.2, 6.2 Hz, 1H), 2.53 (dd, *J* = 17.7, 5.9 Hz, 1H), 2.29 (dd, *J* = 17.7, 10.3 Hz, 1H), 1.91 (d, *J* = 1.1 Hz, 3H), 1.17 (s, 3H). **^{13}C NMR** (126 MHz, $CDCl_3$) δ 215.67, 159.45, 143.95, 129.88, 129.77, 114.01, 94.39, 83.83, 77.98, 71.74, 70.92, 69.04, 55.44, 45.43, 42.83, 24.83, 18.13. **IR** (neat): ν_{max} (cm^{-1}) = 2935, 1758, 1514, 1248, 1103, 1043, 820. $[\alpha]_D^{20}$= +46.2 (*c* 1.13 in CH_2Cl_2). **HRMS** (ESI^+) calc. for $C_{19}H_{25}INaO_5$ $[M+Na]^+$ 483.0639, found 483.0636.

Synthesis of PMBM ether 187

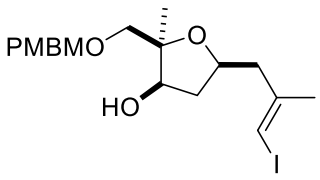

To a cold, -78 °C stirred solution of ketone 186 (300 mg, 0.653 mmol, 1.0 eq.) in DCM (6.5 mL) was added DIBAL (1.0 M in DCM, 1.63 mL, 1.63 mmol, 2.5 eq). The resulting mixture was stirred for 1 hour at -78 °C after which complete consumption of the ketone was observed by TLC analysis. The reaction mixture was diluted with a saturated solution of Rochelle's salt (10 mL) and stirred vigorously for 2 hours. The phases were separated, and the aqueous phase was then washed with DCM (3 x 10 mL). The organic layers were combined, and washed with brine, dried with $MgSO_4$, filtered, and concentrated under reduced pressure. The resulting oil was purified by flash chromatography (gradient of EtOAc:hexanes 1:9 to 1:4) to afford PMBM ether 187 as a clear oil (277 mg, 92%).

^{1}H NMR (500 MHz, $CDCl_3$) δ 7.27 (d, *J* = 8.5 Hz, 2H), 6.92 – 6.86 (m, 2H), 5.97 (q, *J* = 1.2 Hz, 1H), 4.78 (d, *J* = 6.5 Hz, 1H), 4.76 (d, *J* = 6.5 Hz, 1H), 4.55 (s, 2H), 4.15 – 4.09 (m, 2H), 3.81 (s, 3H), 3.74 (d, *J* = 10.0 Hz, 1H), 3.66 (d, *J* = 10.0 Hz, 1H), 2.93 (d, *J* = 6.2 Hz, 1H), 2.59 (dd, *J* = 13.9, 6.6 Hz, 1H), 2.43 (dd, *J* = 13.9, 6.4 Hz, 1H), 2.36 (dt, *J* = 13.2, 6.7 Hz, 1H), 1.86 (d, *J* = 1.1 Hz, 3H), 1.69 (ddd, *J* = 12.6, 7.1, 5.1 Hz, 1H), 1.18 (s, 3H). **^{13}C NMR** (151 MHz, $CDCl_3$) δ 159.56, 145.15, 129.73, 129.55, 114.09, 95.04, 83.80, 78.79, 76.96, 74.56, 72.21, 69.66, 55.46, 46.35, 40.54, 24.68, 22.80. **IR** (neat): ν_{max} (cm^{-1}) = 3465, 2970, 1514, 1248, 1104, 1037, 820. $[\alpha]_D^{20}$= -13.6 (*c* 0.71 in CH_2Cl_2). **HRMS** (ESI^+) calc. for $C_{19}H_{27}INaO_5$ $[M+Na]^+$ 485.0795, found 485.0796.

Synthesis of TIPS ether 151

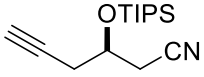

TIPS ether 151 was prepared according to the reported procedure. Data in agreement with that presented in the literature.[123]

Synthesis of vinyl iodide 152

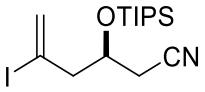

To a cold, 0 °C stirred solution of TIPS ether 151 (2.97 g, 11.2 mmol, 1.0 eq.) in hexanes (55.9 mL) was added 9-iodo-9-BBN (1.0 M in hexanes, 16.8 mL, 16.8 mmol, 1.5 eq) dropwise. The resulting mixture was stirred for 4 hours at 0 °C. Glacial acetic acid (3.21 mL, 55.9 mmol, 5.0 eq) was added and the resulting mixture was stirred for 30 minutes at 0 °C. NaOH (1M in H_2O, 7.5 mL), H_2O_2 (30% in H_2O, 15 mL), and $NaHCO_3$ (sat. solution in H_2O, 50 mL) were added and the resulting mixture was warmed to room temperature and stirred for 1 hour before the reaction mixture was diluted with Et_2O (50 mL). The phases were separated, and the aqueous phase was then washed with Et_2O (3 x 50 mL). The organic layers were combined, and washed with a saturated solution of $Na_2S_2O_3$ (100 mL), dried with $MgSO_4$, filtered, and concentrated under reduced pressure. The resulting oil was purified by flash chromatography (Et_2O:hexanes 1:99) to afford vinyl iodide 152 containing a 10% inseparable protodeiodinated by-product as a clear oil (2.99 g, 68%).

^{1}H NMR (600 MHz, $CDCl_3$) δ 6.28 (s, 1H), 5.84 (d, *J* = 1.5 Hz, 1H), 4.34 (dq, *J* = 8.8, 4.4 Hz, 1H), 2.81 (dd, *J* = 14.2, 4.8 Hz, 1H), 2.71 (dd, *J* = 14.2, 8.9 Hz, 1H), 2.61 (dd, *J* = 16.6, 4.4 Hz, 1H), 2.50 (dd, *J* = 16.6, 4.0 Hz, 1H), 1.16 – 1.06 (m, 21H). **^{13}C NMR** (151 MHz, $CDCl_3$) δ 129.86, 117.03, 104.43, 67.31, 51.83, 25.14, 18.18, 12.47. **IR** (neat): ν_{max} (cm^{-1}) = 2944, 2867, 2253, 1464, 1110, 1069, 883, 740. $[\alpha]_D^{20}$= +2.5 (*c* 0.88 in CH_2Cl_2). **HRMS** (ESI$^+$) calc. for $C_{15}H_{32}IN_2OSi$ $[M+NH_4]^+$ 411.1323, found 411.1325.

Synthesis of acetal 168

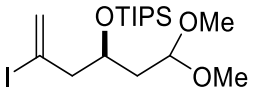

To a cold, -78 °C stirred solution of vinyl iodide 152 (3.14 g, 7.98 mmol, 1.0 eq.) in toluene (40.0 mL) was added DIBAL (0.9 M in CH_2Cl_2, 13.2 mL, 12.0 mmol, 1.5 eq) dropwise. The resulting mixture was stirred for 1 hour at -78 °C. A solution of citric acid

(10% in H_2O, 40 mL) was added, and the mixture was warmed to room temperature and stirred for 1 hour. The reaction was diluted with Et_2O (40 mL), the phases were separated, and the aqueous phase was then washed with Et_2O (3 x 50 mL). The organic layers were combined and washed with brine, dried with $MgSO_4$, filtered, and concentrated under reduced pressure to afford the crude aldehyde 153. Due to the relative instability of the product, the resulting crude material was filtered through a silica plug, eluting with Et_2O, and used without further purification.

To a room temperature stirred solution of crude aldehyde 153 (2.60 g, 7.21 mmol, 1.0 eq.) in methanol (54.1 mL) and trimethoxyorthoformate (18.0 ml) was added $KHSO_4$ (98.2 mg, 0.721 mmol, 0.1 eq). The resulting mixture was stirred for 3 hours at room temperature. The reaction mixture was then diluted with a saturated solution of $NaHCO_3$ (50 mL) and CH_2Cl_2 (100 mL). The phases were separated, and the aqueous phase was then washed with CH_2Cl_2 (3 x 50 mL). The organic layers were combined, dried with $MgSO_4$, filtered, and concentrated under reduced pressure. The resulting oil was purified by flash chromatography (Et_2O:hexanes 1:39) to afford acetal 168 containing a 10% inseparable protodeiodinated by-product as a clear oil (3.02 g, 85% over two steps).

^{1}H NMR (400 MHz, $CDCl_3$) δ 6.12 (q, *J* = 1.3 Hz, 1H), 5.77 (s, 1H), 4.64 (dd, *J* = 6.7, 4.7 Hz, 1H), 4.22 (ddt, *J* = 8.2, 7.0, 4.6 Hz, 1H), 3.33 (s, 3H), 3.31 (s, 3H), 2.68 (dd, *J* = 13.8, 4.7 Hz, 1H), 2.56 (ddd, *J* = 13.9, 8.3, 1.0 Hz, 1H), 1.91 (ddd, *J* = 14.1, 6.7, 4.4 Hz, 1H), 1.67 (ddd, *J* = 14.0, 7.0, 4.7 Hz, 1H), 1.08 (d, *J* = 6.2 Hz, 22H). **^{13}C NMR** (101 MHz, $CDCl_3$) δ 128.42, 107.02, 101.91, 68.59, 53.48, 53.30, 52.04, 39.04, 18.34, 12.91. **IR** (neat): ν_{max} (cm^{-1}) = 2943, 2867, 1465, 1107, 1060, 883, 754. $[\alpha]_D^{20}$= -10.1 (*c* 0.85 in CH_2Cl_2). **HRMS** (ESI^+) calc. for $C_{17}H_{35}INaO_3Si$ $[M+Na]^+$ 465.1292, found 465.1300.

Synthesis of vinyl stannane 169

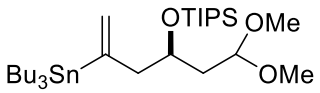

To a cold, -78 °C stirred solution of acetal 168 (2.99 g, 6.75 mmol, 1.0 eq.) and $SnBu_3Cl$ (3.70 mL, 13.5 mmol, 2.0 eq) in THF (67.5 mL) was added *t*BuLi (1.40 M in hexanes, 9.65 mL, 13.5 mmol, 2.0 eq). The resulting mixture was stirred for 1 hour at -78 °C. The

reaction mixture was then diluted with a saturated solution of NH_4Cl (50 mL) and Et_2O (50 mL) and warmed to room temperature. The phases were separated, and the aqueous phase was then washed with Et_2O (3 x 50 mL). The organic layers were combined, dried with $MgSO_4$, filtered, and concentrated under reduced pressure. The resulting oil was purified by flash chromatography on silica pre-washed with a 1% triethylamine in hexanes solution (gradient of Et_2O:hexanes 1:199 to 1:49) to afford vinyl stannane 169 as a clear oil (2.90 g, 71%, 81% based on recovered starting material).

^{1}H NMR (600 MHz, $CDCl_3$) δ 5.72 (t, *J* = 2.3 Hz, 1H), 5.21 (s, 1H), 4.65 (dd, *J* = 8.0, 3.2 Hz, 1H), 4.06 (td, *J* = 9.3, 4.5 Hz, 1H), 3.28 (s, 6H), 2.67 – 2.61 (m, 1H), 2.34 (dd, *J* = 13.6, 10.1 Hz, 1H), 1.89 (ddd, *J* = 14.0, 8.0, 2.9 Hz, 1H), 1.55 – 1.41 (m, 7H), 1.31 (h, *J* = 7.3 Hz, 6H), 1.08 (s, 21H), 0.93 – 0.86 (m, 15H). **^{13}C NMR** (151 MHz, $CDCl_3$) δ 150.90, 128.22, 102.33, 68.86, 53.04, 52.36, 50.23, 39.66, 29.25, 27.63, 18.41, 18.38, 13.83, 13.00, 9.61. **IR** (neat): ν_{max} (cm^{-1}) = 2928, 1465, 1382, 1106, 1063, 883, 754. $[\boldsymbol{\alpha}]_{\boldsymbol{D}}^{\boldsymbol{20}}$= -20.9 (*c* 1.0 in CH_2Cl_2). **HRMS** (ESI^+) calc. for $C_{29}H_{62}NaO_3SiSn$ $[M+Na]^+$ 629.3353, found 629.3387.

Synthesis of aldehyde 166

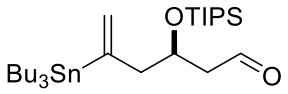

To a cold, 0 °C stirred solution of acetal 169 (3.75 g, 6.19 mmol, 1.0 eq.) and 2,6-lutidine (4.31 mL, 37.2 mmol, 6.0 eq) in CH_2Cl_2 (61.9 mL) was added trimethylsilyl triflate (4.58 mL, 24.8 mmol, 4.0 eq). The resulting mixture was stirred for 3 hours at 0 °C. The reaction mixture was then diluted with a saturated solution of $NaHCO_3$ (50 mL) and Et_2O (50 mL) and warmed to room temperature. The phases were separated, and the aqueous phase was then washed with Et_2O (3 x 50 mL). The organic layers were combined, dried with $MgSO_4$, filtered, and concentrated under reduced pressure. The resulting oil was purified by flash chromatography on silica pre-washed with a 0.5% triethylamine in hexanes solution (Et_2O:hexanes 1:99) to afford aldehyde 166 as a clear oil (1.49 g, 43%).

^{1}H NMR (600 MHz, $CDCl_3$) δ 9.88 (t, *J* = 2.6 Hz, 1H), 5.73 (t, *J* = 2.3 Hz, 1H), 5.26 (d, *J* = 3.1 Hz, 1H), 4.42 (ddt, *J* = 10.5, 6.1, 4.2 Hz, 1H), 2.76 (dd, *J* = 13.5, 4.2 Hz, 1H), 2.56 (ddd, *J* = 15.8, 4.3, 2.1 Hz, 1H), 2.51 – 2.41 (m, 2H), 1.55 – 1.39 (m, 7H), 1.31 (h, *J* = 7.4 Hz, 8H), 1.07 (s, 21H), 0.93 – 0.85 (m, 15H). **^{13}C NMR** (101 MHz, $CDCl_3$) δ 202.57, 150.54, 129.25, 68.47, 50.06, 49.76, 29.25, 27.56, 18.30, 13.78, 12.72, 9.79. **IR** (neat): ν_{max} (cm^{-1}) = 2927, 1726, 1464, 1102, 1011, 883. $[\alpha]_D^{20}$= -10.1 (*c* 0.85 in CH_2Cl_2). **HRMS** (ESI^+) calc. for $C_{27}H_{57}O_2SiSn$ $[M+H]^+$ 561.3149, found 561.3158.

Synthesis of phosphonate 125

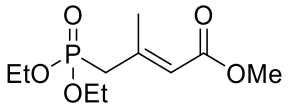

Phosphonate 125 was prepared according to the reported procedure. Data in agreement with that presented in the literature.[104]

Synthesis of diene 178

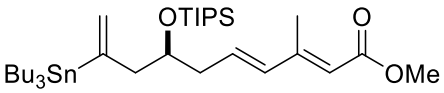

A 1.0M solution of lithium diisopropylamine was prepared. To a cold, 0 °C stirred solution of diisopropylamine (1.0 mL, 7.0 mmol) in THF (3.08 mL) was added n-BuLi (2.4 M, 2.92 mL, 7.0 mmol). The resulting mixture was stirred for 1 hour at 0 °C and used in the following reaction.

To a cold, -78 °C stirred solution of phosponate 125 (1.01 g, 4.02 mmol, 1.5 eq.) in THF:HMPA (1:1, 17.9 mL) was added the prepared LDA solution (4.02 mL, 4.02 mmol, 1.5 eq). The resulting mixture was stirred for 30 minutes at -78 °C. Aldehyde 166 (1.50 g, 2.68 mmol, 1.0 eq) in THF (9.0 mL) was added to the reaction at -78 °C and allowed to slowly warm to -40 °C over 1 hour. The resulting mixture was then stirred at -40 °C for 1 hour. The reaction mixture was then diluted with a saturated solution of NH_4Cl (30 mL)

and Et_2O (30 mL) and warmed to room temperature. The phases were separated, and the aqueous phase was then washed with Et_2O (3 x 30 mL). The organic layers were combined, dried with $MgSO_4$, filtered, and concentrated under reduced pressure. The resulting oil was purified by flash chromatography on silica pre-washed with a 0.5% triethylamine in hexanes solution (Et_2O:hexanes 1:199 to 3:197) to afford diene 178 as a clear oil (1.57 g, 89%, 3:1 *E*/*Z*).

^{1}H NMR (500 MHz, $CDCl_3$) δ 6.26 (dt, *J* = 14.9, 7.2 Hz, 1H), 6.10 (d, *J* = 15.3 Hz, 1H), 5.70 (ddd, *J* = 2.9, 1.9, 0.9 Hz, 1H), 5.67 (s, 1H), 5.25 – 5.19 (m, 1H), 4.02 (ddt, *J* = 10.1, 5.8, 4.2 Hz, 1H), 3.70 (d, *J* = 9.2 Hz, 3H), 2.63 – 2.54 (m, 1H), 2.47 – 2.36 (m, 2H), 2.27 (d, *J* = 1.2 Hz, 3H), 2.26 – 2.17 (m, 1H), 1.52 – 1.38 (m, 6H), 1.31 (h, *J* = 7.3 Hz, 3H), 1.07 (s, 21H), 0.98 – 0.81 (m, 15H). **^{13}C NMR** (126 MHz, $CDCl_3$) δ 167.90, 153.09, 151.02, 135.90, 134.23, 128.29, 117.35, 71.26, 51.08, 49.67, 39.70, 29.27, 27.60, 18.36, 13.88, 13.81, 12.76, 9.74. **IR** (neat): ν_{max} (cm^{-1}) = 2927, 2868, 2109, 1722, 1437, 1240, 1156, 1111, 882, 724. $[\alpha]_D^{20}$= -23.2 (*c* 0.83 in CH_2Cl_2). **HRMS** (ESI^+) calc. for $C_{33}H_{65}O_3SiSn$ $[M+H]^+$ 657.3726, found 657.3713.

Synthesis of ester S4

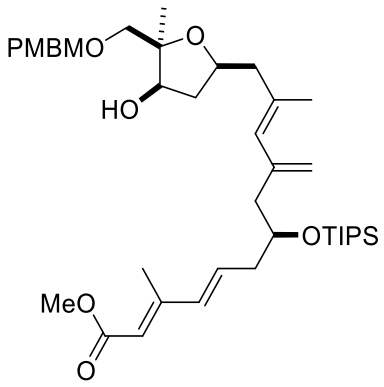

To a room temperature stirred solution of THF 187 (40.0 mg, 86.5 µmol, 1 eq.) and vinyl stannane 178 (102 mg, 156 µmol, 1.8 eq) in DMSO (0.9 mL) was added copper (I) thiophene carboxylate (33.0 mg, 173 µmol, 2.0 eq) and tetrakis(triphenylphosphine)-palladium (20.0 mg, 17.3 µmol, 0.2 eq). The resulting mixture was heated to 60 °C and stirred for 1 hour. The reaction mixture was then cooled to room temperature and diluted with a saturated solution of NH_4Cl (3 mL) and EtOAc (3 mL). The phases were

separated, and the aqueous phase was then washed with EtOAc (3 x 5 mL). The organic layers were combined, dried with $MgSO_4$, filtered, and concentrated under reduced pressure. The resulting oil was purified by flash chromatography on silica pre-washed with a 0.5% triethylamine in hexanes solution (gradient of EtOAc:hexanes 1:9 to 1:4) to afford ester S4 as a mixture of *E*/*Z* isomers (29.2 mg, 48%, 3:1 C2 *E*/*Z*).

^{1}H NMR (601 MHz, $CDCl_3$) δ 7.27 (d, *J* = 8.5 Hz, 2H), 6.88 (d, *J* = 8.5 Hz, 2H), 6.27 – 6.21 (m, 1H), 6.10 (d, *J* = 15.7 Hz, 1H), 5.69 (s, 1H), 5.61 (s, 1H), 5.01 (s, 1H), 4.84 (s, 1H), 4.77 (qd, *J* = 6.5, 1.6 Hz, 2H), 4.55 (s, 2H), 4.11 (td, *J* = 6.6, 5.0 Hz, 2H), 3.97 (dq, *J* = 9.6, 4.8 Hz, 1H), 3.80 (s, 3H), 3.75 (d, *J* = 10.1 Hz, 1H), 3.70 (s, 3H), 3.66 (d, *J* = 10.0 Hz 1H), 2.88 (d, *J* = 6.7 Hz, 1H), 2.48 (dd, *J* = 13.4, 5.9 Hz, 1H), 2.44 – 2.38 (m, 1H), 2.38 – 2.32 (m, 2H), 2.27 (d, *J* = 0.9 Hz, 3H), 2.26 – 2.20 (m, 3H), 1.81 (d, *J* = 1.0 Hz, 3H), 1.70 (ddd, *J* = 13.1, 7.7, 5.5 Hz, 1H), 1.20 (s, 3H), 1.05 (s, 21H). **^{13}C NMR** (151 MHz, $CDCl_3$) δ 167.87, 159.54, 153.05, 142.45, 135.96, 135.89, 134.19, 129.73, 129.60, 128.04, 117.42, 116.10, 114.06, 94.98, 83.36, 79.01, 75.12, 72.22, 71.11, 69.56, 55.44, 51.09, 47.27, 46.00, 40.81, 39.79, 29.86, 22.67, 18.96, 18.32, 12.73. **IR** (neat): ν_{max} (cm^{-1}) = 3476, 2942, 1714, 1612, 1247, 1159, 1040, 884. $[\alpha]_D^{20}$= -11.5 (*c* 0.32 in CH_2Cl_2). **HRMS** (ESI^+) calc. for $C_{40}H_{64}NaO_8Si$ $[M+Na]^+$ 723.4263, found 723.4266.

Synthesis of seco acid 188

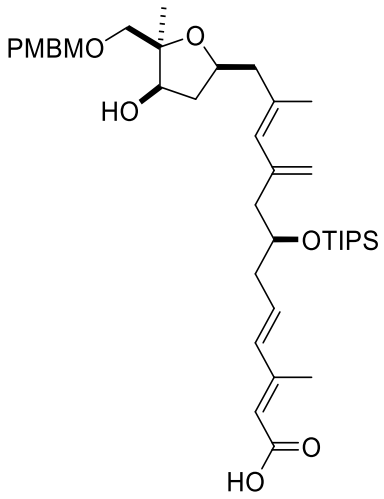

To a room temperature stirred solution of ester S4 (37.5 mg, 53.5 μmol, 1 eq.) in MeOH (0.6 mL) was added barium hydroxide octahydrate (169 mg, 535 μmol, 10.0 eq). The

resulting mixture was stirred at room temperature for 4 days. The reaction mixture was then diluted with a saturated solution of NH_4Cl (3 mL) and CH_2Cl_2 (3 mL). The phases were separated, and the aqueous phase was then washed with CH_2Cl_2 (3 x 5 mL). The organic layers were combined, dried with $MgSO_4$, filtered, and concentrated under reduced pressure. The resulting oil was purified by flash chromatography on silica pre-washed with a 0.5% triethylamine in hexanes solution (gradient of EtOAc:hexanes 3:7 to 1:1 then MeOH:DCM 1:4) to afford seco acid 188 as a mixture of *E*/*Z* isomers (26.4 mg, 71%, 3:1 *E*/*Z*).

^{1}H NMR (601 MHz, $CDCl_3$) δ 7.29 – 7.22 (m, 2H, overlap), 6.90 – 6.87 (m, 2H), 6.29 (dt, *J* = 14.9, 7.2 Hz, 1H), 6.13 (d, *J* = 15.7 Hz, 1H), 5.72 (s, 1H), 5.61 (s, 1H), 5.02 (s, 1H), 4.85 (s, 1H), 4.78 (d, *J* = 6.6 Hz, 1H), 4.76 (d, *J* = 6.6 Hz, 1H), 4.56 (s, 2H), 4.14 – 4.09 (m, 2H), 3.98 (dq, *J* = 9.4, 4.7 Hz, 1H), 3.80 (s, 3H), 3.75 (d, *J* = 10.1 Hz, 1H), 3.66 (d, *J* = 10.1 Hz, 1H), 2.49 (dd, *J* = 13.4, 5.8 Hz, 1H), 2.42 (dt, *J* = 12.2, 5.5 Hz, 1H), 2.39 – 2.32 (m, 2H), 2.28 (s, 3H), 2.27 – 2.20 (m, 3H), 1.81 (d, *J* = 1.4 Hz, 3H), 1.70 (ddd, *J* = 13.0, 7.7, 5.5 Hz, 1H), 1.20 (s, 3H), 1.05 (s, 21H). **^{13}C NMR** (151 MHz, $CDCl_3$) δ 169.48 (assigned by HMBC), 159.54, 155.25, 142.40, 135.92, 135.85, 135.15, 129.74, 129.59, 128.04, 116.27, 116.14, 114.07, 94.98, 83.37, 79.02, 77.37, 77.16, 76.95, 75.12, 72.22, 71.12, 69.58, 55.44, 47.27, 45.98, 40.80, 39.81, 22.68, 18.97, 18.32, 14.07, 12.72. **IR** (neat): ν_{max} (cm^{-1}) = 2958, 1611, 1380, 1249, 1042, 883. $[\alpha]_D^{20}$= +13.1 (*c* 0.40 in CH_2Cl_2). **HRMS** (ESI^+) calc. for $C_{39}H_{66}NO_8Si$ $[M+NH_4]^+$ 704.4552, found 704.4549.

Synthesis of macrocycle 189

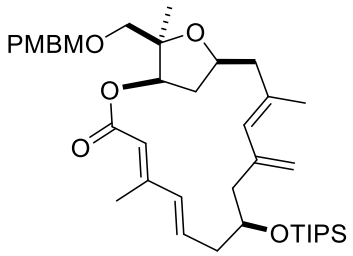

To a room temperature stirred solution of sodium bicarbonate (621 mg, 7.39 mmol, 200 eq.) and 2-bromo-1-ethylpyridinium tetrafluoroborate (203 mg, 739 μmol, 20 eq) in CH_2Cl_2 (68 mL) was added seco acid seco acid 188 (25.4 mg in 6.0 mL of CH_2Cl_2, 37.0

μmol, 1.0 eq) by syringe pump over 48 hours at a flow rate of 2.08 μL/min. After addition, the reaction was stirred for a further 24 hours. The reaction mixture was then diluted with a saturated solution of NH_4Cl (50 mL) and CH_2Cl_2 (50 mL). The phases were separated, and the aqueous phase was then washed with CH_2Cl_2 (3 x 50 mL). The organic layers were combined, dried with $MgSO_4$, filtered, and concentrated under reduced pressure. The resulting oil was purified by flash chromatography (gradient of EtOAc:hexanes 1:19 to 3:7) to afford macrocycle 189 as a mixture of *E*/*Z* isomers (17.8 mg, 72%)

^{1}H NMR (500 MHz, $CDCl_3$) δ 7.29 (ddd, *J* = 8.6, 5.2, 2.9 Hz, 2H), 6.89 (ddd, *J* = 8.6, 5.1, 2.9 Hz, 2H), 6.09 (d, *J* = 16.1 Hz, 1H), 5.84 (ddd, *J* = 15.6, 11.6, 4.2 Hz, 1H), 5.66 (s, 1H), 5.23 (s, 1H), 5.13 (d, *J* = 11.5 Hz, 1H), 4.89 (t, *J* = 2.0 Hz, 1H), 4.77 (s, 2H), 4.72 (s, 1H), 4.57 (d, *J* = 11.4 Hz, 1H), 4.53 (d, *J* = 11.5 Hz, 1H), 4.49 (ddt, *J* = 11.5, 8.4, 4.4 Hz, 1H), 4.10 (tdd, *J* = 10.2, 4.2, 1.8 Hz, 1H), 3.83 (d, *J* = 9.6 Hz, 1H), 3.81 (s, 3H), 3.65 (d, *J* = 9.6 Hz, 1H), 2.81 (dt, *J* = 12.6, 4.2 Hz, 1H), 2.63 – 2.55 (m, 1H), 2.47 (d, *J* = 15.6 Hz, 1H), 2.35 – 2.24 (m, 2H), 2.19 – 2.09 (m, 1H), 2.07 (d, *J* = 1.1 Hz, 3H), 1.82 (dd, *J* = 15.6, 10.4 Hz, 1H), 1.58 (s, 3H), 1.56 (d, *J* = 9.4 Hz, 1H), 1.29 (s, 3H), 1.12 – 1.03 (m, 21H). **^{13}C NMR** (126 MHz, $CDCl_3$) δ 167.71, 159.38, 151.95, 142.37, 133.85, 133.35, 133.06, 132.85, 130.13, 129.66, 118.31, 113.98, 113.05, 94.76, 83.94, 79.35, 76.91, 73.58, 71.37, 68.97, 55.45, 48.41, 45.23, 44.69, 35.03, 24.03, 18.25, 16.99, 13.88, 12.45. **IR** (neat): ν_{max} (cm^{-1}) = 2941, 1723, 1611, 1514, 1248, 1060. $[\alpha]_D^{20}$= +64 (*c* 0.13 in CH_2Cl_2). **HRMS** (ESI^+) calc. for $C_{39}H_{61}O_7Si$ $[M+H]^+$ 669.4181, found 669.4185.

Synthesis of macrocycle 190

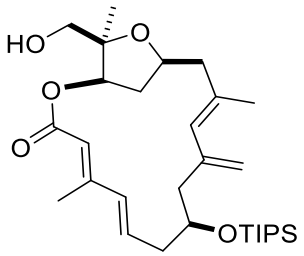

To a room temperature stirred solution of macrocycle 189 (7.6 mg, 11 μmol, 1.0 eq.) in DCE (0.37 mL) was added trimethoxybenzene (0.96 mg in 0.1 mL of DCE, 5.7 μmol, 0.5 eq) and silver hexafluoroantimonate (0.29 mg in 0.1 mL of DCE, 0.85 μmol, 0.075 eq).

The resulting mixture was heated to 40 °C and stirred for 6 hours after which complete consumption of the PMBM ether was observed by TLC analysis. The reaction mixture was filtered through silica by eluting with a solution of EtOAc and hexanes (1:1) and concentrated under reduced pressure. The resulting oil was purified by flash chromatography (gradient of EtOAc:hexanes 1:19 to 1:4) to afford macrocycle 189 as a clear oil (3.4 mg, 57%).

^{1}H NMR (500 MHz, $CDCl_3$) δ 6.14 (d, *J* = 15.5 Hz, 1H), 5.87 (ddd, *J* = 15.6, 11.6, 4.3 Hz, 1H), 5.72 (s, 1H), 5.25 (s, 1H), 5.13 (d, *J* = 4.7 Hz, 1H), 4.91 (s, 1H), 4.73 (s, 1H), 4.50 (ddd, *J* = 12.7, 8.3, 5.7 Hz, 1H), 4.11 (tdd, *J* = 10.3, 4.2, 2.2 Hz, 1H), 3.81-3.71 (m, 2H), 3.76 (s, 1H, OH), 2.82 (dt, *J* = 12.2, 4.2 Hz, 1H), 2.57 (dd, *J* = 13.3, 5.4z Hz 1H), 2.47 (d, *J* = 15.5 Hz, 1H), 2.30 (m, 1H, ovlp), 2.30 (m, 1H, ovlp), 2.19 – 2.10 (m, 1H), 2.08 (d, *J* = 1.1 Hz, 3H), 1.83 (dd, *J* = 15.5, 10.3 Hz, 1H), 1.59 (s, 3H), 1.58 (d, *J* = 14.3 Hz, 1H, ovlp), 1.26 (s, 3H), 1.16 – 1.04 (m, 28H). **^{13}C NMR** (151 MHz, $CDCl_3$) δ 167.66, 152.49, 142.33, 133.77, 133.42, 133.24, 132.87, 118.06, 113.18, 84.61, 79.91, 73.52, 66.82, 48.30, 45.18, 44.65, 35.20, 23.85, 18.25, 17.05, 13.98, 12.42. **IR** (neat): ν_{max} (cm^{-1}) = 3596, 3439, 2931, 1724, 1463, 1235, 1062, 885, 703. $[\alpha]_D^{20}$= +30 (*c* 0.15 in CH_2Cl_2). **HRMS** (ESI^+) calc. for $C_{30}H_{51}O_5Si$ $[M+H]^+$ 519.3504, found 519.3500.

Synthesis of C1-C23 fragment 201

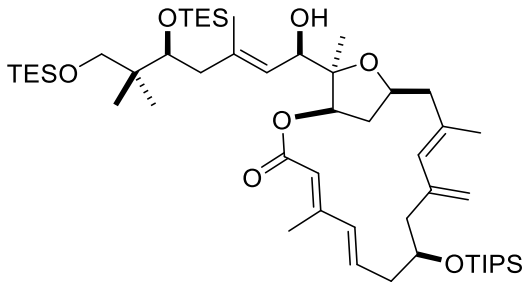

To a room temperature stirred solution of macrocycle 190 (9.3 mg, 18 µmol, 1.0 eq.) in CH_2Cl_2 (0.9 mL) was added Dess-Martin periodinane (30 mg, 72 µmol, 4.0 eq.). The resulting mixture was stirred for 3 hours at room temperature after which complete consumption of the alcohol was observed by TLC analysis. The reaction mixture was diluted with CH_2Cl_2 (3 mL) and a 1:1:1 solution of sat. NaS_2O_3:sat. $NaHCO_3$:H_2O (3 mL). This mixture was stirred vigorously for 2 hours. The phases were separated, and the

aqueous phase was then washed with CH_2Cl_2 (3 x 5 mL). The organic layers were combined, washed with brine, dried with $MgSO_4$, filtered, and concentrated under reduced pressure to afford macrocyclic aldehyde 198. Due to the instability of the product on solid-phase purification media, the material was quickly filtered through a small Fluorosil plug with Et_2O (20 mL) and used in the next step.

A solution of vinyl iodide 199 (14.8 mg, 29 µmol, 6 eq.) in dry Et_2O (0.20 mL) was cooled to -78 °C. A solution of *t*Butyl lithium (37 µL, 1.56 in hexanes, 58 µmol, 12 eq.) was added and the resulting mixture stirred at -78 °C for 5 minutes. A prepared solution of $MgBr_2$ (0.26 mL, 0.3 M in 3:1 Et_2O:benzene, 77 µmol, 16 eq.) was then added and the resulting mixture was stirred for an additional 15 minutes at -78 °C. Aldehyde 198 (2.5 mg, 4.8 µmol, 1.0 eq.) in Et_2O (0.4 mL) was then added and the resulting mixture was stirred for 1 hour at -78 °C. The reaction mixture was then diluted with sat. NH_4Cl solution (3 mL), and CH_2Cl_2 (5 mL) and allowed to warm to room temperature. The phases were separated, and the aqueous phase was then washed with CH_2Cl_2 (3 x 5 mL). The organic layers were combined, washed with brine, dried with MgSO4, filtered, and concentrated under reduced pressure. The resulting oil was purified by flash chromatography (gradient of EtOAc:hexanes) to afford C1-C23 fragment 201 as a 5:1 mixture of C2 E/Z isomers as a clear oil (2.9 mg, 3.2 µmol, 68%).

^{1}H NMR (601 MHz, $CDCl_3$) δ 6.16 (d, *J* = 15.4 Hz, 1H), 5.87 (ddd, *J* = 15.7, 11.6, 4.2 Hz, 1H), 5.80 (s, 1H), 5.34 (d, *J* = 8.8 Hz, 1H), 5.30 (s, 1H), 5.17 (d, *J* = 4.4 Hz, 1H), 4.91 (s, 1H), 4.73 (s, 1H), 4.69 (dd, *J* = 9.0, 4.3 Hz, 1H), 4.48 (dt, *J* = 14.0, 6.1 Hz, 1H), 4.15 – 4.08 (m, 1H), 3.85 (dd, *J* = 8.0, 2.9 Hz, 1H), 3.37 (d, *J* = 9.5 Hz, 1H), 3.33 (d, *J* = 9.5 Hz, 1H), 2.82 (d, *J* = 12.4 Hz, 1H), 2.63 – 2.57 (m, 1H), 2.50 – 2.45 (m, 1H), 2.37 – 2.27 (m, 4H), 2.19 – 2.14 (m, 1H), 2.09 (s, 3H), 2.08 – 2.04 (m, 1H), 1.88 – 182 (m, 1H), 1.78 (s, 3H), 1.58 (s, 3H), 1.57 (m, 1H), 1.17 (s, 3H), 1.08 (m, 21H), 0.95 (tt, *J* = 6.9, 3.2 Hz, 18H), 0.86 (s, 3H), 0.80 (s, 3H), 0.62-0.55 (m, 12H). **^{13}C NMR** (151 MHz, $CDCl_3$) δ 167.74, 152.16, 142.41, 139.03, 133.90, 133.33, 133.18, 132.87, 125.69, 118.45, 113.26, 87.20, 79.90, 77.37, 77.16, 76.95, 76.81, 74.02, 73.73, 70.31, 69.82, 48.42, 45.15, 44.76, 44.35, 40.99, 34.87, 21.03, 20.57, 18.26, 17.16, 17.01, 14.01, 12.46, 7.39, 7.02, 5.72, 4.62. $[\alpha]_D^{20}$= +94 (*c* 0.10 in CH_2Cl_2). **IR** (neat): ν_{max} (cm^{-1}) = 3321, 2917, 1724, 1462, 1237, 1092, 1014, 740. **HRMS** (ESI^+) calc. for $C_{51}H_{94}NaO_7Si_3$ $[M+Na]^+$ 925.6299, found 925.6200.

A.2.4. Experimental Procedures for the Synthesis of Nucleoside Analogues

Ketofluorohydrins containing nucleobases or nucleobase analogues were prepared[70] or purchased from WuXi Chemistry. Data for the prepared compounds match the reported literature data.

Preparation of silyl ether 231

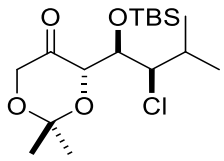

To a cold, 0 °C, stirred solution of alcohol 233 (81 mg, 0.323 mmol, 1.0 eq) in THF (2.58 mL) and CH_2Cl_2 (0.65 mL) under N_2 was added 2,6-lutidine (0.262 mL, 2.26 mmol, 7.0 eq) followed by TBSOTf (0.26 mL, 1.13 mmol, 3.5 eq). The resulting mixture was maintained at 0 °C and stirred for an additional 1 hour. The reaction mixture was then diluted with saturated NH_4Cl solution (5 mL) and allowed to warm to room temperature. The mixture was then diluted with CH_2Cl_2, (5 mL) and the phases were separated. The aqueous phase was washed with CH_2Cl_2 (3 x 10 mL) and the organic phases were combined and washed with brine, dried over $MgSO_4$, filtered, and concentrated under reduced pressure. The resulting oil was purified by flash chromatography (EtOAc:hexanes 1:19) to afford silyl ether 231 as a clear oil (114.2 mg, 97%).

^{1}H NMR (601 MHz, $CDCl_3$) δ 4.33 (dd, *J* = 3.3, 1.4 Hz, 1H), 4.22 (dd, *J* = 16.7, 1.5 Hz, 1H), 4.18 (dd, *J* = 6.8, 4.5 Hz, 1H), 4.13 (dd, *J* = 6.8, 3.3 Hz, 1H), 3.96 (d, *J* = 16.7 Hz, 1H), 2.00 (hept, *J* = 6.6, 4.5 Hz, 1H), 1.47 (s, 3H), 1.45 (s, 3H), 1.05 (d, *J* = 6.5 Hz, 3H), 0.96 (d, *J* = 6.6 Hz, 3H), 0.88 (s, 8H), 0.16 (s, 3H), 0.10 (s, 3H). **^{13}C NMR** (151 MHz, $CDCl_3$) δ 206.96, 101.27, 75.68, 74.25, 71.39, 67.46, 30.61, 26.18, 24.27, 23.55, 21.29, 18.61, 17.16, -3.75, -4.18. **IR** (neat): ν_{max} (cm^{-1}) = 2961, 2932, 1752, 1379, 1224, 1095, 988, 778, 735 $[\alpha]_D^{20}$= -99.7 (*c* 1.08 in CH_2Cl_2). **HRMS** (ESI^+) calc. for $C_{17}H_{33}ClNaO_4Si$ $[M+Na]^+$ 387.1729, found 387.1739.

Preparation of aldol 232

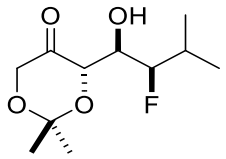

To a 0 °C stirred solution of isovaleraldehyde (1.00 ml, 9.11 mmol, 1.5 eq) in DMF (12 mL) was added $NaHCO_3$ (766 mg, 9.11 mmol, 1.5 eq), L-proline (1.05 g, 9.11 mmol, 1.5 eq), and N-fluorobenzenesulfonimide (2.87 g, 9.11 mmol, 1.5 eq). The resulting mixture was maintained at 0 °C and stirred for 2 hours until analysis by ^{1}HNMR aliquot indicated consumption of the aldehyde. A solution of 2,2-dimethyl-1,3-dioxan-5-one (0.73 mL, 6.08 mmol, 1.0 eq) in CH_2Cl_2 (120 mL) was added and the reaction warmed to room temperature. The resulting mixture was maintained at room temperature and stirred for 18 hours. The mixture was then diluted with a saturated solution of $NaHCO_3$ (100 mL) and the phases were separated. The aqueous phase was washed with CH_2Cl_2 (3 x 100 mL) and the organic phases were combined and washed with brine, dried over $MgSO_4$, filtered, and concentrated under reduced pressure. The resulting oil was purified by flash chromatography (gradient of acetone:hexanes 1:19 to 3:37) to afford aldol 232 as a clear oil solid (814.1 mg, 57%).

Data for the prepared compound matches the reported literature data.[69]

Synthesis of aldol 233

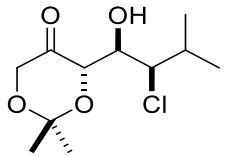

To a room temperature stirred solution of isovaleraldehyde (1.0 mL, 9.1 mmol, 1.0 eq) in CH_2Cl_2 (45 mL) was added L-proline (0.84 g, 7.3 mmol, 0.8 eq) and N-chlorosuccinimide (1.3g, 9.6 mmol, 1.05 eq). The resulting mixture was stirred for 1 hour and 2,2-dimethyl-1,3-dioxan-5-one (1.15 mL, 9.6 mmol, 1.05 eq) was added. The resulting mixture was stirred for 24 hours. The mixture was then diluted with sat. NH_4Cl (50 mL) and the phases were separated. The aqueous phase was washed with CH_2Cl_2 (3 x 50 mL) and

the organic phases were combined and washed with brine, dried over $MgSO_4$, filtered, and concentrated under reduced pressure. The resulting oil was purified by flash chromatography (EtOAc:hexanes 7.5:92.5) to afford aldol 233 as a yellow solid (1.32 g, 58%, d.r. 8.0:1).

Data for the prepared compound matches the reported literature data.[68]

Synthesis of aldol 234

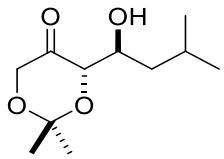

To a cold, 0 °C, stirred solution isovaleraldehyde (200 mg, 2.32 mmol, 1.0 eq) in DMF (4.64 mL) was added L-proline (53.3 mg, 0.46 mmol, 0.2 eq) and 2,2-dimethyl-1,3-dioxan-5-one (0.833 mL, 6.97 mmol, 3.0 eq). The resulting mixture was maintained at 0 °C and stirred for an additional 120 hours. The reaction mixture was then diluted with saturated NH_4Cl (5 mL) and EtOAc (5 mL) and the phases were separated. The aqueous phase was washed with EtOAc (3 x 5 mL) and the organic phases were combined and washed with brine, dried over $MgSO_4$, filtered, and concentrated under reduced pressure. The resulting oil was purified by flash chromatography (gradient of EtOAc:hexanes 1:9 to 1:4) to afford aldol 234 as a clear oil (356 mg, 71%).

Data for the prepared compound matches the reported literature data.[223]

Preparation of diol 235a

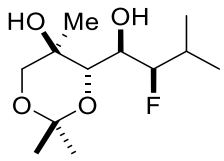

To a cold, -78 °C, stirred solution of aldol 232 (97.6 mg, 0.417 mmol, 1.0 eq) in CH_2Cl_2 (6.1 mL) under N_2 was added MeMgI (0.69 mL, 3.0 M in diethyl ether, 2.08

mmol, 5.0 eq) slowly (along interior wall of flask). The resulting mixture was maintained at -7 °C and stirred for an additional 5 hours. The reaction mixture was then quenched with a 1:1 mixture of saturated NH_4Cl and MeOH solution (10 mL) and allowed to warm to room temperature. The mixture was then diluted with CH_2Cl_2, (10 mL) and the phases were separated. The aqueous phase was washed with CH_2Cl_2 (3 x 10 mL) and the organic phases were combined and washed with brine, dried over $MgSO_4$, filtered, and concentrated under reduced pressure. The resulting oil was purified by flash chromatography (gradient of EtOAc:hexanes 1:9 to 3:7) to afford diol 235a as a white solid (62.4 mg, 60%, d.r. 7.8:1).

MP 45-48 °C**.** **^{1}H NMR** (400 MHz, $CHCl_3$) δ 4.26 (ddd, *J* = 46.9, 8.8, 1.4, 1H), 3.79 (overlap, d, *J* = 6.0 Hz, 1H), 3.80 – 3.75 (overlap, m, 1H), 3.73 (d, *J* = 11.3 Hz, 1H), 3.50 (d, *J* = 11.3 Hz, 1H), 3.03 (s, 1H), 2.29 (s, 1H), 2.17 – 2.02 (m, 1H), 1.46 (s, 3H), 1.42 (s, 3H), 1.38 (s, 3H), 1.06 (dd, *J* = 6.6, 1.3 Hz, 3H), 0.95 (dd, *J* = 6.8, 0.9 Hz, 3H). **^{13}C NMR** (101 MHz, Chloroform-*d*) δ 99.46, 96.57 (d, *J* = 173.4 Hz), 72.45 (d, *J* = 3.8 Hz), 71.22 (d, *J* = 18.9 Hz), 70.34, 68.20, 28.93, 28.67 (d, *J* = 20.0 Hz), 20.11, 19.24, 18.65 (d, *J* = 5.4 Hz), 18.37 (d, *J* = 8.7 Hz). **IR** (neat): ν_{max} (cm^{-1}) = 3625, 3399, 2967, 1473, 1382, 1200, 1131, 1044, 864. $[\alpha]_D^{20}$= -23.5 (*c* 1.13 in MeOH). **HRMS** (ESI^+) calc. for $C_{12}H_{23}FNaO_4$ $[M+Na]^+$ 273.1473, found 273.1482.

Synthesis of carbonate S5

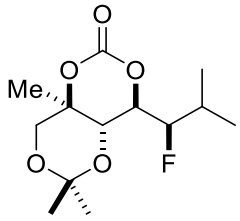

To a room temperature stirred solution of diol 235a (20 mg, 0.080 mmol, 1.0 eq) in THF (0.40 mL) was added N,N'-carbonyldiimidazole (26 mg, 0.16 mmol, 2.0 eq). The resulting mixture was maintained at room temperature and stirred for an additional 18 hours. N,N'-carbonyldiimidazole (26 mg, 0.16 mmol, 2.0 eq) was then added again and the resulting mixture was maintained at room temperature and stirred for an additional 6 hours. The reaction mixture was then diluted with saturated NH_4Cl (3 mL) and CH_2Cl_2 (3

mL). The phases were separated. The aqueous phase was washed with CH_2Cl_2 (3 x 5 mL) and the organic phases were combined and washed with brine, dried over $MgSO_4$, filtered, and concentrated under reduced pressure. The resulting oil was purified by flash chromatography (EtOAc:hexanes 1:9) to afford carbonate S5 as a clear oil (18.8 mg, 85%).

^{1}H NMR (400 MHz, $CDCl_3$) δ 4.38 (ddd, *J* = 25.4, 10.1, 1.1 Hz, 1H), 4.19 (d, *J* = 10.4 Hz, 1H), 4.11 (dd, *J* = 44.9, 9.3 Hz, 1H), 3.90 (d, *J* = 10.7 Hz, 1H), 3.71 (d, *J* = 10.7 Hz, 1H), 2.33 (tp, *J* = 9.7, 6.7 Hz, 1H), 1.59 (s, 2H), 1.53 (s, 3H), 1.45 (s, 3H), 1.09 (d, *J* = 6.6 Hz, 3H), 0.96 (d, *J* = 6.8 Hz, 3H). **^{13}C NMR** (101 MHz, $CDCl_3$) δ 147.08, 101.64, 93.69 (d, *J* = 183.0 Hz), 76.42 (d, *J* = 18.4 Hz), 73.09, 68.23, 65.07 (d, *J* = 6.7 Hz), 29.10, 28.07 (d, *J* = 20.3 Hz), 19.02 (d, *J* = 4.4 Hz), 18.96, 17.97 (d, *J* = 9.1 Hz), 17.31. **IR** (neat): ν_{max} (cm^{-1}) = 2968, 1765, 1357, 1200, 1086, 848. $[\alpha]_D^{20}$= -29.0 (*c* 1.0 in CH_2Cl_2). **HRMS** (ESI^+) calc. for $C_{13}H_{22}FO_5$ $[M+H]^+$ 277.1446, found 277.1445.

Synthesis of diol 236a

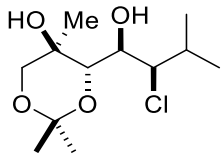

To a cold, -78 °C, stirred solution of ketone 233 (118 mg, 0.471 mmol, 1.0 eq) in CH_2Cl_2 (6.8 mL) under N_2 was added MeMgI (0.94 mL, 3.0 M in diethyl ether, 2.82 mmol, 6.0 eq) slowly (along interior wall of flask). The resulting mixture was maintained at -78 °C and stirred for an additional 5 hours. The reaction mixture was then quenched with a 1:1 mixture of saturated NH_4Cl and MeOH solution (15 mL) and allowed to warm to room temperature. The mixture was then diluted with CH_2Cl_2, (15 mL) and the phases were separated. The aqueous phase was washed with CH_2Cl_2 (3 x 15 mL) and the organic phases were combined and washed with brine, dried over $MgSO_4$, filtered, and concentrated under reduced pressure. The resulting oil was purified by flash chromatography (gradient of EtOAc:hexanes 1:9 to 3:7) to afford diol 236a as a white solid (98.2 mg, 78%, d.r. 5.5:1).

MP: 79-85 °C**. ^{1}H NMR** (601 MHz, $CDCl_3$) δ 4.06 (dd, *J* = 7.6, 1.5 Hz, 1H), 3.93 (td, *J* = 9.1, 1.5 Hz, 1H), 3.77 (d, *J* = 9.1 Hz, 1H), 3.72 (d, *J* = 11.2 Hz, 1H), 3.48 (d, *J* = 11.2 Hz, 1H), 3.09 (d, *J* = 1.6 Hz, 1H), 2.37 (d, *J* = 9.1 Hz, 1H), 2.10 (dh, *J* = 7.7, 6.6 Hz, 1H), 1.47 – 1.45 (m, 3H), 1.42 (d, *J* = 0.8 Hz, 3H), 1.38 – 1.36 (m, 3H), 1.12 (d, *J* = 6.6 Hz, 3H), 1.06 (d, *J* = 6.7 Hz, 3H). **^{13}C NMR** (151 MHz, $CHCl_3$) δ 99.52, 73.77, 72.19, 71.15, 70.28, 68.07, 32.83, 28.95, 20.58, 20.41, 20.22, 19.17. **IR** (neat): ν_{max} (cm^{-1}) = 3726, 3420, 2968, 2875, 1381, 1198, 1157, 1045, 944, 866. $[\alpha]_D^{20}$= -26.2 (*c* 0.96 in CH_2Cl_2). **HRMS** (ESI$^+$) calc. for $C_{12}H_{23}ClNaO_4$ $[M+Na]^+$ 289.1177, found 289.1180.

Synthesis of THF S6

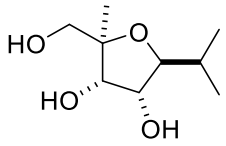

A solution of diol 236a (20 mg, 0.075 mmol, 1.0 eq) in MeOH (2.5 mL) was heated to 120 °C in a sealed tube in a microwave, reaching a pressure of 20 PSI. The reaction was maintained at 120 °C for 2 hours. The reaction mixture was then cooled and concentrated under reduced pressure. The resulting oil was purified by flash chromatography (EtOAc:hexanes 4:1) to afford diol S6 as a clear oil (13.6 mg, 98%).

^{1}H NMR (601 MHz, $CHCl_3$) δ 4.04 (dd, *J* = 6.6, 1.3 Hz, 1H), 3.93 (dd, *J* = 6.7, 5.2 Hz, 1H), 3.59 (dd, *J* = 6.5, 5.2 Hz, 1H), 3.52 (d, *J* = 11.5 Hz, 1H), 3.46 (d, *J* = 11.5 Hz, 1H), 1.82 – 1.73 (m, *J* = 6.8 Hz, 1H), 1.18 (s, 3H), 0.97 (d, *J* = 6.8 Hz, 6H). **^{13}C NMR** (151 MHz, $CHCl_3$) δ 87.40, 83.38, 73.26, 72.12, 67.53, 31.37, 18.60, 18.43, 16.84. **IR** (neat): ν_{max} (cm^{-1}) = 3390, 2934, 1466, 1271, 1098, 962, 874, 737. $[\alpha]_D^{20}$= -8.7 (*c* 1.2 in $CHCl_3$). **HRMS** (ESI$^+$) calc. for $C_9H_{19}O_4$ $[M+H]^+$ 191.1278, found 191.1280.

Synthesis of diol 273a

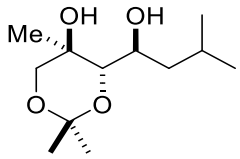

To a cold, -78 °C, stirred solution of aldol 234 (50 mg, 0.23 mmol, 1.0 eq) in CH_2Cl_2 (7.7 mL) under N_2 was added MeMgI (0.39 mL, 3.0 M in diethyl ether, 1.20 mmol, 5.0 eq) slowly (along interior wall of flask). The resulting mixture was maintained at -78 °C and stirred for an additional 5 hours. The reaction mixture was then quenched with a 2:1 mixture of saturated NH_4Cl and MeOH solution (10 mL) and allowed to warm to room temperature. The mixture was then diluted with CH_2Cl_2, (10 mL) and the phases were separated. The aqueous phase was washed with CH_2Cl_2 (3 x 10 mL) and the organic phases were combined and washed with brine, dried over $MgSO_4$, filtered, and concentrated under reduced pressure. The resulting oil was purified by flash chromatography (gradient of EtOAc:hexanes 1:19 to 3:7) to afford diol 237a as a clear oil (31.4 mg, 58%, d.r. 1.8:1).

^{1}H NMR (400 MHz, $CDCl_3$) δ 3.79 (tdd, *J* = 9.4, 4.0, 2.4 Hz, 1H), 3.68 (d, *J* = 11.2 Hz, 1H), 3.54 (s, 1H), 3.46 (d, *J* = 11.2 Hz, 1H), 3.42 (d, *J* = 9.0 Hz, 1H), 2.13 (d, *J* = 4.2 Hz, 1H), 1.83 – 1.72 (m, 1H), 1.59 (ddd, *J* = 14.2, 10.1, 2.5 Hz, 1H), 1.43 (s, 3H), 1.40 (s, 3H), 1.36 (s, 3H), 1.29 (ddd, *J* = 14.1, 9.7, 4.4 Hz, 1H), 0.97 (d, *J* = 6.6 Hz, 3H), 0.93 (d, *J* = 6.5 Hz, 3H). **^{13}C NMR** (151 MHz, $CDCl_3$) δ 99.17, 77.01, 71.21, 70.35, 68.47, 43.86, 29.00, 24.13, 24.03, 21.75, 20.30, 19.17. **IR** (neat): ν_{max} (cm^{-1}) = 3381, 2956, 2872, 1381, 1199, 1157, 1044, 867. $[\alpha]_D^{20}$= -23.3 (*c* 1.0 in CH_2Cl_2). **HRMS** (ESI^+) calc. for $C_{12}H_{25}O_4$ $[M+H]^+$ 233.1747, found 233.1749.

Synthesis of carbonate S7

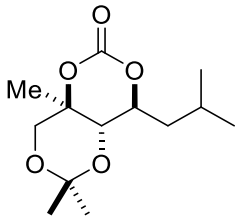

To a room temperature stirred solution of diol 237a (18.1 mg, 0.078 mmol, 1.0 eq) in THF (0.39 mL) was added N,N'-carbonyldiimidazole (50.5 mg, 0.31 mmol, 4.0 eq). The resulting mixture was maintained at room temperature and stirred for an additional 24 hours. The reaction mixture was then diluted with saturated NH_4Cl (3 mL) and CH_2Cl_2 (3 mL). The phases were separated. The aqueous phase was washed with CH_2Cl_2 (3 x 5 mL) and the organic phases were combined and washed with brine, dried over $MgSO_4$, filtered, and concentrated under reduced pressure. The resulting oil was purified by flash chromatography (EtOAc:hexanes 1:19) to afford carbonate S7 as a clear oil (14.8 mg, 74%).

^{1}H NMR (500 MHz, $CDCl_3$) δ 4.37 (dt, *J* = 9.9, 6.2 Hz, 1H), 3.84 (d, *J* = 10.7 Hz, 1H), 3.69 (d, *J* = 7.9 Hz, 1H), 3.67 (d, *J* = 8.9 Hz, 1H), 1.98 (dh, *J* = 13.6, 6.8 Hz, 1H), 1.58 (s, 3H), 1.55 (dd, *J* = 7.8, 5.5 Hz, 2H), 1.50 (s, 3H), 1.44 (s, 3H), 0.97 (d, *J* = 6.8 Hz, 3H), 0.95 (d, *J* = 6.7 Hz, 3H). **^{13}C NMR** (126 MHz, $CDCl_3$) δ 147.63, 101.32, 77.47, 73.36, 70.68, 68.18, 42.00, 29.15, 23.78, 23.55, 21.73, 18.96, 17.71. **IR** (neat): ν_{max} (cm^{-1}) = 2958, 1763, 1386, 1199, 1104, 1075, 856, 732. $[\alpha]_D^{20}$= -29.1 (*c* 1.0 in CH_2Cl_2). **HRMS** (ESI^+) calc. for $C_{13}H_{23}O_5$ $[M+H]^+$ 259.1540, found 259.1541.

Synthesis of alcohol 238

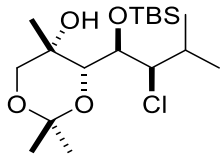

To a cold, -78 °C, stirred solution of ketone 231 (60.6 mg, 0.116 mmol, 1.0 eq) in CH_2Cl_2 (5.5 mL) under N_2 was added MeMgI (0.33 mL, 3.0 M in diethyl ether, 0.99

mmol, 6.0 eq) slowly (along interior wall of flask). The resulting mixture was maintained at -78 °C and stirred for an additional 8 hours. The reaction mixture was then quenched with a 1:1 mixture of saturated NH_4Cl and MeOH solution (10 mL) and allowed to warm to room temperature. The mixture was then diluted with CH_2Cl_2, (10 mL) and the phases were separated. The aqueous phase was washed with CH_2Cl_2 (3 x 10 mL) and the organic phases were combined and washed with brine, dried over $MgSO_4$, filtered, and concentrated under reduced pressure. The resulting oil was purified by flash chromatography (gradient of EtOAc:hexanes 1:39 to 1:9) to afford alcohol 231 as a clear oil (33.5 mg, 53%).

^{1}H NMR (500 MHz, $CDCl_3$) δ 4.13 (dd, *J* = 6.2, 3.9 Hz, 1H), 4.08 (t, *J* = 6.0 Hz, 1H), 4.05 (s, 1H), 3.76 (d, *J* = 3.9 Hz, 1H), 3.55 (d, *J* = 11.7 Hz, 1H), 3.48 (d, *J* = 11.7 Hz, 1H), 2.11 (dq, J = 12.9, 6.5 Hz, 1H), 1.43 (s, 3H), 1.40 (s, 3H), 1.20 (s, 3H), 1.05 (d, *J* = 6.6 Hz, 3H), 1.01 (d, *J* = 6.5 Hz, 3H), 0.94 (s, 9H), 0.22 (s, 3H), 0.18 (s, 3H). **^{13}C NMR** (151 MHz, $CDCl_3$) δ 99.51, 77.00, 74.12, 71.19, 70.70, 69.45, 30.87, 28.24, 26.39, 23.19, 21.30, 19.69, 18.80, 17.93, -2.87, -3.72. **IR** (neat): ν_{max} (cm^{-1}) = 3471, 1383, 1254, 1108, 1072, 857, 777. $[\alpha]_D^{20}$= +14.3 (*c* 1.0 in CH_2Cl_2). **HRMS** (ESI^+) calc. for $C_{18}H_{38}ClO_4Si$ $[M+H]^+$ 381.2222, found 381.2225.

Alcohol 231 was deprotected with according to the following procedure:

To a cold, 0 °C, stirred solution of alcohol 231 (12.5 mg, 34.0 µmol, 1.0 eq.) in THF (0.34 mL) was added TBAF (51 µL, 51.4 µmol, 1.5 eq). The resulting mixture was maintained at 0 °C and stirred for 30 minutes. The mixture was then diluted with CH_2Cl_2 (3 mL) and a saturated solution of NH_4Cl (3 mL) and the phases were separated. The aqueous phase was washed with CH_2Cl_2 (3 x 5 mL) and the organic phases were combined and washed with brine, dried over $MgSO_4$, filtered, and concentrated under reduced pressure.

Data for the prepared compound matches the data for the minor diastereomer from the preparation of diol 236a.

Synthesis of diol 240

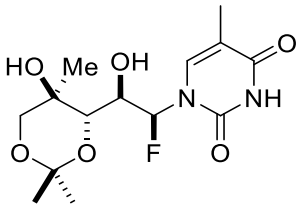

To a cold, -78 °C, stirred solution of ketone 239 (15 mg, 0.047 mmol, 1.0 eq) in CH_2Cl_2 (3.2 mL) under N_2 was added MeMgI (80 µL, 3.0 M in diethyl ether, 0.24 mmol, 5.0 eq) slowly (along interior wall of flask). The resulting mixture was maintained at -78 °C and stirred for an additional 5 hours. The reaction mixture was then quenched with a 1:1 mixture of saturated NH_4Cl and MeOH solution (5 mL) and allowed to warm to room temperature. The mixture was then diluted with CH_2Cl_2, (5 mL) and the phases were separated. The aqueous phase was washed with CH_2Cl_2 (3 x 5 mL) and the organic phases were combined and washed with brine, dried over $MgSO_4$, filtered, and concentrated under reduced pressure. The resulting oil was purified by flash chromatography (gradient of EtOAc:hexanes 1:1 to 4:1) to afford diol 240 as a white solid (9.6 mg, 61%, d.r. 6.0:1).

MP 151-156 °C**.** **^{1}H NMR** (500 MHz, MeCN-d_3) δ 7.45 (q, *J* = 1.3 Hz, 1H), 6.38 (dd, *J* = 43.8, 3.8 Hz, 1H), 3.96 (ddd, *J* = 19.6, 9.4, 3.8 Hz, 1H), 3.80 (d, *J* = 9.4 Hz, 1H), 3.68 (d, *J* = 11.2 Hz, 1H), 3.39 (d, *J* = 11.2 Hz, 1H), 2.17 (s, 2H), 1.84 (d, *J* = 1.3 Hz, 3H), 1.39 (s, 3H), 1.32 (s, 3H), 1.25 (s, 3H). **^{13}C NMR** (126 MHz, MeCN-d_3) δ 164.31, 151.03, 137.59 (d, *J* = 3.0 Hz), 111.01, 100.02, 93.49 (d, *J* = 206.8 Hz), 73.29 (d, *J* = 3.4 Hz), 72.22 (d, *J* = 24.1 Hz), 70.62, 68.37, 28.92, 19.69, 18.98, 12.35. **IR** (neat): ν_{max} (cm^{-1}) = 3247, 2994, 1772, 1667, 1380, 1278, 1087, 1049, 861, 734. $[\alpha]_D^{20}$= -44.4 (*c* 1.0 in MeOH). **HRMS** (ESI^+) calc. for $C_{14}H_{22}FN_2O_6$ $[M+H]^+$ 333.1462, found 333.1449.

Synthesis of diol 241

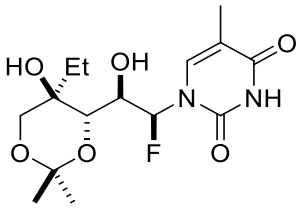

To a cold, -78 °C, stirred solution of ketone 239 (150 mg, 0.474 mmol, 1.0 eq) in CH_2Cl_2 (15.8 mL) under N_2 was added EtMgI (0.79 mL, 3.0 M in diethyl ether, 2.37 mmol, 5.0 eq) slowly (along interior wall of flask). The resulting mixture was maintained at -78 °C and stirred for an additional 5 hours. The reaction mixture was then quenched with a 1:1 mixture of saturated NH_4Cl and MeOH solution (20 mL) and allowed to warm to room temperature. The mixture was then diluted with CH_2Cl_2, (20 mL) and the phases were separated. The aqueous phase was washed with CH_2Cl_2 (3 x 20 mL) and the organic phases were combined and washed with brine, dried over $MgSO_4$, filtered, and concentrated under reduced pressure. The resulting oil was purified by flash chromatography (EtOAc:hexanes 2:3) to afford diol 241 as a white solid (52 mg, 54%, 2.5:1).

MP: 176-180 °C**. ^{1}H NMR** (500 MHz, MeCN-d_3) δ 9.01 (s, 1H), 7.42 (s, 1H), 6.36 (dd, *J* = 43.8, 3.9 Hz, 1H), 4.36 (d, *J* = 4.6 Hz, 1H), 4.07 – 3.97 (m, 1H), 3.85 (d, *J* = 9.6 Hz, 1H), 3.67 (d, *J* = 11.7 Hz, 1H), 3.50 (dd, *J* = 11.7, 1.3 Hz, 1H), 3.35 (s, 1H), 1.96 (ovlp, *assigned via COSY spectrum*, 1H), 1.83 (d, *J* = 1.3 Hz, 3H), 1.52 (dt, *J* = 14.1, 7.5 Hz, 1H), 1.39 (s, 3H), 1.23 (s, 3H), 0.94 (t, *J* = 7.5 Hz, 3H). **^{13}C NMR** (126 MHz, MeCN-d_3) δ 164.35, 151.03, 137.58, 111.03, 100.07, 93.79 (d, *J* = 207.0 Hz), 74.17 (d, *J* = 3.4 Hz), 71.55 (d, *J* = 24.1 Hz), 70.09, 65.73, 28.75, 23.84, 19.17, 12.35, 6.97. **IR** (neat): ν_{max} (cm^{-1}) = 3452, 3365, 2994, 1692, 1666, 1377, 1280, 1085, 861, 741. $[\alpha]_D^{20}$= -37.0 (*c* 1.0 in CH_2Cl_2). **HRMS** (ESI^+) calc. for $C_{15}H_{24}FN_2O_6$ $[M+H]^+$ 347.1613, found 347.1617.

Synthesis of diol 242

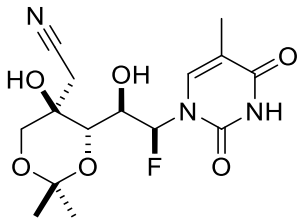

To a cold, -78 °C, stirred solution of MeCN (0.33 mL, 6.35 mmol, 4.0 eq) in THF (19.9 mL) under N_2 was added n-BuLi (2.76 mL, 2.3M in hexanes, 6.35 mmol, 4.0 eq). The resulting mixture was maintained at -78 °C and stirred for 30 min. A prepared solution of MgI_2 (10.6 mL, 0.6M, 6.35 mmol) was added and the resulting mixture was maintained at -78 °C and stirred for an additional 1 hour. A solution of 239 (500 mg, 1.59 mmol, 1.0 eq) in CH_2Cl_2 (60 mL) was added and the resulting mixture was maintained at -78 °C and stirred for an additional 5 hours. The reaction mixture was then quenched with a 1:1 mixture of saturated NH_4Cl and MeOH solution (120 mL) and allowed to warm to room temperature. The mixture was then diluted with CH_2Cl_2, (100 mL) and the phases were separated. The aqueous phase was washed with CH_2Cl_2 (3 x 200 mL) and the organic phases were combined and washed with brine, dried over $MgSO_4$, filtered, and concentrated under reduced pressure. The resulting oil was purified by flash chromatography (EtOAc:hexanes 2:3) to afford diol 242 as a white solid (198.3 mg, 35%, d.r. 1.8:1).

^{1}H NMR (500 MHz, MeCN-d_3) δ 9.19 (s, 1H), 7.33 (s, 1H), 6.32 (dd, *J* = 43.8, 4.3 Hz, 1H), 4.76 (s, 1H), 4.18 (s, 1H), 4.02 – 3.93 (m, 1H), 3.95 (d, *J* = 1.8 Hz, 1H), 3.73 (s, 2H), 3.08 (d, *J* = 16.9 Hz, 1H), 2.72 (d, *J* = 16.9 Hz, 1H), 1.84 (d, *J* = 1.3 Hz, 3H), 1.40 (s, 3H), 1.26 (s, 3H). **^{13}C NMR** (126 MHz, MeCN-d_3) δ 164.24, 150.98, 137.31 (d, *J* = 3.1 Hz), 118.48, 111.30, 100.67, 94.15 (d, *J* = 207.1 Hz), 72.91 (d, *J* = 4.6 Hz), 71.60 (d, *J* = 25.3 Hz), 68.28, 67.27, 28.77, 22.95, 18.75, 12.31. **IR** (neat): ν_{max} (cm^{-1}) = 3432, 1707, 1690, 1662, 1380, 1266, 1201, 1044, 860, 742. $[\alpha]_D^{20}$= -60.4, (*c* 0.74 in CH_2Cl_2). **HRMS** (ESI^+) calc. for $C_{15}H_{21}FN_3O_6$ $[M+H]^+$ 358.1414, found 358.1410.

Synthesis of diol 243

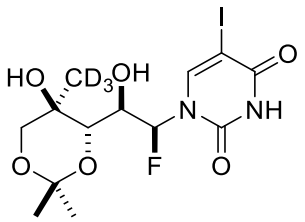

To a cold, -78 °C, stirred solution of iodouracil ketofluorohydrin[70] (214 mg, 0.50 mmol, 1.0 eq) in CH_2Cl_2 (16 mL) under N2 was added methylmagnesium iodide (0.83 mL, 3.0 M, 2.5 mmol, 5.0 eq) slowly and the resulting mixture was maintained at -78 °C and stirred for an additional 5 hours. The reaction mixture was then quenched with a solution of saturated NH4Cl (20 mL) and allowed to warm to room temperature and the phases were separated. The aqueous phase was washed with CH2Cl2 (3 x 20 mL) and the organic phases were combined and washed with brine, dried over MgSO4, filtered, and concentrated under reduced pressure. The resulting oil was purified by flash chromatography (EtOAc:hexanes) to afford diol 243 as a white solid (103 mg, 46%, d.r. 6.2:1).

^{1}H NMR (500 MHz, DMSO-*d*6) δ 11.87 (s, 1H), 8.16 (s, 1H), 6.27 (dd, *J* = 44.0, 4.3 Hz, 1H), 5.98 (d, *J* = 5.7 Hz, 1H), 4.72 (s, 1H), 4.06-4.01 (m, 1H), 3.70 (d, *J* = 9.2 Hz, 1H), 3.59 (d, *J* = 11.2 Hz, 1H), 3.32-3.29 (m, 1H), 1.31 (s, 3H), 1.19 (s, 3H). **^{13}C NMR** (500 MHz, DMSO-*d*6) δ 160.29, 149.76, 145.82, 100.57, 98.38, 93.32 (d, *J* = 207.5 Hz), 72.57, 69.95 (d, *J* = 23.8 Hz), 69.64, 66.66, 28.46, 18.57. **UPLC/MS** calc. for C13H16D3FIN2O6 [M+H]+ 448, found 448.

Synthesis of diol 244

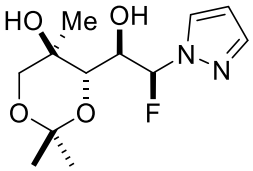

To a cold, -78 °C, stirred solution of pyrazole ketofluorohydrin[70] (35 mg, 0.14 mmol, 1.0 eq) in CH_2Cl_2 (4.5 mL) under N_2 was added methylmagnesium iodide (0.18 mL, 3.0 M in

ethyl ether, 0.54 mmol, 4.0 eq) slowly (along interior wall of flask). The resulting mixture was maintained at -78 °C and stirred for an additional 5 hours. The reaction mixture was then quenched with a 1:1 mixture of saturated NH_4Cl and MeOH solution (5 mL) and allowed to warm to room temperature. The mixture was then diluted with CH_2Cl_2, (5 mL) and the phases were separated. The aqueous phase was washed with CH_2Cl_2 (3 x 5 mL) and the organic phases were combined and washed with brine, dried over $MgSO_4$, filtered, and concentrated under reduced pressure. The resulting oil was purified by flash chromatography (gradient of EtOAc:hexanes 1:4 to 2:3) to afford diol 244 as a white solid (15.1 mg, 51%, d.r. 5:1).

MP: 92-98 °C. **^{1}H NMR** (500 MHz, $CDCl_3$) δ 7.67 (d, *J* = 2.6 Hz, 1H), 7.65 (d, *J* = 1.9 Hz, 1H), 6.39 (t, *J* = 2.2 Hz, 1H), 6.14 (d, *J* = 51.9 Hz, 1H), 4.26 (dd, *J* = 22.6, 9.5 Hz, 1H), 4.06 (dd, *J* = 9.5, 1.1 Hz, 1H), 3.80 (d, *J* = 11.3 Hz, 1H), 3.54 (d, *J* = 11.3 Hz, 1H), 1.53 (s, 3H), 1.43 (s, 3H), 1.41 (s, 3H). **^{13}C NMR** (126 MHz, $CDCl_3$) δ 141.56 (d, *J* = 1.9 Hz), 132.05, 107.12, 99.44, 92.13 (d, *J* = 212.2 Hz), 73.52 (d, *J* = 21.6 Hz), 72.06, 70.10, 67.19, 29.07, 19.98, 19.24. **IR** (neat): ν_{max} (cm^{-1}) = 3362, 2994, 2369, 1380, 1196, 1045, 865, 762. $[\alpha]_D^{20}$= -17.9 (*c* 1.0 in MeOH). **HRMS** (ESI^+) calc. for $C_{12}H_{19}FN_2O_4$ $[M+H]^+$ 275.1402, found 275.1414.

Synthesis of diol 245

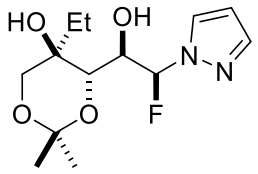

To a cold, -78 °C, stirred solution of pyrazole ketofluorohydrin[70] (30.2 mg, 0.117 mmol, 1.0 eq) in CH_2Cl_2 (3.9 mL) under N_2 was added ethylmagnesium iodide (0.53 mL, 1.1 M in ethyl ether, 0.585 mmol, 5.0 eq) slowly (along interior wall of flask). The resulting mixture was maintained at -78 °C and stirred for an additional 2.5 hours. After this time, further ethylmagnesium iodide (0.27 mL, 1.1 M in ethyl ether, 0.292 mmol, 2.5 eq) was added resulting mixture was maintained at -78 °C and stirred for an additional 2.5 hours. The reaction mixture was then quenched with a 1:1 mixture of saturated NH_4Cl and MeOH solution (5 mL) and allowed to warm to room temperature. The mixture was then

diluted with CH_2Cl_2, (5 mL) and the phases were separated. The aqueous phase was washed with CH_2Cl_2 (3 x 5 mL) and the organic phases were combined and washed with brine, dried over $MgSO_4$, filtered, and concentrated under reduced pressure. The resulting oil was purified by flash chromatography (gradient of EtOAc:hexanes 1:9 to 2:3) to afford diol 245 as a clear viscous oil (17.4 mg, 52%, d.r. 4:1).

^{1}H NMR (500 MHz, $CDCl_3$) δ 7.67 (d, *J* = 2.5 Hz, 1H), 7.65 (d, *J* = 1.7 Hz, 1H), 6.39 (t, *J* = 2.2 Hz, 1H), 6.13 (d, *J* = 52.0 Hz, 1H), 5.95 (s, 1H), 4.32 (dd, *J* = 22.6, 9.7 Hz, 1H), 4.11 (d, *J* = 9.7 Hz, 1H), 3.80 (d, *J* = 11.7 Hz, 1H), 3.62 (dd, *J* = 11.6, 1.3 Hz, 1H), 3.41 (s, 1H), 2.01 (dq, *J* = 14.8, 7.5 Hz, 1H), 1.64 (dq, *J* = 14.6, 7.4 Hz, 1H), 1.54 (s, 3H), 1.40 (s, 3H), 1.02 (t, *J* = 7.4 Hz, 3H). **^{13}C NMR** (126 MHz, $CDCl_3$) δ 141.55, 132.05, 107.11, 99.47, 92.24 (d, *J* = 212.2 Hz), 72.92 (d, *J* = 21.5 Hz), 72.74, 68.81, 65.18, 28.97, 23.38, 19.41, 6.87. **IR** (neat): ν_{max} (cm^{-1}) = 3409, 2918, 2369, 1380, 1198, 1136, 1046, 821, 761. $[\alpha]_D^{20}$= -26.5 (*c* 0.6 in CH_2Cl_2). **HRMS** (ESI^+) calc. for $C_{13}H_{21}FN_2O_4$ $[M+H]^+$ 289.1556, found 289.1558.

Synthesis of carbonate S8

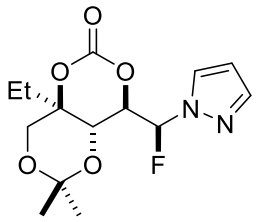

To a room temperature stirred solution of diol 235 (7.8 mg, 27 μmol, 1.0 eq) in THF (0.14 mL) was added N,N'-carbonyldiimidazole (18 mg, 0.11 mmol, 4.0 eq). The resulting mixture was maintained at room temperature and stirred for 18 hours. N,N'-carbonyldiimidazole (18 mg, 0.11 mmol, 4.0 eq) was then added again and the resulting mixture was maintained at room temperature and stirred for an additional 24 hours. The reaction mixture was then diluted with saturated NH_4Cl (3 mL) and CH_2Cl_2 (3 mL). The phases were separated. The aqueous phase was washed with CH_2Cl_2 (3 x 5 mL) and the organic phases were combined and washed with brine, dried over $MgSO_4$, filtered, and concentrated under reduced pressure. The resulting oil was purified by flash

chromatography (gradient of EtOAc:hexanes 1:19 to 1:4) to afford carbonate S8 as a clear oil (4.0 mg, 47%).

^{1}H NMR (500 MHz, $CDCl_3$) δ 7.98 (d, *J* = 2.6 Hz, 1H), 7.62 (d, *J* = 1.7 Hz, 1H), 6.42 (t, *J* = 2.2 Hz, 1H), 6.40 (dd, *J* = 45.7, 1.5 Hz, 1H), 4.75 (ddd, *J* = 18.7, 10.4, 1.7 Hz, 1H), 4.29 (d, *J* = 10.3 Hz, 1H), 4.01 (d, *J* = 11.1 Hz, 1H), 3.77 (dd, *J* = 11.1, 1.7 Hz, 1H), 2.26 (dq, *J* = 15.2, 7.6 Hz, 1H), 1.69 (dqd, *J* = 14.7, 7.4, 1.7 Hz, 1H), 1.54 (s, 4H), 1.42 (s, 3H), 1.08 (t, *J* = 7.4 Hz, 3H). **^{13}C NMR** (151 MHz, $CDCl_3$) δ 145.83, 141.03 (d, *J* = 2.2 Hz), 129.89, 108.52, 101.85, 94.05 (d, *J* = 211.8 Hz), 76.74 (d, *J* = 23.6 Hz), 75.11, 66.60, 63.49, 28.88, 21.28, 18.88, 6.49. **IR** (neat): ν_{max} (cm^{-1}) = 2986, 1779, 1389, 1205, 1106, 1053, 819, 759. $[\alpha]_D^{20}$= -63 (*c* 0.26 in CH_2Cl_2). **HRMS** (ESI^+) calc. for $C_{14}H_{20}FN_2O_5$ $[M+H]^+$315.1351, found 315.1349.

Synthesis of diol 246

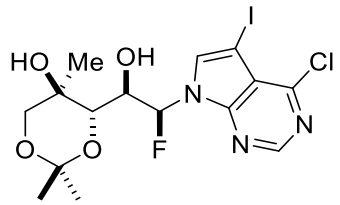

To a cold, -78 °C, stirred solution of chloroiododeazadenine ketofluorohydrin[70] (20.0 mg, 0.043 mmol, 1.0 eq) in CH_2Cl_2 (1.42 mL) under N_2 was added methylmagnesium iodide (0.57 mL, 3.0 M in ethyl ether, 0.17 mmol, 4.0 eq) slowly (along interior wall of flask). The resulting mixture was maintained at -78 °C and stirred for an additional 3 hours. The reaction mixture was then quenched with a 1:1 mixture of saturated NH_4Cl and MeOH solution (1.5 mL) and allowed to warm to room temperature. The mixture was then diluted with CH_2Cl_2, (1.5 mL) and the phases were separated. The aqueous phase was washed with CH_2Cl_2 (3 x 2 mL) and the organic phases were combined and washed with brine, dried over $MgSO_4$, filtered, and concentrated under reduced pressure. The resulting oil was purified by flash chromatography (EtOAc:hexanes 3:7) to afford diol 246 as a white solid (16.1 mg, 78%, d.r. 15:1).

MP: 100-105 °C. **^{1}H NMR** (600 MHz, $CDCl_3$) δ 8.70 (s, 1H), 7.75 (s, 1H), 6.46 (d, *J* = 49.0 Hz, 1H), 6.18 (s, 1H), 4.19 (dd, *J* = 19.3, 9.5 Hz, 1H), 4.02 (d, *J* = 9.5 Hz, 1H), 3.80

(d, *J* = 11.3 Hz, 1H), 3.54 (d, *J* = 11.3 Hz, 1H), 3.40 (s, 1H), 1.49 (s, 3H), 1.44 (s, 3H), 1.38 (s, 3H). **^{13}C NMR** (151 MHz, $CDCl_3$) δ 154.21, 150.86, 135.81, 118.30, 99.73, 92.38 (d, *J* = 213.0 Hz), 72.47, 72.17 (d, *J* = 21.4 Hz), 70.12, 67.77, 54.17, 28.97, 19.87, 19.18. **IR** (neat): ν_{max} (cm^{-1}) = 3285.37, 2958.78, 2928.80, 2859.70, 1721.39, 1461.74, 1268.34, 1117.46, 730.97. $[\alpha]_D^{20}$= +17 (*c* 0.7 in $CHCl_3$). **HRMS** (ESI^+) calc. for $[M+H]^+$ 486.0087 m/z, found 486.0068 m/z.

Synthesis of diol 247

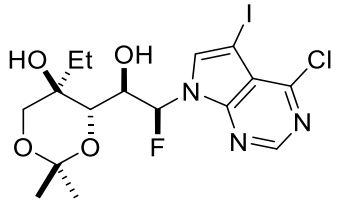

To a cold, -78 °C, stirred solution of chloroiododeazadenine ketofluorohydrin[70] (34.8 mg, 74.1 μmol, 1.0 eq) in CH_2Cl_2 (3.7 mL) under N_2 was added ethylmagnesium iodide (0.257 mL, 1.44 M in ethyl ether, 0.37 mmol, 5.0 eq) slowly (along interior wall of flask). The resulting mixture was maintained at -78 °C and stirred for an additional 5 hours. The reaction mixture was then quenched with a 1:1 mixture of saturated NH_4Cl and MeOH solution (5 mL) and allowed to warm to room temperature. The mixture was then diluted with CH_2Cl_2, (10 mL) and the phases were separated. The aqueous phase was washed with CH_2Cl_2 (3 x 10 mL) and the organic phases were combined and washed with brine, dried over $MgSO_4$, filtered, and concentrated under reduced pressure. The resulting oil was purified by flash chromatography (EtOAc:hexanes 1:9) to afford diol 247 as a white solid (22.8 mg, 61%, d.r. 2.6:1).

MP: 136-143 °C. **^{1}H NMR** (600 MHz, MeCN-d_3) δ 8.64 (s, 1H), 8.20 (s, 1H), 6.94 (dd, *J* = 45.1, 2.5 Hz, 1H), 4.88 (d, *J* = 4.3 Hz, 1H), 4.59 – 4.47 (m, 1H), 3.57 (d, *J* = 11.7 Hz, 1H), 3.26 (dd, *J* = 11.7, 1.3 Hz, 1H), 3.24 (s, 1H), 3.19 (d, *J* = 9.7 Hz, 1H), 1.99 (overlap, dq, *J* = 14.3, 7.5 Hz, 1H), 1.58 (dq, *J* = 14.6, 7.5 Hz, 1H), 1.22 (s, 3H), 0.94 (t, *J* = 7.5 Hz, 3H), 0.71 (s, 3H). **^{13}C NMR** (151 MHz, MeCN-d_3) δ 153.32, 152.62, 152.15, 135.38 (d, *J* = 1.9 Hz), 117.64, 99.85, 91.46 (d, *J* = 202.7 Hz), 74.68 (d, *J* = 5.7 Hz), 71.60 (d, *J* = 25.0 Hz), 69.66, 65.49, 54.55, 28.69, 24.08, 18.61, 6.97. **IR** (neat): ν_{max} (cm^{-1}) = 3369,

2369, 1579, 1444, 1259, 1091, 865, 721. $[\alpha]_D^{20}$= -13.8 (*c* 1.0 in MeOH). **HRMS** (ESI$^+$) calc. for $C_{16}H_{21}ClFIN_3O_4$ $[M+H]^+$ 500.0249, found 500.0220.

Synthesis of carbonate S9

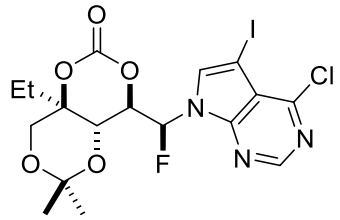

To a room temperature stirred solution of diol 247 (4.0 mg, 8.0 µmol, 1.0 eq) in THF (0.16 mL) was added N,N'-carbonyldiimidazole (13 mg, 80 µmol, 10.0 eq) and the resulting mixture was maintained at room temperature and stirred for 24 hours. The reaction mixture was then diluted with saturated NH_4Cl (3 mL) and CH_2Cl_2 (3 mL). The phases were separated. The aqueous phase was washed with CH_2Cl_2 (3 x 5 mL) and the organic phases were combined and washed with brine, dried over $MgSO_4$, filtered, and concentrated under reduced pressure. The resulting oil was purified by flash chromatography (gradient of EtOAc:hexanes 1:19 to 1:4) to afford carbonate S9 as a white solid (2.3 mg, 55%).

MP: 93-100 °C. **^{1}H NMR** (601 MHz, $CDCl_3$) δ 8.65 (s, 1H), 7.84 (s, 1H), 7.07 (d, *J* = 41.8 Hz, 1H), 5.04 (t, *J* = 9.9 Hz 1H), 3.92 (d, *J* = 11.3 Hz, 1H), 3.54 (d, *J* = 11.1, 2H), 2.31 (dq, *J* = 15.7, 7.4 Hz, 1H), 1.74 (dq, *J* = 15.2, 7.5 Hz, 1H), 1.47 (s, 3H), 1.29 (s, 3H), 1.09 (t, *J* = 7.3 Hz, 3H). **^{13}C NMR** (151 MHz, $CDCl_3$) δ 153.79, 151.73, 151.68, 145.25, 132.64, 117.29, 102.02, 89.32 (d, *J* = 210.0 Hz), 75.07, 66.55 (d, *J* = 5.4 Hz), 63.21, 55.69, 29.86, 28.92, 21.52, 18.72, 6.50. **IR** (neat): ν_{max} (cm^{-1}) = 3418, 1779, 1445, 1211, 1111, 948, 736. $[\alpha]_D^{20}$= -20 (*c* 0.15 in CH_2Cl_2). **HRMS** (ESI$^+$) calc. for $C_{17}H_{19}ClFIN_3O_5$ $[M+H]^+$ 526.0037, found 526.0040.

Synthesis of diol 248

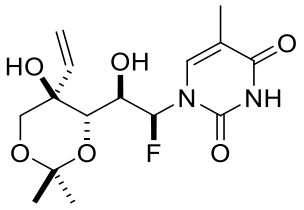

To a cold, -78 °C, stirred solution of ketone 239 (30 mg, 95 µmol, 1.0 eq) in CH_2Cl_2 (3.2 mL) under N_2 was added vinylmagnesium bromide (0.95 mL, 1.0 M in THF, 0.95 mmol, 10.0 eq) slowly (along interior wall of flask). The resulting mixture was maintained at -78 °C and stirred for an additional 5 hours. The reaction mixture was then quenched with a 1:1 mixture of saturated NH_4Cl and MeOH solution (5 mL) and allowed to warm to room temperature. The mixture was then diluted with CH_2Cl_2, (5 mL) and the phases were separated. The aqueous phase was washed with CH_2Cl_2 (3 x 5 mL) and the organic phases were combined and washed with brine, dried over $MgSO_4$, filtered, and concentrated under reduced pressure. The resulting oil was purified by flash chromatography (EtOAc:hexanes 2:3) to afford diol 248 as a white solid (10.5 mg, 32%, d.r. 1:2).

MP: 83-88 °C**. ^{1}H NMR** (500 MHz, MeCN-d_3) δ 9.02 (S, 1H), 7.38 (p, *J* = 1.1 Hz, 1H), 6.40 (dd, *J* = 17.5, 11.0 Hz), 6.35 (dd, *J* = 46.7, 2.7 Hz), 5.45 (dd, *J* = 17.5, 1.9 Hz, 1H), 5.31 (dd, *J* = 11.0, 1.9 Hz, 1H), 4.26 (d, *J* = 4.5 Hz, 1H), 3.90 (d, *J* = 9.3 Hz, 1H), 3.83 (s, 1H), 3.80 (d, *J* = 11.2 Hz, 1H), 3.46 (d, *J* = 11.2 Hz, 1H), 1.83 (d, *J* = 1.3 Hz, 3H), 1.45 (s, 3H), 1.30 (s, 3H). **^{13}C NMR** (126 MHz, MeCN-d_3) δ 164.34, 150.95, 138.31, 137.41 (d, *J* = 3.8 Hz), 115.35, 111.02, 100.31, 93.40 (d, *J* = 206.8 Hz), 73.55 (d, *J* = 3.4 Hz), 72.34 (d, *J* = 24.1 Hz), 70.83, 69.71, 28.76, 18.99, 12.34. **IR** (neat): ν_{max} (cm^{-1}) = 3394, 2995, 2368, 1708, 1676, 1380, 1276, 1087, 1047, 864**.** $[\alpha]_D^{20}$= -51.5 (*c* 1.0 in MeOH). **HRMS** (ESI^+) calc. for $C_{15}H_{22}FN_2O_6$ $[M+H]^+$ 345.1456, found 345.1462.

Synthesis of diol 249

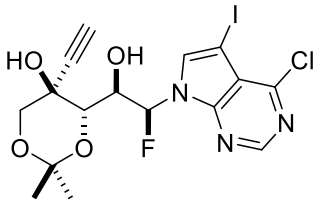

To a cold, -78 °C, stirred solution of chloroiododeazadenine ketofluorohydrin[70] (19.7 mg, 0.042 mmol, 1.0 eq) in CH_2Cl_2 (5.3 mL) under N_2 was added ethynylmagnesium bromide (0.42 mL, 0.5 M in THF, 0.21 mmol, 5.0 eq) slowly (along interior wall of flask). The resulting mixture was maintained at -78 °C and stirred for an additional 5 hours. The reaction mixture was then quenched with a 1:1 mixture of saturated NH_4Cl and MeOH solution (5 mL) and allowed to warm to room temperature. The mixture was then diluted with CH_2Cl_2, (10 mL) and the phases were separated. The aqueous phase was washed with CH_2Cl_2 (3 x 10 mL) and the organic phases were combined and washed with brine, dried over $MgSO_4$, filtered, and concentrated under reduced pressure. NMR internal standard indicated a yield of 6.2 mg, 30%. The two product diastereomers were separated by flash chromatography (gradient of EtOAc:hexanes 1:19 to 3:7). The product proved inseparable from the starting material by flash chromatography and was used as is for the subsequent reaction. An analytical sample was purified by HPLC for characterization to afford diol 249 as a white solid.

MP: 188-192 °C. **^{1}H NMR** (601 MHz, $CDCl_3$) δ 8.71 (s, 1H), 7.70 (s, 1H), 6.62 (s, 1H), 6.45 (d, *J* = 49.3 1H), 4.58 (dd, *J* = 20.0, 9.3 Hz, 1H), 4.37 (s, 1H), 4.02 (d, *J* = 11.3 Hz, 1H), 3.98 (d, *J* = 11.3 Hz, 1H), 3.87 (d, *J* = 11.3 Hz, 1H), 2.51 (s, 1H), 1.50 (s, 3H), 1.44 (s, 3H). **^{13}C NMR** (151 MHz, $CDCl_3$) δ 154.44, 150.83, 149.74, 135.99, 118.50, 100.12, 92.63 (d, *J* = 213.1 Hz), 82.94, 74.23, 73.05 (d, *J* = 21.0 Hz), 72.21, 68.26, 66.51, 54.30, 28.61, 19.23. **IR** (neat): ν_{max} (cm^{-1}) = 3725, 3425, 3285, 2985, 2889. $[\alpha]_D^{20}$= +14.5 (*c* 1.0 in $CHCl_3$). **HRMS** (ESI^+) calc. for $C_{16}H_{16}ClFIN_3NaO_4$ $[M+Na]^+$ 517.9750, found 517.9749.

Synthesis of diol 251

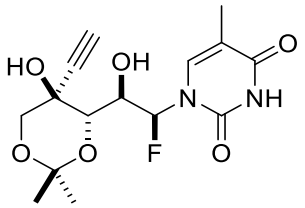

To a cold, -78 °C, stirred solution of ketone 239 (100 mg, 0.316 mmol, 1.0 eq) in CH_2Cl_2 (15.8 mL) under N_2 was added ethynylmagnesium bromide (3.16 mL, 0.5 M in THF, 1.58 mmol, 5.0 eq) slowly (along interior wall of flask). The resulting mixture was maintained at -78 °C and stirred for an additional 5 hours. The reaction mixture was then quenched with a 1:1 mixture of saturated NH_4Cl and MeOH solution (20 mL) and allowed to warm to room temperature. The mixture was then diluted with CH_2Cl_2, (20 mL) and the phases were separated. The aqueous phase was washed with CH_2Cl_2 (3 x 20 mL) and the organic phases were combined and washed with brine, dried over $MgSO_4$, filtered, and concentrated under reduced pressure. The resulting oil was purified by flash chromatography (gradient of EtOAc:hexanes 2:3 to 1:1) to afford diol 251 as a white solid (33.4 mg, 31%, d.r. 1:1).

^{1}H NMR (400 MHz, DMSO-d_6) δ 11.49 (s, 1H), 7.56 (s, 1H), 6.36 (dd, J = 43.6, 4.1 Hz, 1H), 6.23 (d, J = 6.1 Hz, 1H), 5.38 (s, 1H), 3.71 (d, J = 8.8 Hz, 1H), 3.68 (s, 2H), 3.44 (s, 1H), 3.32 (s, 2H), 1.78 (d, J = 1.2 Hz, 3H), 1.33 (s, 3H), 1.21 (s, 3H).

Data in agreement with that presented by Meanwell *et al.*[70]

Synthesis of nucleoside analogue 255

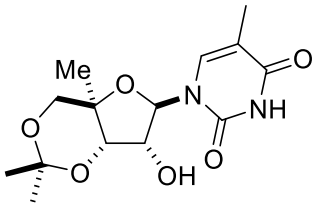

To a room temperature stirred solution of diol 240 (6.0 mg, 18 μmol, 1.0 eq) in MeCN (0.18 mL) was added NaOH (90 μL, 2.0 M in H_2O, 0.18 mmol, 10.0 eq). The

resulting mixture was heated to 60 °C and stirred for 1 hour. The reaction mixture was then quenched with a saturated NH_4Cl solution (3 mL) and cooled to room temperature. The mixture was then diluted with CH_2Cl_2, (5 mL) and the phases were separated. The aqueous phase was washed with CH_2Cl_2 (3 x 5 mL) and the organic phases were combined and washed with brine, dried over $MgSO_4$, filtered, and concentrated under reduced pressure. The resulting oil was purified by flash chromatography (gradient of EtOAc:hexanes 4:1 to pure EtOAc) to afford nucleoside analogue 255 as a white solid (3.6 mg, 61%).

MP: 108-115 °C**. ^{1}H NMR** (500 MHz, MeCN-d_3) δ 8.96 (s, 1H), 7.20 (d, *J* = 1.3 Hz, 1H), 5.84 (d, *J* = 1.5 Hz, 1H), 4.25 (ddd, *J* = 6.1, 4.4, 1.5 Hz, 1H), 3.95 (d, *J* = 9.4 Hz, 1H), 3.74 (d, *J* = 9.5 Hz, 1H), 3.72 (d, *J* = 6.3 Hz, 1H), 3.65 (d, *J* = 4.3 Hz, 1H), 1.85 (d, *J* = 1.2 Hz, 3H), 1.53 (s, 3H), 1.47 (d, *J* = 0.8 Hz, 3H), 1.45 (s, 3H). **^{13}C NMR** (151 MHz, MeCN-d_3) δ 164.40, 151.23, 137.30, 111.48, 102.64, 93.09, 76.78, 76.11, 73.99, 73.05, 29.50, 20.04, 18.31, 12.25. **IR** (neat): v_{max} (cm^{-1}) = 3464, 2921, 2398, 1691, 1274, 1178, 1142, 1103, 1032, 851. $[\alpha]_D^{20}$= -21.1 (*c* 0.4 in MeOH). **HRMS** (ESI^+) calc. for $C_{14}H_{20}N_2O_6$ $[M+H]^+$ 313.1394, found 313.1395.

Nucleoside analogue 255 was deprotected according to the following procedure:

Nucleoside analogue 255 (1.6 mg, 5.1 µmol, 1.0) was dissolved in a solution of acetyl chloride (0.23 µL, 5.1 µmol, 1.0 eq.) in D2O (0.5 mL). The resulting mixture was maintained at room temperature for 2 hours. The reaction was then directly analyzed by NMR analysis.

Data for the prepared compound matches the reported literature data.[239]

Synthesis of nucleoside analogue 256

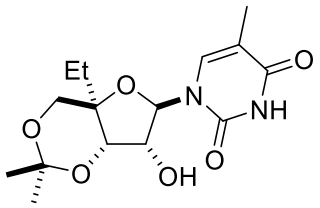

To a room temperature stirred solution of diol 241 (43.6 mg, 126 µmol, 1.0 eq) in MeCN (1.26 mL) was added NaOH (0.63 mL, 2.0 M in H_2O, 1.3 mmol, 10.0 eq). The resulting mixture was heated to 50 °C and stirred for 1 hour. The reaction mixture was then quenched with a saturated NH_4Cl solution (3 mL) and cooled to room temperature. The mixture was then diluted with CH_2Cl_2, (5 mL) and the phases were separated. The aqueous phase was washed with CH_2Cl_2 (3 x 5 mL) and the organic phases were combined and washed with brine, dried over $MgSO_4$, filtered, and concentrated under reduced pressure. The resulting oil was purified by flash chromatography (gradient of EtOAc:hexanes 1:1 to 3:2) to afford nucleoside analogue 256 as a white solid (14.1 mg, 34%).

MP: 102-108 °C**. ^{1}H NMR** (600 MHz, MeCN-d_3) δ 9.08 (s, 1H) 7.22 (s, 1H), 5.78 (d, *J* = 1.7 Hz, 1H), 4.26 (ddd, *J* = 6.4, 4.4, 1.7 Hz, 1H), 3.99 (d, *J* = 9.8 Hz, 1H), 3.79 (d, *J* = 6.6 Hz, 1H), 3.77 (dd, *J* = 9.9, 1.7 Hz, 1H), 3.74 – 3.70 (m, 1H), 2.03 (dqd, *J* = 15.0, 7.5, 1.7 Hz, 1H), 1.93 (overlap, *assigned via COSY spectrum*, 1H), 1.85 (d, *J* = 1.3 Hz, 3H), 1.53 (s, 3H), 1.44 (s, 3H), 0.90 (t, *J* = 7.6 Hz, 3H). **^{13}C NMR** (151 MHz, MeCN-d_3) δ 164.47, 151.28, 137.41, 111.55, 102.47, 92.91, 78.83, 77.00, 73.84, 68.49, 29.43, 20.98, 20.04, 12.24, 6.86. **IR** (neat): ν_{max} (cm^{-1}) = 3411, 2922, 2369, 1705, 1465, 1372, 1267, 1103, 1022, 851. $[\alpha]_D^{20}$= -27 (*c* 0.7 in MeOH). **HRMS** (ESI^+) calc. for $C_{15}H_{23}N_2O_6$ $[M+H]^+$ 327.1551, found 327.1550.

Synthesis of nucleoside analogue 257

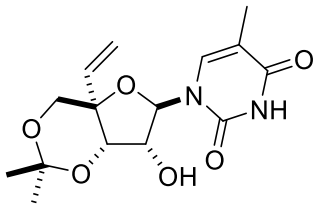

To a room temperature stirred solution of diol 248 (10.8 mg, 31.4 μmol, 1.0 eq) in MeCN (0.31 mL) was added NaOH (0.16 mL, 2.0 M in H_2O, 0.31 mmol, 10.0 eq). The resulting mixture was heated to 50 °C and stirred for 1 hour. The reaction mixture was then quenched with a saturated NH_4Cl solution (3 mL) and cooled to room temperature. The mixture was then diluted with CH_2Cl_2, (5 mL) and the phases were separated. The aqueous phase was washed with CH_2Cl_2 (3 x 5 mL) and the organic phases were combined and washed with brine, dried over $MgSO_4$, filtered, and concentrated under reduced pressure. The resulting oil was purified by flash chromatography (gradient of EtOAc:hexanes 7:3 to pure EtOAc) to afford nucleoside analogue 257 as a white solid (5.9 mg, 58%).

MP: 85-89 °C**. ^{1}H NMR** (500 MHz, MeCN-d_3) δ 9.00 (s, 1H), 7.24 (q, *J* = 1.4 Hz, 1H), 6.51 (dd, *J* = 17.7, 11.1 Hz, 1H), 5.82 (d, *J* = 1.4 Hz, 1H), 5.44 (dd, *J* = 17.8, 1.8 Hz, 1H), 5.27 (dd, *J* = 11.1, 1.7 Hz, 1H), 4.27 – 4.21 (m, 1H), 4.12 (d, *J* = 9.3 Hz, 1H), 3.92 (d, *J* = 6.1 Hz, 1H), 3.82 (d, *J* = 9.3 Hz, 1H), 3.32 (dd, *J* = 5.2, 1.4 Hz, 1H), 1.86 (d, *J* = 1.2 Hz, 3H), 1.58 (s, 3H), 1.49 (s, 3H). **^{13}C NMR** (151 MHz, MeCN-d_3) δ 164.44, 151.25, 138.44, 137.58, 114.52, 111.63, 103.02, 93.19, 77.87, 77.41, 73.92, 73.25, 29.32, 20.06, 12.25. **IR** (neat): ν_{max} (cm^{-1}) = 3459, 2920, 2368, 1706, 1466, 1374, 1271, 1142, 1104, 1032, 989, 855. $[\alpha]_D^{20}$= -13 (*c* 1.0 in MeOH). **HRMS** (ESI^+) calc. for $C_{15}H_{21}N_2O_6$ $[M+H]^+$ 325.1400, found 325.1413.

Synthesis of nucleoside analogue 258

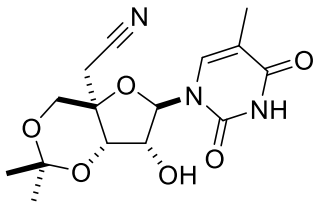

To a room temperature stirred solution of diol 242 (73.8 mg, 207 μmol, 1.0 eq) in MeCN (10.3 mL) was added NaOH (103 μL, 2.0 M in H_2O, 207 μmol, 1.0 eq). The resulting mixture was stirred at room temperature for 72 hours. The reaction mixture was then quenched with a saturated NH_4Cl solution (10 mL). The mixture was then diluted with CH_2Cl_2, (10 mL) and the phases were separated. The aqueous phase was washed with CH_2Cl_2 (4 x 10 mL) and the organic phases were combined and washed with brine, dried over $MgSO_4$, filtered, and concentrated under reduced pressure. The resulting oil was purified by flash chromatography (gradient of EtOAc:hexanes 3:2 to 9:1) to afford nucleoside analogue 258 as a white solid (45.0 mg, 65%).

MP: 143-147 °C. **^{1}H NMR** (500 MHz, MeCN-d_3) δ 8.99 (s, 1H), 7.19 (d, *J* = 1.3 Hz, 1H), 5.86 (d, *J* = 1.3 Hz, 1H), 4.37 (t, *J* = 5.2 Hz, 1H), 4.09 (d, *J* = 10.4 Hz, 1H), 4.04 (dd, *J* = 10.4, 1.8 Hz, 1H), 3.97 (d, *J* = 4.3 Hz, 1H), 3.96 (d, *J* = 6.0 Hz, 1H), 3.26 (dd, *J* = 17.7, 1.8 Hz, 1H), 3.16 (d, *J* = 17.7 Hz, 1H), 1.86 (d, *J* = 1.3 Hz, 3H), 1.55 (s, 3H), 1.47 (s, 3H). **^{13}C NMR** (151 MHz, MeCN-d_3) δ 164.66, 151.27, 137.62, 118.48, 111.76, 103.46, 94.45, 76.52, 75.40, 73.20, 69.75, 29.20, 21.14, 19.97, 12.26. **IR** (neat): ν_{max} (cm^{-1}) = 3405, 2994, 2260, 1705, 1278, 1181, 1134, 1030, 845. $[\alpha]_D^{20}$= -51.7 (*c* 0.9 in MeOH). **HRMS** (ESI$^+$) calc. for $C_{15}H_{20}N_3O_6$ $[M+H]^+$ 338.1352, found 338.1350.

Synthesis of nucleoside analogue 259

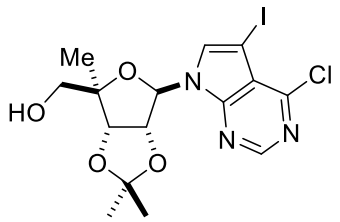

To a room temperature stirred solution of diol 249 (6.5 mg, 13.3 μmol, 1.0 eq) in MeCN (0.2 mL) was added $InCl_3$ (0.6 mg, 2.7 μmol, 0.2 eq). The resulting mixture was stirred at room temperature for 24 hours. Acetone (0.1 mL) and 2,2-dimethoxypropane (4 μL, 2.5 eq) were then added, followed by camphorsulphonic acid (0.5 mg, 0.15 eq). The reaction mixture was then quenched with a saturated sodium bicarbonate solution (0.5 mL). The mixture was then diluted with CH_2Cl_2, (0.5 mL) and the phases were separated. The aqueous phase was washed with CH_2Cl_2 (3 x 1 mL) and the organic phases were combined and washed with brine, dried over $MgSO_4$, filtered, and concentrated under reduced pressure. The resulting oil was purified by flash chromatography (EtOAc:DCM 1:9) to afford nucleoside analogue 259 as a white solid (2.8 mg, 45%).

MP: 112-121 °C. **^{1}H NMR** (601 MHz, $CDCl_3$) δ 8.63 (d, *J* = 2.4 Hz, 1H), 7.49 (d, *J* = 2.5 Hz, 1H), 5.79 (t, *J* = 3.9 Hz, 1H), 5.39 (dt, *J* = 11.4, 2.2 Hz, 1H), 5.30 (t, *J* = 5.2 Hz, 1H), 5.02 – 4.96 (m, 1H), 3.79 – 3.72 (m, 1H), 3.63 (t, *J* = 11.7 Hz, 1H), 1.65 (d, *J* = 2.4 Hz, 3H), 1.37 (d, *J* = 2.4 Hz, 3H), 1.34 (d, *J* = 2.4 Hz, 3H). **^{13}C NMR** (151 MHz, $CDCl_3$) δ 154.06, 150.53, 149.40, 135.30, 119.26, 114.44, 94.89, 88.34, 83.37, 82.70, 69.09, 51.72, 27.72, 25.41, 18.11. **IR** (neat): ν_{max} (cm^{-1}) = 3362.15, 2929.04, 2857.50, 1461.86, 1380.77, 1268.48, 1117.39, 1019.11. $[\alpha]_D^{20}$= +20.3 (*c* 0.3 in MeOH). **HRMS** (ESI^+) calc. for $[M+H]^+$ 466.0025 m/z, found 466.0011 m/z.

Synthesis of nucleoside analogue 260

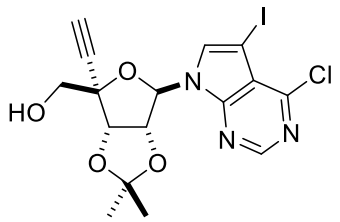

To a room temperature stirred solution of diol 249 (4.9 mg, 9.9 µmol, 1.0 eq) in MeCN (0.2 mL) was added $InCl_3$ (11.0 mg, 49 µmol, 5.0 eq). The resulting mixture was maintained at room temperature with stirring for 18 hours. 2,2-dimethoxypropane (3.0 µL, 25 µmol, 2.5 eq) was then added, followed by camphorsulphonic acid (0.15 mg, 1.5 µmol 0.15 eq) in acetone (0.1 mL). The resulting mixture was maintained at room temperature with stirring for an additional 4 hours. The reaction mixture was then quenched with a saturated $NaHCO_3$ solution (5 mL). The mixture was then diluted with CH_2Cl_2, (5 mL) and the phases were separated. The aqueous phase was washed with CH_2Cl_2 (5 x 5 mL) and the organic phases were combined and washed with brine, dried over $MgSO_4$, filtered, and concentrated under reduced pressure. The resulting oil was purified by flash chromatography (gradient of EtOAc:hexanes 1:9 to 3:7) to afford diol 260 as a white solid (2.1 mg, 44%).

MP: 75-84 °C. **^{1}H NMR** (500 MHz, $CDCl_3$) δ 8.63 (s, 1H), 7.47 (s, 1H), 5.94 (d, *J* = 5.1 Hz, 1H), 5.30 – 5.26 (m, 2H), 5.14 (d, *J* = 6.2 Hz, 1H), 3.98 (dd, *J* = 12.2, 2.4 Hz, 1H), 3.88 (d, *J* = 11.9 Hz, 1H), 2.77 (s, 1H), 1.71 (s, 3H), 1.40 (s, 3H). **^{13}C NMR** (101 MHz, $CDCl_3$) δ 154.25, 150.75, 149.55, 135.01, 119.24, 115.83, 94.61, 84.48, 83.03, 81.86, 78.15, 77.37, 68.05, 52.21, 27.38, 25.57. **IR** (neat): ν_{max} (cm^{-1}) = 3362.15, 2917.58, 2849.93, 1574.23, 1434.09. $[\alpha]_D^{20}$= +20.3 (*c* 0.3 in MeOH). **HRMS** (ESI^+) calc. for $C_{16}H_{16}ClIN_3O_4$ $[M+H]^+$ 475.9869, found 475.9883.

Synthesis of nucleoside analogue 261

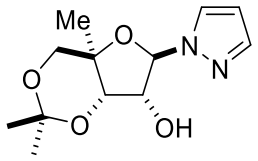

To a room temperature stirred solution of diol 244 (5.0 mg, 18 μmol, 1.0 eq) in MeCN (0.18 mL) was added NaOH (91 μL, 2.0 M in H_2O, 0.18 mmol, 10.0 eq). The resulting mixture was heated to 50 °C and stirred for 30 hours. The reaction mixture was then quenched with a saturated NH_4Cl solution (3 mL) and cooled to room temperature. The mixture was then diluted with CH_2Cl_2, (5 mL) and the phases were separated. The aqueous phase was washed with CH_2Cl_2 (3 x 5 mL) and the organic phases were combined and washed with brine, dried over $MgSO_4$, filtered, and concentrated under reduced pressure. The resulting oil was purified by flash chromatography (gradient of EtOAc:hexanes 1:4 to 2:3) to afford nucleoside analogue 261 as a white solid as a mixture of α and β anomers (2.9 mg, 63%). An analytical sample was purified by HPLC to obtained characterization of the desired β-anomer.

MP: 102-108 °C. **^{1}H NMR** (600 MHz, CD_3CN) δ 7.79 (dd, *J* = 2.5, 0.6 Hz, 1H), 7.56 (d, *J* = 1.7 Hz, 1H), 6.35 (dd, *J* = 2.5, 1.7 Hz, 1H), 5.29 (d, *J* = 1.4 Hz, 1H), 4.16 (t, *J* = 1.6 Hz, 1H), 4.01 (d, *J* = 1.8 Hz, 1H), 3.71 (dd, *J* = 11.2, 1.0 Hz, 1H), 3.41 (d, *J* = 11.1 Hz, 1H), 3.22 (s, 1H), 1.42 (s, 3H), 1.35 (s, 3H), 1.24 (s, 3H). **^{13}C NMR** (151 MHz, CD_3CN) δ 141.72, 130.93, 107.83, 99.82, 72.95, 70.85, 67.01, 64.58, 56.93, 29.13, 20.05, 19.06. **IR** (neat): ν_{max} (cm^{-1}) = 3423, 2959, 2929, 2873, 1461, 1381, 1268, 1102, 908, 731. $[\alpha]_D^{20}$= +20.3 (*c* 0.3 in MeOH). **HRMS** (ESI^+) calc. for $C_{12}H_{19}N_2O_4$ $[M+H]^+$ 255.1339, found 255.1341.